EFFECTS OF NON-BIOCIDAL COATING TECHNOLOGIES ON COLONISATION BY

ECTOCARPOID ALGAE

By

EMMANUELLE MARIE LAETITIA EVARISTE

A thesis submitted to the

University of Birmingham

for the degree of

DOCTOR OF PHILOSOPHY

UNIVERSITY OF BIRMINGHAM

University of Birmingham Research Archive

e-theses repository

ABSTRACT

Algae are well-recognised for their fouling impact on immersed surfaces. During this thesis, the relationships between surface and bulk properties of coatings and the adhesion preferences of a new test species, *Ectocarpus crouaniorum*, a filamentous brown alga and a significant member of fouling communities, were explored. A novel laboratory-based adhesion bioassay for *E. crouaniorum* using small filamentous fragments as inocula was developed. The bioassay was used to screen sets of experimental coatings at an appropriate scale in well-replicated and controlled experiments

Sets of coatings with varying wettability, surface charge or modulus were produced, characterised and assayed. The attachment and adhesion preferences of *E. crouaniorum* were influenced by the surface and bulk properties. These preferences were compared with those of *U. linza*. No linear correlation was observed between the adhesion strength of *E. crouaniorum* and wettability in contrast to the linear relationship observed testing *U. linza*; increase of modulus decreased or increased the adhesion strength of *E. crouaniorum* and *U. linza,* respectively. However, both species had lower adhesion on uncharged xerogel coatings. The performance of test coatings was also assessed in field assays and the results showed that these data were not always similar to the laboratory assay.

ACKNOWLEDGEMENTS

CONTENTS LISTINGS

LIST OF ILLUSTRATIONS

Some titles have been shortened for purposes of clarity.

LIST OF TABLES

Some titles have been shortened for purposes of clarity.

LIST OF DEFINITIONS

Adhesion strength: For soft-fouling organisms such as algae, it is the ease of removal (i.e. % removal) after exposure to a shear stress, while for hard-fouling organisms such as barnacles, it is measured by the application of a mechanical shear force parallel to the base of the organisms to measure the critical removal stress.

Amphiphilic: A term describing molecules or surfaces that simultaneously possess both hydrophobic and hydrophilic properties.

Antifouling coatings: Coatings that prevent the colonisation of biofouling on immersed surfaces.

Axenic: It describes a culture of an organism that is free of all other 'contaminating' organisms.

Biocide: A chemical substance capable of killing living organisms.

Biofilm: An aggregate of microorganisms adhering to each other and to a surface and embedded in a matrix of extracellular polymeric substances (EPS). In the context of marine fouling, a biofilm is a complex community of unicellular organisms including bacteria, diatoms and fungi.

Biofouling: Growth of living organisms upon artificial substrates such as ships' hulls and buoys.

Borosilicate glass: It is a type of glass, which has silica and boron oxide as the main components. Nexterion® glass is a borosilicate glass produced by Schott.

Boundary layer (around the ship): It represents the layer of fluid in the immediate proximity of a bounding surface where the effects of viscosity are significant.

Byssus: A collection of strong filaments by which certain molluscs attach themselves to hard surfaces.

Coefficient of friction: A dimensionless scalar value, which describes the ratio of the force of friction between two surfaces and the force pressing them together.

Contact angle: It is the angle at which a liquid interface meets the solid surface, allowing the category of interactions between the liquid and the surface to be determined. It measures the wettability of the surface.

Copolymer: A polymer derived from two or more monomeric species.

Corrosion: Breakdown of substrate materials due to chemical reactions between water and oxygen.

Cross-linker: A compound that induces the formation of cross-links.

Drag: The force, which resists motion of an object through a fluid.

Dynamic contact angle: It is measured alternative method to measure the wettability of a surface to the static contact angle method. Dynamic contact angle method measures the advancing contact angle and the receding contact angle of surfaces. Advancing contact angle is measured when the water is added to a stable drop of water and the contact angle was relatively stable. The receding angle on the other hand was measured when the water was removed and the contact angle was relatively stable. The difference between these two angles is the contact angle hysteresis that is thought to be a measure of roughness and surface heterogeneity.

Elastomer: It is a polymer with the property of viscoelasticity, generally having low modulus and high elastic strength compared with other materials.

Epoxy: It is a term used for the basic components and the cured-end products of epoxy resins. It is used to produce coatings and adhesives.

Extracellular polymer substances (EPS): They are glue-like compounds secreted by microorganisms, mainly composed of polysaccharides and proteins, which are important for the formation of the biofilm and cells attachment to surfaces.

Fouling-release coatings: Coatings that do not prevent colonisation, but the adhering organisms are so weakly attached that they are 'released' at relatively low hydrodynamic shear stress, such as those created when a vessel moves through the water.

Glass transition region (observed in the DMA results): It is the region where the sample becomes less hard as storage modulus decreases and tan delta peaks.

Glass transition (Tg; observed in the DMA results): It refers to the range of temperature where a material softens.

Hard fouling: One of the categories of the biofouling organisms. Hard fouling organisms are represented by their hard bodies, such as mussels and barnacles.

Hydrophilic: It refers to the physical property of molecules or surfaces that can bond with water molecules through hydrogen bonding. This means that the surface is very wettable, that is, a droplet of water readily spread on such a surface.

Hydrophobic: It refers to a physical property of molecules or surfaces that cannot readily bond with water or other polar molecules. "Superhydrophobic" surfaces are extremely difficult to wet, that is, water droplets roll off when the surface is titled by as little as 10°.

Lipophobicity: It is the chemical property of chemical compounds. It means "fat rejection"; it should decrease the adhesion strength of fouling organisms.

Macrofouling: It represents the category of fouling organisms that are individually visible by eyes including algae (weeds) and animals.

Microfouling: In opposite to macrofouling, it is attributable to the accumulation of unicellular algae (diatoms) and bacteria although other microscopic organisms e.g. protozoa and fungi are often also present (also referred to as "slime"). It is difficult to control on non-biocidal surfaces, having a low surface profile and can remain adherent on ships' hulls at speeds in excess of 30 knots.

Modulus: It is the tendency of the substance such as a coating to be deformed elastically (but not permanently) when a force is applied to it. Two types of modulus were measured: the storage modulus and the elastic modulus, allowing determination of the stiffness of the coating.

PEO: It refers to poly(ethylene oxide), which is a polymer of ethylene oxide; poly(ethylene glycol) PEG is also a polymer of ethylene oxide. The only difference between PEG and PEO is their molecular weight. In general, PEG has a molecular weight below 20000 g mol^{-1}, while PEO has a molecular weight above 20000 g mol^{-1}.

PDMSe: Poly(dimethylsiloxane) elastomer, a rubbery polymer that forms the binder system of many commercial fouling-release coatings.

Precursor (or sol): A compound that participates in the chemical reaction that produces another compound. The most common precursor to produce silica xerogel is tetraethylorthosilicate (TEOS).

Pristine surface: A surface that has its original purity or that has not been soiled.

Pseudobarnacle: A cylindrical metal stud that is glued to the surface using an epoxy adhesive, which is used to simulate the adhesion of a barnacle.

Self-polishing copolymer (SPC): The paint polymer or binder system is made soluble in seawater by hydrolysis. This is a controlled chemical reaction and only occurs at the surface of the coating. SPC technology combines controlled polishing rate and optimum biocide release with inherent self-smoothing for hull roughness control and maximum fuel efficiency.

Settlement: It is the process of the motile spores or larvae to settle on a surface.

Soft fouling: It is one of the categories of the biofouling. Soft fouling represents those organisms, which do not have hard bodies. In the literature, soft fouling are soft-bodied animals, algae and slime. However, for assessments in the field, soft fouling excludes algae and slime.

Surface energy: It is defined as the excess energy at the surface of material compared to the bulk and is a measure of the capacity of a surface to interact spontaneously, using the excess energy, with other materials.

Tangent delta or Tan delta (measured with the DMA): It is the tangent of the phase angle, referring to the ratio of loss to elasticity, which indicates the viscoelasticity of a sample.

Turbulent flow (water channel): It is a flow regime characterised by chaotic and stochastic property changes.

Weed fouling: The most common weed (algae) fouling on ships is the green algae *Ulva spp.* and the brown algae *Ectocarpus spp.* Weed fouling usually occurs where there is available sunlight, i.e. around the water line and a few meters below. It is not usually found on the flat bottom of vessels.

Wettability: It is the ability of maintaining contact with a solid surface and is known by measuring the contact angle.

Xerogel: organosilica-based sol-gels; dried gels produced by evaporation of the solvents.

LIST OF ABBREVIATIONS AND SYMBOLS

AF: Antifouling

AFM: Atomic force microscopy

ANOVA: Analysis of variance

ASW: Artificial seawater

CA: Contact angle

CCAP: Culture Collection of Algae and Protozoa

Chl *a*: Chlorophyll a

DAPI: 4',6-diamidino-2-phenylindole

DMA: Dynamic mechanical analyser

DMSO: Dimethyl sulfoxide

E: Elastic modulus

E': Storage modulus

E'': Loss modulus

EPS: Extracellular polymers

FR: Fouling-release

GEEs: Generalized estimating equations

GeO$_2$: Germanium dioxide

GZLM: Generalized linear models

IS700: Intersleek 700

IS900: Intersleek 900

OWRK equation: Owens, Wendt, Rabel and Kaelble equation

PDMS: Poly(dimethylsiloxane)

PDMSe: Poly(dimethylsiloxane) elastomer

PEG: Poly(ethylene glycol)

PFPE: Perfluoropolyether

R^2: Coefficient of determination of a linear regression

RFU: Relative fluorescence unit

RM ANOVA: Repeated measure ANOVA

SE: Standard error (when used with 2 ± SE)

SE: Surface energy

T2: Silastic® T2

Tan D: Tan Delta

TEOS: Tetraethylorthosilicate

Tg: Glass transition temperature

XPS: X-ray photoelectron spectrometry

In literature and in this thesis, the symbol **θ** was used to represent the contact angle. Several subscripts were used in this thesis in order to explain which contact angle was measured, the method or the liquid used.

$θ_m$: Measured contact angle, which is the contact angle that was measured using the contact angle method.

$θ_c$: Calculated contact angle, which is used for the underwater contact angle method. The internal contact angle was measured ($θ_m$) but only the values of the external contact angle were used ($θ_c$) which was equal to 180°- $θ_m$.

The term θ was also followed by few other subscripts to refer to the different liquids and methods used to measure the contact angle. The subscripts referring to the liquids letters were: 'W' water and 'D' diiodomethane and to the different methods used: 'S' static, 'adv' advancing, 'rec' receding, 'und' underwater. These terms will be explained in more detail in Chapter 2.9.1.

In literature and so in this thesis, the symbol γ referred the surface tension of a liquid γ_L (L meaning liquid) and the surface energy of the solid γ_S (S meaning solid). They both can be split into two polar and dispersive components, which will be represented by superscript P and D. These terms will be explained in more detail in Chapter 2.9.1.

1. GENERAL INTRODUCTION

For decades, numerous studies have been performed in order to understand and to find solutions to control marine biofouling. Marine biofouling is an undesirable accumulation of marine organisms such as bacteria, algae and invertebrates on structures submerged in the sea, leading to damage to surfaces. Biofouling is ubiquitous, regardless of location and season. The deleterious effects of fouling impact a range of industries, including shipping, the leisure craft market, the power industry, oceanographic monitoring and aquaculture. In addition, surfaces of living marine organisms can also be fouled (i.e. epibiosis) leading to economic and production issues in aquaculture of seaweeds and shellfish (Fitridge et al. 2012).

Fouling has been an economic problem for shipping for centuries as it increases drag and thus more fuel is required to maintain speed (Pritchard 1988; Schultz 2007; Schultz et al. 2011). Modern antifouling (AF) paints that contain biocides control fouling efficiently, but environmental regulations have led to research into 'environmentally benign' technologies that prevent fouling organisms adhering -i.e. do not kill the cells and larvae that initially attach- and are not harmful for the marine environment. These newer technologies include non-biocidal, 'fouling-release' (FR) paints. Numerous studies have shown that these coatings do not prevent colonisation of surfaces per se; rather they decrease the adhesion strength of the attached organisms, especially hard fouling organisms such as barnacles, as well as algal species such as *Ulva linza* (Anderson et al. 2003; Callow and Callow 2011 for reviews)*.* However, some organisms, notably diatoms, adhere strongly to these coatings (Holland et al. 2004; Thompson et al. 2008). In addition, ectocarpoid algae are reported to be able to colonise and adhere to non-biocidal, FR coatings on test panels and ships' hulls (International Paint, D. Williams, personal communication). Ectocarpoid algae have been well

studied for their ecology and genetics, but only a few studies have been reported on their fouling behaviour.

1.1. Problems due to biofouling

The high interest in biofouling is due to associated economic and environmental consequences for shipping and other industries. Settlement and subsequent growth of fouling organisms on ships' hulls increase roughness and therefore increase fuel consumption in order to maintain speed to counteract the extra hydrodynamic drag that is imposed. It has been estimated that biofouling may account for a powering penalty of up to 86 % for a heavily fouled hull and even if the hull is only fouled by a light layer of slime, the powering penalty can reach 10-16 % (Schultz 2007). In the same way, biofouling increases the roughness and therefore the diameter of offshore-submerged structures, which amplifies the effects of waves, current loadings and drag forces (Edyvean et al. 1985; Edyvean 2010 for review).

Biofouling also increases the cost of hull maintenance due to inspection, dry-docking, cleaning, paint removal and repainting. Then if the hull is damaged, for example by corrosion of steel surfaces, more time will be needed in order to repair the hull. A recent analysis of the economic impact of a range of marine biofouling (from biofilm to weeds and small calcareous fouling) for the US Navy estimated a cost of $56 million per annum for an Arleigh Burke DDG-51 destroyer, which represents 30 % of the US Navy fleet (Schultz et al. 2011). If the analysis is extrapolated to the entire fleet, the approximate annual cost for maintenance associated with hull fouling would be between $180 and 260 million per annum (Schultz et al. 2011). Maréchal and Hellio (2009 for review) estimated a cost of $150 billion per year for the world cost of fouling (including transport delays, hull repairs, cleaning of desalination units and biocorrosion).

The emission of greenhouse and acid rain gases is increased by biofouling via the increase of fuel consumption needed to maintain ship power. An indirect consequence of biofouling is the release of biocides into the environment from biocidal AF coatings. The presence of biocides influences biotic and abiotic processes such as bioconcentration, food web mechanisms, temperature, salinity, pH and interaction with organic matter. In addition, biocides such as copper that has been the main AF compound used since Roman times, are accumulated in sediments of marinas, shipyards and harbours (Harino et al. 2007; Srinivasan and Swain 2007). These accumulations raise some environmental concerns on the negative effects on non-target organisms living in surrounding environments.

Furthermore, fouled hulls along with ballast water are important vectors for the introduction of non-indigenous marine species to non-native environments (e.g. Hewitt 2002; Hewitt et al. 2004; Floerl 2005; Schaffelke et al. 2006; Barry et al. 2008). The ecological impacts of invasive species include competition with the native organisms, possibility of habitat change and effect on trophic levels. Economic consequences include environmental management costs for eradication or control. A notable example of invasive species is the introduction of zebra mussels (*Dreissena polymorpha*) into the Great Lakes from Europe through ballast water in the mid-1980s. Hewitt et al. (2004) estimated the number of introduced and cryptogenic species in Port Phillip Bay, Victoria, Australia to be over one hundred because the majority of them were concentrated around the shipping ports.

1.2. Solutions to biofouling

In order to solve the biofouling problem, scientists have researched solutions such as the development of coatings to protect ships. Two types of coatings are mostly used commercially: biocidal AF coatings and non-biocidal FR coatings. Biocidal AF coatings prevent the colonisation by marine organisms on immersed structures by killing the organisms that settle on the surfaces. FR coatings do not primarily prevent colonisation but

organisms that attach to surfaces have a weak adhesion and are released at low hydrodynamic shear forces (Swain et al. 2000).

In addition to coatings, other technologies to contend with biofouling have been developed, especially mechanical techniques, which when combined with non-biocidal paints provide better ship husbandry. The developed technologies are mostly focussed on underwater scrubbing (or grooming), which allows removal of fouling underwater without having to dry dock the ship (Tribou and Swain 2010). During the last decades, the number of commercial scrubbing systems has increased. However, the use of these instruments needs to be monitored carefully to reduce the risk of dispersion of non-indigenous marine species in new environments (Lewis and Coutts 2010 for review). Mechanical technologies should then be used before the vessels leave marinas or harbours where the fouling has originated.

Other non-coating solutions have been tested over the last 50 years, such as the use of electricity, magnetism, heat or even radiation (Finnie and Williams 2010 for review). The use of electricity, which is the release of current or charge along the hull surface, was the most effective but unfortunately, it is too complex to be able to use this technique on a large scale.

At the present time, both biocidal and non-biocidal AF paints are available for use on vessels. The present, non-tin-based biocidal AF paints contain a range of alternative biocidal compounds including copper (or cuprous oxide, a derived compound) and zinc pyrithione that prevent the settlement and growth of fouling organisms. Non-biocidal solutions are mainly represented by FR coatings that have specific surface and bulk properties in order to minimise the adhesion strength of organisms and make removal by water flow easier (Swain et al. 2000; Finnie and Williams 2010). Technologies that will cost less, be more durable and allow the removal of fouling at lower speeds are also being researched (Callow and Callow 2011 for review).

According to the different components of the coating, surface properties vary. These parameters can affect the settlement and adhesion of spores and larvae as well as the adhesion of adult plants and animals. By examining the adhesion of fouling organisms to surfaces presenting different properties, new knowledge into the mechanism of adhesion can be gained. In AF research, for example using *U. linza* and diatoms as test organisms, many surface parameters have been studied including surface chemistry and charge (Ederth et al. 2008; Cao et al. 2009), wettability (Callow et al. 2005; Krishnan et al. 2006b; Akesso et al. 2009a; Akesso et al. 2009b), friction (Howell and Behrends 2006; Bowen et al. 2007), electrostatic interactions (Rosenhahn et al. 2009) and topography (Callow et al. 2002; Genzer and Efimenko 2006; Cooper et al. 2011). The response of cells, spores and larvae to wettability varies according the species. For example, cells of the diatom *Navicula incerta* typically adhere more strongly to hydrophobic surfaces while settled spores and sporelings of *U. linza* typically adhere less strongly to hydrophobic surfaces (Krishnan et al. 2006b; Schilp et al. 2007; Bennett et al. 2010; Finlay et al. 2010). However, these are generalisations and exceptions to these observations do occur, for example, amphiphilic coatings, which contain both hydrophobic and hydrophilic functionalities, are particularly effective in FR laboratory assays (Grozea et al. 2009; Callow and Callow 2011 for reviews) and form the basis of some current leading commercial technologies such as Intersleek® 900 (IS900). Over-generalisation on the influence of surface properties on coating performance should therefore be avoided.

1.2.1. Biocidal coatings

Biocidal AF coatings such as self-polishing copolymer AF paints prevent the colonisation of marine organisms by releasing biocides at a more or less controlled rate from the coating surface. During this process, some AF paints lose thickness due to the release of the biocide into the surrounding environment (i.e. its decrease in the paint film) (Finnie and Williams 2010; Dafforn et al. 2011). Biocidal paints contain one or more biocides; the most used and

effective is copper, usually in the form of cuprous oxide that is known to be active against many invertebrate fouling organisms but it is usually less effective against algae. It is generally used in combination with other biocides in order to provide activity against a wide range of organisms. Tributyltin self-polishing copolymer biocidal AF paint was highly effective, but is now banned due to its environmental effects on non-target marine organisms. Progressively stringent legislation has regulated the choice and use of biocides, in order to protect human health and the marine environment (Chambers et al. 2006; Pereira and Ankjaergaard 2009 for reviews).

1.2.2. Non-biocidal coatings

1.2.2.1. Fouling-release coatings

For a number of years, researchers have been investigating non-biocidal, non-fouling strategies including FR coatings. Two types of materials are mostly used to create FR coatings: silicones and fluoropolymers. FR coatings do not primarily prevent the colonisation of organisms on immersed surfaces, but the surface properties of these coatings minimise the adhesion and facilitate the removal of fouling organisms at low hydrodynamic shear forces, such as the movement of the ship through the water (Finnie and Williams 2010). These polymers and coatings incorporating them are typically characterised by their low surface energies. FR coatings are more effective for high-speed craft (>15 knots) that do not spend much time in port (Finnie and Williams 2010). Current research aims for a new generation of coatings, which will be suitable for low speed vessels that spend time in the port, such as fluoropolymer-based coatings (Finnie and Williams 2010).

Wettability and surface energy are the most studied FR coating properties. Wettability is the ability of a liquid to maintain contact with a solid surface and is determined by measuring the contact angle. Surface energy is defined as the excess of energy at the surface of a material compared to the bulk (Brady and Singer 2000) and is calculated from the contact angle

measurements of at least two liquids using the Owens, Wendt, Rabel and Kaelble equation (see Chapter 2.9.1.3). In principle, the lower the surface energy is, the less interaction will be possible between the surface and other molecules such as cells and proteins. Baier and DePalma (1971; Dexter et al. 1975) studied polymer surface properties and suggested that adhesion would be minimal in a range of surface tensions (which is related to the surface energy) between 20 and 30 mN m^{-1}. The "Baier curve", indicated that there was a relationship between the critical surface tension of a coating and the relative amount of adhesion by attaching cells/organisms (Dexter et al. 1975; Dexter 1976; Dexter 1979). Other studies have demonstrated that not only is surface tension (or surface energy) linked to adhesion, but also other materials properties such as elastic modulus also influence the adhesion of marine organisms (Berglin et al. 2003).

Previous laboratory studies showed that surface energy and wettability are important parameters to predict attachment and/or adhesion strength of marine fouling organisms on surfaces (Brady and Singer 2000 for review). Fouling organisms do not have similar behaviour. Cypris larvae ('cyprids') of *Balanus improvisus* prefer to settle on surfaces with low surface energy (Dahlström et al. 2004), while cyprids of *Balanus amphitrite* prefer high surface energy (Rittschof and Costlow 1989; Finlay et al. 2010). However, a recent study showed that the settlement of cyprids seemed to be influenced by the surface charge, and not only by the wettability per se (Petrone et al. 2011a). Zoospores of *U. linza* prefer to settle on surfaces with low surface energy (Callow et al. 2000; Schilp et al. 2007; Bennett et al. 2010). In contrast, surfaces with high surface energy had higher adhesion strength of sporelings of *U. linza* (Akesso et al. 2009a; Akesso et al. 2009b; Bennett et al. 2010).

Commercial FR coatings are mostly based on poly(dimethylsiloxane) elastomers (PDMSe or silicone) (Finnie and Williams 2010, Lejars et al. 2012). Generally, these coatings, which are non-polar and hydrophobic and so have low surface energy (~22 mN m^{-1}), are expected to show low adhesion of polar molecules such as adhesive proteins because there are less

opportunities for hydrogen bonding and polar interactions (Callow and Callow 2011 for review). In general, they also have low elastic moduli and the release of hard-fouling is proportional to $(\gamma E)^{1/2}$, where γ is the surface energy and E is the modulus (Brady and Singer 2000).

Fluoropolymers have a low surface energy and general chemical stability, which have generally been thought to be essential properties for FR coatings (Finnie and Williams 2010). Finnie and Williams (2010) have listed the most studied fluoropolymer-based coatings developed and tested since 1976. The first coating of this kind that has been tested was a fluorinated poly(urethane) coating (Field 1976). Fluoropolymers are known for their high hydrophobicity and non-stick properties. Only a few studies have been done on these polymers compared to the silicones (Krishnan et al. 2006b; Martinelli et al. 2008; Wang et al. 2011). For example, Yarbrough et al. (2006) showed that spores of *U. linza* had lower adhesion (as in Hu et al. 2009) and higher removal on fluorinated coatings than standard surfaces (glass and PDMSe surfaces).

Amphiphilic coatings are FR technology, which contain a hydrophobic and a hydrophilic component. One way these coatings can be made is the blending of immiscible polymers or contrasting chemistries of block copolymers, which are generally a hydrophobic and a hydrophilic component. The hydrophobic component, which is often fluorinated, has non-polar, low surface energy properties; these properties reduce polar and H-bonding interactions with the bioadhesives produced by the fouling organisms. The hydrophilic component, which is often poly(ethylene glycol) PEG, brings protein-repellency properties (Du et al. 1997). IS900, which is a commercialised coating produced by International Paint is amphiphilic. Amphiphilic coatings have a dynamic surface that differs locally in surface chemistry, topography and mechanical properties due for example to the separation phase of mutually incompatible copolymers (review in Callow and Callow 2011). Gudipati et al. (2005) showed that cross-linked hyperbanched fluoropolymer and PEG amphiphilic networks were

effective against settlement of spores of *U. linza* and decreased the adhesion strength of sporelings of *U. linza*. Other researchers have used amphiphilic coatings in which a thin amphiphilic surface-active block copolymer is deposited over a thick, elastomeric base layer (Krishnan et al. 2006a; Martinelli et al. 2008). These coatings also showed weaker adhesion of *U. linza* sporelings and *Navicula* sp*.*

Another approach to control fouling is the use of zwitterionic materials, which seem to deter the adsorption of proteins and cells (Krishnan et al. 2008). These effects might be due a superhydrophobic surface produced by a hydration layer that is electrostatically induced. A zwitterion is a neutral molecule that has a positive and a negative electrical charge at different locations within the molecule. Two zwitterionic molecules are the most studied, poly(sulfobetaine) and poly(carboxybetaine). These materials are relatively cheap and chemically stable (Jiang and Cao 2010). Aldred et al. (2010) showed that poly(sulfobetaine methacrylate) polySBMA and poly(carboxybetaine methacrylate) polyCBMA inhibited settlement of cyprids. In addition, these materials are resistant to the adsorption of proteins and animal cells (Zhang et al. 2006). The settlement of spores of *U. linza* and the attachment of diatom cells were almost fully inhibited by polySBMA (Zhang et al. 2009).

1.2.2.2.   Other non-biocidal technologies

Organosilica-based sol-gels ('xerogels') are a well-known, robust coating technology but have not been extensively used to control marine biofouling (Selvaggio et al. 2009; Gunari et al. 2011). They are 'environmentally friendly' (i.e. do not contain biocides), which is an important aspect in the development of new biofouling solutions. Recent studies have shown that they have both AF and FR properties in laboratory assays against several fouling organisms such as *B. amphitrite, U. linza* and *Navicula perminuta* (Tang et al. 2005; McMaster et al. 2009; Bennett et al. 2010; Finlay et al. 2010). The efficacy of this technology has been demonstrated in the field using Aquafast[®], an organically-modified hybrid xerogel. This has been applied to approximately 100 boats and on metal materials supporting an

underwater camera at a marine archaeological site (Selvaggio et al. 2009; Gunari et al. 2011).

In the natural environment, many marine organisms are free of fouling organisms, which is attributed to physical defence mechanisms such as nano- or micro-topographical ridges on their skin surface. For example, the pilot whale *Globicephala melas* has nanoridge enclosed pores on the surface of its skin, which reduce surface available for the adhesion and attachment of fouling organisms (Baum et al. 2002). In addition, shark's skin has been the most studied model recently because it has been observed that all shark species are protected against biofouling apparently due to the presence of microtopographical ridges on their skins, which have different patterns according to the species (Reif et al. 1985 cited in Bechert et al. 2000). Non-toxic biomimetic technologies, which copy, or are inspired by these natural physical defence mechanisms, have been recently developed (Magin et al. 2010; Salta et al. 2010; Scardino and de Nys 2011). Micro-textured surfaces inhibit the settlement of several fouling organisms but the response of fouling organisms to topographic surfaces varies. Settlement of the barnacle *B. improvisus* is lower on micro-textured surfaces than smooth surfaces (Berntsson et al. 2000). For *U. linza*, Callow et al. (2002) showed the attachment of spores increased in valleys and around pillars of 5 µm depth and width; dimensions similar to the size of the spores. These studies led to the Sharklet AF topography surfaces, which is a surface of 2 µm wide rectangular-like periodic features (4, 8, 13 and 16 µm in length) of 4 µm height spaced 2 µm apart. Sharklet AF reduced spore settlement of *U. linza* by 85 % compared to smooth PDMS surfaces (Carman et al. 2006). However, the size of different categories of fouling organisms varies enormously –i.e. the length scale for bacteria is, for example, approximately 1 µm, whereas the spore of *U. linza* is around 5 µm and barnacle larvae may be several hundreds of micrometers in size. It is therefore difficult to envisage that coatings with only one size of topographic feature will have universal AF properties.

For over 20 years, researchers have investigated the use of enzymes in AF/FR coatings (Banerjee et al. 2011). Many fouling organisms attach to the surface using adhesives at least partly composed of proteins, so enzymes such as proteases should be capable of degrading these adhesives. The effects of the enzymes could occur at two different stages; during settlement, the enzymes could have a repellent effect by being released into the surrounding seawater and then after settlement, the enzymes could degrade the adhesives (Olsen et al. 2007 for review). Previous studies showed that several commercial enzymes had an effect on the settlement and adhesion strength of several fouling organisms (Pettitt et al. 2004; Huijs et al. 2006). In addition, Dobretsov et al. (2007) demonstrated that some proteases inhibited the settlement of bryozoan larvae.

Hydrogels are also being investigated as the basis of novel AF technologies. Hydrogels are cross-linked networks of hydrophilic polymer chains. They are highly water absorbent, which causes them to swell, depending on the degree of cross-linking. Typical hydrophilic polymers being investigated include polyHEMA (hydroxyethyl methacrylate) and PEG. Inhibition of settlement of cyprids of *B. amphitrite* was observed on PEG-based hydrogels (Ekblad et al. 2008) and also on PVA-SbQ hydrogels (polyvinyl alcohol substituted with light-sensitive stilbazolium groups) (Rasmussen et al. 2002). In addition, PEG-based hydrogels showed inhibition of the settlement of *U. linza* spores, cells of *N. incerta* and some species of bacteria (Ekblad et al. 2008). Magin et al. (2011) also showed decrease of the adhesion of cells of *Navicula incerta* and *Cobetia marina*, a bacterium, on hydrogels based on poly(ethyleneglycol) dimethacrylate 'PEGMA'.

1.2.3. Assessment of coatings: laboratory and field assays

Laboratory and field assays are used to screen numerous coatings in order to down-select them before testing them on ships' hulls and eventual commercialisation. Laboratory assays do not and are not intended to reflect the complexity of "real world". Their main purpose is to evaluate the intrinsic AF/FR properties of experimental coatings that are often available in

only small quantities. The assays are performed under controlled conditions (species, temperature and medium) with a defined challenge, typically by single organism. They are generally easy to perform and thus for a relatively low cost (facilities and amount of materials) provide a rapid assessment of the relationship between the structure and properties of a coating and its biological performance. This enables down-selection of coatings for further development and testing. In addition, laboratory assays may reveal any coating toxicity issues associated with catalysts or unpolymerised monomers. Laboratory assays also lend themselves well to hypothesis-driven experiments on fundamental aspects of settlement and adhesion.

Compared to laboratory assays, field tests are expensive. Facilities have to be available for application of the test coatings to panels. Static immersion is typically performed on moored rafts or from piers and requires frequent inspections and an associated infrastructure. Rafts require maintenance. Test patches may also be applied to hulls and are therefore constrained by dry docking schedules. Subsequent inspections may require divers. Field tests are also less controlled: in the natural environment, organisms interact with each other and seasonal factors (variation in fouling pressure, environmental factors) influence the development of fouling. The results of field assays may therefore vary between repeat exposures because the organisms and the environmental factors are uncontrolled (Sanchez and Yebra 2009 for a review). However, field assays are representive of the real world allowing the observation of colonisation of fouling organisms in real time and in consequence to assess the 'real' performance of the test coatings.

1.3. Fouling organisms

There are two broad classes of biofoulers, microfoulers and macrofoulers. Microfoulers are primarily bacteria and diatoms, which form a biofilm and macrofoulers are macroalgae and invertebrates such as barnacles and tubeworms. Biofouling starts within seconds/minutes after a pristine surface is immersed through the formation of a molecular "conditioning" layer

caused by the adsorption of dissolved organic materials. The surface conditioning layer will change the surface properties such as surface charge and wettability (Thome et al. 2012) and this could influence the next steps in the biofouling process. Many reviews refer to the temporal 'succession' of fouling organisms (Fig. 1.1 and (Bailey-Brock 1989; Wahl 1989; Benedetti-Cecchi 2000; Callow and Callow 2002; Anderson et al. 2003; Callow and Callow 2011)). Thus, it is often observed that the first colonisers are unicellular organisms –i.e. bacteria and diatoms that produce a biofilm or slime layer within hours. 'Secondary' and 'tertiary' colonisers are considered to include macrofoulers such as seaweeds and invertebrates respectively, the fouling by these organisms being macroscopically visible after 1-several weeks. However, as Callow and Callow (2011) have pointed out, it is important to realise that the temporal succession, as depicted in Fig. 1.1, is an over-simplification and must be viewed with caution. In particular, the apparently later stages of colonisation by macrofoulers may merely reflect the rate of development of the different types of macrofoulers towards the formation of macroscopically visible fouling (Clare et al. 1992). Therefore, for example, whilst it may take weeks before fouling by seaweeds and invertebrates becomes visible to the naked eye, in reality, the settlement stages of these organisms (e.g. spores of algae, larvae of barnacles) are able to colonise a freshly immersed surface within minutes (Roberts et al. 1991; Holm et al. 1997).

A second problem arising from the simplistic view presented in Fig. 1.1 is that it is often suggested (Abarzua and Jakubowski 1995; Yebra et al. 2004) that the succession of different fouling organisms is causally related, e.g. that macrofoulers need the presence of a biofilm to settle (Kirschner and Brennan 2012). Whilst it is true that some macrofouling invertebrates, such as the tubeworm *Hydroides elegans,* do require a biofilm for larval settlement (Lau et al. 2002; Huggett et al. 2009; Ganesan et al. 2010), equally, larvae of other invertebrates such as barnacles (Berntsson et al. 2000; Aldred et al. 2006) and spores of seaweeds such as *U. linza* can settle on a pristine, freshly immersed surface without a biofilm. In addition, where

the influence of single-species biofilms has been studied, both positive and negative effects on settlement have been reported, e.g. for spores of *U. linza* and cells of *N. incerta* (Wieczorek and Todd 1998; Patel et al. 2003; Mieszkin et al. 2012).

macrofouling

microfouling

tertiary colonizers

secondary colonizers

primary colonizers

organic film

Substrate

1 min	1 - 24 h	1 week	2 - 3 weeks
adhesion of organic particles (e.g. protein)	**bacteria** (e.g.Pseudo monas putrefaciens, Vibrio alginofyticus) **diatoms** (e.g. Achnantes brevipes, Amphiprora paludosa. Amphora coffeaeformis, Licmophora abbreviata Nifzschia pusilla)	**spores of macroalgae** (e.g. Enteromorpha intestinalis, Ulothrix zonata [Chlorophyta]) **protozoa** (e.g. Vaginicola sp., Vorticella sp., Zoolhamnium sp., [CiliataJ)	**larvae of macrofoulers** (e.g. Balanus amphitrite [Crustacea] Electra crustulenta [Bryozoa] Laomedia flexuosa [Coelenterata] Mytilus edulis [Mollusca] Spirorbis borealis [Polychaeta] Styela coriacea [Tunicata])

Figure 1.1: Simplified hypothetical temporal structure of biofouling settlement (Abarzua and Jakubowski 1995).

1.3.1. Test organisms and their systems of adhesion

In order to produce good fouling resistant paints, a diversity of fouling organisms has to be studied, especially their adhesion mechanisms (including adhesives). However, the processes of adhesion of marine fouling organisms are not well known. It is known that the capacity of fouling organisms to attach and grow on a submerged surface depends on the interactions between the adhesive and the surface (Callow and Callow 2011).

The diversity of fouling organisms differs due to numerous factors (environmental, material, chemical). It was observed that the important fouling organisms belong to algal and invertebrate groups: Algae, Mollusca, Crustacea, Bryozoa, Annelida, Tunicata, Cnidaria and Porifera. Estimations of the fouling diversity were previously compiled, in 1952 the number of

fouling species was estimated to 2000 species (WHOI 1952) while Anderson and Hunter (2000) estimated the community at over 4000 species.

Marine biofilms are composed of different species of bacteria, *Archaea* and unicellular organisms such as diatoms (Callow and Callow 2006). They are dynamic and complex systems, due to the diversity of species and their density (Qian et al. 2007; Dobretsov 2010). Moreover, biofilms are influenced by physical, chemical and biological factors (i.e. surface properties, nutrient availability, competition and predation).

The adhesion of marine bacteria and diatoms to inanimate substrates involves secretion of a glue-like compound of extracellular polymers (EPS), which is mainly polysaccharides and proteins in nature (Christensen 1989; Molino and Wetherbee 2008 for reviews). Biofilms produce chemical signals, which influence the settlement of cells, spores and larvae of other fouling organisms such as *U. linza* (Gram et al. 2002; Patel et al. 2003; Tait et al. 2005; Mieszkin et al. 2012).

The community of invertebrates is diverse and many are known to foul ships' hulls including barnacles, tunicates, hydroids and mussels. It was shown that these fouling invertebrates adhere to surfaces using different adhesives (Flammang et al. 2009; Kamino 2010; Stewart et al. 2011). The most studied hard-fouling animals are barnacles, well-known for their ability to settle on submerged structures. Due to their relatively large size, their hard calcareous shell plates and their high adhesion strength, they increase the drag of ships and can damage protective paints. The colonisation of submerged surfaces is through cyprids, which use a pair of sensory antennules to determine whether the surface is suitable for settlement (Clare and Aldred 2009 for review). The adhesion of barnacles occurs in three phases. The cyprids temporarily attach to the surface while they are exploring it using their antennules, and leave footprints that contain a settlement pheromone, which facilitates gregarious settlement. After the exploration phase when they find an adequate location, they secrete

cyprid cement to settle and then around 40 days later, the adult barnacles secrete adult cement; these cements allow the barnacles to be permanently fixed to the surface (Walker 1973).

Tubeworms produce a permanent proteinaceous cement that allows the organism to 'glue' fragments of shell and sand grains together to produce the wall of a protective tube within which the worm remains fully mobile. Hamer and Walker (2001) showed that the settlement of *Spirorbis spirorbis* can be induced by the presence of a biofilm and algae.

A quite different adhesion mechanism is shown by mussels, which attach to surfaces using elastic byssus threads. Even though the byssus threads are used for permanent attachment, the mussels can cleave them in order to change their locations and they will produce new threads at the new site (review in Wiegemann 2005). The proteins that make up the mussel byssus have been extensively characterised biochemically and the mussel adhesives inspired the production of new coatings and adhesives (Silverman and Roberto 2007 for review; Lee et al. 2011; Yu et al. 2011).

Algae are ubiquitous and colonise a wide range of structures such as buoys, ships, aquaculture nets. In order to find a solution against algal fouling, the different strategies of colonisation have to be known. Many macroalgal species contribute to marine fouling but two genera are more cited than others: *Ulva* and *Ectocarpus* (Pyefinch 1950; Terry and Picken 1986). For a number of years, the Birmingham Biofouling Group has worked with *U. linza* (syn. *Enteromorpha linza*), which is an important fouling green alga that colonises a variety of man-made structures including ships' hulls (Callow 1996). *Ulva* is a common genus found throughout the world in the upper intertidal zone. Its dispersal is achieved mainly through the release of a large number of motile, quadriflagellete zoospores (5-7 µm diameter). Callow et al. (1997) showed that colonisation of surfaces involves the transition from a free-swimming spore to an adhered non-motile spore, and the secretion of an adhesive. Spore germination

occurs within few hours; cell division and growth produce sporelings- young plants that are also firmly attached to the substratum by adhesive secreted by the rhizoids. Previous studies showed that the settlement of spores of *U. linza* is higher on hydrophobic surfaces (Callow et al. 2000), whilst adhesion strength of settled spores is strongest on a hydrophilic surface (Finlay et al. 2002).

Recent field observations by International Paint showed that some filamentous brown algae, determined as members of the Ectocarpales, are able to colonise specific types of non-biocidal, FR coatings (Fig. 1.2).

Figure 1.2: Ship's hull protected with FR/AF coating and colonised by filamentous brown algae, identify as ectocarpoid species (Photo: Callow J.A.).

1.3.2. Ectocarpales

The order Ectocarpales is in the class Phaeophyceae (brown algae), which belongs to the phylum Heterokontophyta (also named Stramenopiles) that is phylogenetically distant from the other algae (green and red algae) and the terrestrial plants that belong to the Archaeplastida (Table 1.1, (Baldauf 2003; Baldauf 2008; Silberfeld et al. 2010)).

The main studied genera are *Ectocarpus, Hincksia* and *Pilayella*. They are distributed in temperate regions worldwide, and rarely present in tropical regions. *Ectocarpus,* which is the most studied genus, is present on the seashore from high intertidal pools to the sublittoral zone and has a high range of salinity tolerance from low-salinity habitats, even a freshwater site in Australia (West and Kraft 1996), to a salt-polluted river in Germany (Geissler 1983).

Table 1.1: Phylogeny of ectocarpoid algae.

Phylum	Heterokontophyta	
Class	Phaeophyceae	
Order	Ectocarpales (Setchell et Gardner)	
Family	Ectocarpaceae (C. Agardh)	Acinetosporaceae (G. Gamel ex J. Feldmann)
Genus	*Ectocarpus*	*Hincksia* *Pylaiella*

Within the Phaeophyceae, the range of form and diversity of morphology are high such as the size and the shape of the thallus. However, within the order Ectocarpales, the morphological diversity is lower. For years, this order of brown algae was considered as archaic because of the simple morphology represented by uniseriate filaments, but recent molecular phylogenetic research shows that the family Ectocarpaceae was created by a recent divergence inside the class Phaeophyceae (Charrier et al. 2008; Phillips et al. 2008; Silberfeld et al. 2010), meaning that the Ectocarpales is closer to the family Laminariaceae that has a more complex morphology and life cycle compared to all the other families of the Phaeophyceae (such as Dictyotales, Fucales).

Members of the Ectocarpales are known to be ship-fouling algae (Pyefinch 1950; Fletcher 1980; Mineur et al. 2007) and are some of the dominant fouling algae present on fish cages for aquaculture (de Nys and Guenther 2009 for review). The genera of Ectocarpales found on ships and raft panels seem to be predominately *Ectocarpus* and *Hincksia* (Greer and Amsler 2002; Mineur et al. 2007).

There has been extensive discussion for many years on the taxonomic status of *Ectocarpus* species (Cardinal 1964; Müller and Eichenberger 1994). For example, 487 taxa of *Ectocarpus* are listed in www.algaebase.org with 75 that are currently accepted taxonomically (at 16-10-2012). Numerous strains are available at CCAP in Oban, Scotland (Gachon et al. 2007), but only 4 species are recognised by Cardinal (1964), with seven varieties of *Ectocarpus siliculosus* and three varieties of *Ectocarpus fasciculatus*. In addition, two species are listed by Coppejans and Kling (1995) with three varieties for *Ectocarpus confervoides* and one for *E. fasciculatus*. *E. siliculosus, E. fasciculatus* and *Ectocarpus crouaniorum* are recognised as the three common species present in Europe (Peters et al. 2010). One of the problems for identification is the high plasticity of the common features that are observed in order to identify species (habit, branching pattern and size of sporangia).

For experimental purposes, the Ectocarpales provide good models. They have a small size and are relatively easy to cultivate, and do not need constant care (subculturing). The life cycle for *Ectocarpus* spp. typically takes 3 months in the laboratory (Müller 1977; Charrier et al. 2008).

For this project, two genera within the Ectocarpales are most important, *Ectocarpus* and *Hincksia*. They are both uniseriate branched filamentous macroalgae and are widely distributed as fouling algae (Cardinal 1964; Fletcher 1980). Both genera have prostrate and erect filaments, but they are differentiated by a number of ramifications associated with intercalary growth and the number of pyrenoids in the chloroplast (Russell 1973 for review). The largest distinctions between the two genera are based on the chloroplast form and the position of the sporangia. Their life cycles are complex, and they produce unilocular and plurilocular sporangia and gametangia (Fig. 1.3).
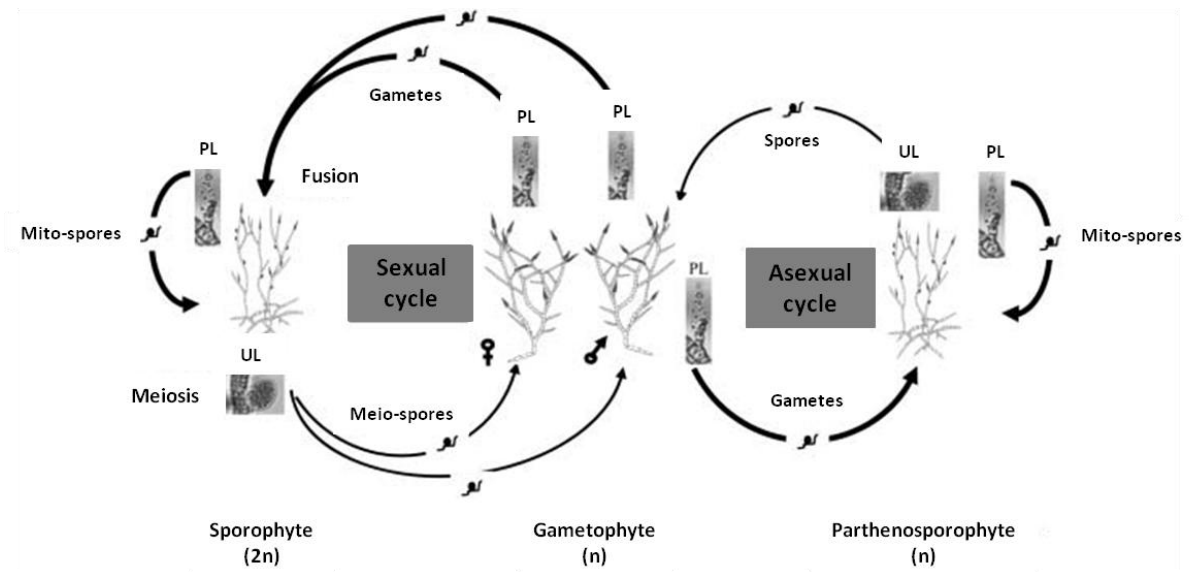
Figure 1.3: Life cycle of *E. siliculosus*. Unilocular sporangia (UL) produced by diploid sporophytes contain meiospores, which grow into male and female gametophytes. Gametophytes produce gametes in plurilocular gametangia (PL). A zygote produced by the fusion of gametes grows into a diploid sporophyte. Parthenosporophytes may grow from unfused gametes and are identical from the sporophyte. By the production of mitospores contained in plurilocular sporangia, parthenosporophytes and sporophytes can reproduce themselves asexually (Charrier et al. 2008).

Ectocarpus has a filamentous and branched thallus (Fig. 1.4a); the diploid sporophyte and haploid gametophyte are isomorphic plants. *Ectocarpus* cells contain one or several elongated plastids with different forms and several pyrenoids. Sporangia are unilocular or plurilocular; the latter being elongated and of various sizes according the species (Fig. 1.4b). The *Ectocarpus* life cycle is complex because in addition to the sporophyte and gametophyte generations, the alga can reproduce by parthenogenesis from non-fecundate gametes that produce haploid parthenosporophytes (Müller 1967). The zooids are biflagellate; zoospores measure around 6-μm length, swim from a few minutes to 24h until they settle with the secretion of adhesive materials (Baker and Evans 1973).
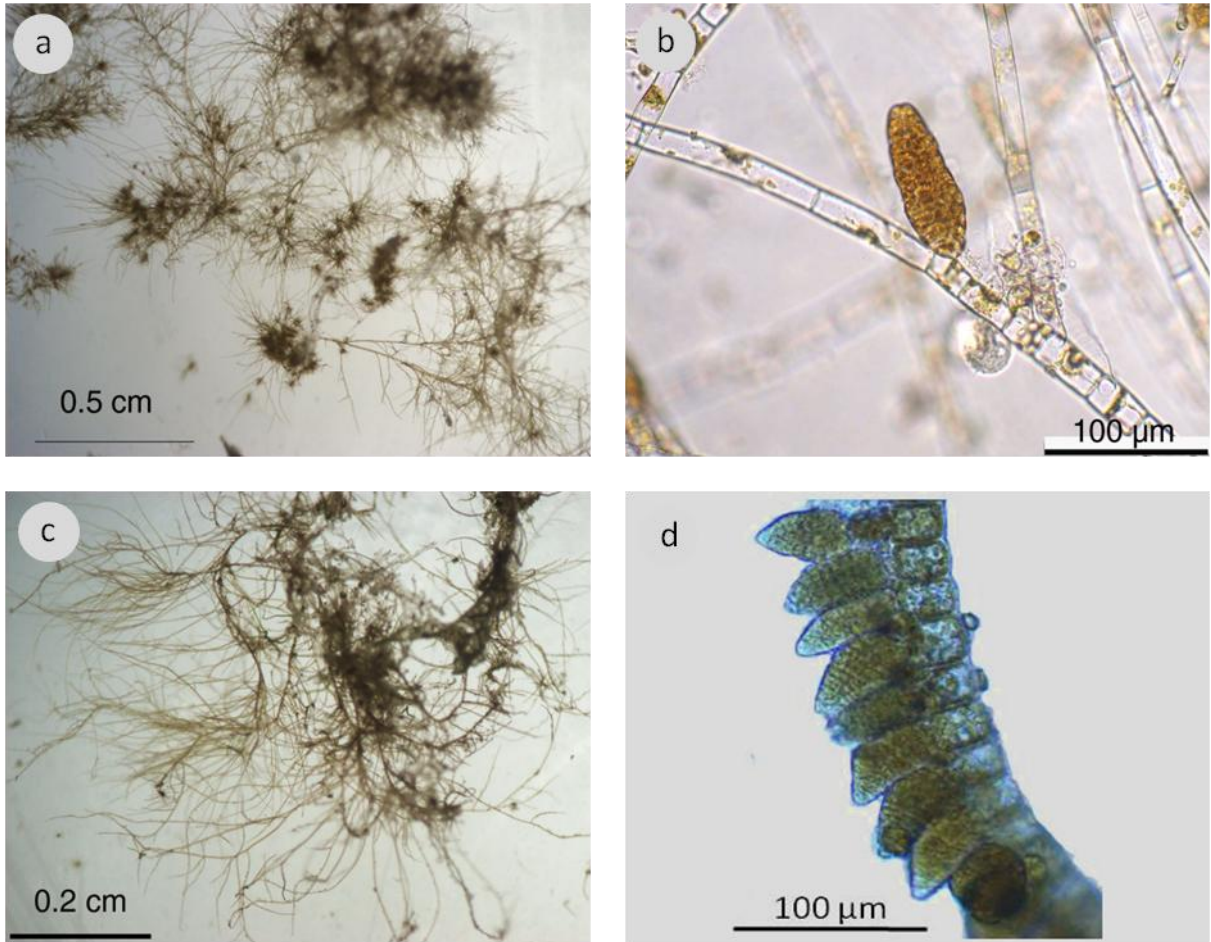
Figure 1.4: *Ectocarpus* **sp. (a and b) and** *Hincksia* **sp. (c and d) isolates from Hartlepool Marina and Newton Ferrers.** Individuals of *Ectocarpus* sp. from Hartlepool Marina (a) and a plurilocular sporangium attached to an erect filament (b). Individual of Hincksia sp. from Newton Ferrers (c) and a line of plurilocular sporangia attached to an erect filament.

Hincksia has a filamentous, haplostic and branched thallus in common with *Ectocarpus* (Fig. 1.4c); its cells contain several discoidal plastids with pyrenoids. In contrast to *Ectocarpus*, the plurilocular sporangia are globular (Fig. 1.4d).

In numerous papers, researchers explained that *Ectocarpus* sporophyte has three different structures: rhizoids, prostrate and erect filaments in contrast to the gametophyte, which has only two structures: rhizoids and upright filaments (Peters et al. 2008; Le Bail 2009). Prostrate filaments are attached to the surface, with numerous ramifications. These filaments are the basal structures of the organism; their cells contain several chloroplasts and can

have reproductive structures (Peters et al. 2004). The prostrate filaments have round cells around the spore and cells on the periphery are more cylindrical, elongated shape (Fig. 1.5; Peters personal observations).
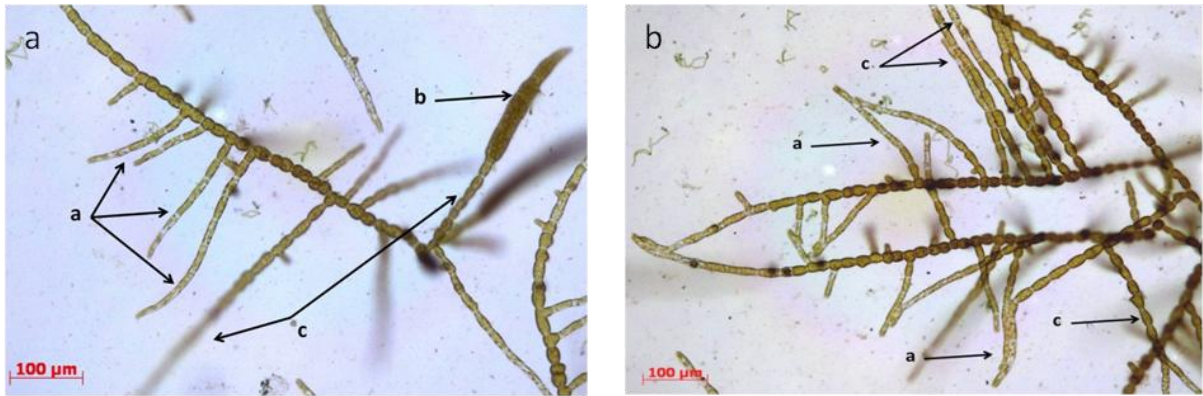
Figure 1.5: Different structures of *Ectocarpus sp.* Prostrate filaments (a), sporangium (b) and erect filaments (c).

Rhizoids are root-like filaments consisting of narrow cells (3-5 μm), which have a wavy-appearance and are produced only by upright filaments (Peters et al. 2008). They do not have reproductive structures. *E. crouaniorum* may not have any rhizoids as it has not been recorded in papers and was not observed (Peters personal comments). Erect filaments that are created from prostrate filaments have low levels of ramification and have reproductive structures (Le Bail 2009). Cell diameters are from 10 to 40 μm (Peters et al. 2008).

Ectocarpoid species are also interesting as fouling organisms because studies have shown that *Ectocarpus* is tolerant to copper, which is a major component in many AF paints (Russell and Morris 1970; Hall et al. 1979; Hall 1980; Hall and Baker 1985; Hall and Baker 1986).

Some studies have shown that spore and individual behaviour among members of Ectocarpales varies according to surface properties. Settlement of spores of *Hincksia irregularis* is promoted by a hydrophobic surface and a dark environment (Greer and Amsler

2002). However, Greer and Amsler (2004) showed that the settlement of spores of *H. irregularis* could vary according to the ecological fitness of the individuals and their habitat within the marine environment. Anecdotal observations suggest that the sporophyte of *E. siliculosus* adheres more strongly to both glass (hydrophilic) and polystyrene (hydrophobic) than the gametophyte (Peters et al. 2008). The spores are strongly resistant to AF paint toxins such as copper (Hall and Baker 1985 and 1986) and the preference of surfaces for spores to settle varies according the species. It was shown that zoospores of *Ectocarpus* spp*.* (certainly *E. siliculosus*) have no preference for settlement on surfaces of different textures (Baker 1971 cited in Fletcher and Callow 1992) whilst Linskens (1966 cited in Fletcher and Callow 1992) showed that *E. siliculosus* prefers a rough surface to adhere and *E. fasciculatus* prefers smooth surfaces*.* However, most of these earlier reports on adhesion preferences must be treated with caution since they do not represent systematic, well-controlled studies.

1.4.   Aims and objectives of the project

1.4.1. Aims

Much effort has been expended by the Birmingham group to explore the relationship between coating parameters such as wettability and roughness and the settlement of spores of *U. linza* and the adhesion strength of the attached spores and sporelings. Whilst *U. linza* has provided a very good model system for such studies, recent field observations by International Paint showed that ectocarpoid species are becoming increasingly important as colonisers of the more recent generation of commercial non-biocidal coatings and therefore there is merit in studying the surface preferences of this species. The overall aim of this project, therefore, was to develop laboratory scale fouling bioassays for ectocarpoid algae, and then to apply these to understand more about the adhesion characteristics of these algae in relation to the physico-chemical parameters of coatings.

1.4.2. Objective 1: Acquire isolates of a range of ectocarpoid algae and culture these on a large scale

For this project, specific strains of *Ectocarpus* and *Hincksia* species were therefore cultured, axenically or non-axenically in the laboratory; these cultures were from field collections and from the culture collection of SAMS (Scottish Association for Marine Science, Oban, Scotland). From these cultures, quantification of biomass (filaments) was used to test the AF/ FR properties of various model and practical coating types. Three cultures of *Ectocarpus* were obtained from Dr. C. Gachon (SAMS): *E. siliculosus CCAP 1310/4* from Peru, *E. siliculosus CCAP 1310/56* from New Zealand, *E. crouaniorum CCAP 1310/300* from Oban (Scotland). The taxonomic status of *E. crouaniorum CCAP 1310/300* has only recently been defined (Gachon et al. 2009; Peters et al. 2010). These three species were selected because they grow quickly, are easy to cultivate, they produce numerous sporangia and they appeared to stick to surfaces -i.e. the culture flasks in which they grow (Gachon, pers. comm.). Isolates of species of *Ectocarpus* and *Hincksia* were also cultured from FR coatings on raft panels at the International Paint laboratory in Newton Ferrers and on boats moored in Hartlepool Marina.

1.4.3. Objective 2: Development of a reproducible laboratory bioassay for the attachment and adhesion of ectocarpoid algae to test surfaces

In the case of laboratory bioassays to assess the performance of novel coatings with *U. linza,* the standard approach is based on the settlement of zoospores released from plants collected from the wild. The experimental design for such evaluations typically requires a high density of synchronously-released spores (typically 1×10^6 ml^{-1}) in large volumes (up to 1 l). The settled spores are then counted as a measure of initial surface colonisation. The spores are then allowed to develop into sporelings for 6-7 days before assessing their adhesion strength using either a water channel or a water jet. At the start of this project, it was realised that this approach was not feasible for *Ectocarpus* spp*.* Therefore, a different approach was adopted using cultured alga as a source of inoculum, the intention being to

'seed' test coatings on glass microscope slides with fragments of cultured filaments obtained by blending. The expectation was that adhered fragments would grow and divide, colonising the surfaces. The adhesion strength of the attached alga could then be assessed by either of the hydrodynamic methods mentioned above.

1.4.4. Objective 3: Prepare or acquire test coatings and apply the novel bioassay to these test coatings

To clarify the kind of surfaces that ectocarpoid species prefer to settle on and which surfaces promote adhesion, experiments employing coatings, which have been characterised in terms of those surface and bulk properties known to influence fouling organisms, are required. A significant proportion of the project has therefore involved the preparation and characterisation of test coatings at International Paint (Gateshead). Within the different series of coatings tested, a series of silicone coatings with a range of wettabilities was also used to explore the influence of immersion on the surface wettability of coatings under laboratory and field conditions.

1.4.5. Objective 4: Compare the results obtained using the novel bioassay with the results from field assays and the adhesion strength of *U. linza*

While laboratory bioassays under precisely controlled conditions provide valuable information on the preferences of fouling organisms, and the intrinsic performance of test coatings, such assays may not predict performance in the field. A series of field experiments was therefore carried out using test panels placed under static immersion at Hartlepool Marina and at the International Paint laboratory in Newton Ferrers, Devon. In 2010, a set of coatings based on PDMS with varying moduli (and wettabilities) and on fluoropolymers with varying moduli (and wettabilities) were immersed for 4 months. In 2011, a series of silicone-based coatings with varying wettability/surface energy were immersed for 5 months. In 2012, a set of coatings based on different molecular weight of silicone, which gave a small range of moduli was

immersed for almost three months. In addition, the adhesion strength of *U. linza* was compared with the adhesion strength of ectocarpoid algae on the different test coatings.

2. GENERAL MATERIALS AND METHODS

2.1. Unialgal cultures from the field

Ectocarpoid algae were collected from boats moored in Hartlepool Marina (54°69'N; 1°20'E, Fig. 2.1 and 1.2) and from panels on rafts moored in the Yealm estuary at Newton Ferrers (50°31'N; 4°05'W, Fig. 2.1) in order to identify the genera of fouling organisms and to obtain wild cultures. Isolates were placed in Petri dishes with ½-strength enriched Provasoli medium (hereafter referred to as "Provasoli medium", Appendix 1) in order to keep them in good condition until selection. The selection of algae was made in the laboratory within a few days after the collection; only the uniseriate, filamentous ectocarpoid algae were kept.

Figure 2.1: Map of the two locations (represented by the yellow stars), Hartlepool Marina and Newton Ferrers where ectocarpoid algae were collected (from Google map).

To obtain uni-algal cultures, small tufts of filaments were transferred to Petri dishes with artificial seawater (ASW, 33.3ppt, pH=8.2, Tropic Marin®). Using surgical scissors, filaments

were cut into 5-10 cell fragments under a binocular microscope (magnification x10). Filaments that appeared to be uncontaminated with epiphytes and with a characteristic morphology and colour were transferred to 24-well plates with Provasoli medium. In the natural environment, algae, diatoms and bacteria co-inhabit, but in culture, diatoms can be invasive. In order to eliminate them, all the cultures were treated with germanium dioxide (GeO_2), following the method in Shea and Chopin (2007). The cultures were inoculated with a GeO_2 solution (0.05% in ASW) for 10 days before changing the medium. After treatment with GeO_2, the culture medium was changed every 2 weeks for 2 months, then every 2-3 months in order to obtain a larger quantity of algae. An initial culture bank of 100 ectocarpoid isolates was maintained in this way. All isolates with typical morphology and colour were observed microscopically (transmitted light and fluorescence) in order to identify the genus (and species, if possible), using the criteria outlined in Table 2.1. Initially two genera of Ectocarpales were identified as being present: *Hincksia* (30 cultures) and *Ectocarpus* (70 cultures); no *Pilayella* was collected. After 18 months, this initial bank was reduced to 8 isolates (5 of *Hincksia* and 3 of *Ectocarpus*) by removing obvious duplicates, keeping only those cultures that looked healthy. Some isolates also died due to overgrowth by bacteria and green algae.

Table 2.1: Different features of the three most represented genera of ectocarpoid algae: *Hincksia, Ectocarpus* and *Pilayella* (Coppejans and Kling 1995).

Genus	Chloroplast	Zoïdocyst
Hincksia sp.	Round	Lateral/terminal
Ectocarpus sp.	Elongated	Lateral/terminal
Pilayella sp.	Round	Intercalary

2.2. The selection of cultures from CCAP

Cultures of three different *Ectocarpus* spp. were obtained from the Culture Collection for Algae and Protozoa (CCAP, Dunstaffnage, Oban, Scotland): *Ectocarpus crouaniorum* CCAP 1310/300; *Ectocarpus siliculosus* CCAP 1310/4 and *E. siliculosus* CCAP 1310/56. Both axenic and non-axenic cultures were provided.

Preliminary observations showed that both isolates of *E. siliculosus* adhered less well to standard surfaces (glass, Silastic® T2, Intersleek® 700 (IS700) and Intersleek® 900 (IS900)) than *E. crouaniorum*. Therefore, it was decided to use *E. crouaniorum* CCAP 1310/300 for the studies reported in this thesis.

E. crouaniorum CCAP 1310/300 is a diploid sporophyte that was isolated and transferred into culture in 2006. The individual plants measure less than 3 cm in nature and up to 2 cm in the laboratory (Fig. 2.2).
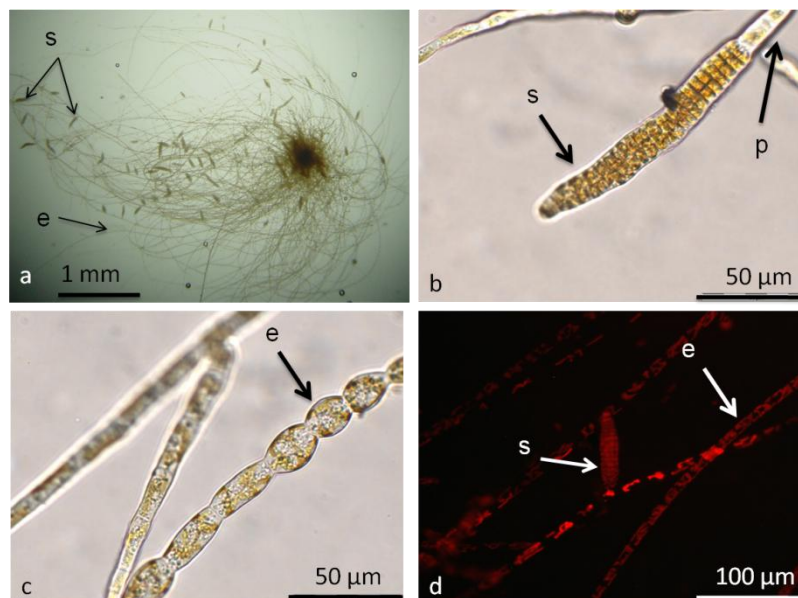
Figure 2.2: *E. crouaniorum CCAP 1310/300*. a) Individual with filaments of 7 mm length with erect filaments (e) and sporangia (s); b) Plurilocular sporangium (s) with peduncle (p); c) Erect filaments (e) with ribbon-shaped chloroplasts and d) Autofluorescent chloroplasts in cells of erect filaments (e) and plurilocular sporangium (s) observed by UV fluorescence microscopy ($300\text{-}390 \text{ nm}_{ex}\text{-}420 \text{ nm}_{em}$).

2.3. Culture methods

Wild isolates and *E. crouaniorum* were maintained in unialgal cultures in 650 ml flasks (Cellstar filter cap suspension culture flask, Greiner Bio-One) containing 200 ml of Provasoli medium (Starr and Zeikus 1987) prepared using autoclaved ASW. Cultures were grown statically, without aeration at 15°C with a 12:12 h light:dark cycle (light intensity 20 μE m^{-2} s^{-1}) and subcultured every 2-3 months.

2.4. Growth rate and morphology of axenic and non-axenic cultures

A pilot experiment was conducted to observe the variation of biomass and morphology between axenic and non-axenic cultures of *E. crouaniorum* in order to decide which type of culture would be used for subsequent assays.

All the preparations for the experiment were performed in a sterile culture cabinet. Approximately 1 g wet biomass was transferred into 300 ml of Provasoli medium prepared using autoclaved ASW and was kept on a stirrer prior to transferring aliquots (5 ml) into 70 ml sterile flasks to which 10 ml of Provasoli medium were added. Twenty-five replicates for each treatment were made, including five for initial measurement of biomass. In order to quantify the algal biomass used to inoculate the test samples, chlorophyll *a* (chl *a)* was measured (Chapter 2.5). Every three weeks for 12 weeks, the algal biomass of five replicates of each treatment was measured by chl *a* extraction. At the same time, the medium was changed for all the other flasks using a nylon cell strainer filter (mesh size 100 μm, BD Falcon) to retain all the filaments. Every three days throughout the experiment, the flasks were randomly placed in the incubator so all flasks received the same degree of illumination.

No difference in growth rate was observed as represented by the slopes of the lines in Fig. 2.3, until the final harvest when there was a substantial increase biomass in the non-axenic cultures. Observations of morphology showed that in the axenic cultures, the organisms grew as tufts of small filaments (around 2 mm of length) whereas in the non-axenic cultures the

organisms grew as larger tufts with filaments measuring at least 7 mm in length (Fig. 2.4). The morphology of plants in the non-axenic cultures was more representative of *Ectocarpus* spp. in the natural environment.
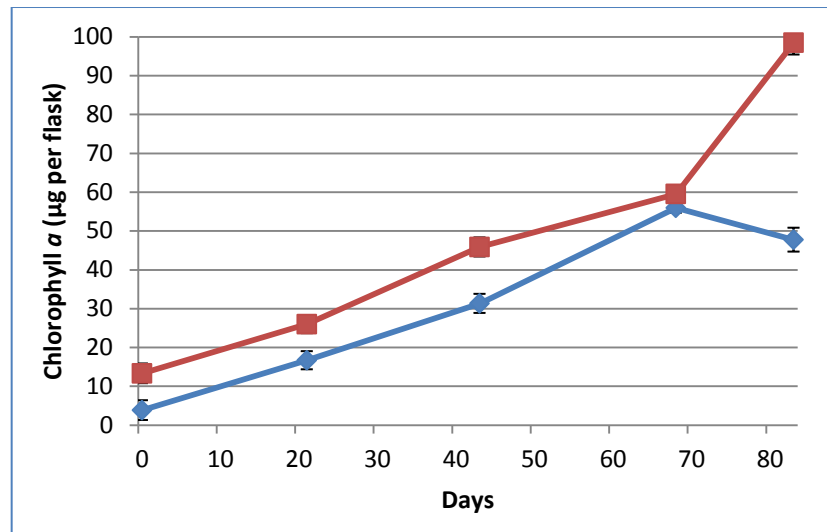
Figure 2.3: Biomass of *E. crouaniorum* measured as chl *a* for 83 days of culture. Axenic and non-axenic cultures are respectively represented by the blue and the red lines. Means of 5 replicates ± 2 x SE.
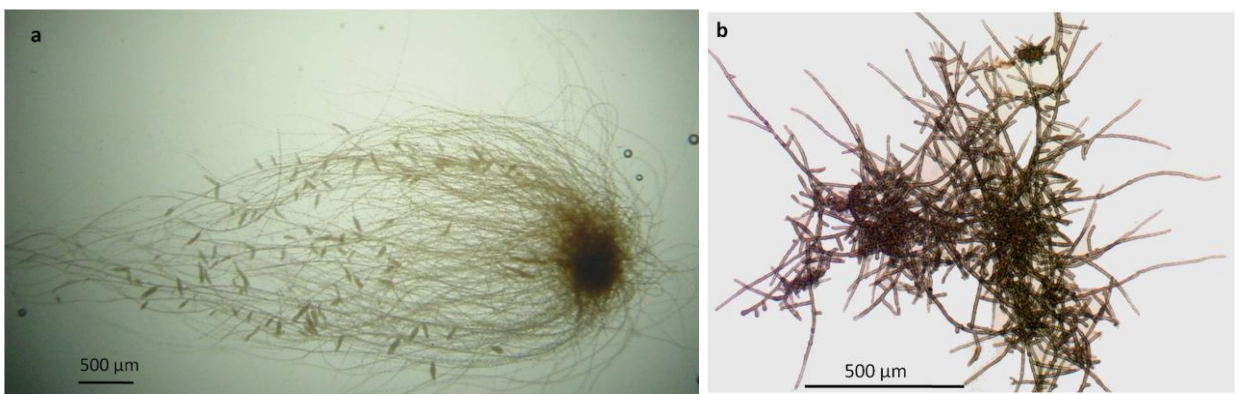
Figure 2.4: Variation of morphology between non-axenic (a) and axenic (b) cultures of *E. crouaniorum*. The different sizes of the plants under the two conditions necessitated the use of different magnifications.

In conclusion, variations of the growth and the morphology between axenic and non-axenic cultures were observed. Previous studies showed that the typical growth form of *Ulva linza* is

dependent on bacteria and some bacteria stimulate the settlement of spores (Provasoli and Pintner 1980; Dobretsov and Qian 2002; Marshall et al. 2006). Amin et al. (2009) showed there are beneficial interactions between marine bacteria and phytoplankton. The study indicated that subsequent experiments should be performed with non-axenic cultures because the morphology was more typical of field organisms. Therefore, in the experiments described in the rest of this thesis, only non-axenic cultures were used.

2.5. Biomass determination by extraction of chlorophyll *a*

The biomass of filaments in the filtrate used as the inoculum was quantified as chl *a* content. Three 15 ml replicate samples of filaments were harvested onto 3 μm cellulose nitrate filters, then chl *a* was extracted with 2 ml of DMSO (Shoaf and Lium 1976). The filaments were left in DMSO for 10 min in the dark after which absorbance at 664 nm and 630 nm was measured, using DMSO as reference. The chl *a* concentration in the filtrate was calculated using the formula for diatoms (Jeffrey and Humphrey 1975), where SV is the volume of DMSO and MV is the volume of ASW containing the filaments.

Chl *a* (μg ml^{-1} of starting inoculum) = $(11.47(A_{664}) - 0.4(A_{630}))$ * (SV/MV)

The concentration of filaments in the inoculum (as chl *a*) was then adjusted to 0.04 to 0.12 μg ml^{-1} of chl *a*, depending on the species (Chapter 3.2.1).

For the determination of biomass of unattached filaments in the developed adhesion assay (Chapter 3.2.3), chl *a* was determined by the same method using the following formula:

Chl *a* (μg) = $(11.47(A_{664}) - 0.4(A_{630}))$ * (SV)

2.6. Testing of adhesion strength using a calibrated water channel

Since fouling-release (FR) coatings do not prevent settlement, a water channel apparatus is one of the methods used to quantify the adhesion strength of fouling organisms such as

algae (Schultz et al. 2000). The apparatus provides a rapid, repeatable test for determining the shear stress necessary to remove the test organisms from a range of test surfaces (Fig. 2.5). The water channel was designed to provide fully turbulent flow and is thus a good indicator of the conditions necessary for detachment of these organisms from the ship's hull because boundary layers around ships are turbulent (Schultz et al. 2003). The fully-developed channel flow allows determination of accurate wall shear stress from a simple pressure gradient measurement. Turbulent flow is created in a 60 cm long low aspect ratio test section of channel preceding the slides. The shear stress in the test section can vary from 8 Pa to 50 Pa generated by a flow of ASW up to 4.9 m s^{-1}. Six individual microscope slides can be tested for each run. The explanation of how the apparatus was used to generate adhesion strength data is outlined in Chapters 2.7 and 3.2.4.

Using the formulae from Schultz et al. (2003), the shear stress of 50 Pa represents a ship velocity of 9.1 m s^{-1} (17.7 knots or 20.5 mph) at downstream distance of 50 m while the shear stress of 8 Pa represents a ship velocity of 3.6 m s^{-1} (7 knots or 8 mph) at the same downstream distance.

The term 'adhesion strength' of soft-fouling organisms such as algae refers to the ease of removal (i.e. % removal) after exposure to a shear stress, while for hard-fouling organisms such as barnacles and tubeworms, the adhesion strength is measured by the application of a mechanical shear force parallel to the base of the organisms to measure the critical removal stress (Swain and Schultz 1996; Kavanagh et al. 2001).
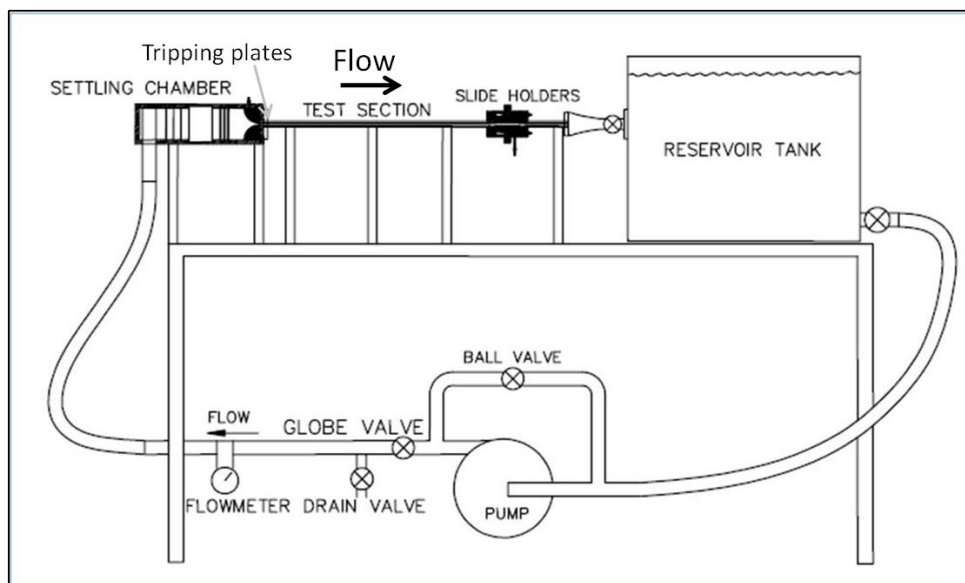
Figure 2.5: Representative layout of the water channel system (from Schultz et al. (2000)). The pumped flow of ASW from the 265-liter tank enters the settling chamber, which creates the turbulent flow. The turbulent flow enters 'tripping plates' (0.5 mm in height) at the start of the test section, which ensures that the flow is fully developed and turbulent. The mounting apparatus for the test slides is downstream of the tripping plates. The slide holders can accommodate six slides (three at the top and three at the bottom), which are arranged with their long axes parallel to the direction of the flow. Each mounting position has a mechanism to enable correct alignment of each slide flush with the channel walls and for differences in coating thickness to be accommodated. The test slides are held in place by a vacuum applied to the reverse (non-test) side of each slide, which is lightly greased with silicone grease.

2.7.   Measurement of biomass using a fluorescent plate reader

Before using the water channel, the attached biomass on each test slide was quantified, non-destructively, by measuring the fluorescence of chlorophyll in a fluorescence plate reader (excitation = 430 nm, emission = 670 nm, TECAN GeniosPlus) (Finlay et al. 2008). Fluorescence was measured as relative fluorescence units (RFU). The RFU value for each slide was the mean of 168-point fluorescence readings, taken within an area 6 x 1.9 cm along the central longitudinal axis of the slide. Uninoculated test surfaces that had been hydrated in ASW were used to blank the plate reader. There was a linear correlation

(R^2=0.85) between the attached biomass measured using by chlorophyll fluorescence in the plate reader and biomass determined by chl *a* extraction (Fig. 2.6).
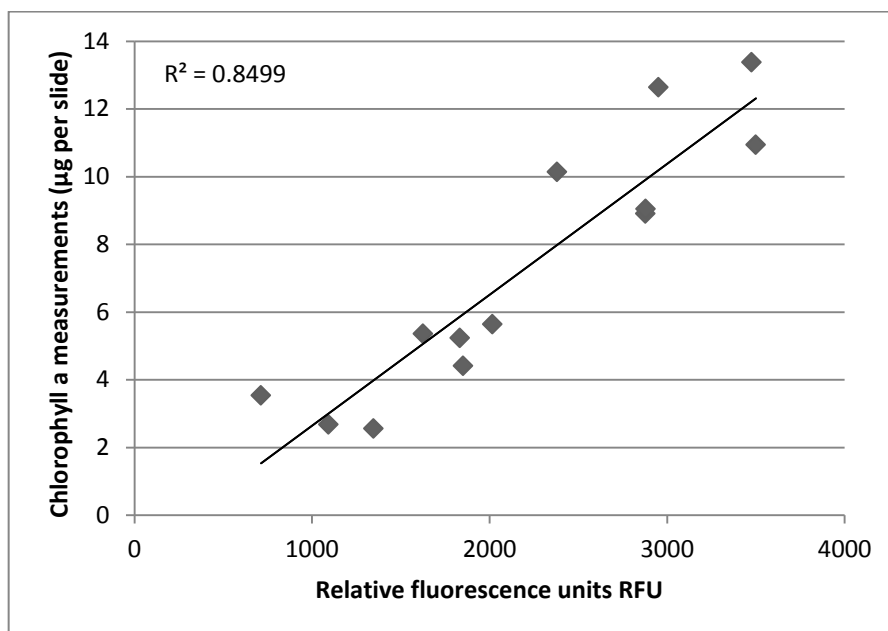
Figure 2.6: Relationship between chl *a* measured by chlorophyll extraction and in situ fluorescence in the TECAN fluorescent plate reader. The attached biomass (13-replicate slides) was measured using the plate reader and then the filaments were removed from each slide using a cell scraper and were placed in 10 millilitres of ASW before measuring chl *a* content using the method in Chapter 2.5.

2.8. Adhesion assays with sporelings of the green alga *Ulva linza*

In order to put results for ectocarpoid algae into a broader fouling context, adhesion assays on test surfaces were also performed with the green alga *U. linza* (syn. *Enteromorpha linza*), which is used extensively by the Birmingham group as a model macrofouling test organism. Fronds of *U. linza* were collected from Llantwit Major, Wales (51°40'N; 3°48'W) and a suspension of zoospores (1.0 x 10^6 spores ml^{-1}) was prepared by the following method (Cooper et al. 2011). The collected fronds were brought back to the laboratory and kept overnight at 5°C. The following day, the reproductive tips were cut and transferred to a beaker with sufficient ASW to cover the plants for 5-10 min. As soon as spores were

released, the medium was filtered into a clean beaker using three layers of nylon mesh of decreasing pore size (100 µm (top), 50 µm and 20 µm (bottom)). The meshes removed any debris such as sand grains and diatoms. The beaker containing the spore suspension was then placed in crushed ice to concentrate the spores, which swam towards the bottom of the beaker, while gametes and dead spores stayed at the ASW surface. The concentrated spore suspension was pipetted into another beaker placed in crushed ice in order to concentrate the spores again before transferring the suspension to a final beaker. The final concentrated spore suspension was diluted with ASW to obtain an absorbance of 0.15 at 660 nm, which is equivalent to 1.0×10^6 spores ml^{-1} (Callow ME personal communication). Spores were kept in the dark by wrapping the vessel with aluminium foil and placed on a magnetic stirrer to prevent settlement.

For bioassay of test surfaces, six replicate slides of each treatment were placed in Quadriperm dishes (Greiner Bio-One) and 10 ml of zoospore suspension were added to each compartment. After 45 min in darkness, the Quadriperm dishes that contained the slides were gently rinsed in ASW to remove unsettled (swimming) spores. The spores that attached to the surfaces were cultured as sporelings in supplemented ASW medium in an illuminated incubator at 18°C with a 16h:8h light:dark cycle, for six to seven days. The culture medium (Appendix 2) (Starr and Zeikus 1987) was changed every two days. Sporeling biomass was measured *in situ* by measuring the fluorescence of chlorophyll *a* in a fluorescence plate reader, as described in Chapter 2.7.

2.9. Characterisation of bulk and surface properties of test coatings

2.9.1. Wettability and surface energy

Measurement of contact angle θ, especially the static water contact angle formed by a droplet of water, in air, is the most widely used method to describe the wetting properties of a surface. Low values of θ indicate a strong interaction between liquid and solid, in which the

liquid spreads over (i.e. 'wets') the solid surface, while high values of θ indicate a weak interaction and low wetting. Contact angle measurements using a minimum of two liquids with different, known surface tensions are used to calculate surface energy and its polar and dispersive components.
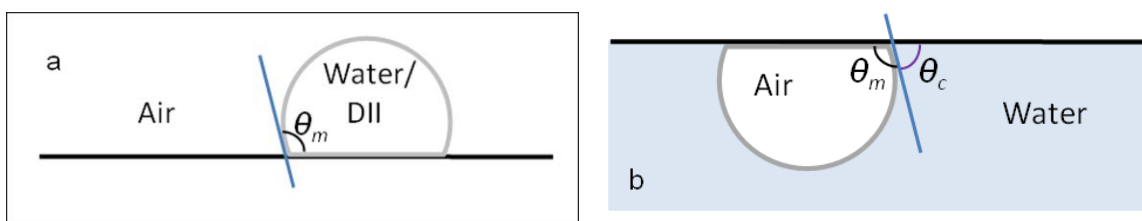
Figure 2.7: Representative layout of the method to measure wettability in air (a) and in water (b) on a test surface. For both methods, in this thesis the internal angle θ_m was measured. For some purposes for the underwater method, the external angle θ_c is then calculated (180 - θ_m). DII: diiodomethane.

2.9.1.1. Wettability in air

The contact angle is the angle at which a liquid interface meets the solid surface, allowing interaction between the liquid and the surface to be determined (Fig. 2.7a). Static contact angles of the test surfaces for water and diiodomethane (five drops on each of three-replicate slides) were measured in the laboratories of International Paint using a Dataphysics instrument and Sca20 software. Diiodomethane (syn. methylene iodide) was chosen because it is non-polar due to its molecular symmetry, compared to water, which is well known as a polar solvent. It is important to use polar and non-polar liquids in order to calculate surface energy and its components (Chapter 2.9.1.3). The drop size was 3.5 µl for the water and 1.8 µl for the diiodomethane. After a drop of test liquid is placed on a surface, there is a strong relaxation of the drop shape before it becomes stable. The best moment to measure the contact angle is therefore after the relaxation of the drop. In order to determine this, relaxation curves for the two test liquids were compared on different surfaces (IS700,

IS900 and the first series of silicone elastomer coatings). As a result, relaxation measurement times of 140 s for water and 60 s for diiodomethane were chosen since by these times the drops on each surface were stable.

While the measurement of static contact angles in air is the most common method to characterise surface wettability, additional information can be obtained by 'dynamic contact angle analysis' and this was applied to the silicone 'hybrid' coatings (see Chapter 4.2). The same instrument and software was used as the static contact angle method. A 3.5 µl water drop was provided by a micro-syringe on the slide. The dynamic contact angle was then continuously recorded after a relaxation time of 140 s. Further water was added continuously (15 µl at 0.25 µl s^{-1}), and after 60 s of delay time the same amount of water (15 µl) was removed from the drop at the same rate (Fig. 2.8a). The video acquisition rate was 10 frames per second. A graph was produced for each drop showing the contact angle as a function of diameter of the drop (Fig. 2.8b). The advancing angle θ_{Wadv} was measured when the water was added and the contact angle was relatively stable. The receding angle θ_{Wrec} on the other hand was measured when the water was removed and the contact angle was relatively stable. The difference between these two angles is the contact angle hysteresis that is thought to be a measure of roughness and surface heterogeneity (Good and Koo 1979; Schwartz and Garoff 1985).
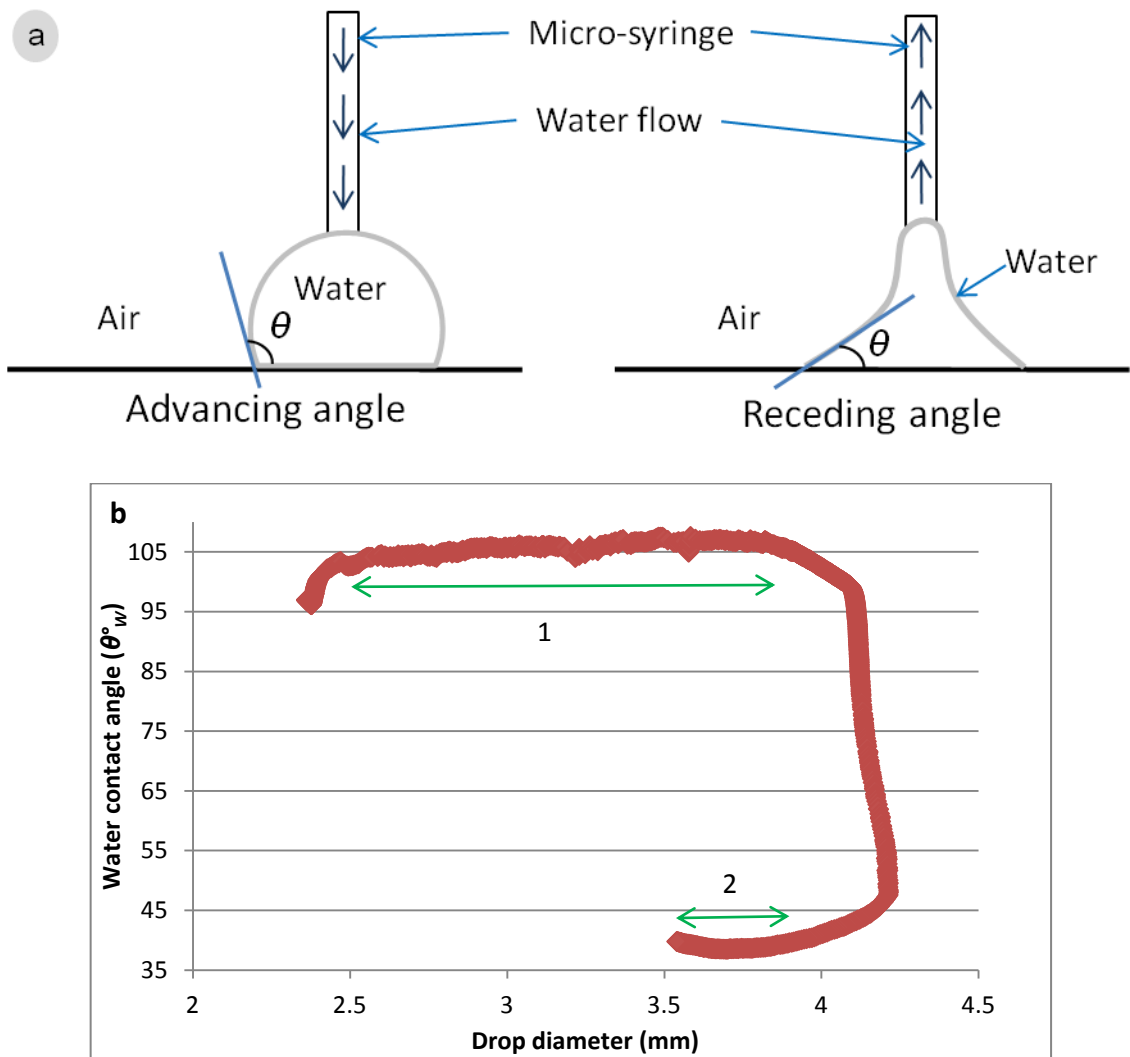
Figure 2.8: Dynamic technique (advancing and receding contact angles). a) Advancing and receding angle layouts; b) Tracking of the dynamic water contact angle as a function of the drop diameter. The means of all the contact angles within the arrows 1 and 2 represent respectively the advancing and receding contact angle.

2.9.1.2. Underwater wettability

While measurement of either static or dynamic contact angles in air is the most commonly used method to characterise the surface wettability of test coatings, further information can be obtained by measuring the contact angle of an air bubble, underwater, i.e. when coatings are hydrated by immersion in MilliQ water or ASW (Figs. 2.9a/b). It is argued that this provides a better measure of the wettability properties of a coating as perceived by a fouling

organism. Underwater contact angles were measured using a Dataphysics instrument and Sca20 software. Surfaces were immersed in a Dataphysics GC20 glass cell filled with MilliQ water and then the air bubble was created using a Dataphysics SNC 052/026 dosing needle (stainless steel) as shown on Figure 2.9. For each slide, static underwater contact angle, which was the internal angle ('air-side'; Fig. 2.7b), was measured for three bubbles of 2 µl of air. The measurements were taken after 10 s, to allow for relaxation of the air bubble. However, the values reported in this thesis are for the external angle ('water-side'; i.e. 180°-θ_m) in order to provide consistency of terminology. In this way, a hydrophobic coating, for example is always associated with a high contact angle, irrespective of whether the contact angle is determined in air, or underwater.
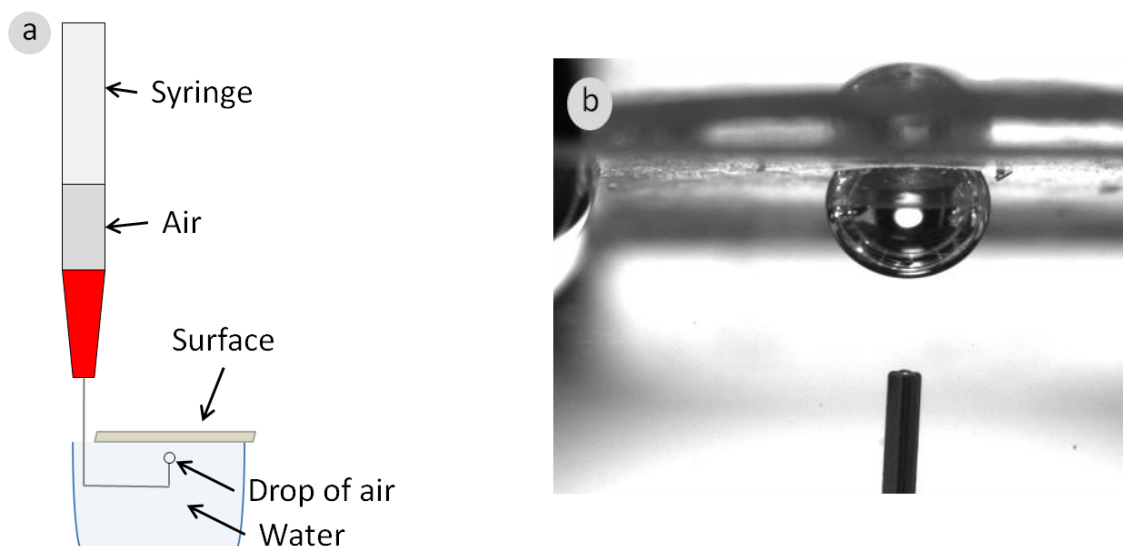
Figure 2.9: Underwater system. a) Syringe system with the needle that deposed the air bubble into the surface; b) End of the syringe where the bubble exited and an air bubble attached to the surface.

2.9.1.3.   Surface energy

A surface parameter that is often linked to surface wettability is the 'surface energy'. Surface energy is defined as the excess energy at the surface of material compared to the bulk and is a measure of the capacity of a surface to interact spontaneously, using the excess energy,

with other materials. In this thesis, total surface energy and the proportions of polar and dispersive components were determined from measuring static contact angles with two liquids (water and diiodomethane as explained above) and the Owens, Wendt, Rabel and Kaelble (OWRK) equation. This is an equation commonly used in the literature for experimental FR coatings and is the standard method employed within International Paint. When a surface has a high polar component, then the coating allows interactions with water, whereas when the coating has a high dispersive, non-polar fraction, the coating has less interaction with water (Owens and Wendt 1969).

OWRK equation is: $$(1+ \cos(\theta))^*\gamma_L = 2 \sqrt{(\gamma_S^D * \gamma_L^D)} + 2\sqrt{(\gamma_S^P * \gamma_L^P)}$$

Where θ is the angle measured (with water or diiodomethane); γ_L is the surface tension of the liquid (water or diiodomethane), which is split up into a polar γ_L^P and a dispersive fraction γ_L^D and γ_S is the surface energy of the solid (i.e. test surface), which is also split up into a polar γ_S^P and a dispersive component γ_S^D.

Two liquids are needed due to the two unknown values on the equation (the polar and dispersive component for the surface). By choosing a second liquid, which has no polar component (i.e. diiodomethane), the equation used for the second liquid (diiodomethane used as DII in the following formulae) is simplified, giving:

$$(1+ \cos(\theta))^*\gamma_L = 2 \sqrt{(\gamma_S^D * \gamma_L^D)}$$

because diiodomethane has no polar component.

2.9.2. Modulus

The modulus is the tendency of a material such as a coating to be deformed elastically (but not permanently) when a force is applied to it. Two types of modulus were measured: the storage modulus using the dynamic mechanical analyser (DMA) and the elastic modulus

using an elongation measurement method. The first method was used at the start of the project but after further discussion, it was realised that the elongation measurement method would be more meaningful for this project, as in FR studies, the elastic modulus is more studied than the storage modulus.

2.9.2.1. Dynamic mechanical analyser DMA

DMA (Perkin Elmer Pyris Diamond Dynamic Mechanical Analyser) is a thermoanalytical technique whereby a small deformation is applied to a sample in a cyclic manner and allows the materials to respond to stress, temperature, frequency and other tested factors. It characterises the viscoelastic behaviour of a coating, allowing the measurement of storage modulus (E') and Tan Delta (Fig. 2.10). E' is a measure of the stiffness of the coating. If the coating has a high storage modulus, it is a stiff material. Tan Delta is an indicator of the viscoelasticity of a sample but is also used to assign the glass transition temperature (Tg), which is represented by the peak in Tan Delta. Tg is the temperature at which an amorphous material transitions from a hard, brittle glass state to a rubbery state (Fig. 2.10). The smaller the Tan Delta, the more viscous the material is. On the other hand, the higher the Tan Delta value, the more elastic the material is (Perkin Elmer 2008).

DMA method was used on the condensation-cured silicone elastomer coatings with PDMS or PDMS/PEO (S1, S2 and S3, see Chapters 4 and 5) and the fluoropolymer coatings (Chapter 6). For each coating, the measurements were done using a thick layer of coating (2 replicates) cut in a rectangular shape (approximately 20 mm by 8 mm and 3 mm thick), which was placed in the instrument. The DMA instrument applied a sinusoidal deformation at a range of temperatures (from -130°C to 55°C) with a heating rate of 2-3°C min^{-1}.
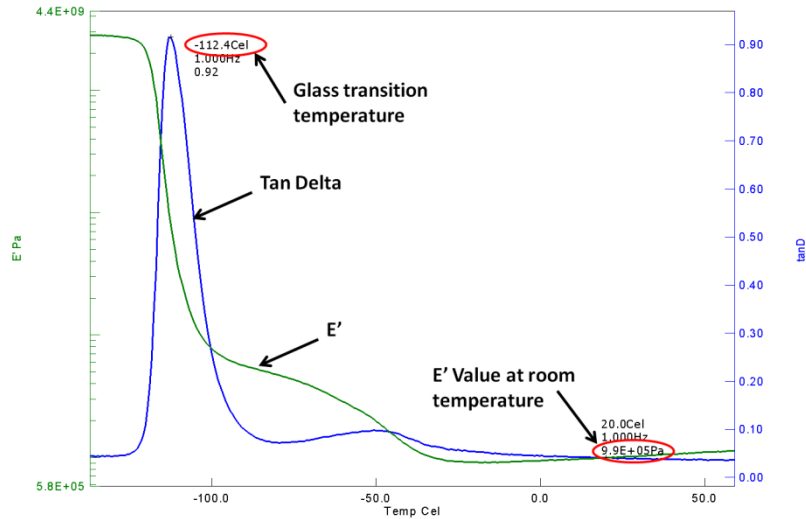
Figure 2.10: Results from a DMA analysis of S3 coating. The peak of blue Tan Delta curve represents Tg, the glass transition temperature. The green curve represents the storage modulus E', which is the stiffness of the coating. The value used is the data obtained at room temperature (red circle).

2.9.2.2. Elastic modulus

The modulus was measured using an elongation measurement method: laser extensometer, which is used to measure changes in the length of the coating (using Zwick Tensile Test Machine and Free Film Tensile v3-vi Front Panel software). It also allows the measurement of different parameters associated with the modulus. The instrument performed stress/strain measurements of thin layer of coating around 0.6 mm thick (3 replicates), the data were then transmitted to Free Film Tensile v3-vi Front Panel software. The thin layers of coating were cut in rectangular shapes (approximately 80 mm by 12 mm) and marked. The distance between these markers was tracked in the data file on the computer while the thin layer was stretched. The loading speed was 50 mm min^{-1}; the width and the thickness were measured for each replicate before the experiment.

Figure 2.11a explains that the results of stress applied on the layer of coating can be separated in two different stresses: the elastic and plastic strains. The elastic strain is also named linear deformation. It is from that part of the graph from which the modulus is calculated using the equation: E=σ/ε. E is the Young's modulus, σ is the stress exerted and ε

43

is the strain. In that first phase, the thin layer of coating can return to its original size. The plastic strain is also named plastic deformation. From that point, the thin layer cannot return to its original size.

The elastic modulus can also be linked to the storage modulus obtained by DMA (see above) as shown in Fig. 2.11b using the equation $|E|^2 = (E')^2 + (E'')^2$, where E' is the storage modulus, which is the stored energy (representing the elastic portion of the coating), E'' is the loss or dissipated energy (representing the viscous portion of the coating).
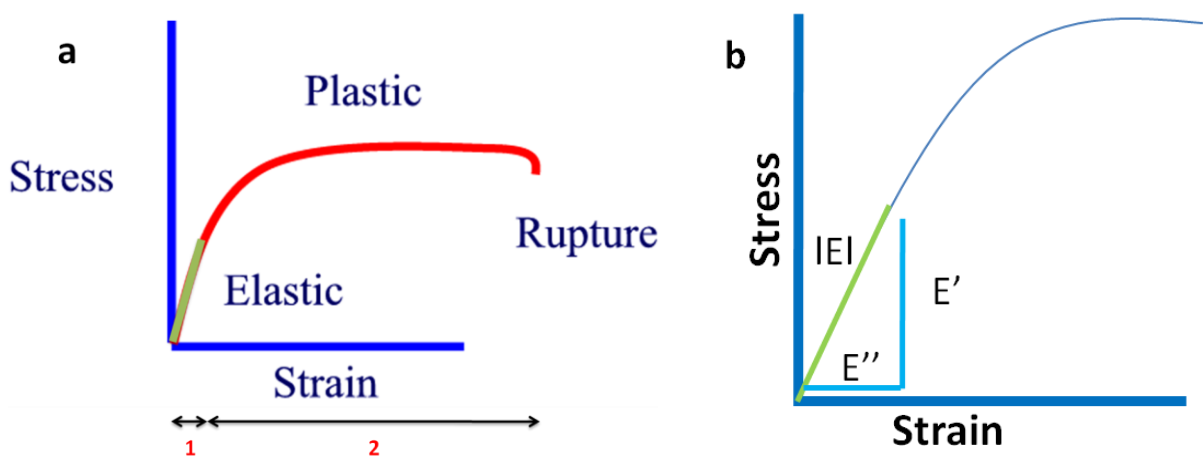
Figure 2.11: Result of stress applied on a thin layer of coating. a) General graph result. The higher the stress (force exert), the higher the strain is. The strain can be separated in two parts: 1: the elastic strain (represented by the green line) and 2: the plastic strain. When the stress is too high, the thin layer breaks (rupture). b) Relationship between the absolute value of elastic modulus (|E|), storage modulus E' and loss modulus E''.

Different results are obtained from this method: maximum force, elastic modulus, tensile strength and strain to failure, but only the elastic modulus was used for this thesis. The elastic modulus (MPa), here represented by the Young's modulus is a measure of the stiffness of the material, which describes the tendency of the coating to deform along an axis when opposing forces applied along that axis. It is calculated as the gradient of the stress/strain plot in the elastic regime (Fig. 2.11a and b).

This method was used for the silicone wettability series (Chapters 4 and 6) and for the silicone "modulus" series (Chapters 4 and 8).

2.9.3. Surface roughness by profilometry

The Nanofocus Scan[R] profilometer is an instrument, which measures a surface's profile along a 5 cm line on each test slide (3 replicates), in order to quantify its roughness and its flatness, using μScan version 6.1 software. Surface roughness can have an important role in the settlement and adhesion strength of algae (Granhag et al. 2004; Schumacher et al. 2007). The most interesting parameter obtained from the profilometer is Ra (Fig. 2.12). Ra represents the arithmetic average of roughness-height; it is the average of the magnitudes of all peaks and valleys of the measured surface (μm).

$$R_a = \frac{1}{n}\sum_{i=1}^{n}|a_i|$$
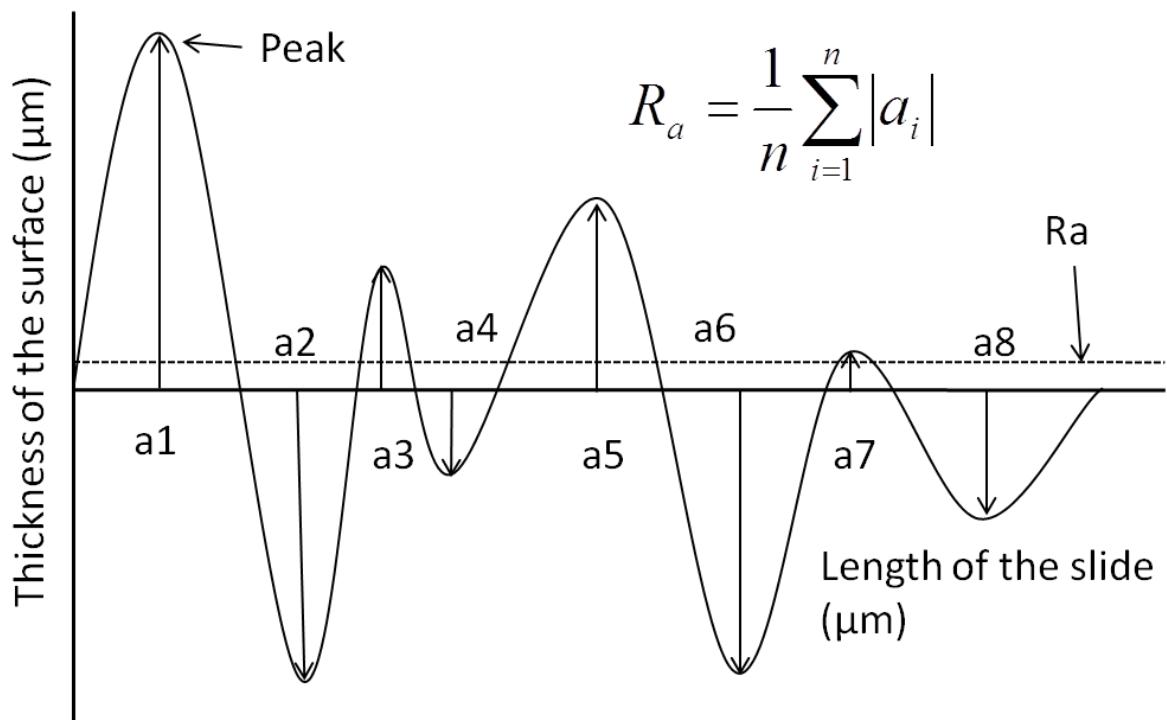
Figure 2.12: Ra on a coated surface explaining its calculation. The peaks show that the surface is not perfectly smooth. In the formula, a represents the amplitude of the peaks a_1, a_2 etc.

2.10. Statistical methods

- Laboratory experiments

Single metric analyses of coating performance (GZLM – SPSS)

Generalized linear modelling (GZLM, SPSS) with pairwise comparisons was used to assess coating performance as measured by each individual biomass metric (8 days unattached biomass, 14 days attached biomass, percentage biomass removal). Generalized linear modelling gives flexibility over a classical ANOVA to account for a non-normal distribution of the response variable (biomass metric). Different statistical models of the relationship between the predictor (coating) and response variables were modelled by changing the link function, and the best model for the data was determined by maximum likelihood estimation (i.e. the model with the lowest Akaike's information criterion (AIC value, Quinn and Keough 2002). Pairwise comparisons between coatings were performed using the resulting models. GZLM was also used to analyse the data for *U. linza*.

Multiple metric analyses of coating performance (RM ANOVA – SPSS)

Repeated-measures analysis of variance (RM ANOVA, SPSS) was used to assess coating combined performance by looking at two metrics: accumulated biomass after 14 days and the biomass remaining after exposure to shear. RM ANOVA is an experimental design based on an unreplicated two-factor crossed ANOVA design where experimental units are recorded repeatedly through time (Quinn and Keough 2002). Biomass data before and after shear were tested for equality of variance (Levene's test, Minitab). In cases where variance was not equal, the data were transformed using log-transformation. The coatings were compared using post hoc REGWQ (Ryan-Einot-Gabriel-Welsch, SPSS), which is one of the most powerful comparison procedures (Quinn and Keough 2002). The Post Hoc REGWQ separated coatings into groups, giving a significance value for each group.

- Field statistics

Single metric analyses of coating performance (GZLM – SPSS) for field assay in 2010

Generalized linear modelling (GZLM, SPSS) with pairwise comparisons was used to assess coating performance and the difference observed for each data collection using separately the data from microfouling, weeds, soft- and hard-bodied animals. The method used to compare the data was similar to that used in laboratory experiments (explained above).

Generalized estimating equations for field assay in 2011-12

Generalized estimating equations (GEEs, SPSS) with pairwise comparisons (with Sequential Bonferroni correction) were used to assess the performance of the test coatings. GEEs are an extension of GZLM to model correlated data (Quinn and Keough 2002). This method allows for a fixed response variable (the percentage of microfouling, weeds, soft and hard-bodied animals or total % fouling) to determine the effect of the coatings whilst taking into account the effect of panel, row, column and inspection date. As for the GZLM method, different statistical models of the relationship between the response variable and the predictors (panel, row, column, inspection date) were modelled by changing the link function. In addition, as for GZLM, the maximum likelihood estimation, i.e. the lowest Akaike's information criterion (AIC), was used to determine the best model for the data set.

Results of laboratory and field experiments were shown with either plus or minus standard deviation (SD) when the number of replicates was equal to or smaller than 5 and for the other cases 2x standard error (SE) was used.

3. DEVELOPMENT AND CHARACTERISTICS OF AN ADHESION BIOASSAY FOR ECTOCARPOID ALGAE

3.1. Introduction

Macroalgae (seaweeds) are known to foul panels, buoys' fishnets and ships' hulls. The common fouling green alga *Ulva linza* has been used extensively as a model fouling species for fundamental studies on the influence of properties as explained in Chapter 1.2. *U. linza* has also been used for over a decade in laboratory-based evaluations of experimental coatings that are candidates for practical application (see Callow and Callow 2011 for review). However, there are few comparable studies on other species of macrofouling algae.

Ectocarpoid algae are known to colonise ships' hulls and other submerged surfaces as explained in Chapter 1. Two genera of ectocarpoid algae are typically found on ships and raft panels -*Ectocarpus* and *Hincksia* (Greer and Amsler 2002; Mineur et al. 2007). In recent years, ectocarpoid algae have also been found growing on non-biocidal, 'fouling-release' (FR) coatings, both on raft panels and boat hulls (International Paint, unpublished data). This, and the growing interest in exploring non-biocidal, FR (i.e. 'low adhesion') technologies for fouling control (Callow and Callow 2011 for review) suggests that more extensive research on ectocarpoid algae is warranted and the first requirement is a robust, laboratory-based adhesion bioassay comparable to the *U. linza* assay. The bioassay has to able to down-select test coatings by providing a rapid assessment of the adhesion behaviour of the test organisms (Chapter 1.2.3). The main purpose of the present Chapter is to report on the development and characteristics of such an assay.

The starting point for bioassays using *U. linza* is the colonisation of surfaces by motile spores synchronously released from fertile fronds of the alga collected from the seashore. For a typical assay of multiple coatings, a litre of synchronously-released spores at a concentration of 1 x 10^6 per ml can readily be obtained, which is sufficient to assay 9 replicates of 8-10

coatings in microscope slide format using a standard protocol (e.g. Bennett et al. 2010). Although spores can be released from *Ectocarpus* spp., it is not remotely possible to obtain the quantities outlined for *U. linza*. However, in addition to settlement of spores, colonisation of substrata by ectocarpoid algae occurs through the production of creeping (i.e. prostrate) filaments: this forms the basis of the assay described in this paper. *Ectocarpus crouaniorum* was chosen as the test organism based on observations that it had a fast rate of growth and stronger adhesion to surfaces of culture vessels compared to other strains or species of *Ectocarpus* (Gachon pers. observations). Other ectocarpoid algae obtained from the field were also tested in order to validate the method and to observe any differences in adhesion between cultivated species and species from the field. The adhesion of ectocarpoid algae on a set of standard surfaces was evaluated in order to test the potential of the method to discriminate between surfaces with different properties.

3.2. Bioassay methods

3.2.1. Cultivation of ectocarpoid algae

The main test species used in this study was *Ectocarpus crouaniorum* CCAP 1310/300, which was grown as non-axenic, unialgal cultures as described in Chapter 2.3. The assay was then applied to unialgal cultures of two ectocarpoid algae collected from the field (Newton Ferrers, Devon, UK, Nov. 2009); an isolate of *Ectocarpus* (referred to here as '*Ectocarpus* sp.' since the precise species was not identifiable) and *Hincksia secunda* (Coppejans and Kling 1995), as explained in Chapter 2.1. Culturing conditions for these isolates were the same as for *E. crouaniorum.*

The assay was also applied to a mixed population of 'wild' ectocarpoid algae (genera *Ectocarpus, Hincksia* and *Pilayella)* collected from non-biocidal test panels exposed in Hartlepool Marina, UK in May 2011. The algal material was tested directly after

transportation to the laboratory, without any prior culturing. The algae were washed in artificial seawater (ASW) and cleaned using a paintbrush to remove most of the surface epiphytes such as diatoms.

3.2.2. Preparation of algal inoculum

To prepare the algal inoculum for the bioassay, approximately 2 g (wet wt.) of cultured or wild alga were blended with a hand-held kitchen homogeniser (setting 4 on a 650 W Russell Hobbs blender model 14333) for 1 min in 100 ml of ½-strength Provasoli medium. The blended alga was filtered through a nylon cell strainer (mesh size 100 µm, BD Falcon); large fragments were retained on the filter, which was discarded. The filtrate, consisting of small filaments, was used as the inoculum.

For the mixture of uncultivated ectocarpoid algae, this process was modified to reduce diatom contamination. The filtrate after blending was discarded since it contained many diatoms. The large filaments retained on the filter were then re-blended and filtered through a new nylon cell strainer. The filtrate from this second homogenisation was used as the inoculum.

The biomass of filaments in the filtrate used as the inoculum was quantified as the concentration of chlorophyll *a* (chl *a*) as described in Chapter 2.5*.*

The filtrate was diluted with ½-strength Provasoli medium to a chl *a* concentration of approximately 0.04 µg ml^{-1} for *E. crouaniorum*, 0.07 µg ml^{-1} for *Hincksia secunda*, 0.09 µg ml^{-1} for *Ectocarpus* sp. and 0.12 µg ml^{-1} for the mixture of 'wild' ectocarpoid algae. The concentrations used for the cultivated 'wild' species (*Ectocarpus* sp. and *Hincksia secunda*) were higher because a proportion of filaments was pale in colour and for the non-cultivated, wild preparation, the mixture contained other organisms, notably diatoms.

3.2.3. Preparation of the test surfaces

The test surfaces were three FR elastomeric coatings: Intersleek® 700 (IS700, International Paint) and Silastic® T2 (Dow-Corning Corporation), which are poly(dimethylsiloxane) (PDMS)-based (i.e. silicone) and the fluoropolymer technology Intersleek® 900 (IS900, International Paint) and Nexterion® glass B slides (Schott). Nexterion® glass is a hydrophilic borosilicate glass that is smooth and ultrasonically cleaned.

IS700 (grey) and IS900 (grey) are both 3-pack commercial FR coatings, which were prepared as explained in Chapter 4.2.4.

Glass microscope slides coated with Silastic® T2 (T2) were provided by Dr. P. Willemsen (TNO, Den Helder). T2 is a PDMS elastomer (Dow-Corning Corporation) and was prepared as described in D'Souza et al. (2010). The T2 mixture (60% in xylene) was sprayed onto primed glass microscope slides and cured at 50°C for 5 h. The characterisation of all test surfaces is explained in Chapter 4.5.

All the slides of Intersleek were leached in a 30-liter tank of deionised water, recirculated through a carbon filter (flow rate 72 ml s^{-1}) containing a polypropylene sediment cartridge (Cale Parmer, 1 μm pore) and filled with activated charcoal (Sigma-Aldrich, Daroc®, 12-20 mesh), for a minimum of 4 weeks in order to remove residual curing agents. The slides were placed in racks allowing the water to pass across the surfaces. Immediately prior to the start of the bioassay, the IS slides were rinsed with MilliQ water and gently wiped with a sponge in order to remove any bacteria that had adhered to the surface. Slides of T2 were put into MilliQ water for 24 hours to hydrate them. All test samples were incubated for 2 hours in ASW prior to the start of the bioassay.

3.2.4. Adhesion bioassay for ectocarpoid algae

The developed test protocol enables two measurements of adhesion performance on different surfaces: a) a measure of initial attachment, assessed after 14 days of incubation with the test inoculum; and b) a measure of adhesion strength of the attached filaments after exposure to shear stress, assessed by measuring the proportion of attached filaments removed after exposure to a shear stress in a water channel.

Test surfaces (9 replicates) each contained in individual compartments of Quadriperm polystyrene culture dishes (Greiner Bio-One), were inoculated with 15 ml aliquots of blended filaments prepared as described in 3.2.2, and incubated under the same conditions as those used for algal cultivation. After 8 days, non-adhered filaments were removed by gently rinsing each slide in ASW (5 gentle movements per slide). The rinsed slides were put back into the Quadriperm dishes in ½-strength Provasoli medium and incubated for a further 6 days. The unattached biomass in each test compartment after 8 days was retained and the biomass of unattached filaments was estimated through determination of chl *a* content as described in Chapter 2 (3 replicates).

After a total incubation period of 14 days, test slides were gently rinsed in seawater to remove any remaining unattached filaments, then attached biomass on each test slide was quantified, non-destructively, by measuring the fluorescence of chlorophyll in a fluorescence plate reader (excitation = 430 nm, emission = 670 nm, TECAN GeniosPlus) as explained in Chapter 2.7. Fluorescence was measured as relative fluorescence units (RFU).

To measure the adhesion strength of attached filaments, the 9 replicates of each test surface were exposed to a wall shear stress of 8 Pa for 5 min in a water channel producing fully-developed turbulent flow (see Chapter 2.6.; Schultz et al. 2000; Schultz et al. 2003). The biomass that remained after exposure in the water channel was quantified as RFU as described above. Percentage removal was determined by comparison of the biomass (RFU)

before and after exposure to shear stress. Slides were observed under a microscope to observe the filament morphology using transmitted light for the transparent surfaces and UV light (300-390 nm_{ex}, 420 nm_{em}) for the two opaque Intersleek coatings. In order to facilitate the microscopic observations on the two Intersleek coatings, the cell wall of *E. crouaniorum* was stained using the fluorescent brightener Calcofluor White (Sigma-Aldrich, 0.01% in seawater) for 10 min and then was rinsed with seawater. Calcofluor White binds to β-linked polysaccharides like cellulose and hence is used to stain cell walls of algae and higher plants (Herth and Schnepf 1980). All assays were performed at least twice to demonstrate consistency: results from one representative assay are illustrated below.

3.2.5. Comparative assays with sporelings of the green alga *Ulva linza*

Comparative assays using sporelings of *U. linza* were performed following the method in Chapter 2.8. To assess the adhesion strength of the sporelings, the slides were exposed to a wall shear stress of 50 Pa for 5 min in a water channel (a higher shear stress was used for *U. linza* because this alga adhered more strongly to the test coatings compared with *Ectocarpus* spp.). Percentage removal was determined from RFU values before and after exposure to shear, as described for ectocarpoid algae (see above; Chapters 2.6 and 2.7). Statistical analysis of the adhesion data is explained in Chapter 2.10, and statistical tables for the whole Chapter are presented in Appendix 3.

3.3. Results

3.3.1. Algal morphology of *E. crouaniorum*

After blending and filtration, the starting inoculum for adhesion assays consisted of small filaments averaging 6.3 ± 1 cells (mean of 50 observations ± 2 x SE, Fig. 3.1a). After 6 days'

incubation with test surfaces, filaments that had adhered grew by cell division (Fig. 3.1b). After 14 days, test surfaces were typically colonised by an extensive growth of prostrate and erect filaments, the latter bearing some sporangia (Fig. 3.1c). There was no evidence of toxicity associated with any of test surfaces.
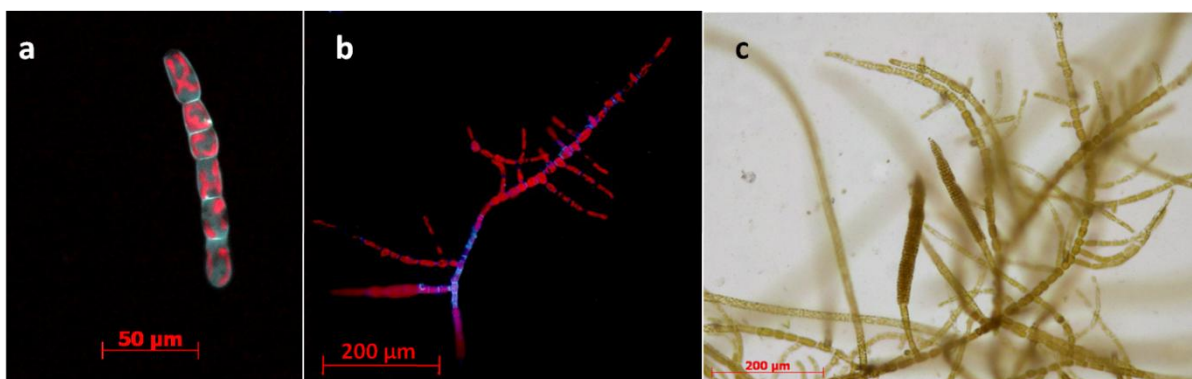
Figure 3.1: Different stages of growth of filaments of *E. crouaniorum.* a) Starting inoculum of fragmented filaments of *E. crouaniorum*, stained with the fluorescent brightener Calcofluor White (0.01%, Sigma-Aldrich), visualised by UV fluorescence microscopy (300-390 nm_{ex}, 420 nm_{em}). The red fluorescence is autofluorescence of chlorophyll. b) Filaments after 6 days' growth under UV fluorescence. The starting inoculum was pre-stained with Calcofluor White (0.01%, Sigma-Aldrich): new growth is shown as Calcofluor White-negative cells. c) Bright field image of inoculated test surface after 14 days' growth showing prostrate and erect filaments, some bearing plurilocular sporangia.

3.3.2. Adhesion strength in relation to applied shear stress using *E. crouaniorum*

To examine the relationship between the adhesion strength of attached filaments and the applied shear stress, the water channel was used to impose a range of shear stresses to filaments attached to IS700. Results showed a linear relationship between adhesion strength (as % removal) and the applied shear stress (Fig. 3.2). Maximum removal from this test surface (IS700) was ca. 60 % at the highest pressure available (50 Pa).
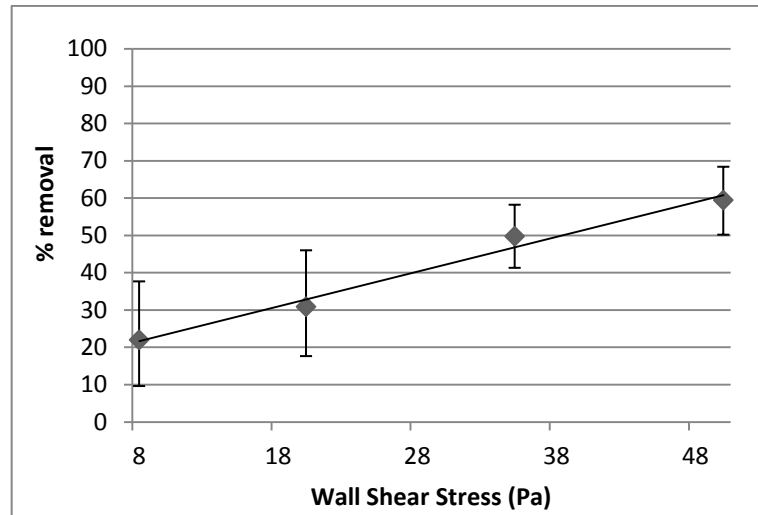
Figure 3.2: Percentage removal of *E. crouaniorum* from IS700 as a function of wall shear stress.
Biomass measured as relative fluorescence units. Mean of 3 replicates ± SD.

3.3.3. Comparative assay of adhesion strength of several algae on a range of standard coatings

To examine the characteristics of the assay, comparative bioassays were performed on a range of test surfaces. After 8 days' incubation with the starting inoculum, non-attached filaments were removed and quantified through chl *a* determination. For each alga, there were marked differences between surfaces in the amount of unattached filaments recovered from the culture dishes (Table 3.1). This may be the result of differences in the initial adhesion of inoculum, but could also be due to differences in the growth of unattached inoculum during the 8 days of incubation. Hence, the measure of unattached filaments must be used with caution and cannot strictly be regarded as indicating differences in initial adhesion per se. Unfortunately, it was not possible to obtain an accurate direct measure of attached biomass after 8 days because for some coatings, insufficient biomass had attached to give reliable readings in the plate reader. For all the starting inocula, except *Hincksia,* the amount of unattached filaments in dishes containing Nexterion slides was significantly greater than for all the other coatings ($p \leq 0.05$; GZLM, Pairwise comparison) suggesting

weaker adhesion to this surface. In the case of *Hincksia,* there was significantly more unattached biomass on IS900 (p≤0.05; GZLM, Pairwise comparison).

Table 3.1: Unattached biomass after 8 days' incubation of test surfaces with filaments, as measured by chl *a*. Mean of 3 replicates ± SD.

	Total unattached biomass (μg chl *a*)			
	Cultivated algae			Uncultivated ectocarpoid algae
	E. crouaniorum	Unidentified *Ectocarpus sp.*	*Hincksia secunda*	
IS700	0.23 ± 0.1	1.4 ± 0.87	0.16 ± 0.04	0.4 ± 0.02
IS900	0.26 ± 0.07	1.2 ± 0.6	0.64 ± 0.15	0.45 ± 0.26
T2	0.28 ± 0.08	0.8 ± 0.5	0.14 ± 0.11	0.42 ± 0.11
Nexterion	0.95 ± 0.28	8.8 ± 3.5	0.11 ± 0.06	1.04 ± 0.19

After removing the unattached filaments, the test surfaces were incubated in fresh culture medium for a further 6 days (i.e. 14 days in total) before exposure to a shear stress of 8 Pa. Different amounts of biomass were attached and different proportions of the attached biomass were removed from the test surfaces by exposure to shear (Figs. 3.3b, 3.5b, 3.6b).

E. crouaniorum.

Significant differences in the biomass of attached filaments were observed after a total of 14 days of growth (Fig. 3.3a). Biomass on Nexterion was lowest, T2 was intermediate while IS700 and IS900 together had the highest attached biomass (p≤0.05, GZLM, Pairwise comparison).

The amount of biomass remaining on the coatings after exposure to 8 Pa shear stress is shown in Figure 3.3a. Comparison of biomass before and after exposure to the shear stress (expressed as % removal) is a measure of adhesion strength. The results (Fig. 3.3b) show that *E. crouaniorum* adhered weakly to IS900 and Nexterion, both surfaces showing high percentage removal, up to 90 %. Adhesion to IS700 and T2 was stronger with 38 % and 18

% removal, respectively. The adhesion strength of filaments was higher on T2 than on IS700, although more filaments were attached initially on IS700 compared to T2. The statistical analyses showed that removal from IS700 was significantly higher than from T2 and lower than from IS900 and Nexterion (p≤0.05, GZLM, Pairwise comparison).
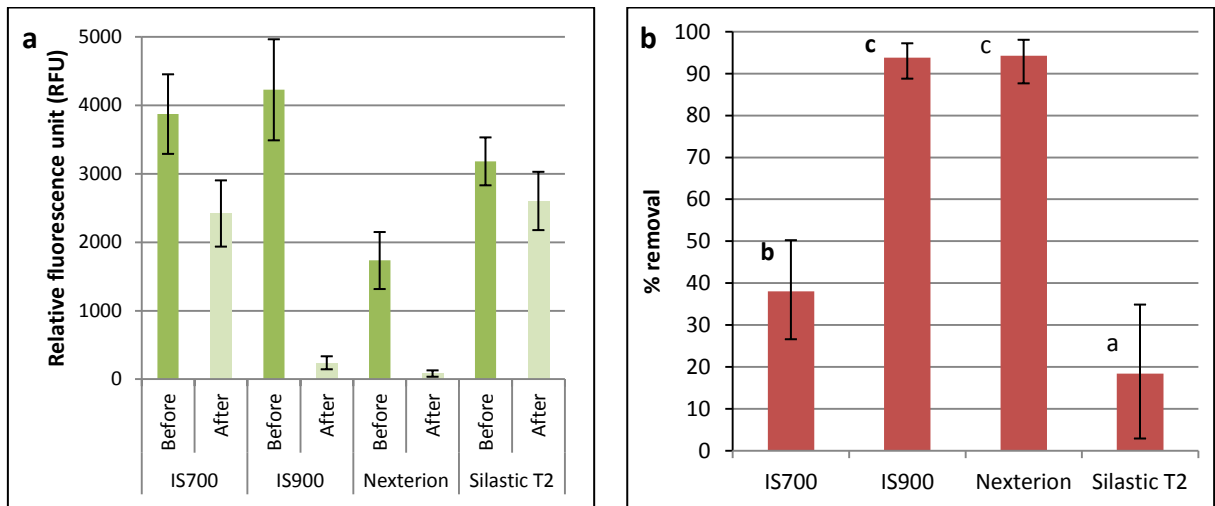
Figure 3.3: Adhesion assays with *E. crouaniorum.* a) Biomass of attached alga before and after exposure to a wall shear stress of 8 Pa, on 4 different surfaces, after 14 days of incubation at 15°C. Biomass was measured as relative fluorescence units. b) Percentage removal after exposure to 8 Pa shear stress, calculated from data presented in a). Means from 9 replicates ± 2 x SE. Values that are significantly different at p≤0.05 in GZLM test are indicated by different letters above the bars.

Statistical analysis of the combined performance of the surfaces (i.e. analysing together the amount of biomass before and after exposure to shear stress) revealed three groups. IS700 and T2 formed one group; both had relatively high biomass before and after exposure to shear showing that *E. crouaniorum* attached most strongly to these surfaces in terms of both initial attachment and adhesion strength. IS900 and Nexterion formed two separate groups; although both had low biomass after exposure to shear stress, there was a difference in biomass before exposure to shear (p≤0.05, RM ANOVA, Post Hoc REGWQ).

The differences between surfaces reported here were reproducible: in 3 separate experiments IS900 consistently gave a higher percentage removal of filaments under shear

than IS700, (69-80 % and 25-39 %, respectively). The release of filaments was consistently higher from Nexterion than T2 (% removal 53-90 % and 11-24 %, respectively).
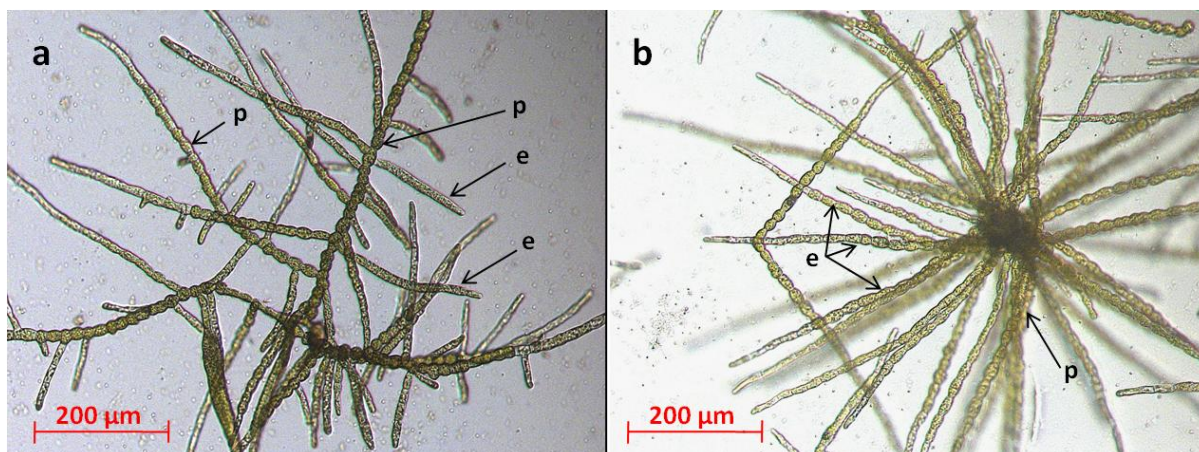
Figure 3.4: Two different morphotypes of *E. crouaniorum* on surfaces. a) organism with equal prostrate (p) and erect filaments (e). b) 'star' morphotype: organism with more erect than prostrate filaments (below the plane of focus).

After 14 days' growth, two different morphotypes were observed on all the surfaces (Fig. 3.4). However, after exposure to shear stress, morphotype A with both erect and prostrate filaments was predominant, i.e. there was preferential loss of morphotype B, although on Nexterion and IS900, adhered filaments were rarely seen.

***Ectocarpus* sp.**

Assays with this species were performed twice; the pattern of results presented below was observed in both experiments. Significant differences in the biomass of attached filaments were observed after a total of 14 days of growth (Fig. 3.5a). Nexterion had the lowest biomass, T2 had an intermediate amount of biomass and IS700 and IS900 both had the highest biomass ($p \leq 0.05$, GZLM, Pairwise comparison). These results are similar to those observed for *E. crouaniorum*. The assessment of adhesion strength on the 3 silicone-based coatings gave similar results to *E. crouaniorum,* adhesion to IS900 being the weakest (97 %

removal) followed by IS700 and T2 (Fig. 3.5b, p≤0.05, GZLM, Pairwise comparison). Adhesion strength on Nexterion was greater than that obtained for *E. crouaniorum*. However, the value for percentage removal from Nexterion has to be treated with care, because it was based on a very low starting value for biomass and therefore there is some uncertainty attached to the percentage removal data.
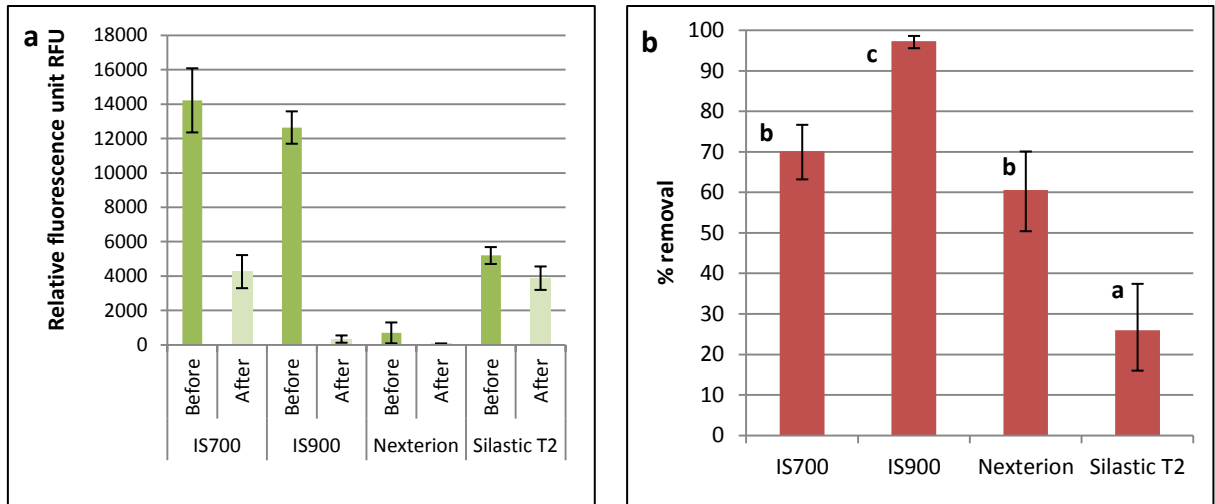
Figure 3.5: Adhesion assays with *Ectocarpus* sp. a) Biomass of attached alga before and after exposure to a wall shear stress of 8 Pa, on 4 different surfaces, after 14 days of incubation at 15°C. Biomass was measured as relative fluorescence units. b) Percentage removal after exposure to 8 Pa shear stress, calculated from data presented in a). Means from 9 replicates ± 2 x SE. Values that are significantly different at p≤0.05 in GZLM test are indicated by different letters above the bars.

Statistical analysis of the combined performance of the surfaces (i.e. analysing together the amount of attached biomass, and that remaining after exposure to shear stress) showed that all of the surfaces were different from each other for this particular *Ectocarpus* sp. (p≤0.05, RM ANOVA, Post Hoc REGWQ).

Taken together these results were broadly similar to those for *E. crouaniorum* and as for *E. crouaniorum*, the 'star' morphotype (Fig. 3.4b) was rarely observed on the test surfaces after exposure to shear stress. On Nexterion and IS900, adhered filaments were rarely seen after exposure to shear. The morphologies of the filaments were identical to those of *E.*

crouaniorum, whereby only those with both erect and prostrate filaments attached strongly to the surfaces.

Hincksia secunda

Significant differences in the biomass of attached filaments were observed after a total of 14 days of growth (Fig. 3.6a). Adhesion was weak on both Intersleek surfaces (Fig. 3.6b). Adhesion to Nexterion was strong with only 15 % of filaments being removed under shear. The experiment was performed twice, and the results showed that this pattern was reproducible.
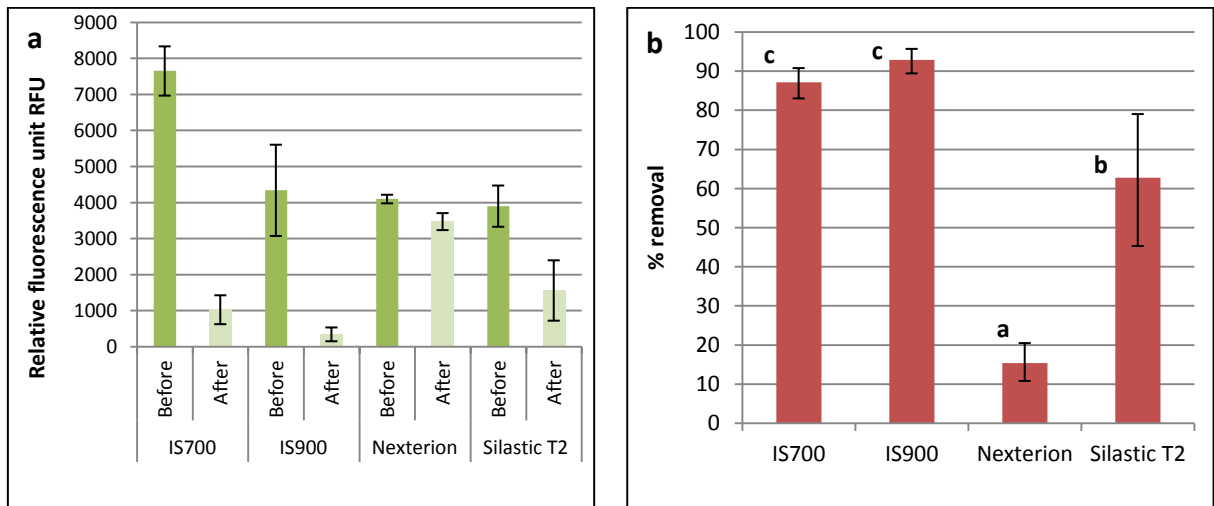
Figure 3.6: Adhesion assays with *Hincksia secunda.* a) Biomass of attached alga before and after exposure to a wall shear stress of 8 Pa, on 4 different surfaces, after 14 days of incubation at 15°C. Biomass was measured as relative fluorescence units. b) Percentage removal after exposure to 8 Pa shear stress, calculated from data presented in a). Means from 9 replicates ± 2 x SE. Values that are significantly different at p≤0.05 in GZLM test are indicated by different letters above the bars.

Statistical analysis of the combined performance of the surfaces (i.e. analysing together the amount of attached biomass, and that remaining after exposure to shear stress) revealed three performance groups in the order IS900=T2>IS700>Nexterion (p≤0.05, RM ANOVA, Post Hoc REGWQ).

Mixture of uncultivated 'wild' ectocarpoid algae

The biomass after 14 days' growth (Fig. 3.7a) was higher on IS700 and IS900 compared with T2 and Nexterion (p≤0.05, GZLM, Pairwise comparison). Adhesion strength, measured as percentage removal under shear (Fig. 3.7b) showed high removal values, up to 78% for IS900. The variation between surfaces was not statistically significant except between IS900 and T2 (p≤0.05, GZLM, Pairwise comparison). Statistical analysis of the combined performance of the surfaces (i.e. analysing together the amount of attached biomass, and that remaining after exposure to shear stress) revealed three performance groups IS900/T2>T2/Nexterion>IS700 (p≤0.05, RM ANOVA, Post Hoc REGWQ). Comparable results were obtained in a repeat experiment conducted on a separate collection of wild material.
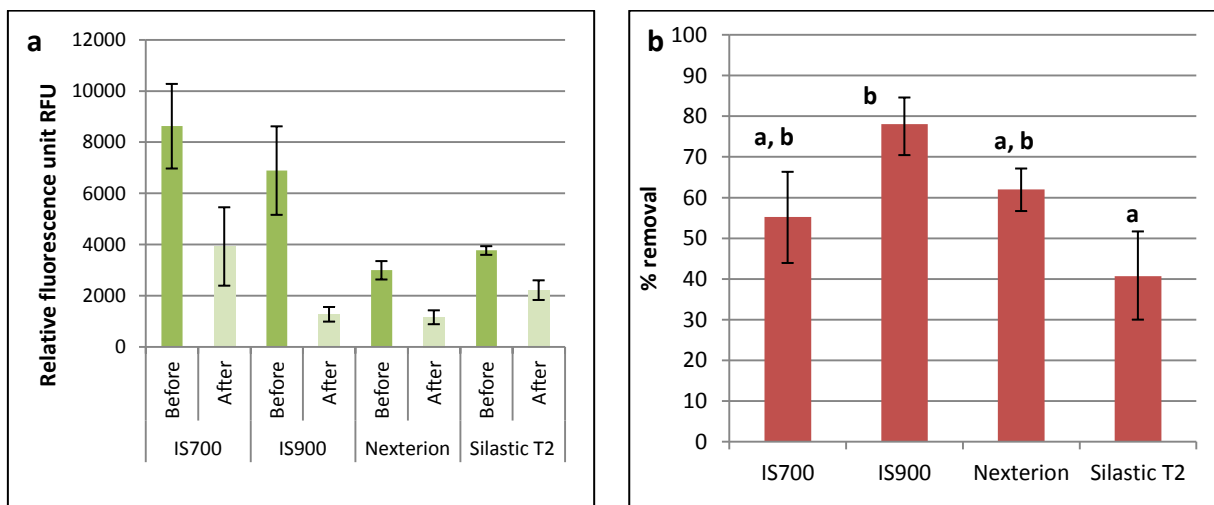
Figure 3.7: Adhesion assays with 'wild' ectocarpoid algae. a) Biomass of attached alga before and after exposure to a wall shear stress of 8 Pa, on 4 different surfaces, after 14 days of incubation at 15°C. Biomass was measured as relative fluorescence units. b) Percentage removal after exposure to 8 Pa shear stress, calculated from data presented in a). Means from 9 replicates ± 2 x SE. Values that are significantly different at p≤0.05 in GZLM test are indicated by different letters above the bars.

Microscopic observation showed that there were many erect and prostrate filaments on all the slides both before and after exposure to shear stress. Many diatoms were also observed on all test surfaces, particularly on Nexterion. On T2 and IS900, before exposure to shear stress, *Ectocarpus* was the main colonising genus although *Hincksia* and *Pilayella* were also present. After exposure to shear stress, only *Ectocarpus* and *Hincksia* were observed suggesting that *Pilayella* has weaker adhesion compared to the other two genera. Differences between genera were also observed for T2 and Nexterion. Both of these surfaces were colonized by *Ectocarpus* and *Hincksia* (with a few filaments of *Pilayella*) but after exposure to shear, there was proportionally more *Hincksia* than *Ectocarpus* remaining on Nexterion and vice versa for T2.

Ulva linza

The biomass that developed on the test surfaces was a consequence of germination and growth of spores that adhered during the settlement assay. Significant differences in the biomass of sporelings were observed after 6 days of growth (Fig. 3.8a), which probably reflects the density of spores that settled on the test surfaces. Higher biomass was observed on IS700 and IS900 compared to Nexterion and T2.
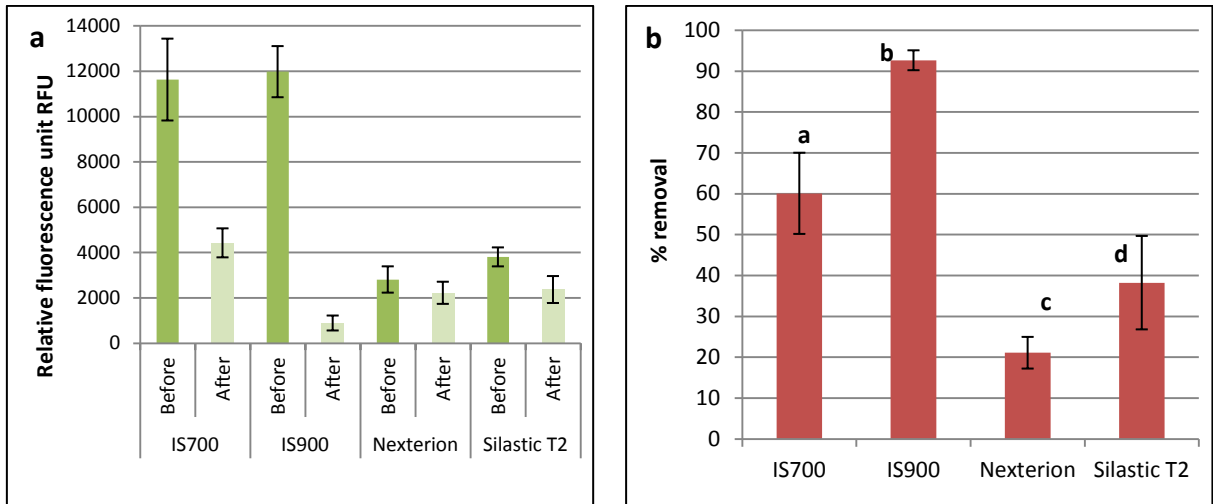
Figure 3.8: Adhesion assays with *Ulva linza.* a) Biomass of attached sporelings before and after exposure to a wall shear stress of 50 Pa, on 4 different surfaces, after 6 days of incubation at 18°C. Biomass was measured as relative fluorescence units. b) Percentage removal after exposure to 50 Pa shear stress, calculated from data presented in a). Means from 6 replicates ± 2 x SE. Values that are significantly different at p≤0.05 in GZLM test are indicated by different letters above the bars.

Biomass after exposure to 50 Pa shear stress showed further differences between the surfaces. Adhesion of sporelings was weak on IS900 (Fig. 3.8b) compared to Nexterion from which only 21 % of sporelings were removed. Sporelings had higher adhesion strength on T2 than on IS700 (p≤0.05, GZLM, Pairwise comparison).

3.4.   Discussion

The challenge of finding effective, environmentally friendly coatings has led researchers to improve their laboratory tools and to set up new bioassays (Briand 2009). These new tools and assays allow testing with more fouling organisms and a larger quantity or variety of test surfaces. The main purpose is to assess the intrinsic antifouling (AF) or FR properties of experimental coatings, enabling down-selection for further experiments or field assays. Laboratory-scale assays do not, and are not intended to reflect the complexities of the "real

world". In the natural marine environment, organisms interact with each other and there are seasonal influences (variations in fouling pressure, environment) leading to an essentially uncontrolled situation. In contrast, laboratory-scale assays are relatively easy to perform; they provide for a low cost (facilities and amount of materials), a rapid assessment of the test coatings, in reproducible conditions (temperature, medium and species). They also allow the elucidation of underlying settlement and adhesion mechanisms leading to a more informed understanding of how coatings work, or do not work.

A requirement for a good laboratory-based bioassay for non-biocidal AF/FR coatings is that the test organism should be capable of providing sufficient levels of starting inoculum (spores, cells, filaments, larvae) to permit the simultaneous testing of several coatings (e.g. if a compositional 'ladder' is to be studied), with sufficient replicates for good statistics, and within the same experiment to facilitate direct comparability. The test organism should be collectable from the wild without undue seasonal dependence, or capable of being cultured, at relatively low cost. The assay results should be also consistent and reproducible from experiment to experiment. While biological and seasonal variability, especially of material collected from the wild, may mean that absolute levels of e.g. spore settlement, or adhesion strength will vary from one bioassay to another, it would be anticipated that relative performance should be consistent. For example, a reliable assay should place the performance of a standard set of coatings in the same rank order and be capable of discriminating sensitively between coatings with different properties.

The study has reported the development of a protocol to investigate the growth and adhesion strength of ectocarpoid algae that meets the above requirements. The assay is based on the inoculation of test surfaces with small filaments of non-axenic *E. crouaniorum* (although it is possible to culture *Ectocarpus* spp. axenically, the plants that develop do not have a morphology typical of those collected from the wild, which may influence adhesion characteristics, see Chapter 2.4). Cultured ectocarpoid algae, especially *Ectocarpus* spp. are

good models for such assays due to their small size, facile culturability and rapid growth (life cycle completed in 3 months in the laboratory), allowing sufficient algal material to be collected in a short culture period. The protocol of the bioassay established above is easy to perform and to repeat under the same environmental conditions (temperature, culture medium, light). Each of the experiments was repeated at least once and results showed that the protocol was reproducible, allowing the replicated testing of different coatings and different ectocarpoid species.

This study showed that an inoculum of short filaments of ectocarpoid algae obtained by blending, produced all the morphological structures of a normal organism observed in the wild (prostrate and erect filaments, and sporangia) after less than 2 weeks. The production of attached prostrate filaments was essential for this study since there are structures that attached to surfaces. After a few days, it was possible to observe the first prostrate filaments and the production of ramifications, which allowed the organisms to adhere more strongly. After 14 days, sporangia were observed on erect and prostrate filaments, which may allow further colonisation of the surface through the release of motile spores. The morphology of the filaments seemed to follow the same development as sporelings (Le Bail et al. 2008; Peters et al. 2008). After a few days, the cut filaments that attached to the surface, produced new cells of prostrate filaments in one or both directions, then after a few more days, erect filaments were produced.

Two different morphotypes were observed for all the cultivated ectocarpoid species growing on the test surfaces. Morphotype A ('normal') had both prostrate and erect filaments in equal quantity, whilst morphotype B consisted of more erect filaments in the form of a radiating star. The star morphotype was mostly present before exposure to shear stress, while the normal morphotype was more typical after shear stress. These observations indicate that the star morphotype had lower adhesion strength than the normal morphotype and confirm the importance of the prostrate filaments for adhesion.

The experiments with *E. crouaniorum* showed that the bioassay was reproducible across replicated assays and the results obtained from *E. crouaniorum* and *Ectocarpus* sp. collected from the field, were similar. The data demonstrated that two different isolates from two different locations and cultivated for different lengths of time (4 years versus 1.5 years) behaved in a similar way.

Regarding the ability of the test protocol to enable adhesion preferences on different types of coating to be discriminated, a range of coatings/surfaces was used with different properties. These properties are fully described in Chapter 4, but in brief, the results of the surface energy measurements (Table 4.10) confirm the expectation that both PDMS-based coatings (T2 and IS700) are hydrophobic, low surface energy coatings with water contact angles >100° and a very low proportion of polar surface energy. By contrast, the amphiphilic IS900 gave a much lower water contact angle, and while its total surface energy was similar to IS700, as anticipated the polar contribution to total surface energy was substantial (52.9%). Nexterion glass had a high surface energy, with a high proportion of the polar component, as anticipated for a hydrophilic surface. All three commercial test coatings had a low elastic modulus (1.17–1.42 MPa) and Ra roughness was in the submicron range (0.2–0.32 mm). The results of the assays on these coatings described in this Chapter showed that the assay protocol did discriminate between coatings with these different properties. *E. crouaniorum* attached weakly to the amphiphilic IS900 and more strongly to the more hydrophobic, silicone coatings (T2 and IS700). Similar results were obtained for the cultured *Ectocarpus* sp. collected from the wild and in this respect, the results for both cultivated *Ectocarpus* strains are rather similar to the results obtained for the sporelings of the green alga *U. linza*, which have been shown to adhere less strongly to amphiphilic than hydrophobic elastomeric coatings (e.g. Martinelli et al. 2008; Sundaram et al. 2011). However, there are differences between *Ectocarpus* spp. and *U. linza* in their relative adhesion to hydrophilic (Nexterion) glass surfaces. *U. linza* adhered strongly to Nexterion glass whereas *E. crouaniorum* and

Ectocarpus sp. showed weak adhesion to glass, both in terms of the initial attachment of inoculum, and subsequent adhesion strength of attached filaments. In this respect, *Ectocarpus* spp. appears to be more similar in adhesion characteristics to the three raphid diatoms studied by Holland et al. (2004), which attached more strongly to T2 than to glass.

Comparing now the adhesion characteristics between different ectocarpoid genera, the experiments with *H. secunda* indicated that members of the same order (Ectocarpales) do not necessarily have the same preferences for adhesion since *H. secunda* attached more strongly to hydrophilic Nexterion glass than to T2. These data are different from previous observations made by Greer and Amsler (2002 and 2004) showing that spores of *Hincksia irregularis* preferred to settle more on hydrophobic surfaces compared to hydrophilic negatively charged surfaces. However, the preference of spores for settlement cannot be taken as an indicator of adhesion strength of young plants as shown for *U. linza* (e.g. Bennett et al. 2010).

The experiment with the mixed, non-cultured ectocarpoid algae collected from the wild was performed in order to assess whether culturing influenced adhesion preferences. The collected algae were cleaned, but it was technically impossible to separate individual genera in sufficient quantity to perform replicated bioassays from the tufted, intermingled samples collected. A mix of genera was therefore observed, which may more accurately reflect the fouling potential of ectocarpoid algae in the wild. The results showed that the adhesion characteristics of the mixed wild inoculum broadly reflected those of the cultured *Ectocarpus*, although less distinctly. Visual observation showed that *Ectocarpus* was the dominant genus in the wild population with small proportions of *Hincksia* and *Pilayella*. These results suggest that the adhesion preferences obtained from the bioassay based on cultured *Ectocarpus* are broadly representative of the population of wild ectocarpoid algae if *Ectocarpus* is the dominant genus.

In conclusion, this Chapter reports the development of a routine protocol to perform laboratory-based adhesion assays on test surfaces, using the readily cultivated species *E. crouaniorum*. The results of the *E. crouaniorum* model were consistent with those obtained for *Ectocarpus* sp. that was more recently put into cultivation, and a mixture of non-cultivated wild species. The assay is rapid (2 weeks) and has been shown to be reproducible; the species is easy to cultivate and at a relatively low cost (provided suitable hydrodynamic apparatus is available). The results showed that the assay discriminates between surfaces with different properties, reproducibly, allowing reliable down-selection of test surfaces for further testing or field assay.

The work described in this Chapter has contributed to a paper (*Evariste E, Gachon CMM, Callow ME, Callow JA. 2012. Development and characteristics of an adhesion bioassay for ectocarpoid algae. Biofouling 28: 15-27.*) (Appendix 14).

4. THE PREPARATION AND CHARACTERISATION OF TEST COATINGS

4.1. Introduction

One of the aims of the project was to understand the interactions between ectocarpoid algae and the surface and bulk properties of coatings that are most relevant to fouling-release (FR) performance -viz. wettability, surface energy and modulus. In Chapter 3, the discriminatory power of the developed adhesion bioassay was tested using a range of standard commercial coatings. Whilst the properties of these coatings differ, a proper analysis of the influence of properties on performance is best conducted via hypothesis-driven experiments with purpose-made test coatings in which properties (ideally only one) are systematically changed. In practice, the production of a series of coatings, which has similar chemistry and has only one property changed is difficult because there are links between most of the properties. In this Chapter, the preparation and characterisation of several sets of test coatings is described (Table 4.1). The coatings were prepared in the laboratory of International Paint in Gateshead and were used in laboratory and field assays, the results of which are described in subsequent Chapters.

As explained in Chapter 1, two types of hydrophobic (and in the case of fluoropolymers, lipophobic) polymers are used to produce commercial FR coatings, silicone elastomers and fluoropolymers. For this project, they were used to produce four sets of experimental-scale FR coatings, which had different properties.

Table 4.1: Coatings and date of production.

Name	Coating series	Year Prepared	Results Chapter No.
Condensation cured perfluoropolyether coatings	mD10 / mD10-H / mE10-H (A small set of coatings for initial investigations of the effects of modulus)	March 2010	5,9
Condensation cured silicone elastomer coatings	S1, S2 and S3[1] (A small set of coatings for initial investigations of the effects of modulus)	March 2010	5,9
	Silicone 'hybrid' wettability series (A series of coatings for systematic studies on the effect of surface energy and hydrophobic/hydrophilic balance)	January 2011	6,10
	Silicone 'modulus' series (A series of coatings for systematic studies of the effects of modulus/molecular weight)	March 2012	8,11
Intersleek	IS700 / IS900 (Standards)	March 2010 ; January 2011	

Fluoropolymer coatings. In 2010, a set of three coatings was produced for initial studies on the effect of modulus. These were based on modified hydroxyl-functionalised proprietary perfluoropolyethers Fluorolink D10, Fluorolink D10-H and Fluorolink E10-H. The coatings mD10, mD10-H and mE10-H were designed to have different modulus but similar surface energies. They all had different modulus as planned, but mE10-H was more hydrophilic than the other coatings on account of its content of poly(ethylene oxide) PEO.

Silicone-based FR coatings. In 2010, a small set of three silicone elastomer coatings were prepared for initial investigations of the effects of modulus. They were designed to have different moduli but similar wettabilities/surface energies. S1 coating was based on a medium molecular weight poly(dimethylsiloxane) PDMS (viscosity 4000 mPa s^{-1}) while S2 coating was based on a low molecular weight PDMS (viscosity 750 mPa s^{-1}). Both should have a low

---

[1] Previously named LSE, MMO and HSE, respectively

surface energy being based on PDMS but since modulus is inversely proportional to polymer molecular weight (Brazel and Rosen 2012 referred to the rubber theory) it was anticipated that there would be distinct differences in modulus. In addition, a third coating S3 was designed to have different modulus than the two other coatings, but it also had a higher surface energy since it incorporated a proprietary trimethoxysilyl-terminated poly(dimethylsiloxane)-poly(ethylene oxide) PDMS-PEO block copolymer.

Based on the results from the three coatings made in 2010, two more sets of coatings were prepared in 2011 and 2012 to test specific hypotheses regarding the influence of surface energy and modulus respectively. An extended range of six silicone 'hybrid' coatings, which is referred to as the 'wettability series', was made in 2011 with different surface energies and hydrophilic/hydrophobic balance. This was achieved by blending PDMS and a proprietary PDMS-PEO block copolymer in different ratios.

In 2012, a range of low surface energy silicone coatings was made using different molecular weights (and viscosities) of PDMS to vary the modulus, while keeping surface energies similar.

Commercial standards. The two commercial standard coating Intersleek® 700 (IS700) and 900 (IS900) were produced in the laboratories of International Paint while Silastic® T2 (T2, Dow-Corning Corporation) and Nexterion® glass B slides were provided respectively by Dr. P. Willemsen (TNO, Den Helder) and Schott. T2 and Nexterion® glass were used in Chapter 3 for the development of the ectocarpoid algae bioassay while both Intersleek coatings were used as standards for most of the assays during the project.

4.2. Materials and methods

All the coatings described in this Chapter were characterised using the methods explained in Chapter 2.9. The wettability/surface energy was measured using the contact angle methods;

the modulus was either measured using dynamic mechanical analyser or the elongation measurement method and the roughness was also measured using profilometer.

4.2.1. Preparation of condensation cured perfluoropolyether coatings (fluoropolymer coatings)

Components

Chemically modified perfluoropolyethers were selected as condensation cure systems in which the glass transition temperature and surface energy can be modified in a controlled manner. These proprietary systems are based on Solvay's hydroxyl functional perfluoropolyethers know as Fluorolink D10, D10-H and E10-H. These have the general formula $(CH_3O)_3Si-X-CF_2-O-(CF_2-CF_2-O)_p-(CF_2O)_q-CF_2-X-Si(OCH_3)_3)$. The ratio of p and q values is between 1.9:1 and 1:1 dependent on the manufacturing route. As supplied these are non-reactive materials; they were converted to reactive species by International Paint, and for clarity the modified polymers were re-named mD10, mD10-H and mE10-H. The functional groups for the modifications were as follows: $X = -CH_2O-$ (i.e. formaldehyde) for mD10 and mD10-H: and $X = -CH_2(OCH_2CH_2)_nO-$ (i.e. poly(ethylene oxide)) for mE10-H.

The surface energy of the resulting polymer is dependent on the X functionality "D" or "E" and the modulus of the resultant coating is dependent on the molecular weight of the polymer (H = High). The molecular weight was 700 kg mol^{-1} for mD10-H, 500 kg mol^{-1} for mD10 and 750 kg mol^{-1} for mE10-H. From these, it was assumed that the coatings mD10-H and mE10-H would have slightly different modulus but possibly mE10-H would be more hydrophilic due to the presence of PEO and the coating mD10 should have similar surface energy to mD10-H (i.e. due to similar X functionality) but higher modulus than mD10-H and mE10-H as the molecular weight of mD10 was the lowest.

The fluoropolymer formulations were a mix of 150 g polymer and 1.5 g of catalyst (*bis* (2-ethylhexyl) hydrogen phosphate (EHHP).

4.2.2. Preparation of condensation cured silicone elastomer coatings

S1, S2 and S3 coatings prepared in 2010 (Table 4.2):

Three test coatings were produced based on PDMS (two viscosities) or PDMS-PEO in order to have different moduli.

Polymers: Hydroxyl-terminated PDMS

- Low mol. wt. (Rhodorsil 48V750, viscosity 750 mPa s^{-1})

- Medium mol. wt. (DC 3-0213, viscosity 4000 mPa s^{-1})

$$\text{HO-(Si(CH}_3)_2\text{O)}_n\text{-H}$$

Trimethoxysilyl-terminated   PDMS-PEO   copolymer   (IP   Polymer XX/00843)
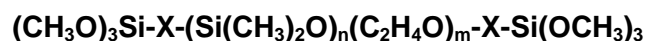
$$(\text{CH}_3\text{O})_3\text{Si-X-(Si(CH}_3)_2\text{O)}_n(\text{C}_2\text{H}_4\text{O})_m\text{-X-Si(OCH}_3)_3$$

Crosslinker: Prehydrolysed tetraethylorthosilicate (TEOS)

$$\text{C}_2\text{H}_5\text{-(OSi(OC}_2\text{H}_5)_2\text{O)}_n\text{-C}_2\text{H}_5$$

Catalyst: *Bis* (2-ethylhexyl) Hydrogen Phosphate (EHHP)

$$[\text{CH}_3(\text{CH}_2)_3\text{CH}(\text{C}_2\text{H}_5)\text{CH}_2\text{O}]_2\text{PO}_2\text{H}$$

Solvent: Xylene

$$\text{C}_6\text{H}_4(\text{CH}_3)_2$$
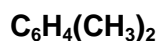
Table 4.2: Composition of the S1, S2 and S3 coatings.

	Function	Name	Quantity (g)
S1	Polymer	PDMS (DC 3-0213)	103.09
	Crosslinker	TEOS	4.64
	Catalyst	EHHP	0.83
	Solvent	Xylene	34.02
S2	Polymer	PDMS (Rhodorsil 48V750)	445.09
	Crosslinker	TEOS	20.03
	Catalyst	EHHP	2.22
	Solvent	Xylene	19.46
S3	Polymer	PDMS-PEO (Polymer XX/00843)	38.29
	Catalyst	EHHP	0.33
	Solvent	Xylene	8.89

Condensation cured silicone 'hybrid' coatings of different wettability/surface energy prepared in 2011

In order to modify systematically the surface energy of silicone-based coatings, PDMS was blended with different proportions of a proprietary, trimethoxysilyl-terminated PDMS-PEO block copolymer (Table 4.3).

Polymers: Hydroxyl-terminated PDMS (viscosity 4000 mPa s^{-1})

$$HO-(Si(CH_3)_2O)_n-H$$

Trimethoxysilyl-terminated PDMS-PEO copolymer (IP XX/00843)

$$(CH_3O)_3Si-X-(Si(CH_3)_2O)_n(C_2H_4O)_m-X-Si(OCH_3)_3$$

Crosslinker: Prehydrolysed tetraethylorthosilicate (TEOS)

$$C_2H_5-(OSi(OC_2H_5)_2O)_n-C_2H_5$$

Catalyst: Dioctyltin dilaurate (DOTDL) + 2,4-Pentanedione (catalyst stabiliser)

$((CH_2)_7CH_3)_2Sn(OCO(CH_2)_{10}CH_3)_2$ **$CH_3COCH_2COCH_3$**

Solvent: Xylene

$C_6H_4(CH_3)_2$
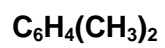
Table 4.3: Composition of the silicone 'hybrid' (PDMS-PEO) coatings of different wettability.

	Function	Name	Quantity (g)
H	Polymer	PDMS	103.09
	Crosslinker	TEOS	4.64
	Catalyst	DOTDL + stabiliser	8.42
	Solvent	Xylene	34.02
H1	Polymers	PDMS	113.36
		PDMS-PEO	11.40
	Crosslinker	TEOS	3.65
	Catalyst	DOTDL + stabiliser	6.60
	Solvent	Xylene	15.00
H2	Polymers	PDMS	100.00
		PDMS-PEO	25.00
	Crosslinker	TEOS	3.65
	Catalyst	DOTDL + stabiliser	6.60
	Solvent	Xylene	15.00
H3	Polymers	PDMS	88.00
		PDMS-PEO	36.75
	Crosslinker	TEOS	3.65
	Catalyst	DOTDL + stabiliser	6.6
	Solvent	Xylene	15.00
H7	Polymers	PDMS	36.75
		PDMS-PEO	88.00
	Crosslinker	TEOS	3.65
	Catalyst	DOTDL + stabiliser	6.6
	Solvent	Xylene	15.00
H10	Polymer	PDMS-PEO	124.75
	Catalyst	DOTDL + stabiliser	6.6
	Solvent	Xylene	18.65

Condensation cured silicones of different modulus prepared in 2012

To vary the modulus of silicone coatings systematically, while keeping surface energies similar, PDMS with different viscosities (molecular weights), were used (Table 4.4). The expectation was that the modulus would be inversely proportional to the molecular weight/viscosity (i.e. the lower the viscosity, the harder the coating and the higher the modulus).

Polymers:　　　　Hydroxyl-terminated PDMS at different molecular weight/viscosity.

Viscosity of different PDMS: 72 mPa s^{-1}; 4000 mPa s^{-1}; 6000 mPa s^{-1}; 14000 mPa s^{-1} and 50000 mPa s^{-1} (Dow Corning, data provided by the supplier).

$$HO\text{-}(Si(CH_3)_2O)_n\text{-}H$$

Crosslinker:　　　　Prehydrolysed tetraethylorthosilicate (TEOS)

$$C_2H_5\text{-}(OSi(OC_2H_5)_2O)_n\text{-}C_2H_5$$

Catalyst:　　　　Dioctyltin dilaurate (DOTDL) + 2,4-Pentanedione (catalyst stabiliser)

$$((CH_2)_7CH_3)_2Sn(OCO(CH_2)_{10}CH_3)_2 \qquad CH_3COCH_2COCH_3$$

Solvent:　　　　Xylene

$$C_6H_4(CH_3)_2$$
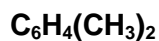
Table 4.4: Composition of the silicone 'modulus' coatings.

	Function	Name	Quantity (g)
M1	Polymer	PDMS (72 mPa s^{-1})	288
	Crosslinker[2]	TEOS	78
	Catalyst[2]	DOTDL + stabiliser	46
M2	Polymer	PDMS (4000 mPa s^{-1})	288
	Crosslinker	TEOS	39
	Catalyst	DOTDL + stabiliser	23
M3	Polymer	PDMS (6000 mPa s^{-1})	288
	Crosslinker	TEOS	39
	Catalyst	DOTDL + stabiliser	23
M4	Polymer	PDMS (14000 mPa s^{-1})	288
	Crosslinker	TEOS	39
	Catalyst	DOTDL + stabiliser	23
	Solvent[3]	Xylene	10
M5	Polymer	PDMS (50000 mPa s^{-1})	288
	Crosslinker	TEOS	39
	Catalyst	DOTDL + stabiliser	23
	Solvent[3]	Xylene	40

---

[2] A higher ratio of catalyst and cross-linker was needed to properly cure the coating M1.

[3] PDMS polymers with a viscosity of 14000 and 50000 mPa s^{-1} were more viscous than the other PDMS polymers with lower viscosity. In order to produce coatings with similar dry film thickness, a solvent was therefore used for the production of M4 and M5 to lower the viscosity of the blends.

4.2.3. Preparation of standard coatings

Three standard, silicone-based commercial coatings were used: T2, IS700, IS900, plus Nexterion® glass. The preparation of the coatings was explained in Chapter 3.2.3.

IS700 (grey) and IS900 (grey) are both 3-pack commercial FR coatings (Table 4.5). IS700 is a hydrophobic silicone providing a smooth, non-stick surface (http://www.international-marine.com/Product%20Datasheets/147+M+eng+A4.pdf). IS900 is a PDMS-based fluoropolymer that produces an amphiphilic coating, i.e. a surface that simultaneously possesses both hydrophobic and hydrophilic functionalities (http://www.international-pc.com/MPYAPCPCProductDatasheets/3852+P+eng+A4.pdf). Both Intersleek coatings were applied over a tie coat according to manufacturer's instructions. The same tie coat, Intersleek® 731 (IS731), was applied for both Intersleek® coatings, to glass microscope slides that had been cleaned with xylene, using a roller, and then dried overnight. IS731 was composed of a base (Part A, pink, 58.92 g) mixed with a curing agent (Part B, clear, 41.01 g). The top coats (i.e. finish coat) were applied by brush and allowed to cure overnight at room temperature before characterizing the surface properties.

Table 4.5: Composition of Intersleek® coatings.

	Function	Name	Quantity (g)
Intersleek® 700 Grey	Polymer, pigment and fluid	IS700 Part A grey	76.7
	Curing agent	IS700 Part B	18.5
	Catalyst	IS700 Part C	4.8
Intersleek® 900 Grey	Polymer, pigment and fluid	IS900 Part A grey	77.2
	Curing agent	IS900 Part B	12.9
	Catalyst	IS900 Part C	9.9

4.2.4. Application of the test coatings

To coat all the glass slides together and quickly, they were attached to panels, cleaned using xylene and then coated using a roller with an unpigmented Veridian tie coat (International Paint) with 5-10 ml of xylene as solvent; another tie coat IS731 was used for the two Intersleek coatings as explained above. Unpigmented Veridian tie coat, which is a clear acrylic polymer, dries after 4 hours at room temperature. A tie coat was used because the top coats do not adhere well to glass. The top coats were applied using a brush to have a good thickness of coating (>100 μm for a dry film) and cured at room temperature (~20°) and 40% relative humidity (RH).

4.3. Coating Characterisation: Results and Discussion

All the experimental test coatings were transparent, facilitating microscope observations. The two Intersleek coatings were opaque.

4.3.1. Condensation cured fluoropolymer coatings (2010)

The coatings mD10 and mD10-H were hydrophobic, with water contact angle ca. 92.5° and had low surface energy with a low polar component (Table 4.6). As expected, they had different moduli; mD10 had the highest modulus with 20 MPa, followed by mD10-H with 7.75 MPa. In comparison, the storage modulus of mE10-H was only 1.95 MPa compared with 7.75 and 20 MPa for mD10-H and mD10, respectively. However, mE10-H containing poly(ethylene oxide) groups, was hydrophilic, with a mean water contact angle of 56.3° and a high total surface energy (44.2 mN m^{-1}). This is reflected in a substantially higher polar component of surface energy for mE10-H (Table 4.6). All the three coatings were 'smooth' in the micrometer range with Ra roughness lower than 0.3 μm.

Table 4.6: Properties of the fluoropolymer coatings. The number of replicates was 3 for contact angle, 2 for the storage modulus and 5 for the roughness. Values shown are mean ± SD. The modulus was measured using the DMA (Chapter 2.9.2.1).

Coatings		mE10-H	mD10-H	mD10
Molecular weight (kg mol^{-1})		750	700	500
Modulus (using DMA)	Storage Modulus E' at 20°C (MPa)	1.95 ± 1.4	7.75 ± 2.3	20 ± 12.5
Contact angle	Static Water Contact Angle ($\theta°_{Ws}$)	56.3 ± 0.9	92.8 ± 1.3	92.3 ± 1.6
	Static Diiodomethane Contact Angle ($\theta°_{Ds}$)	68.2 ± 1.1	95.6 ± 1.5	83.1 ± 6.7
	Total Surface Energy γ_S (mN m^{-1})	44.2 ± 0.4	16.9 ± 0.9	19.8 ± 2.4
	Dispersive Surface Energy γ_D (mN m^{-1})	16.8 ± 0.7	7.7 ± 0.5	13.2 ± 3
	Polar Surface Energy γ_P (mN m^{-1})	27.4 ± 1.1	9.2 ± 0.4	6.6 ± 0.6
	% Polar surface energy	62	54.6	33.3
Roughness	Ra (µm)	0.25 ± 0.02	0.19 ± 0.04	0.16 ± 0.01

4.3.2. Condensation cured silicone elastomer coatings (2010 series)

As expected, all three coatings had different moduli. For S1 and S2, the molecular weights of the starting PDMS were different and this was reflected in differences in moduli (0.34 cf. 0.6 MPa). In addition, the modulus of S3 was almost 3x higher than that for S1 modulus, although still below 1 MPa showing they were both relatively 'soft' with moduli below those of the two Intersleek formulations (Table 4.11). However, the surface properties of these three coatings were different. S1 and S2 coatings, being solely PDMS-based, were hydrophobic, with water contact angles of ca. 90° and similarly low total surface energies (24-25 mN m^{-1}) (Table 4.7). Both coatings had low polarity. The S3 coating had a higher surface energy than S1 and S2 by virtue of containing a polar PDMS-PEO copolymer. This is reflected in a higher total surface energy and a much higher proportion of the polar surface energy component

(Table 4.7). All three coatings were 'smooth' in the micrometer range with Ra roughness lower than 0.3 μm.

Table 4.7: Properties of the coatings based on PDMS or PDMS-PEO block copolymer. Ra: arithmetic average of roughness-height. The number of replicates was 3 for contact angle, 2 for the storage modulus and 5 for the roughness. Values shown are mean ± SD. The modulus was measured using the DMA (Chapter 2.9.2.1.).

Coatings		S1	S2	S3
Viscosity (mPa s^{-1})		4000	750	unknown
Modulus (using DMA)	Storage Modulus E' at 20°C (MPa)	0.34 ± 0.01	0.6 ± 0.02	0.96 ± 0.05
Contact angle/ Surface energy	Static Water Contact Angle ($\theta°_{Ws}$)	91.7 ± 1.1	89.7 ± 1	56.3 ± 1.5
	Static Diiodomethane Contact Angle ($\theta°_{Ds}$)	71.4 ± 0.6	69.7 ± 2.5	68.2 ± 2.4
	Total Surface Energy γ_s (mN m^{-1})	24 ± 0.2	25.3 ± 0.9	44.1 ± 0.8
	Dispersive Surface Energy γ_D (mN m^{-1})	19.5 ± 0.5	20.3 ± 1.5	16.8 ± 1.4
	Polar Surface Energy γ_P (mN m^{-1})	4.7 ± 1.1	5 ± 0.5	27.4 ± 1.7
	% Polar surface energy	19.6	19.8	62.0
Roughness	Ra (µm)	0.15 ± 0.01	0.05 ± 0.01	0.23 ± 0.06

4.3.3. Condensation cured silicone hybrids (2011 series)

Table 4.8: Wettability and surface energy of the silicone 'hybrid' wettability series. The number of replicates was 3 for all measurements. Values shown are mean ± SD. The different methods used to measure contact angle are shown using different cell colours. For the measurement of the static contact angle after one month of leaching, the slides were cleaned with a sponge and dried in air for three days before measurements.

Coatings		H	H1	H2	H3	H7	H10
Static Contact Angle (before leaching)	Static Water Contact Angle ($\theta°_{Ws}$)	101.1 ± 0.4	97.7 ± 0.1	83.3 ± 0.9	76.4 ± 0.4	70.4 ± 0.3	64 ± 0.4
	Static Diiodomethane Contact Angle ($\theta°_{Ds}$)	69.6 ± 1.6	67.1 ± 0.8	64.7 ± 0.4	64.7 ± 0.8	63.8 ± 1.1	59.8 ± 0.1
	Total Surface Energy γ_S (mN m^{-1})	23.3 ± 0.8	24.8 ± 0.4	29.4 ± 0.5	32.3 ± 0.4	35.7 ± 0.4	40.6 ± 0.2
	Dispersive Surface Energy γ_D (mN m^{-1})	22 ± 1	23 ± 0.5	22.3 ± 0.2	21.3 ± 0.4	21 ± 0.5	22.4 ± 0.1
	Polar Surface Energy γ_P (mN m^{-1})	1.3 ± 0.2	1.9 ± 0.1	7.1 ± 0.5	11 ± 0.2	14.7 ± 0.2	18.1 ± 0.3
	% Polar Surface Energy	5.6	7.5	24.1	34.0	41.1	44.7
Static Contact Angle (after 1 month of leaching)	Static Water Contact Angle ($\theta°_{Ws}$)	106.2 ± 0.2	97.9 ± 0.4	82.1 ± 1.2	75.6 ± 0.4	71.2 ± 1.1	65.2 ± 0.7
	Static Diiodomethane Contact Angle ($\theta°_{Ds}$)	70.6 ± 0.2	67.4 ± 1	66.4 ± 0.2	65.2 ± 0.3	65.2 ± 0.3	61 ± 0.2
	Total Surface Energy γ_S (mN m^{-1})	22.3 ± 0.1	24.1 ± 0.5	28.2 ± 0.5	31.7 ± 0.7	34.1 ± 0.7	38.8 ± 0.4
	Dispersive Surface Energy γ_D (mN m^{-1})	21.8 ± 0.1	22 ± 0.6	19.1 ± 0.3	18.6 ± 0.2	17.7 ± 0.2	18.9 ± 0.3
	Polar Surface Energy γ_P (mN m^{-1})	0.5 ± 0.3	2.1 ± 0.5	9.1 ± 0.7	13.1 ± 0.7	16.5 ± 0.8	19.8 ± 0.6
	% Polar Surface Energy	2.4	8.5	32.3	41.4	48.2	51.2
Dynamic Contact Angle (no leaching)	Advancing Water Contact angle ($\theta°_{Wadv}$)	108.7 ± 0.5	102.9 ± 2.6	97.1 ± 1.6	97.3 ± 2.4	92.9 ± 1.6	94.2 ± 0.8
	Receding Water Contact angle ($\theta°_{Wrec}$)	64.1 ± 1.9	43.8 ± 4.8	33.6 ± 0.4	32.4 ± 2.7	29.8 ± 1.2	25.4 ± 0.5
	Contact Angle Hysteresis ($\theta°_{Wadv}$ - $\theta°_{Wrec}$)	44.7	59.2	63.5	64.9	63.1	68.8
Air Underwater Contact Angle ($\theta°_{Wund}$)	Contact Angle before leaching	89.2 ± 3.3	87.1 ± 0.9	85.3 ± 0.4	84.8 ± 0.6	82.2 ± 1.2	65.5 ± 1
	Contact Angle after 1 month of leaching	91.6 ± 2.2	76 ± 1.2	68.3 ± 1.7	68.6 ± 1	70.5 ± 1.5	60.8 ± 1.5

The silicone 'hybrid' coatings produced with different blended ratios of PDMS polymer and PDMS-PEO copolymer had a graduated range of wettabilities/surface energies. Static water contact angles (measured on dry coatings in air) showed a range of wettability from 64° to 101.1° (Table 4.8 before leaching). This was reflected in a similarly wide range of total surface energies (23.3 to 40.6 mN m^{-1}) and in the ratio of polar to dispersive surface energy components (Table 4.8; Fig. 4.1a (before leaching)). Measurements of static contact angle and surface energy were also obtained after a month of leaching (in deionised water), followed by drying in air, in order to explore the stability of the coatings after immersion. The results showed that the coatings after immersion had very similar wettabilities (from 65.2° to 106.2°) and surface energies (from 21.8 to 38.8 mN m^{-1}) compared with coatings before immersion, demonstrating that the surface properties of the coatings did not change substantially after immersion and re-drying (Fig. 4.1a and Table 4.8). Thus, the original design criterion to produce a set of stable coatings with different hydrophobic/hydrophilic balances was obtained.

However, it could be argued that any change in properties as a consequence of immersion could have been reversed by drying the coatings in air before remeasuring their static contact angles. Therefore further information on wettability and stability of hydrated coatings was obtained by the 'captive bubble' method in which the contact angle of air bubbles was measured underwater before (i.e. the measurements were obtained after 30 s to 1 min of immersion in MilliQ water) and after one month of leaching (Table 4.8 and Fig. 4.1b). The data of the underwater contact angles before one month's leaching came from an experiment described in Chapter 10, but for the purpose of observing the effect of immersion on the wettability it was necessary to introduce the results in this Chapter. These measurements showed that a range of wettabilities was also observed on immersed coatings before leaching and as expected, the greater the proportion of polar PEO in the blend, the lower the contact angle/the greater the wettability. However, the range of wettabilities was somewhat

narrower than that obtained from static contact angle measurements on dry coatings. Two effects were observed: a) the wettabilities of coatings between the two extremes tended to become more uniform; b) coatings containing the highest proportion of PDMS (H, H1) appeared to become less hydrophobic after immersion. The latter effect can be anticipated since it has been demonstrated that in air, the non-polar methyl groups (i.e. $-CH_3$) of the PDMS backbone orient themselves towards the air interface in order to reduce the surface energy of the system (Chen et al. 2004). However, underwater, in a more hydrophilic environment, it would be anticipated that the methyl groups would bury themselves in the bulk, and this would be reflected in reduced water contact angles- as observed.

Leaching the coatings for 1 month tended to further reduce the captive bubble contact angles, i.e. make the coatings more hydrophilic, except for H, the most hydrophobic coating containing no PEO (Table 4.8, Fig 4.1b). The tendency of amphiphilic coatings containing PEG to become more hydrophilic following immersion, albeit for shorter periods of time than those used here, was recently demonstrated by Cho et al. (2012) using the captive bubble method. They attributed this to progressive exposure of the polar PEG groups.

Finally, the dry coatings (no immersion) were examined by dynamic contact angle analysis. This provides values for the advancing and receding contact angles of a water droplet and as discussed in Chapter 2, the resulting values, in particular the difference between advancing and receding angles, known as 'contact angle hysteresis' is often taken to indicate the degree of surface reconstruction following immersion (Schmidt et al. 2004). All coatings showed substantial contact angle hysteresis with progressively increasing values as the proportion of PEO in the coatings increased. Similar effects were noted for amphiphilic coatings containing PEG (Cho et al. 2012). Taken together with the captive bubble measurements, these results suggest significant surface restructuring of the coatings following immersion, i.e. reorganisation of PEO and PDMS domains bringing more PEO to the surface.
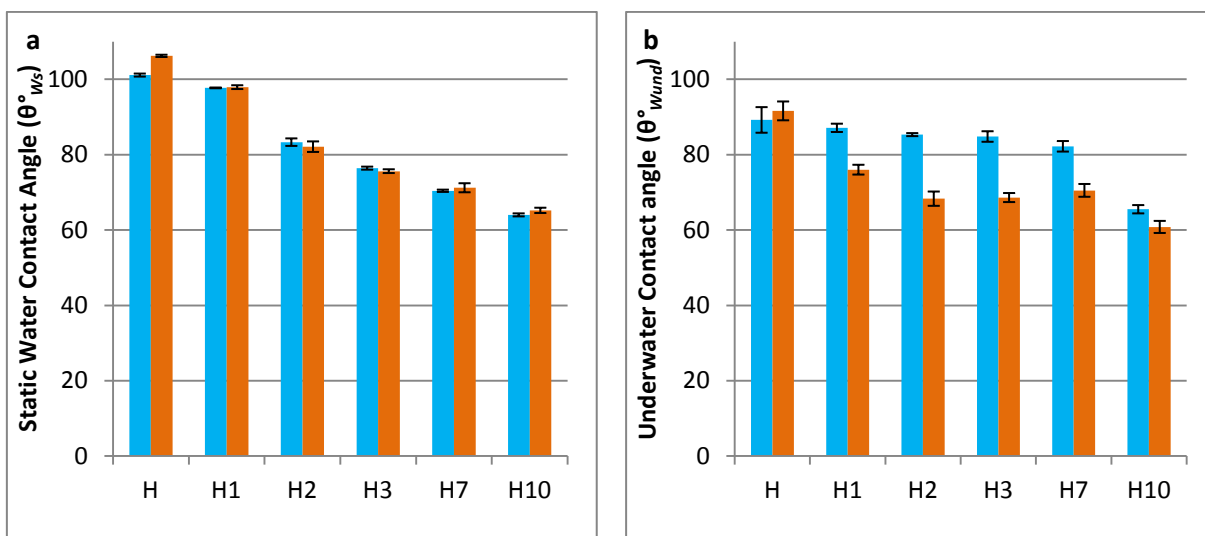
Figure 4.1: Comparison of surface properties of silicone 'hybrid' coatings before and after a month of leaching. a) Static water contact angle before leaching (blue bars) and after one month leaching in deionised water followed by drying in air (orange bars). b) Underwater contact angle before leaching (blue bars) and after one month leaching in deionised water (orange bars). Values shown are mean of three replicates ± SD. The values are also presented in Table 4.7.

Silicone 'hybrid' coatings had similar mechanical properties in terms of elastic modulus (Fig. 4.9). All these coatings were 'smooth' in the micrometer range with Ra roughness lower than 0.3 μm (Fig. 4.9).

In conclusion, this series of coatings had similar mechanical properties and a range of wettability, they thus provide a good test of the effect of wettability/surface energy/polarity on the attachment and adhesion strength of ectocarpoid algae.

Table 4.9: Properties of the silicone 'hybrid' series. Ra: arithmetic average of roughness-height. The number of replicates was 3 for all the property measurements. The modulus was measured using the elongation measurement method (Chapter 2.9.2.2.). Values shown are mean ± SD.

Coatings		H	H1	H2	H3	H7	H10
Elastic Modulus (MPa)		1.02 ± 0.09	0.92 ± 0.03	0.94 ± 0.03	0.94 ± 0.03	0.98 ± 0.07	1.07 ± 0.06
Roughness	Ra (μm)	0.23 ± 0.05	0.07 ± 0.00	0.09 ± 0.07	0.24 ± 0.16	0.21 ± 0.04	0.25 ± 0.29
Dry Film Thickness (μm)		284 ± 45	291 ± 7	483 ± 154	314 ± 31	231 ± 14	155 ± 10

4.3.4. Condensation cured silicone elastomer coatings with different modulus (2012 series).

The five silicone elastomer coatings produced with PDMS polymers with different viscosities/molecular weights, were designed to show a range of elastic moduli. As anticipated, being PDMS-based, all coatings were hydrophobic, with similar water contact angles, ca. 100° and similar surface energies (~23 mN m^{-1}) (Table 4.10). All the coatings were 'smooth' in the micrometer range as Ra roughness was 0.21 μm or less. The thickness of this series of coatings was similar between the coatings and was higher than 100 μm, so the thickness should not affect the adhesion strength of fouling organisms as Chaudhury et al. (2005) showed that thickness of coatings has an effect on the adhesion strength of spores and sporelings of *U. linza*, if it is lower than 100 μm. Results showed that all the elastic modulus values of the coatings were significantly different (Table 4.10; p≤0.05, GZLM, Pairwise comparison). However, whilst it was anticipated that the use of PDMS with such wide differences in viscosity/molecular weight would give moduli differing by at least by an order of magnitude, the determined values only ranged between 0.7 to 1.5 MPa.

Table 4.10: Properties of the silicone "modulus" series. Ra: arithmetic average of roughness-height. The number of replicates was 3 for all the property measurements. The modulus was measured using the elongation measurement method (Chapter 2.9.2.2). Values shown are mean ± SD.

Coatings		M1	M2	M3	M4	M5
PDMS viscosity (mPa s^{-1})		72	4000	6000	14000	50000
Elastic Modulus (MPa)		1.5 ± 0.02	1.04 ± 0.02	0.91 ± 0.03	0.85 ± 0.04	0.73 ± 0.03
Contact angle	Static Water Contact Angle ($\theta°_{Ws}$)	102.6 ± 0.7	100.8 ± 1.1	99.4 ± 1	99.5 ± 0.5	99.1 ± 1.8
	Static Diiodomethane Contact Angle ($\theta°_{Ds}$)	70.4 ± 0.6	69.7 ± 0.6	69.1 ± 0.8	69 ± 0.3	69 ± 2.5
	Total Surface Energy γ_S (mN m^{-1})	22.3 ± 0.3	22.7 ± 0.3	23.2 ± 0.6	23.2 ± 0.1	23.2 ± 1.4
	Dispersive Surface Energy γ_D (mN m^{-1})	21.2 ± 0.4	21.2 ± 0.4	21.3 ± 0.3	21.4 ± 0.3	21.3 ± 1.2
	Polar Surface Energy γ_P (mN m^{-1})	1.2 ± 0.2	1.5 ± 0.3	1.8 ± 0.3	1.8 ± 0.2	1.9 ± 0.2
	% Polar Surface Energy	5.2	6.5	7.8	7.6	8.1
Rough-ness	Ra (μm)	0.05 ± 0.02	0.04 ± 0.02	0.04 ± 0.01	0.07 ± 0.02	0.21 ± 0.13
Dry Film Thickness (μm)		200 ± 56	278 ± 22	268 ± 33	314 ± 78	252 ± 27

4.3.5. Characterisation of standard coatings

Three standard, silicone-based commercial coatings were used during this project: T2, IS700, IS900, plus Nexterion® glass. The surface properties of these standard surfaces are shown in Table 4.11. IS700, being a PDMS-based coating, was hydrophobic, with a water contact angle ca. 102°, a surface energy of 32 mN m^{-1} and almost no polar component. However, IS900 was amphiphilic, with a water contact angle ca. 75.9°, similar surface energy than IS700 and a equal ratio of polar and dispersive components, reflecting its amphiphilic design. They both had similar elastic moduli (1.3 MPa) and they were 'smooth' surfaces in the micrometer range with Ra roughness lower or equal to 0.3 μm.

T2, being a PDMS-based coating, was a hydrophobic surface with a water contact angle ca. 100.9° and it had no polar component in contrast to Nexterion® glass, which was hydrophilic with water contact angle ca. 12.1° and a high polar component. T2 had an elastic modulus similar to the two Intersleek materials, while Nexterion®, being a hard glassy surface, had a much higher elastic modulus. Both surfaces were 'smooth' in the micrometer range with Ra roughness lower than 0.3 μm.

Table 4.11: Properties of standard surfaces. Ra: arithmetic average of roughness-height. The number of replicates was 3 for all the property measurements. The modulus was measured using the elongation measurement method (Elastic modulus; Chapter 2.9.2.2) and also using DMA (storage modulus; Chapter 2.9.2.1) for both Intersleek coatings. The elastic modulus value for T2 was taken from Feinberg et al. (2003). Values shown are mean of 3 replicates ± SD. Elastic modulus and Ra values for Nexterion® glass were that provided by the manufacturer (http://www.schott.com/nexterion/english/application/faq/general.html?so=uk&lang=english.

	Coatings	IS700 grey	IS900 grey	T2	Nexterion glass
Contact angle	**Static Water Contact Angle ($\theta°_{Ws}$)**	102 ± 0.5	75.9 ± 0.53	100.9 ± 0.8	12.1 ± 1.2
	Static Diiodomethane Contact Angle ($\theta°_{Ds}$)	54.4 ± 1.1	74.2 ± 1	69.9 ± 0.9	37.5 ± 1.8
	Surface Energy γs (mN m^{-1})	32 ± 0.7	29.1 ± 0.7	23.3 ± 0.4	70.8 ± 0.3
	Dispersive Surface Energy γD (mN m^{-1})	31.7 ± 0.8	13.7 ± 1.1	23.2 ± 0.4	24.1 ± 0.8
	Polar Surface Energy γP (mN m^{-1})	0.3 ± 0.1	15.4 ± 0.6	0.06 ± 0.0	46.7 ± 0.3
	% Polar surface energy	0.8	52.9	0.3	66
Elastic modulus (MPa)		1.4 ± 0.0	1.2 ± 0.1	1.4	6.4 x 10^4
Storage modulus (MPa)		1.1	1		
Roughness	**Ra (μm)**	0.2 ± 0.0	0.3 ± 0.1	0.2 ± 0.05	0.003
Dry film Thickness (μm)		212 ± 34	311 ± 61	91 ± 21	0

5. INITIAL LABORATORY ASSAYS TO INVESTIGATE THE INFLUENCE OF COATING MODULUS ON THE ADHESION OF *E. CROUANIORUM* AND *U. LINZA*

5.1. Introduction

Biofouling research has been looking at the effect of surface and bulk properties of coatings on the adhesion of marine fouling organisms, especially on the effect of wettability/surface energy. It has been demonstrated that these surface properties influence the attachment and/or the adhesion strength of marine organisms such as the green alga *Ulva linza*, barnacles and bacteria (Chapters 3; e.g. Schilp et al. 2007; Finlay et al. 2010). However, other properties such as modulus and thickness are of importance and are known to have an effect on the attachment and/or the adhesion strength of hard fouling organisms such as barnacles and pseudobarnacles (Berglin et al. 2003; Stein et al. 2003; Kim et al. 2007 and 2008; Kaffashi et al. 2012). In particular, for coatings of equivalent surface energy and thickness, fracture mechanics suggests that the adhesion strength of hard-fouling organisms on elastomeric surfaces should be proportional to $(\gamma E)^{\frac{1}{2}}$ where γ is the surface energy and E is the elastic modulus, i.e. the harder the coating, the stronger the adhesion (Brady and Singer 2000). However, the situation for compliant soft-fouling organisms is somewhat different and in the study of the influence of modulus of PDMS coatings on the adhesion of a marine alga, Chaudhury et al. (2005) showed that the adhesion strength of sporelings of *U. linza* on model PDMS network coatings was strongly influenced by elastic moduli as it was weaker on the coatings having low moduli (0.2 and 0.8 MPa) compared to coatings with higher moduli (2.7 and 9.4 MPa). In addition, Weinman et al. (2009) confirmed that the sporelings of *U. linza* had higher adhesion on a high modulus surface (i.e. 18 MPa) than on a low modulus surface (i.e. 1.2 MPa).

Since the only study of the effect of modulus on adhesion of marine algae was performed with the green alga *U. linza,* at an early stage in the development of this project it was

decided to make some initial studies on the effects of modulus on ectocarpoid algae, using two sets of coatings available within International Paint, viz. a small set of silicone-based coatings with moduli <1 MPa, and a small set of fluoropolymer-based coatings with moduli anticipated to be in the range 2-20 MPa. Although it was realised that these two sets differed significantly in their chemistry it was considered that this initial study would provide a guide to subsequent coating designs based on a single coating chemistry.

Although fluoropolymers are normally associated with attempts to make coatings more hydrophobic, because of the low surface energy donated by fluorine groups, the particular set of fluoropolymers available within International Paint also enabled some coatings to be prepared which differ in modulus. The preparation of these perfluoropolyether (PFPE) or fluoropolymer coatings was described in Chapters 4.2.2. and 4.3.4. They were produced from in-house modifications to Fluorolink D or Fluorolink E, which are polymer modifiers developed by Solvay Solexis to improve the performance of polymeric materials by 'combining' the typical properties of fluorinated compounds with untypical physical properties such as low glass transition temperature and low viscosity. By using modified Fluorolink D materials with different molecular weight, it was possible to produce two coatings with different moduli (20.0 and 7.75 MPa for mD10 and mD10-H respectively), but similar, low surface energies (16.9-19.8 mN m^{-1}, Table 4.6). The initial plan to produce a third coating using Fluorolink E was only partly successful. As shown in Chapter 4.3.4., the modulus of coating mE10-H (1.95 MPa) was significantly different to that of the other two coatings but the total surface energy and the polarity of this coating, was substantially higher compared with the other two coatings on account of the fact that the modified Fluorolink E10-H contains poly(ethylene oxide) PEO groups. This poses certain limitations to the analysis of the results of the adhesion experiments.

The second set of coatings based on silicone was the three PDMS coatings presented in Chapters 4.2.2 and 4.3.2: viz. S1, S2 and S3 (Tables 4.2 and 4.7). The two hydrophobic

coatings S1 and S2 were produced from PDMS polymers with different molecular weight, giving moduli of 0.34 to 0.6 MPa. The third coating S3, produced from PDMS-PEO had a higher modulus of 0.96 MPa, but due to the presence of PEO compound, the coating also had a higher surface energy than S1 and S2. As for the fluoropolymer coatings, the fact that two properties change for one of the coatings poses certain limitations to the analysis of the results of the adhesion experiments.

The aim of this Chapter was to observe how the modulus of coatings could influence the initial attachment and adhesion strength of ectocarpoid algae and to compare the obtained results with the adhesion strength of *U. linza*. The starting hypothesis based on the results of Chaudhury et al. (2005) for sporelings of *U. linza*, was that the increase of moduli of the silicone-based coatings would increase the release of *E. crouaniorum*. However, it was also considered that the increase of moduli presented by the fluoropolymer coatings would have relatively little effect on the increase of adhesion of *E. crouaniorum*, as the range of modulus of the fluoropolymer coatings was higher than the modulus that had an influence on the adhesion of *U. linza* sporelings (Chaudhury et al. 2005).

5.2. Materials and methods

The fluorinated coatings and the PDMS block copolymer coatings were leached for 1 week in a 30-liter tank of deionised water recirculated through a carbon filter before the experiment, while IS700 and IS900 were leached in a similar tank for at least a month, in order to remove residual curing agents (as explained in Chapter 3.2.2). Two algal species were tested: *E. crouaniorum* CCAP 1310/300 and *U. linza,* following the methods explained in Chapters 2.8 and 3.2. Experiments with both sets of coatings were conducted at the same time and with the same set of internal standards (IS900/IS700). However, for clarity the results are presented separately.

After blending and filtration, the starting inoculum (i.e. the filtrate) for adhesion assays with *E. crouaniorum* consisted of small filaments averaging 5 ± 1 cells (mean of 50 observations ± 2 x SE). The experiment was performed twice, the results from both experiments were similar. The results of one experiment are presented. Statistical analysis of the adhesion data is explained in Chapter 2.10, and statistical tables for the whole Chapter are presented in Appendix 4.

5.3. Results

5.3.1. Results with the fluoropolymer coatings

E. crouaniorum

The amount of unattached filaments was quantified after 8 days of growth (Table 5.1) through chlorophyll *a* (chl *a*) determination (Chapter 2.5). Despite all surfaces being inoculated with the same concentration of filaments, there were marked differences between the coatings. The dishes containing the coating mE10-H and the two Intersleek coatings had the lowest amount of unattached biomass (Table 5.1; p≤0.05, GZLM, Pairwise comparison). Unattached biomass in dishes containing the two low surface energy coatings, mD10 and mD10-H was significantly different.

Table 5.1: Unattached biomass after 8 days of growth of tested surfaces, as measured by chl *a*. Means of 3 replicates ± SD. Values that are significantly different at p≤0.05 in GZLM test are indicated by different letters after the unattached biomass values. The three experimental coatings are arranged in order of increasing modulus (mE10-H= 1.95 MPa, mD10-H= 7.75 MPa, mD10=20 MPa).

Coatings	IS700	IS900	mE10-H	mD10-H	mD10
Total unattached biomass (µg chl *a*)	0.2 ± 0.2^a	0.1 ± 0.1^a	0.3 ± 0.3^a	1.1 ± 0.2^b	2.1 ± 0.1^c

Before exposing the attached filaments to a shear stress, they were incubated for a further 6 days of growth (i.e. 14 days in total). The amount of biomass of attached filaments on the different coatings was measured and was different before and after a shear stress exposure of 8 Pa (Figs. 5.1a and b). The relative performance of the standard coatings IS700 and IS900 was consistent with the results reported in Chapter 3, i.e. high initial attached biomass and greater ease of removal under shear from IS900 compared with IS700 ($p \leq 0.05$, RM ANOVA).

All three experimental coatings had a lower initially attached biomass compared with the Intersleek standards. There were also significant differences in initially attached biomass between the three experimental coatings, the biomass of the attached filaments on the coating mD10-H being significantly higher than on the coating mD10 ($p \leq 0.05$, GZLM, Pairwise comparison); while mE10-H had the lowest attached biomass (Fig. 5.1a).

Removal of *E. crouaniorum* from the three experimental coatings under shear was lower than from IS900 and was either greater or similar to IS700 (Fig. 5.1b). Between the three experimental coatings, the attached filaments on mD10-H had significantly higher adhesion than on mD10 and mE10-H, both of which had intermediate levels of removal ($p \leq 0.05$, GZLM, Pairwise comparison). Comparing the two coatings mD10 and mD10-H with similar surface energies, mD10, which had the higher modulus, had lower initial attached filaments and higher percentage removal of these filaments compared to mD10-H. It is therefore possible to conclude that these two coatings showed that the increase of modulus (in the range of 7.75 to 20 MPa) decreases the attachment and adhesion strength of *E. crouaniorum*. However, no conclusion can be drawn from the differences observed on the coating mE10-H as this coating had a different modulus to the other two, but also a very different, and more polar surface energy. It can just be concluded that filaments of *E. crouaniorum* attached to a hydrophilic coating with low modulus seemed to have lower adhesion strength than on harder and more hydrophobic coatings.

As for the experiments using *E. crouaniorum* described in Chapter 3, the two morphologies were present before shear stress exposure i.e. 'star morphology' and 'normal morphology' (in Chapter 3, Fig. 3.5) on all the surfaces. However, after the shear stress exposure, the normal morphology was the most represented.
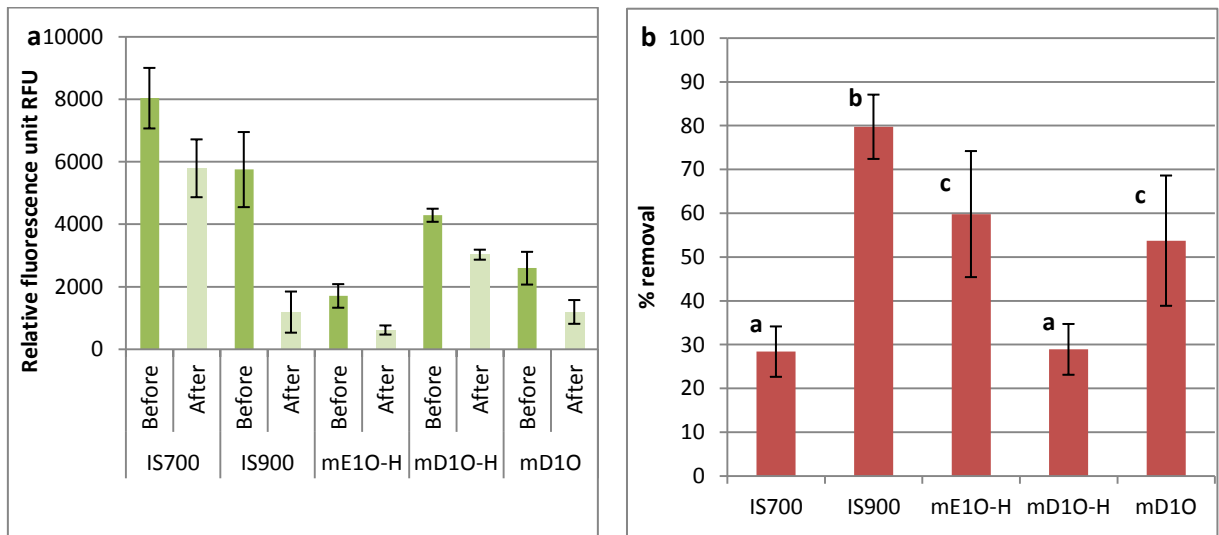
Figure 5.1: Adhesion assays with *E. crouaniorum.* a) Biomass of attached alga before and after exposure to a wall shear stress of 8 Pa, on 5 different surfaces, after 14 days of incubation at 15°C. Biomass was measured as relative fluorescence units. b) Percentage removal after exposure to 8 Pa shear stress, calculated from data presented in a). Means from 9 replicates ± 2 x SE. Values that are significantly different at p≤0.05 in GZLM test are indicated by different letters above the bars. The three experimental coatings are arranged in order of increasing modulus (mE10-H= 1.95 MPa, mD10-H= 7.75 MPa, mD10=20 MPa).

U. linza

After 6 days of growth, sporelings of *U. linza*, covered all surfaces. Growth on all three experimental coatings was not significantly different (Fig. 5.2a; p≤0.05, GZLM, Pairwise comparison). There were similar, high levels of biomass on the standard coatings IS700 and IS900 (Fig. 5.2a), and adhesion strength under shear was substantially weaker on IS900 compared with IS700 (Fig. 5.2b, p≤0.05, GZLM, Pairwise comparison).

Biomass after exposure to 50 Pa shear stress showed distinct differences between coatings and there was no, or very little removal of sporelings under shear from either mD10 or mD10-H whilst removal from mE10-H was almost total (Fig. 5.2b).

Since the percentage removal from mD10 and mD10-H was close to zero, no effect was observed due to the modulus. However, the adhesion strength of the sporelings was significantly different between the two hydrophobic coatings (mD10 and mD10-H) and mE10-H, the sporelings attached weakly to the amphiphilic fluoropolymer coating (with lower modulus) compared to the hydrophobic coating (with high or medium modulus). However, comparisons between these coatings are difficult to make since there were differences in both modulus and surface energy: if two properties are different, it is impossible to conclude if it is one or the combination of both that influences the adhesion strength.
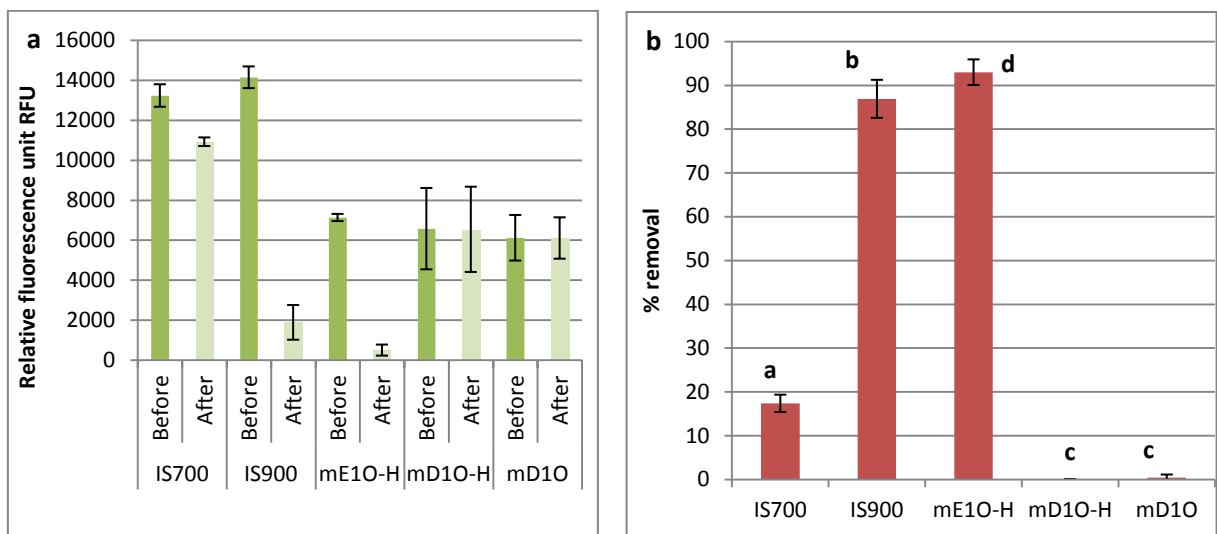
Figure 5.2: Adhesion assays with *U. linza.* a) Biomass of attached sporelings before and after exposure to a wall shear stress of 50 Pa, on 5 different surfaces, after 6 days of incubation at 18°C. Biomass was measured as relative fluorescence units. b) Percentage removal after exposure to 50 Pa shear stress, calculated from data presented in a). Means of 6 replicates ± 2 x SE. Values that are significantly different at p≤0.05 in GZLM test are indicated by different letters above the bars. The three experimental coatings are arranged in order of increasing modulus (mE10-H= 1.95 MPa, mD10-H= 7.75 MPa, mD10=20 MPa).

5.3.2. Results of the silicone coatings

E. crouaniorum

After 8 days of growth, the amount of unattached filaments was quantified (Table 5.2) through chlorophyll *a* (chl *a*) determination (Chapter 2.5). Although all the surfaces had been inoculated with the same concentration of filaments, there were marked differences between the coatings. The biomass of unattached filaments in dishes containing the coating S3 was significantly greater than for all the other coatings (Table 5.2; p≤0.05; GZLM, Pairwise comparison).

Table 5.2: Unattached biomass after 8 days of growth of silicone elastomer coatings, as measured by chl *a*. Means of 3 replicates ± SD. Values that are significantly different at p≤0.05 in GZLM test are indicated by different letters after the unattached biomass values. The three experimental coatings are arranged in order of increasing modulus (S1=0.34 MPa; S2=0.6 MPa and S3=0.96 MPa).

Coatings	IS700	IS900	S1	S2	S3
Total unattached biomass (µg chl *a*)	0.1 ± 0.1^a	0.2 ± 0.2^a	0.7 ± 0.3^a	0.6 ± 0.2^a	1.4 ± 0.4^b

Before the exposure of the attached filaments to 8 Pa shear stress, the coatings were incubated for 6 further days (i.e. 14 days in total). The biomass of attached filaments on the different surfaces was measured and showed differences between the coatings before and after the shear stress exposure (Figs. 5.3a/b).

The differences in initial attached biomass were not as expected from the unattached filament results (Table 5.2 and Fig. 5.3a). The two Intersleek coatings had higher initial biomass attached to their surfaces compared to the test coatings. The statistical analysis showed that the biomass on coating S1 was significantly similar to S3, which had the lowest biomass, but also to S2, which had an intermediate initial biomass (Fig. 5.3a; p≤0.05, GZLM, Pairwise comparison).

Figure 5.3b shows that the adhesion strength of attached filaments on the coatings IS900 and S3 was the lowest with a % removal up to 79 %. The adhesion strength of *E. crouaniorum* on the other coatings was higher with % removal of 22 % for S2, 28 % for IS700 and 56 % for S1. The three test coatings were all significantly different; the filaments attached to their surface had different adhesion strength (Fig. 5.3b; p≤0.05, GZLM, Pairwise comparison).

Comparing the two hydrophobic coatings S1 and S2 with moduli of 0.34 and 0.6 MPa respectively, the attached filaments adhered less strongly to S2. It is therefore possible to conclude that these two coatings showed the anticipated effect of modulus in a range of 0.34 to 0.6 MPa, i.e. lower adhesion on the lower modulus coating. However, the results of S3 were not as anticipated; despite S3 having the highest modulus, the attached filaments had the lowest adhesion strength on this coating. It could maybe be explained by the fact that S3 had a higher surface energy and was more polar than S1 and S2, and as shown in Chapter 3, adhesion of *E. crouaniorum* tends to be weak on more hydrophilic or amphiphilic surfaces.
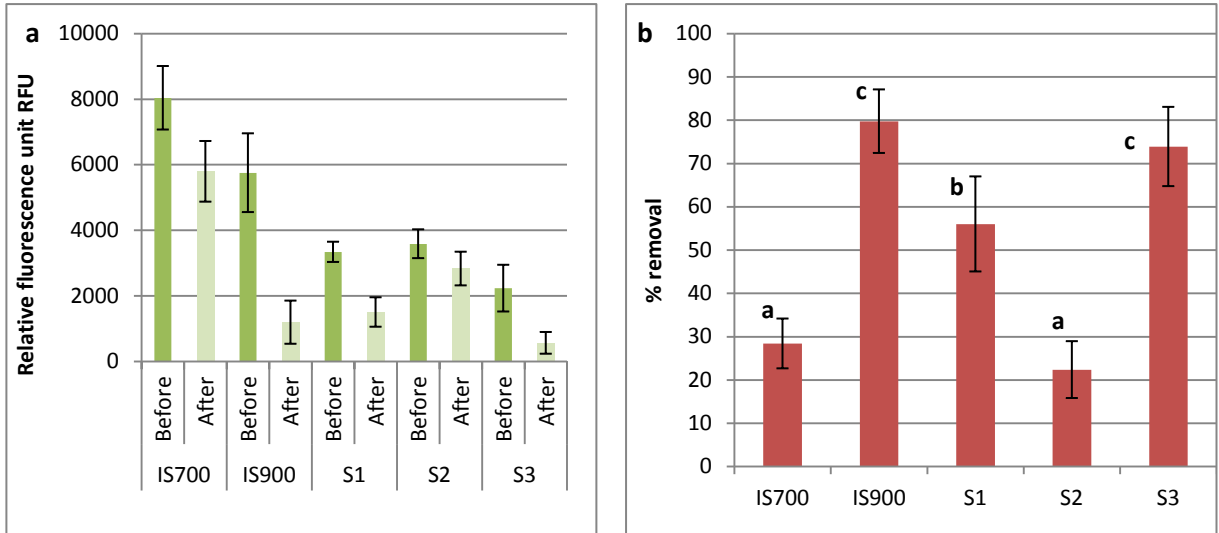
Figure 5.3: Adhesion assays with *E. crouaniorum*. a) Biomass of attached alga before and after exposure to a wall shear stress of 8 Pa, on 5 different surfaces, after 14 days of incubation at 15°C. Biomass was measured as relative fluorescence units. b) Percentage removal after exposure to 8 Pa shear stress, calculated from data presented in a). Means from 9 replicates ± 2 x SE. Values that are significantly different at p≤0.05 in GZLM test are indicated by different letters above the bars. The three experimental coatings are arranged in order of increasing modulus (S1=0.34 MPa; S2=0.6 MPa and S3=0.96 MPa).
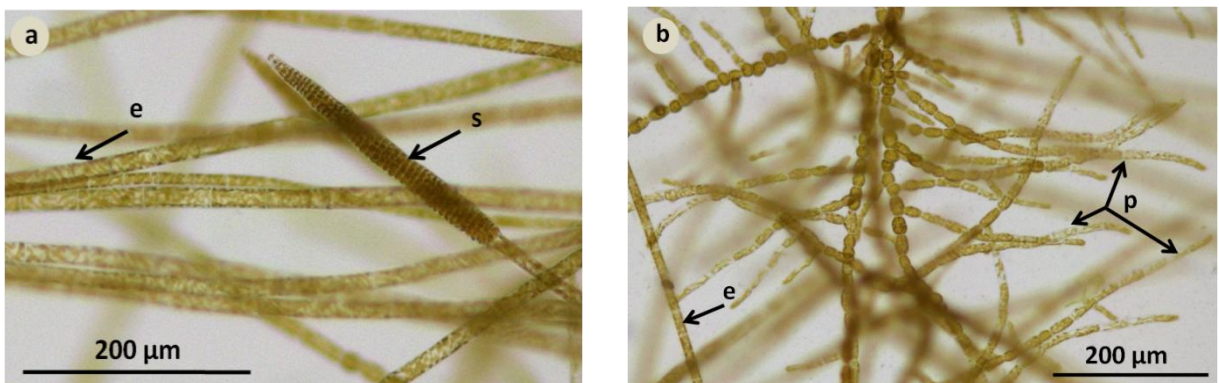
Figure 5.4: Filaments of *E. crouaniorum* on surfaces after exposure to shear stress. Prostrate filaments (p) were paler in colour than the erect filaments (e) due to their lower concentration of chloroplasts inside the cells, and presence of a sporangium (s).

As for the experiments using *E. crouaniorum* described in Chapter 3, before the shear stress exposure, two morphologies were observed: 'star morphology' and 'normal morphology' (in

Chapter 3, Fig. 3.4) on all the surfaces. However, after the shear stress exposure, the normal morphology was the most represented (Fig. 5.4).

U. linza

After 6 days of growth, the biomass of sporelings on the coatings was different, which probably largely reflects differences in the density of spores that settled on the surface. The two Intersleek coatings had the highest initial biomass compared to the other coatings, which had relatively similar initial biomass. The coatings S1 and S2, which had the low biomass were grouped together (Fig. 5.5a; $p \leq 0.05$, GZLM, Pairwise comparison). However, they were significantly different from S3, which had intermediate amount of attached biomass.

After exposure to 50 Pa shear stress, the remaining biomass was different between the coatings. With 87 % removal, sporelings adhered weakly to IS900 compared to all other coatings (Fig. 5.5b). The sporelings on the coating IS700 had high adhesion strength with only 17 % removal, but this was higher than from the test coatings. The adhesion strength of the three test coatings was not significantly different, with a percentage removal up to 9 % and was higher than the two Intersleek coatings ($p \leq 0.05$, GZLM, Pairwise comparison). As the percentage removal was low (<10 %), it was not possible to draw any conclusion from the data. It is possible that the exposure to a higher shear stress values would have shown differences between the coatings.
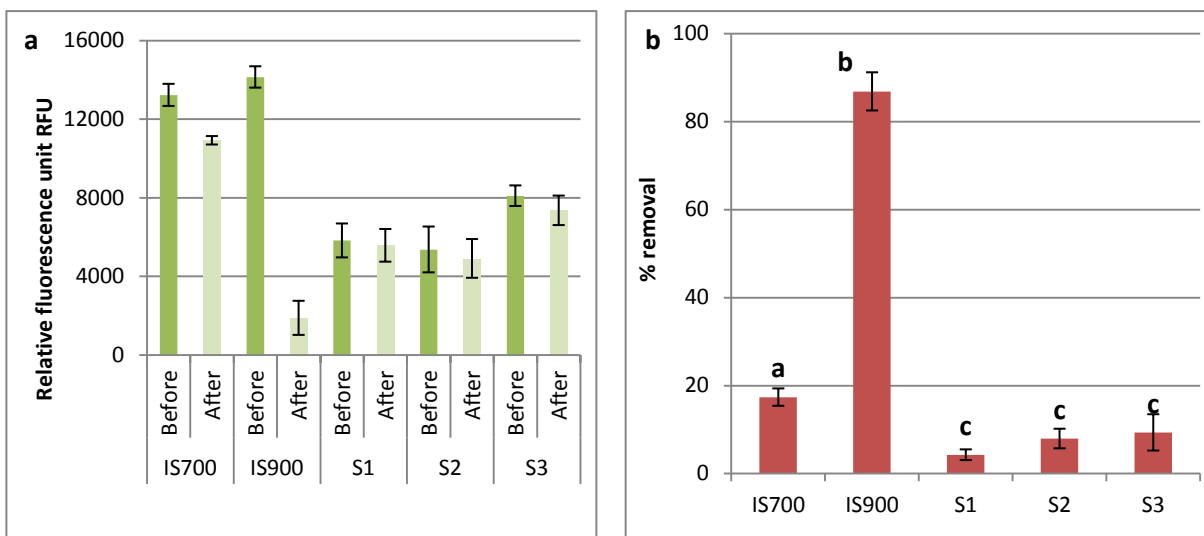
Figure 5.5: Adhesion assays with *U. linza.* a) Biomass of attached sporelings before and after exposure to a wall shear stress of 50 Pa, on 5 different surfaces, after 6 days of incubation at 18°C. Biomass was measured as relative fluorescence units. b) Percentage removal after exposure to 50 Pa shear stress, calculated from data presented in a). Means of 6 replicates ± 2 x SE. Values that are significantly different at p≤0.05 in GZLM test are indicated by different letters above the bars. The three experimental coatings are arranged in order of increasing modulus (S1=0.34 MPa; S2=0.6 MPa and S3=0.96 MPa).

5.4. Discussion

The results on the attachment and adhesion strength of *E. crouaniorum* with the commercial 'standard' coatings IS700 and IS900 were similar to those reported in Chapter 3 -i.e. adhesion strength on the amphiphilic IS900 was significantly weaker than on IS700-demonstrating the consistency of the bioassay between different experiments.

The general starting hypothesis behind these experiments was that the adhesion strength of *E. crouaniorum* would be positively correlated to coating modulus with low adhesion strength on coatings with low modulus (i.e. lower than 3 MPa; the silicone-based coatings) and higher adhesion strength on coatings with higher modulus (the fluoropolymer coatings). To test this hypothesis, a set of three fluoropolymer coatings were used with the following moduli 1.95

MPa (mE10-H), 7.75 MPa (mD10-H) and 20.0 MPa (mD10). The results show that this simple hypothesis was not supported since there was no direct correlation between ease of removal of biomass under shear and modulus, adhesion strength being greatest on mD10-H, the coating of intermediate modulus. However, it must be recalled that whilst coatings mD10 and mD10-H differed in modulus, and had very similar surface energies, coating mE10-H was a very polar coating with a correspondingly high surface energy. This makes it difficult to compare the results for this coating with the other two since two properties were changing simultaneously. When the two coatings with similar surface energies were compared directly, then it appeared that there was an effect of modulus but unexpectedly, attachment and adhesion strength of *E. crouaniorum* was apparently negatively correlated with modulus as the higher the modulus was, the lower the initial attachment and adhesion strength was. This result is impossible to reconcile with any current model of the influence of modulus on release of soft-fouling organisms under shear (e.g. Chaudhury et al. 2005) suggesting that some other parameter may be influencing adhesion of *E. crouaniorum* on these coatings.

However, for the silicone-based coatings, the obtained results were different. The two hydrophobic coatings S1 and S2 performed differently, showing that the determined moduli of these two coatings respectively 0.32 and 0.6 MPa influenced the adhesion strength of *E. crouaniorum*. The results obtained from these two hydrophobic coatings S1 and S2, made from two different molecular weights of PDMS, support the hypothesis since the attached filaments on the coating S1 adhered weakly to the surface compared to S2. However, the results obtained with coating S3 do not support the conclusion. This could be explained as the coating S3 was hydrophilic and *E. crouaniorum* does seem to attach weakly to hydrophilic and amphiphilic surfaces, whatever the modulus is (Chapter 3 and results obtained with the fluoropolymer coatings in this Chapter).

To summarise these results, these two sets of coatings showed different effects on the adhesion strength of *E. crouaniorum*. Both, positive and negative relationships were

observed between the adhesion strength and the modulus of the test coatings. However, the range of moduli was different, the fluoropolymers had a range between 1.95 and 20 MPa while the silicone-based coatings were all below 1 MPa. Moreover, both sets of coatings showed that whatever the modulus was, if the coating was hydrophilic, the adhesion strength of *E. crouaniorum* was relatively weak. In the light of this confusing result, a different, more extensive set of hydrophobic coatings with varying modulus, based on different molecular weight of PDMS, was constructed in 2012 (see Chapter 8) to investigate systematically how cross-link density and modulus influence the adhesion strength of *E. crouaniorum*.

For both sets of coatings, levels of surface colonisation of *U. linza* sporelings were highest on the Intersleek coatings compared to the test coatings (both sets). These differences might reflect differences in the level of initial spore settlement and typically spore settlement in *U. linza* is favoured by low surface energy (Callow and Callow 2005; Bennett et al. 2010). However, spore settlement in the reported experiment was not determined since the main interest was in fouling-release performance. Therefore, it is not possible to comment on the reasons for the observed differences.

With regard to the results with *U. linza*, for the two standard Intersleek coatings the weaker adhesion strength on IS900 compared with IS700 was similar to that shown in Chapter 3 and was similar to the adhesion strength of spores observed in previous studies (Thompson et al. 2010), and in this respect *E. crouaniorum* and *U. linza* were similar. However, it should be noted that removal of *U. linza* from these coatings was achieved at 50 Pa shear stress compared to the 8 Pa used for *E. crouaniorum* – indicating that the adhesion strength of *U. linza* was substantially greater.

6. LABORATORY ASSAYS OF ADHESION TO SILICONE 'HYBRID' COATINGS WITH SYSTEMATIC VARIATIONS IN SURFACE ENERGY AND WETTABILITY

6.1. Introduction

One of the most studied theories to account for the adhesion properties of cells and organisms in relation to substratum properties, is the so-called 'Baier curve'. Baier and DePalma (1971) postulated a complex relationship between adhesion strength of organisms and substratum surface energy (or surface tension) (Fig. 6.1) in which there is a zone of minimal adhesion (the 'Baier minimum') on surfaces with surface energy between 20 and 30 mN m^{-1}. Since then a number of researchers have demonstrated a similar relationship for bacteria on different test surfaces. For example, Dexter et al. (1975; Dexter 1976 and 1979) showed that the number of attached bacteria after immersion in natural seawater followed the 'Baier curve' with lower adhesion around 25 mN m^{-1}. Zhao et al. (2005 and 2007) also showed a minimal adhesion for *Escherichia coli* on Ni-Cu-P-PTFE coatings, which have a surface energy of 25-30 mN m^{-1}. However, all of the previous cited studies have used diverse surfaces (glass, Teflon, steel, fluoropolymer coatings, poly(ethylene)), with widely different physico-chemical properties (polarity, roughness, modulus), not just surface energy.

On the other hand, while systematic studies of the effect of wettability/surface energy of other types of fouling organism have generally shown a relationship between surface wettability and adhesion, such relationships have not been as complex as that postulated by Baier. Furthermore, the nature of the relationship is species-dependent; while Finlay et al. (2002) showed a clear relationship between static contact angle of a range of alkanethiol SAMs and the adhesion of spores of *Ulva linza*, with highest adhesion strength on the most hydrophilic surfaces, the adhesion of the diatom *Amphora coffeaeformis* on the same surfaces showed an inverse relationship. In neither case was there any evidence of a zone of minimal

adhesion analogous to the 'Baier minimum'. Other studies with xerogel surfaces varying systematically in their wettability have demonstrated that adhesion strength of sporelings of *U. linza* was linearly correlated with surface wettability of uncharged fluorocarbon/hydrocarbon-modified xerogels, adhesion being greatest on the more hydrophilic/polar surfaces (Bennett et al. 2010) while adhesion of the diatom *Navicula perminuta* again showed the inverse of this relationship (Finlay et al. 2010). Finlay et al. (2010) also showed that cypris larvae of *Balanus amphitrite* preferred to settle on high energy/hydrophilic surfaces but the adhesion strength of the attached juveniles or the adult barnacles that subsequently developed was not examined and in general it seems that there are no systematic studies of the effect of surface wettability on the adhesion strength of marine invertebrates comparable with those performed on algae, and on surfaces that are designed to vary in just one parameter. However, tests on a wide range of different surfaces (Teflon, silicone coatings and epoxy) suggest that the adhesion strength of adult barnacles is lower on low energy surfaces (Swain and Schultz 1996; Swain et al. 1998).

In Chapter 3, it was shown that *Ectocarpus crouaniorum* adhered less strongly to the amphiphilic IS900 compared to the hydrophobic IS700. Chapter 5 demonstrated that there was similarly weak adhesion to S3 that was a hydrophilic coating containing both PEO and PDMS. In view of these results and the literature as reviewed above, it was decided to prepare and test a range of coatings that present systematic changes in surface energy by varying the ratios of PDMS and a PDMS-PEO copolymer, while keeping other properties, specifically modulus, relatively constant (see Chapter 4, Fig. 4.8). At the ends of the range of the silicone 'hybrid' coatings were a hydrophobic, low surface energy, low polarity coating and a high surface energy, high polarity coating. This range of wettability was lower than the range of wettability tested by Baier, but contained the 'Baier minimal' zone where lower adhesion strength was observed. Depending on the exact proportion of PDMS-PEO; varying degrees of surface amphiphilicity were anticipated. The hypothesis behind the experiments

reported in this Chapter was that there would be an optimal surface energy/wettability at which adhesion strength of *E. crouaniorum* would be at a minimum.
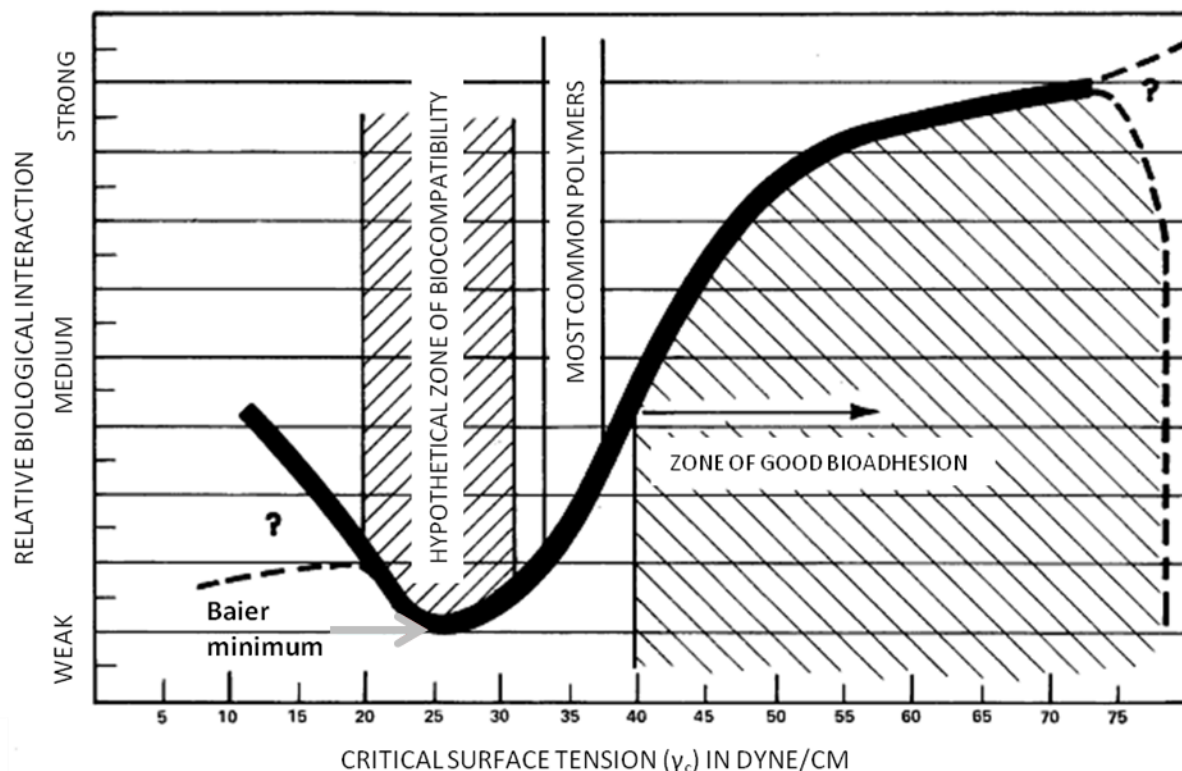
Figure 6.1: 'Baier curve'. It proposes that relative adhesion to test surfaces changes as a complex function of surface tension (or surface energy) (Baier and DePalma 1971). Dyne cm^{-1} is the equivalent of mN m^{-1} used for the surface energy in this thesis.

An implicit assumption behind studies on the relationship between wettability/surface energy, such as that demonstrated by the 'Baier curve', is that the measurement of this surface property, as obtained through measurements of the contact angles of macroscopically visible droplets of test fluids, accurately reflects the interaction between the surface and the adhesives used by fouling organisms, an interaction which occurs at the molecular scale. While this assumption may be true for extremely homogeneous surfaces such as SAMs, it is clearly less likely to be the case for surfaces with chemical and topographic heterogeneity. This is a particularly significant issue for amphiphilic coatings, which, as explained in Chapter 1, are coatings made from the blending of immiscible polymers or contrasting chemistries of

block copolymers, which are generally a hydrophobic and a hydrophilic components. Due to these two components, the surfaces of these coatings are chemically and topographically heterogeneous at a micro/nano-scale and for many coatings, these properties can be dynamic. Some coatings, for example, change on immersion, as the hydrophilic blocks are driven to the wetted surface (Cho et al. 2011 and 2012; Sundaram et al. 2011). In such situations, simple measurements of static contact angle using water droplets are unlikely to capture the properties of a surface, as perceived by the fouling organism. Therefore, in the literature, more investigations are using additional methods to try to relate surface properties to the adhesion of organisms. These methods include measurements of dynamic contact angles (advancing/receding) and the associated contact angle hysteresis and underwater (captive bubble) measurements. More complex surface characterisations of surface heterogeneity include atomic force microscopy (AFM) in dry and wet states, X-ray photoelectron spectrometry (XPS) to determine the chemical composition of the surface (before and after immersion).

The silicone 'hybrid' coatings tested in this chapter were anticipated to show varying degrees of surface amphiphilicity due to their composition. As such, dynamic contact angles (advancing/receding) and the associated contact angle hysteresis and underwater (captive bubble) measurements were made to complement standard static contact angle measures of surface energy.

6.2. Materials and methods

Composition and characterisation of the wettability series

The tested surfaces were the 6 silicone 'hybrid' coatings presented in Chapters 4.2.2 and 4.3.2: H, H1, H2, H3, H7 and H10 and the commercialised standard IS700 (presented in Chapters 4.2.3 and 4.3.5) (Tables 4.8, 4.9 and 4.11). These coatings were leached in a 30-

liter tank of deionised water, recirculated through a carbon filter for at least 2 months, in order to remove residual curing agents. Prior to the start of the experiment, the slides were rinsed with MilliQ water and gently wiped with a sterile sponge in order to remove any bacteria that had adhered to the surfaces. All the slides were equilibrated for 2h in ASW prior to the start of the experiment.

The coating used as a standard in these experiments was IS700. While the intention was also to include IS900, as in previous experiments, the batches of IS900 made for this purpose at International Paint did not show the performance anticipated from experiments reported in Chapters 3 and 5, for reasons that are not clear, as the release of filaments of *E. crouaniorum* and sporelings of *U. linza* was lower than previously observed.

Two algal species were tested: E*. crouaniorum* CCAP 1310/300 and *U. linza*, following the methods explained in Chapters 2 and 3.2, using 8 Pa for *E. crouaniorum* and 20 Pa for *U. linza*. All assays were performed at least twice to demonstrate consistency; results from one representative assay are illustrated below. Statistical analysis of the adhesion data is explained in Chapter 2.10, and statistical tables for the whole Chapter are presented in Appendix 5.

6.3. Results

6.3.1. E. crouaniorum

After blending and filtration, the starting inoculum (i.e. the filtrate) for adhesion assays with *E. crouaniorum* consisted of small filaments averaging 7.3 ± 1.3 cells (mean of 50 observations ± 2 x SE).

After 8 days of growth, the amount of unattached filaments was quantified through chl *a* determination (Chapter 2.5) and differences were observed between the coatings, despite being inoculated with the same concentration of filaments. The biomass of unattached filaments was significantly higher for the dishes containing the coatings IS700, H, H7 and

H10 (Table 6.1; p≤0.05, GZLM, Pairwise comparison). However, the dishes containing the coatings H7 and IS700 were also grouped with the other coatings, which had lower amounts of unattached filaments. These results show that the surface wettability did not significantly influence the unattached biomass except for the two extreme coatings (H and H10), which contained only PDMS or PDMS-PEO, respectively.

Table 6.1: Unattached biomass, after 8 days' incubation of test coatings, as measured by chl *a*. Mean of 3 replicates ± SD. Values, which are significantly different at p≤0.05 in GZLM test, are indicated by different letters after the unattached biomass values.

Coatings	IS700	H	H1	H2	H3	H7	H10
Total unattached biomass (µg chl *a*)	0.43 ± 0.02[a,b]	0.67 ± 0.36[a]	0.28 ± 0.07[b]	0.22 ± 0.05[b]	0.3 ± 0.04[b]	0.37 ± 0.11[a,b]	0.68 ± 0.21[a]

After measurement of the unattached filaments, the coatings were incubated for a 6 further days (i.e. 14 days in total) before their exposure to 8 Pa shear stress. The amount of biomass attached to the coatings was measured and differences were observed between the coatings before and after the shear stress exposure (Figs. 6.2a/b).

There were differences in initial attached biomass between the coatings after 14 days of growth, but not as expected from the unattached filament results (Table 6.1 and Fig. 6.2a). Figure 6.2a showed that the initial biomass before the exposure to the shear stress of the test coatings was different between the coatings, the lowest attached biomass was observed on the most hydrophobic coatings H, H1 and H2 while the highest biomass was observed on the most hydrophilic coatings H3, H7 and H10. Statistical analysis of the results from the silicone 'hybrid' coatings revealed three significant groups: the initial biomass on H was the lowest, followed by the coatings H1 and H2 grouped together while the coatings H3, H7 and H10 had the highest initial attached biomass on their surface (Fig. 6.2a; p≤0.05, GZLM, Pairwise comparison).

Figures 6.2b,c show that the adhesion strength of *E. crouaniorum* (as % removal under shear) varied with wettability and total surface energy. Adhesion was weakest on the two

most hydrophilic coatings H7 and H10, with a percentage removal around 80 %. The four other test coatings had attached filaments with higher adhesion strength, with % removal between 39 % and 68 %. The biomass on coating IS700 had high adhesion strength, as the percentage removal was only 26 % showing that the test coatings were more effective than IS700. Statistical analyses showed that the attached filaments on the coating H2 had the highest adhesion strength, followed by the coatings H1 and H3 that were grouped together (Figs. 6.2b,c; p≤0.05, GZLM, Pairwise comparison). Adhesion strength of *E. crouaniorum* filaments on the coating H was intermediate with 68 % removal while the adhesion on the coatings H7 and H10 was weak. The results show that surface wettability/energy clearly influenced adhesion, but there was not a direct or simple correlation, in fact that shape of the removal curve resembled an 'inverse Baier curve', i.e. there was a total surface energy of approx. 30 mN m^{-1}, at which adhesion was **maximal.**

The relationship between % removal and % polar surface energy (Fig. 6d) was similar to that shown for total surface energy. Possible relationships between adhesion and contact angle hysteresis and underwater contact angles (generally taken to reflect dynamic surface reorganisation events and the influence of immersion) are explored by plots shown in Figures 6.2e-f. In neither case, was there an apparent relationship between either of these surface measurements and ease of removal suggesting that other surface properties were determining adhesion strength.
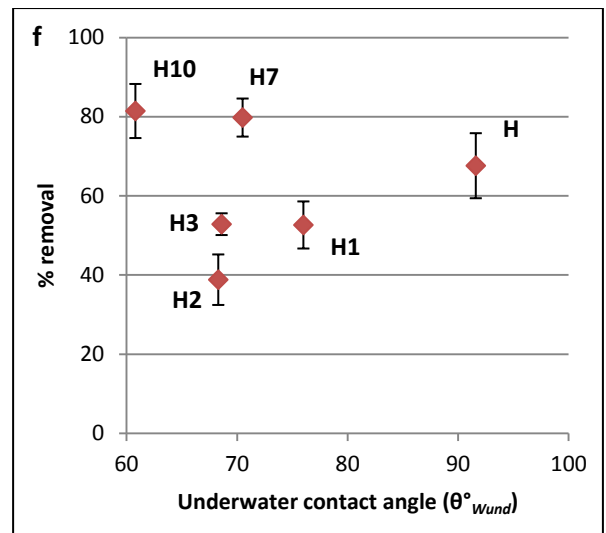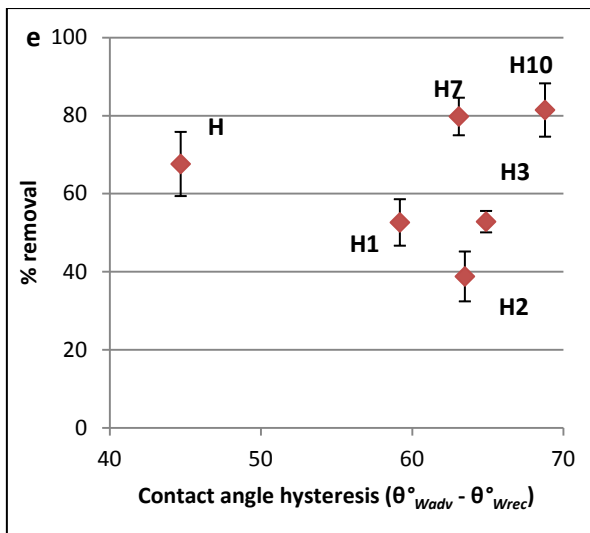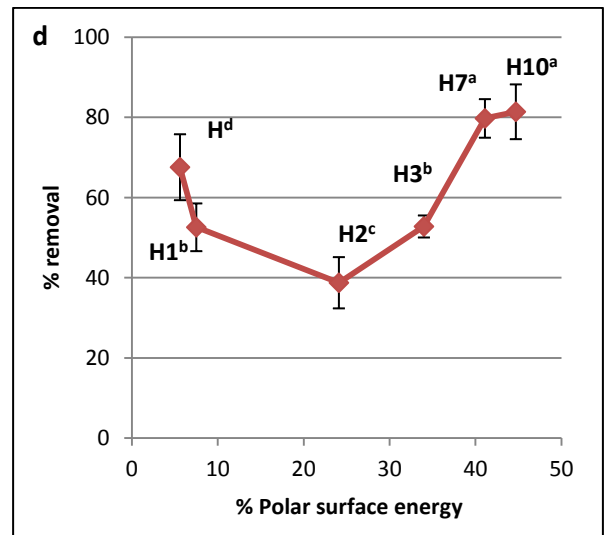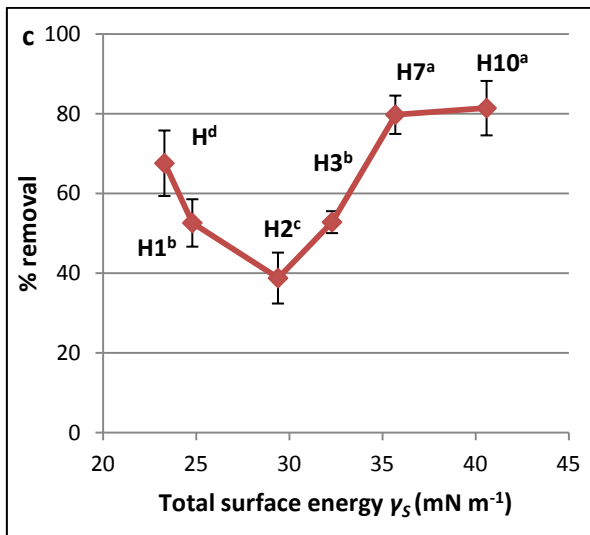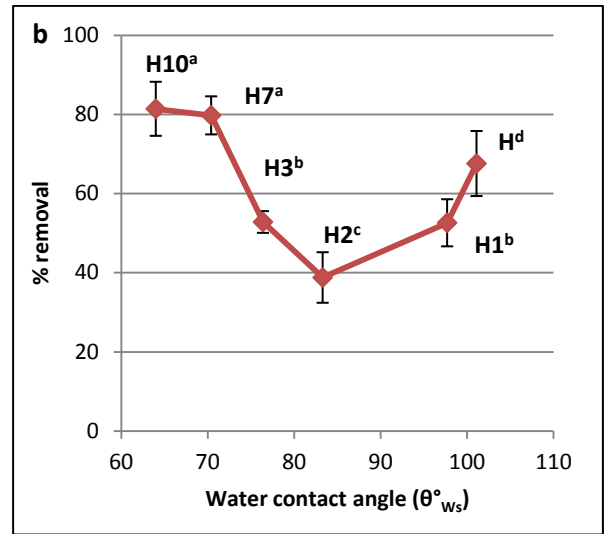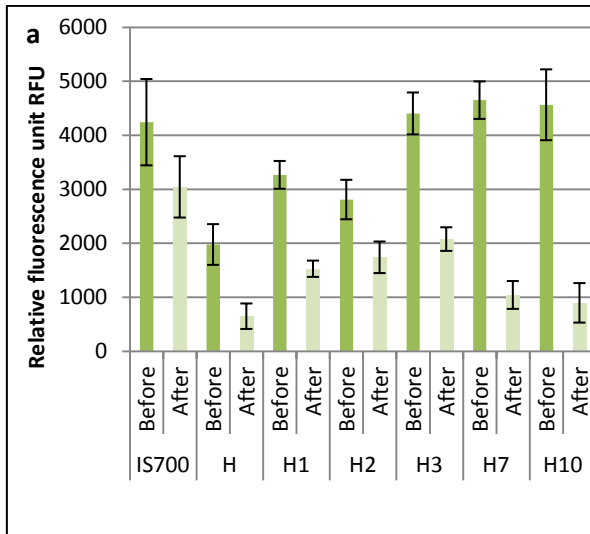
Figure 6.2: Adhesion assays with *E. crouaniorum*. a) Biomass of attached alga before and after exposure to a wall shear stress of 8 Pa, on 7 different surfaces, after incubation for 14 days at 15°C. Biomass was measured as relative fluorescence units. Percentage removal of the wettability series after exposure to shear stress of 8 Pa, calculated from data presented in (a) represented as a function of the wettability (b), total surface energy (c), % polar surface energy (d), contact angle hysteresis (e) and underwater contact angle (θ_{Wund} refers to the external angle of the air bubble (i.e. the 'water-side' calculated angle; see Chapter 2.9.1)) after a month of leaching (f). Means of nine replicates ± 2 x SE. Values that are significantly different at p≤0.05 in GZLM test are indicated by different letters above bars. IS700 was not included in the statistical analysis since the purpose was to test the significance of the results in relation to the hypothesis based on the silicone hybrid series. Measurements of static and underwater contact angles were performed before and after one-month leaching. Analysing the two methods separately, contact angles before and after leaching were slightly different, but had similar relationship to the % removal, so it was decided to plot only one set of data (before immersion for the static contact angle and after immersion for the underwater contact angle).

6.3.2. *U. linza*

The biomass that developed on the coatings was a consequence of the germination and growth of spores of *U. linza* that adhered during the settlement assay. The coating IS700 had higher biomass of sporelings attached to the surface than the test coatings. Significant differences were observed in the initial biomass of sporelings after 7 days of growth (Fig. 6.3a; p≤0.05, GZLM, Pairwise comparison). Lower sporeling biomass was observed on the coating H compared to the other test coatings (Fig. 6.3a). These differences probably reflect differences in the density of spores that settled on the surfaces.
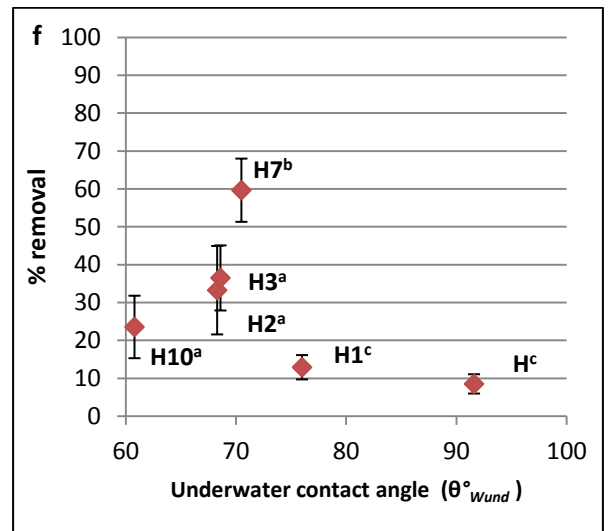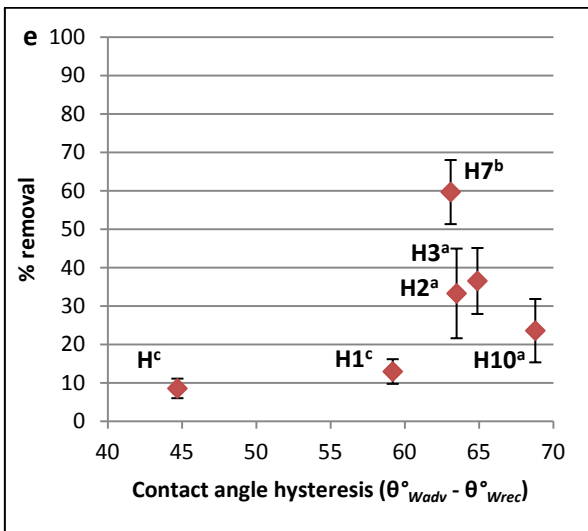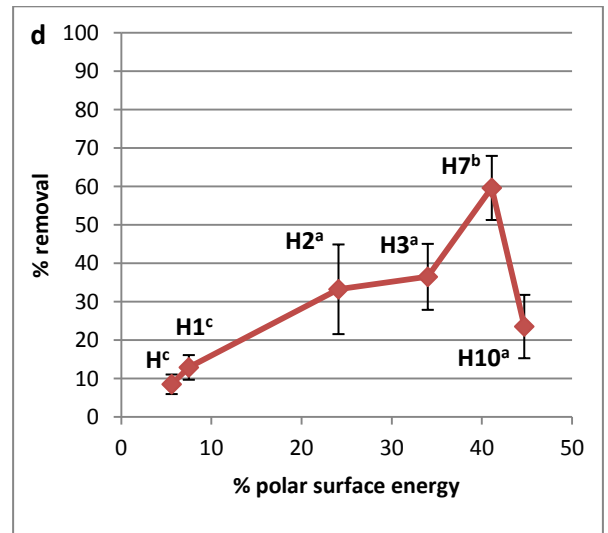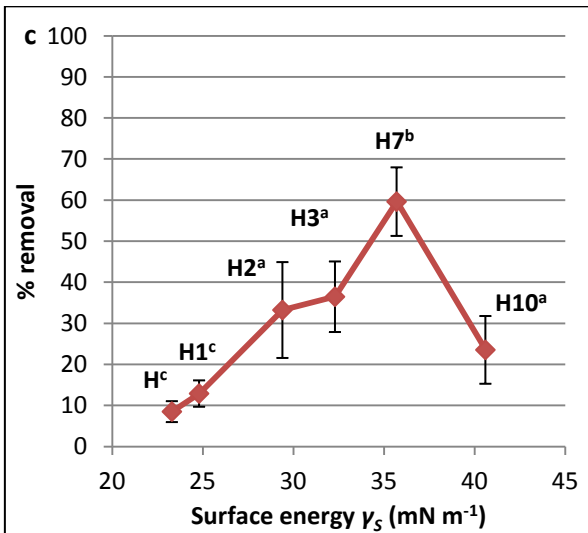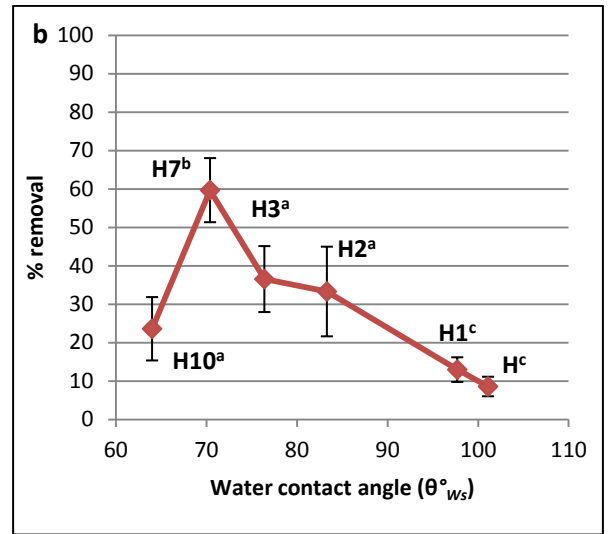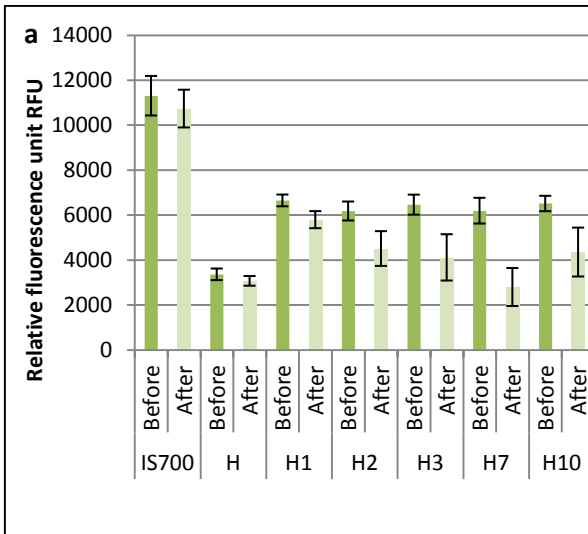
Figure 6.3: Adhesion assays with *U. linza*. a) Biomass of sporelings before and after exposure to a wall shear stress of 20 Pa, on 7 different surfaces, after incubation for 7 days at 18°C. Biomass was measured as relative fluorescence units. Percentage removal of the wettability series after exposure to shear stress of 20 Pa, calculated from data presented in (a) represented as a function of the wettability (b), total surface energy (c), % polar surface energy (d), contact angle hysteresis (e) and underwater contact angle after a month of leaching (f). Means of six replicates ± 2 x SE. Values that are significantly different at p≤0.05 in GZLM test are indicated by different letters above bars. IS700 was not included in the statistical analysis since the purpose was to test the significance of the results in relation to the hypothesis based on the silicone hybrid series. Measurements of static and underwater contact angles were performed before and after one-month leaching. Analysing the two methods separatly, contact angles before and after leaching were slightly different, but had similar relationship to the % removal, so it was decided to plot only one set of data (before immersion for the static contact angle and after immersion for the underwater contact angle).

Remaining biomass after the exposure to 20 Pa shear stress showed further differences between the surfaces. IS700 had the lowest removal (5 %) compared to the experimental silicone hybrids. For coatings H-H7, sporeling adhesion strength was strongly related to surface wettability (Fig. 6.3b), total surface energy (Fig. 6.3c), and relative polarity (Fig. 6.3d), and, adhesion was weaker as hydrophilicity increased. However, one coating, H10, the most polar and hydrophilic, did not follow this trend. These results could also be observed as complex relationship between the adhesion strength of sporelings of *U. linza* and the wettability/surface energy where adhesion to H7 would be minimal due to unmeasured properties. These results were in marked contrast to those with *E. crouaniorum*. There was no clear relationship between adhesion strength and either contact angle hysteresis, or captive bubble contact angle underwater (Figs. 6.3e,f).

6.4. Discussion

Amphiphilic coatings containing PEG as the hydrophilic component and generally fluorinated groups as the hydrophobic component showed good FR properties (Gudipati et al. 2005; Wang et al. 2011), but PDMS has recently been used as hydrophobic components

(Sundaram et al. 2011) and also showed good performance against sporelings of *U. linza* and the diatom *Navicula*.

A new design of coatings developed by International Paint, using different ratios of the blending of PDMS with PDMS-PEO to produce a series of coatings with a graduated range of wettability, was presented in Chapter 4.2.2 and 4.3.3 and they were tested in this Chapter against filaments of *E. crouaniorum* and sporelings of *U. linza*. This series of coatings was well-characterised and provided a good test to observe the influence of wettability since modulus was relatively constant across the range (i.e. 1 MPa) and all surfaces had Ra roughness values in the sub-micron range (<0.3 μm; Table 4.9). The starting hypothesis behind the experiments reported in this Chapter was that there would be an optimal surface energy, at which adhesion strength of the two species tested would be at a minimum.

Considering *E. crouaniorum* first, the results presented in this Chapter partially support this hypothesis since lowest adhesion was obtained on the coatings with a total surface energy between 35.7 and 40.6 mN m^{-1}. However, the data were also confusing since overall there was no obvious relationship between total surface energy or surface polarity, in fact H, the least polar coating, also showed good release performance and the relationship between the total surface energy and the adhesion strength of *E. crouaniorum* can be seen as an inverse 'Baier curve', with the highest adhesion strength around 30 mN m^{-1}, close to the region where Baier and DePalma (1971) postulated lowest adhesion.

In trying to account for these rather surprising results, the amphiphilic nature of these coatings should be considered. One of the characteristics of amphiphilic coatings is that they are chemically heterogeneous at the micro-nano scale. One possible explanation of the pattern of the results reported in this Chapter is that some other parameter that is not captured by measurements of total surface energy and wettability is also varying across the series. Martinelli et al. (2008), who assessed the performance of amphiphilic fluorinated

block copolymer coatings, showed that the ratios of surface atomic composition, measured using XPS, were different before and after immersion, showing that these amphiphilic surfaces are subjected to surface reorganisation. In addition, immersion of the surface changed the roughness and morphology of the surface and it was suggested that it could then affect the preference and performance of the two tested algae (Martinelli et al. 2008; Sundaram et al. 2011). It was observed for amphiphilic coatings containing PDMS and PEG that PDMS chains migrate away from the surface while PEG chains move to the surface (Sundaram et al. 2011), which would happen during the reorganisation.

For this experiment, it was hoped that measurements of contact angle hysteresis and underwater contact angle might have shed some light onto the influence of surface changes, but the results did not give any clear relationships (Figs. 6.2e and 6.3e). However, the different measurements of contact angles showed that the test coatings were subjected to some surface changes occurring during the one-month leaching as the contact angles before and after (underwater contact angles) were different (i.e. between 2.4° (for H) and 17° (for H3) of difference ; Chapter 4, Table 4.8, Fig. 4.1). In addition, the surface changes seemed to be different between the coatings as the hysteresis was higher with the increase of PDMS-PEO copolymer, varying from 45° for H to 69° for H10. Further studies on the surface properties of these coatings using AFM and XPS for example, are clearly necessary to explore the possibility that the surface changes were due to surface reorganisation and to link these changes to the adhesion strength of both test algae, but such studies were outside the scope of this thesis.

The results obtained with *U. linza* are more easily interpreted. Previous studies showed that sporelings of *U. linza* adhere more strongly to hydrophilic than hydrophobic coatings (Akesso et al. 2009a and 2009b; Bennett et al. 2010). The results presented in this Chapter for *U. linza* broadly support this, with adhesion to H7 being minimal and there was no evidence of a 'Baier minimum' in the region of 20-30 mN m^{-1} total surface energy. The one coating that did

not follow this trend was H10. The reasons for this anomalous performance are not known, again presumably some surface property, not captured by measurements of contact angle, surface energy, R_a roughness and modulus, was sufficiently different from the other coatings that the otherwise clear trend in performance was disrupted. Inspection of Table 4.9 reveals that H10 was deposited at a much lower thickness (155 μm) compared with the other coatings, but previous studies have shown that the thickness of elastomer coatings in this range has no effect on the release of sporelings of *U. linza* (Chaudhury et al. 2005). One explanation of the anomalous results with H10 could be that the segregation of hydrophilic and hydrophobic phases was at a scale that generated a sub-optimal patterning of surface domains, resulting in poor release properties.

Taking the two species together, and considering potential applied aspects of this series of coatings, the results appear to indicate that a coating composition of 70 % PDMS-PEO–30 % PDMS, with a surface energy of 36 mN m^{-1} (H7), brings optimal properties that decrease the adhesion strength of two different algae that in general have completely different adhesion characteristics. It would be interesting to test a coating series created from different materials and with graduated wettability ranges but invariant additional surface properties against the two algal species to further investigate the influence of surface energy on adhesion and if that relationship is linked to coating chemistry and/or materials. Further follow up studies could include testing the hybrid series of coatings, plus the additional wettability series of different materials, against diatoms and of course, macrofouling organisms other than seaweeds. These investigations could further clarify the role of surface wettability as a determinant of coating performance. The field performance of the silicone 'hybrid' series of coatings is reported in Chapter 10.

7. LABORATORY ASSAYS OF ADHESION TO XEROGEL FILMS VARYING IN SURFACE ENERGY AND CHARGE

7.1. Introduction

In previous chapters (Chapters 3, 5, 6), it has been demonstrated that the surface energy of coatings influences the adhesion strength of *Ectocarpus crouaniorum*. Studies on fouling-release (FR) coatings have mainly focussed on silicone polymers, which have low-modulus, low surface energy and low micro-roughness (see Chapter 1.5). However, silicone polymers are expensive, and easily damaged (Swain 1999). By comparison, organosilica-based sol-gels ('xerogels') are inexpensive and their higher modulus makes them more robust. They are environmentally friendly (i.e. do not contain biocides), which are important attributes in the development of new biofouling solutions. They have been shown to have both fouling-resistant and FR features in laboratory assays against several fouling organisms such as *Balanus amphitrite, Ulva linza* and *Navicula perminuta* (Tang et al. 2005; McMaster et al. 2009; Bennett et al. 2010; Finlay et al. 2010). The efficacy of these coatings has been demonstrated using Aquafast®, an organically-modified, hybrid xerogel, by field-testing on approximately 100 boats and on metal materials supporting an underwater camera in a marine archaeological site (Selvaggio et al. 2009; Gunari et al. 2011). In view of these previous studies, it was of interest to test similar xerogel materials against ectocarpoid algae.

Xerogel coatings, which are porous sol-gel materials, refer to dried gels produced by evaporation of the solvents. By mixing tetraethylorthosilicate (TEOS), which is the most common precursor (or sol), with different silanes containing fluorocarbon, aminopropyl and hydrocarbon groups, a gel is obtained. Subsequent drying of the gel at room temperature to remove the solvent (which is generally an alcoholic solution and located within the pores of the material) leads to a dried gel called 'xerogel'. Sol-gel-derived xerogel films can be applied to surfaces by a variety of means including spraying, brushing, dip coating and spin coating.

For this study, the coatings were spin cast onto glass microscope slides to provide thin xerogel films of reproducible thickness and uniformity (Jordan et al. 1998).

Xerogel surfaces have uniform surface roughness and can be tuned to provide surfaces with a wide range of wettability, total surface energy and charge (Tang et al. 2005; Bennett et al. 2010; Finlay et al. 2010). A particular feature of these coatings is that they vary not only in total surface energy, but also in the relative proportion of polar and dispersive components, allowing a more detailed analysis of the role of surface energy in bioadhesion. The resulting xerogel coatings are typically hard, i.e. modulus values are in the GPa range.

Wettability and surface energy are the most studied coating properties to predict the attachment and adhesion strength of fouling organisms as explained in previous Chapters (Chapters 1, 3 and 6). Zoospores of *U. linza* prefer to settle on xerogel surfaces with low surface energy (Bennett et al. 2010). However, high settlement of cyprids of *B. amphitrite* was observed on the same xerogel coatings with high surface energy/high wettability (Finlay et al. 2010). In addition, higher adhesion strength of sporelings of *U. linza* was observed on high surface energy xerogel (Bennett et al. 2010). It has also been shown in Chapter 6 that *E. crouaniorum* has lower adhesion strength on silicone-based coatings with high surface energy and a high percentage polar component.

In the present study, the initial attachment and adhesion strength of *E. crouaniorum* were tested on two series of xerogel coatings. The first set of coatings (SET 1) had a wide range of surface wettabilities and had been previously tested against *U. linza* (Bennett et al. 2010) and diatoms (Finlay et al. 2010). In addition to the information provided in these papers, new data on the surface properties of these coatings after immersion in seawater are presented since this is more likely to reflect the condition of coatings as perceived by the fouling organisms compared to characterisations of dry, pristine coatings presented in the previous papers. The results with *E. crouaniorum* indicated that surface charge might be an important

factor in controlling adhesion rather than wettability. However, a complicating factor in the interpretation of the results was that for some of the SET 1 coatings, surface wettability was changed by incorporating charged, polar aminopropyl silanes. Thus, two factors –i.e. wettability and charge- were being changed at the same time. Consequently, a second series of coatings (SET 2) was evaluated with a smaller range of surface wettabilities after immersion, but different surface charge properties. This second set of coatings was tested with both *E. crouaniorum* and *U. linza*.

7.2. Materials and methods

7.2.1. Composition of xerogel coatings provided by SUNY, Buffalo

Two sets of xerogel coatings were provided by Prof. M. Detty (Department of Chemistry, University of Buffalo, The State University of New York (SUNY)). The preparation of the coatings provided is fully described in published papers (Bennett et al. 2010). For the purposes of this thesis, only brief compositional details are provided, plus a summary of surface and bulk properties. The coatings were prepared at SUNY by mixing two cross-linkers tetraethylorthosilicate (TEOS) and alkyltrialkoxysilane with different modified silanes: 3-aminopropyltrimethoxysilane (AP), 3-methylaminopropyltrimethoxysilane (MAP), 3-di methylaminopropyltrimethoxysilane (DMAP), 3,3,3-trifluoropropyltrimethoxysilane (TFP), phenyltriethoxysilane (PH), *n*-octadecyltrimethoxysilane (C18), *n*-octyltrimethoxysilane (C8), tridecafluorooctyltriethoxysilane (TDF). The final sol/xerogel composition is designed in terms of the molar ratio of Si-containing precursors. Thus, a 1:1 PH/TEOS composition contains 50 mole-% PH and 50 mole-% TEOS. Two solvents and a catalyst were used to produce these coatings ethanol, water and hydrochloric acid (HCl), respectively.

Xerogel films were formed as described by Bennett et al. (2010) by spin casting 400 µl of the sol precursor onto pre-cleaned 25 mm x 75 mm glass microscope slides. Slides were cleaned by soaking in 'piranha solution' for 24 h, rinsed with copious quantities of deionised

water, soaked in isopropanol for 10 min, air dried and stored at ambient temperature until used. A model P6700 spin coater was used at 100 rpm for 10 s to deliver the sol and at 3000 rpm for 30 s to coat. All coated surfaces were dried at ambient temperature for at least one-day prior to analysis of the surface properties. They were then shipped to Birmingham.

7.2.2. Characteristics of xerogel coatings determined by SUNY

Contact angles and surface energies of all coatings provided to Birmingham, were determined at SUNY using the methods described by Bennett et al. (2010). Measurements were made on dry coatings and after immersion in artificial seawater ASW for 24 h followed by 1 h in deionised water to remove salts. Immersed coatings were dried in air under ambient conditions for 3 h, before contact angles were measured. Contact angles measured after the immersion in seawater are more likely to reflect the condition of coatings as perceived by the fouling organisms compared to characterisations of dry, pristine coatings presented in the previous papers (Bennett et al. 2010, Finlay et al. 2010).

The test methods used in this study are explained in Chapter 3.2. The test species used were *E. crouaniorum* CCAP 1310/300 and *U. linza*. Statistical analysis of the adhesion data is explained in Chapter 2.10, and statistical tables for the whole Chapter are presented in Appendix 6.

7.3. Results

7.3.1. Characteristics of xerogel coatings determined by SUNY

Table 7.1 shows the properties of the first set of xerogel coatings (SET 1) determined at SUNY (data provided by Prof. M. Detty).

Prior to immersion of SET 1 coatings in ASW, the contact angles and the surface energies were respectively from 49° to 107.9° and 12.4 mN m^{-1} to 53.5 mN m^{-1}. After immersion, values of $\theta°_{Ws}$ decreased by 15° to 25° for each coating to give a smaller range of 31° to 91°, and so the surface energy increased and varied from 27 mN m^{-1} to 64 mN m^{-1}. In addition,

the % polar component of the total surface energy varied from 27.6 % to 53.4 %; the two most polar coatings (DMAP/TEOS and MAP/TEOS) reflected the aminoalkyl functionalities of the silanes used.

Table 7.1: Properties of xerogel coatings (SET 1). Values are the average of 3-5 replicate runs. Error limits are ± SD. * indicates values of R_{rms} and Young's modulus from Bennett et al. (2010).

Composition/ name	1:9 DMAP/TEOS	1:9 MAP/TEOS	1:1 PH/TEOS	1:1 TFP/TEOS	1:1 C8/TEOS	5:45:50 C18/C8/TEOS	1:1 TDF/TEOS
Stored in air							
Static Water Contact Angle ($\theta°_{ws}$)	50 ± 3	49 ± 1	80.4 ± 0.6	82.6 ± 1.4	96 ± 6	107.9 ± 0.7	105 ± 3
Total Surface Energy γ_S (mN m^{-1})	53 ± 2	53.5 ± 0.8	38.2 ± 0.3	25.7 ± 0.7	25 ± 1	22.0 ± 0.4	12.4 ± 0.8
Immersed 24h in ASW							
Static Water Contact Angle ($\theta°_{ws}$)	31 ± 3	32.6 ± 0.8	54 ± 2	64.2 ± 0.2	80 ± 5	91 ± 3	83 ± 2
Total Surface Energy γ_S (mN m^{-1})	64 ± 2	63.6 ± 0.3	53 ± 1	39.3 ± 0.3	35 ± 2	27 ± 1	27 ± 2
Dispersive Surface Energy γ_D (mN m^{-1})	29.7 ± 0.1	30.5 ± 0.1	30.5 ± 0.1	19.5 ±0.1	24.1 ± 0.0	19.5 ±0.1	16.1 ±0.5
Polar Surface Energy γ_P (mN m^{-1})	34.1 ± 0.2	33.1 ± 0.1	22.0 ± 0.2	19.8 ± 0.1	11.1 ± 0.5	7.5 ± 0.2	10.9 ± 0.4
% Polar surface energy	53.4 ± 0.2	52 ± 1	41.8 ± 0.2	50.5 ± 0.1	32 ± 1	27.6 ± 0.2	40.5 ± 0.4
Surface Roughness R_{rms} (nm)	0.6 ± 0.1*	0.5 ± 0.1	0.39 ± 0.0*	0.55 ± 0.1*	0.81 ± 0.1*	0.20 ± 0.1	0.70 ± 0.1
Modulus (GPa)	17.2 ± 2.2*	8.5 ± 0.2	0.07 ± 0.0*	1.17 ± 0.2*	0.06 ± 0.0*	0.2 ± 0.1	1.2 ± 0.2

Profilometric studies conducted at SUNY showed that the xerogel films were 1.0 ± 0.1 µm thick. The surface roughness was low (~ 1 nm or less) for all the coatings. The elastic modulus values ranged from 0.06 to 17.2 GPa. In comparison with silicones, these are relatively hard coatings and since the softest (0.06 GPa) is well above the range (by an order of magnitude) where modulus affects release of sporelings of *Ulva* (Chaudhury et al. 2005). It

is unlikely that these differences in xerogel modulus would influence FR properties against *E. crouaniorum* (the influence of modulus is more extensively discussed in Chapter 8).

Table 7.2: Properties of SET 2 xerogel coatings with charged/uncharged surfaces (i.e. amine-/non-amine-containing surfaces): data provided by Prof. M. Detty. Modulus and roughness data for AP/TEOS and DMAP/TEOS xerogels are from Bennett et al. (2010). Means of 3-5-replicate runs ± SD.

Composition /name	1:9 AP/TEOS	1:9 MAP/TEOS	1:9 DMAPTEOS	1:4 TFP/TEOS	1:4 PH/TEOS
Stored in air					
Static Water Contact Angle ($\theta°_{ws}$)	56 ± 1	47 ± 2	48 ± 3	83 ± 1	81 ± 1
Total Surface Energy γ_s (mN m-1)	52 ± 1	54 ± 1	53 ± 2	25.9 ± 0.9	36.8 ± 0.2
Immersed 24 h in ASW Water					
Static Water Contact Angle ($\theta°_{ws}$)	39 ± 2	33 ± 3	24 ± 6	44 ± 9	59 ± 2
Total Surface Energy γ_s (mN m^{-1})	62.2 ± 0.4	66 ± 2	69 ± 3	55 ± 6	50 ± 1
Dispersive Surface Energy γ_D (mN m^{-1})	35.5 ± 0.1	35.6 ± 0.2	33.1 ± 0.1	23.9 ± 0.1	34.8 ± 0.1
Polar Surface Energy γ_P (mN m^{-1})	26.6 ± 0.1	29.9 ± 0.1	36.1 ± 0.2	31.1 ± 0.6	15.1 ± 0.1
% Polar surface energy	46.4 ± 0.1	47.8 ± 0.1	51.1 ± 0.2	53 ± 1	40 ± 1
Surface Roughness R_{rms} (nm)	1.60 ± 0.05	0.5 ± 0.1	0.60 ± 0.03	0.20 ± 0.09	0.23 ± 0.09
Modulus (GPa)	23.1 ± 3.2	8.5 ± 0.2	17.2 ± 2.2	6.2 ± 0.4	1.5 ± 0.5

The second set of coatings (SET 2) had similar chemistries to SET 1, but their composition was adjusted so their wettability, surface energy and relative polarity had a smaller range of values, following immersion in ASW. Before immersion in ASW, total surface energies ranged from 25.9-54 mN m^{-1} (Table 7.2), but after immersion, the range of surface properties

was reduced to 50-69 mN m^{-1}. However, three of the coatings incorporated the aminoalkyl silanes, AP, MAP and DMAP; at the pH of seawater (i.e. 8.2), the amino groups were protonated providing a net positive surface charge (M. Detty pers. comm). The other two coatings incorporating TFP and PH were uncharged.

The surface roughness of the SET 2 coatings after immersion was similar to those of SET 1 (0.2-1.6 nm) and the elastic modulus values were also in the GigaPascal range (1.5 to 23.1 GPa). For the same reasons as SET 1, it is unlikely that the differences of modulus would influence FR properties against *E. crouaniorum*.

7.3.2. Adhesion strength of *E. crouaniorum* on SET 1 coatings

After blending and filtration, the starting inoculum (i.e. the filtrate) for adhesion assays with *E. crouaniorum* consisted of small filaments averaging 8.4 ± 1.1 cells (mean of 50 observations ± 2 x SE).

After 8 days of growth, non-attached filaments were removed and quantified through chlorophyll *a* (chl *a*) determination (Chapter 2.5). All test surfaces were inoculated with a similar concentration of filaments and after 8 days, there were marked differences in the amount of unattached filaments removed from the culture dishes that contained the different coatings (Table 7.3). This could be due to differences in the initial attachment of inoculum and in the growth of unattached filaments. It is therefore important to use these measurements with caution knowing they might not indicate differences in adhesion *per se*. After 8 days, the amount of attached biomass was insufficient to be measured using the plate reader. The biomass of unattached filaments in dishes containing TFP/TEOS slides was significantly greater than for all the other coatings (Table 7.3; p≤0.05; GZLM, Pairwise comparison). However, no significant difference was observed for most of the other coatings.

Table 7.3: Unattached biomass after 8 days' incubation of SET 1 xerogel coatings with filaments, as measured by chl *a*. Means of 3 replicates ± SD. Values, which are significantly different at p≤0.05 in GZLM test are indicated by different superscript letters after the amount of unattached biomass.

Composition	Unattached biomass as chl *a* (µg)
1:9 DMAP/TEOS	0.21 ± 0.06^a
1:9 MAP/TEOS	0.2 ± 0^a
1:1 PH/TEOS	0.34 ± 0.02^b
1:1 TFP/TEOS	0.52 ± 0.08^c
1:1 TDF/TEOS	$0.28 \pm 0.09^{a,b}$
5:45:50 C18/C8/TEOS	$0.23 \pm 0.09^{a,b}$
1:1 C8/TEOS	$0.22 \pm 0.07^{a,b}$

Before exposure to shear stress, attached filaments were incubated for six further days (i.e. 14 days in total). The amount of biomass of attached filaments on the different surfaces was measured using the plate reader and significant differences were found before and after exposure to 8 Pa shear stress (Figs. 7.1a/b; p≤0.05, GZLM, Pairwise comparison).

After 14 days of growth, significant differences in the biomass of attached filaments were found; three groups were observed (Fig. 7.1a). DMAP/TEOS was grouped to MAP/TEOS, which had the highest attached biomass but was also grouped to C18/C8/TEOS and C8/TEOS, which had lower biomass (p≤0.05, GZLM, Pairwise comparison). However, there was no significant difference between the other coatings.

The adhesion strength of *E. crouaniorum* (i.e. % removal) is shown in Figure 7.1b. DMAP/TEOS and MAP/TEOS had low percentage removal (15-20 %) showing that the filaments were attached strongly to these two coatings compared to all the others, which had high percentage removal (80-95 %). Statistical analyses separated the coatings into three significant groups. DMAP/TEOS and MAP/TEOS formed a group due to their lowest percentage removal. C18/C8/TEOS was grouped to TDF/TEOS, which had lower % removal

but also to the other three coatings, which had the highest percentage removal (p≤0.05, GZLM, Pairwise comparison).

Statistical analysis of the combined performance of the surfaces (i.e. analysing together the amount of attached biomass and that remaining after exposure to shear stress) showed that two significant groups could be observed. DMAP/TEOS and MAP/TEOS formed the first group and all the other coatings the second (p≤0.05, RM ANOVA, post hoc REGWQ).

Figures 7.1c, d and e show the correlation between the surface properties and the percentage removal. These graphs show that the adhesion strength of *E. crouaniorum* was the highest on the two most hydrophilic coatings (DMAP/TEOS and MAP/TEOS). However, no simple relationship was observed between the surface properties and the percentage removal.
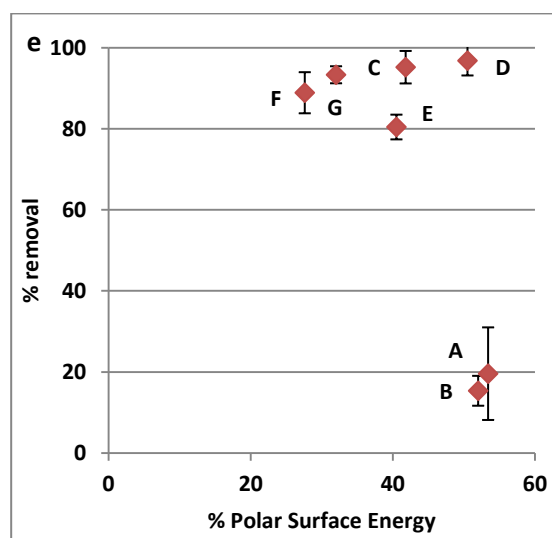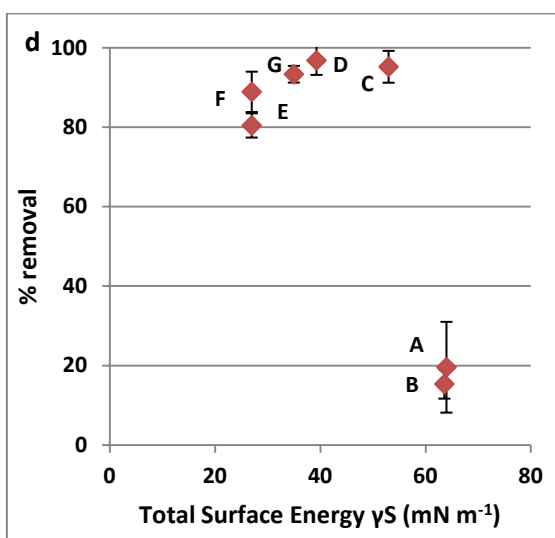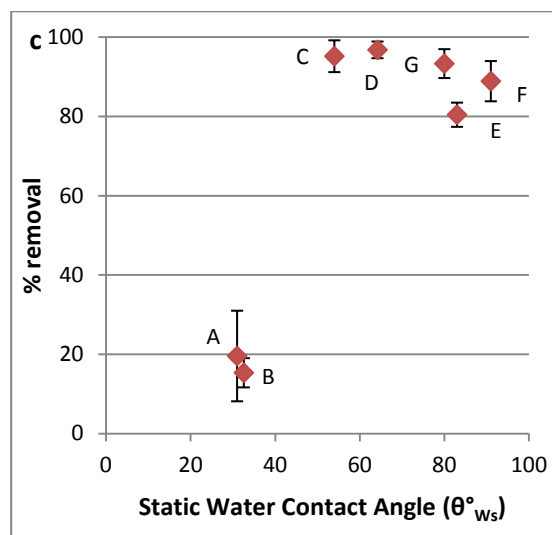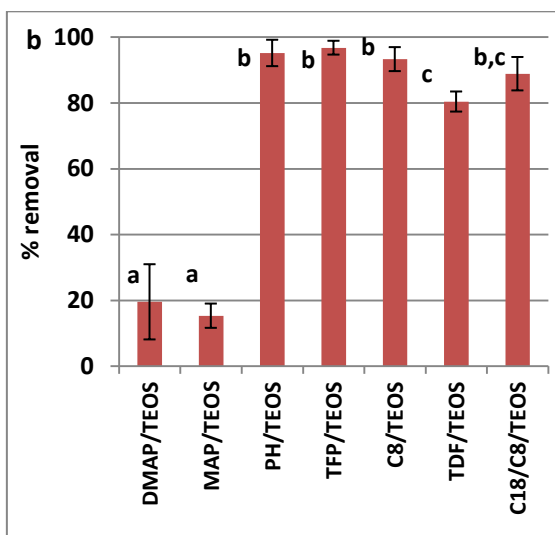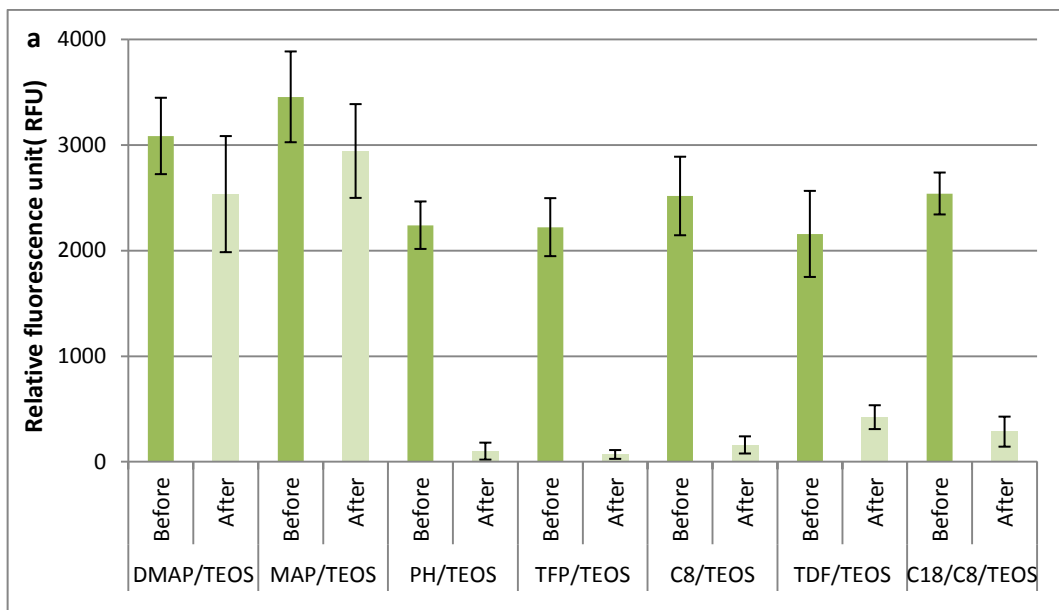
Figure 7.1: Adhesion assays on SET 1 coatings with *E. crouaniorum.* a) Biomass of attached alga before and after exposure to a wall shear stress of 8 Pa on 7 different surfaces, after incubation for 14 days at 15°C. Biomass was measured as relative fluorescence units. b) Percentage removal after exposure to shear stress of 8 Pa, calculated from data presented in (a). Values that are significantly different at p≤0.05 in GZLM test are indicated by different letters above the bars. For Figs. 8.1a and b, the coatings are shown in order of wettability. (c), (d) and (e) show the relationship between percentage removal and surface properties after immersion in ASW: static water contact angle (c), total surface energy (d) and % polar surface energy (e). Means of nine replicates ± 2 x SE. In Figs 7.1c, d and e, the letters associated with data points refer to coating codes: A=DMAP/TEOS; B=MAP/TEOS; C=PH/TEOS; D=TFP/TEOS; E=TDF/TEOS; F=C18/C8/TEOS and G=C8/TEOS.

7.3.3. Adhesion strength of *E. crouaniorum* on SET 2 coatings

After blending and filtration, the starting inoculum (i.e. the filtrate) for adhesion assays with *E. crouaniorum* consisted of small filaments averaging 7.3 ± 1.3 cells (mean of 50 observations ± 2 x SE).

Table 7.4: Unattached biomass after 8 days of growth of charged/uncharged xerogel surfaces, as measured by chl *a*. Means of 3 replicates ± SD. Values, which are significantly different at p≤0.05 in GZLM test are indicated by different superscript letters after the amount of unattached biomass.

Coatings	AP/TEOS	DMAP/TEOS	MAP/TEOS	1:4 TFP/TEOS	1:4 PH/TEOS
Unattached biomass as chlorophyll *a* (µg)	0.03 ± 0.02^a	0.04 ± 0.01^a	0.02 ± 0.01^a	0.41 ± 0.05^b	0.23 ± 0.07^b

As for the previous experiment (above), the amount of unattached filaments was quantified after 8 days of growth (Table 7.4) through chl *a* determination (Chapter 2.5). All the surfaces were inoculated with the same concentration of filaments (i.e. inoculum), but there were marked differences between the coatings for the amount of unattached filaments. The dishes containing the surfaces prepared with aminoalkyl silanes (AP/TEOS, DMAP/TEOS, and MAP/TEOS) had significantly less unattached biomass than the other coatings, which were grouped together (by a factor of 10-20 fold) (Table 7.4; p≤0.05, GZLM, Pairwise comparison).
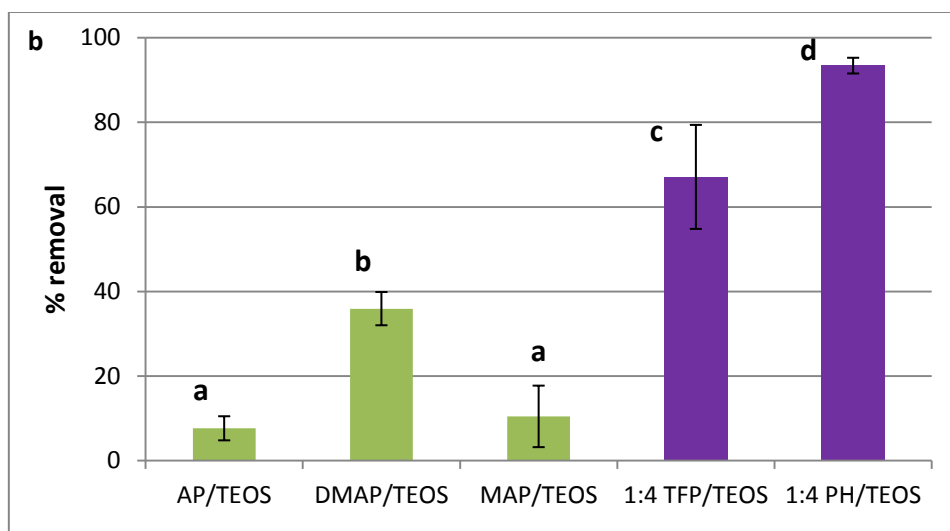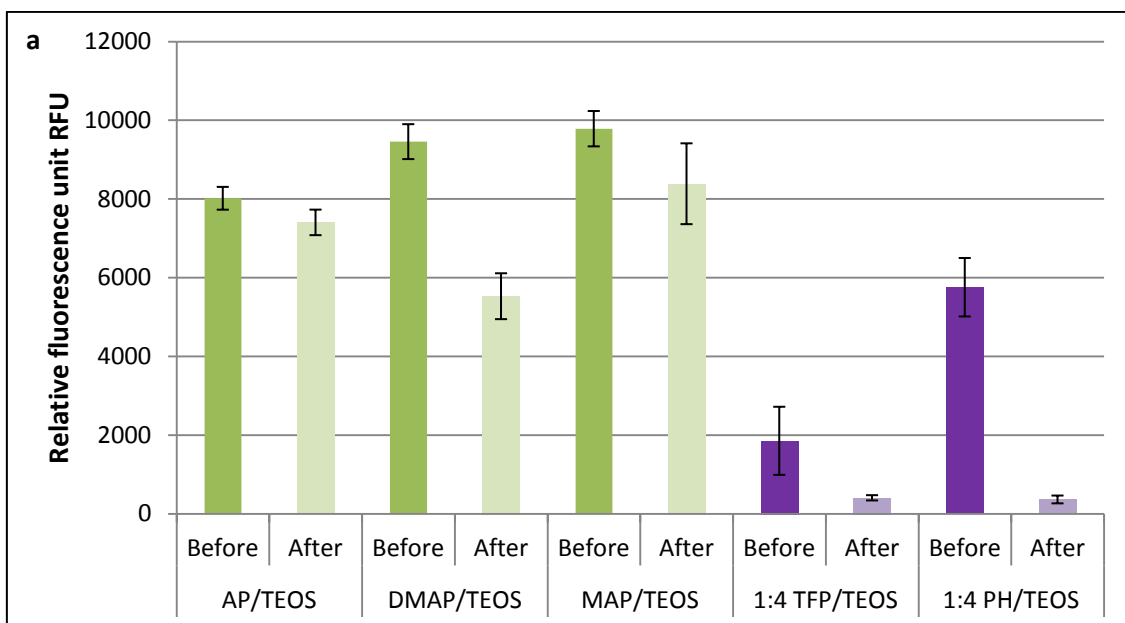
Figure 7.2: Adhesion assays on SET 2 coatings with *E. crouaniorum.* a) Biomass of attached alga before and after exposure to a wall shear stress of 8 Pa, on 5 different surfaces, after 14 days of incubation at 15°C. Biomass was measured as relative fluorescence units. b) Percentage removal after exposure to 8 Pa shear stress, calculated from data presented in a). Means from 9 replicates ± 2 x SE. Values that are significantly different at p≤0.05 in GZLM test are indicated by different letters above the bars. The green and the purple colours in the graphs represented respectively the positively charged and the uncharged surfaces.

The uncharged coatings (1:4 TFP/TEOS and 1:4 PH/TEOS) prepared using uncharged side-chains had lower attached biomass than the charged coatings (AP/TEOS, DMAP/TEOS and MAP/TEOS; Fig. 7.2a) prepared with positively charged organic side-chains. Significant

differences were observed in the biomass of attached filaments after 14 days of growth. The positively charged coatings MAP/TEOS and DMAP/TEOS had significantly the highest biomass, followed closely by the coating AP/TEOS ($p \leq 0.05$, GZLM, Pairwise comparison). The coating 1:4 PH/TEOS had an intermediate amount of biomass attached to the slides while the coating 1:4 TFP/TEOS had the lowest biomass ($p \leq 0.05$, GZLM, Pairwise comparison).

The adhesion strength data (i.e. percentage removal, Figs. 7.2b and 7.3) show that *E. crouaniorum* adhered weakly to the coatings 1:4 TFP/TEOS and 1:4 PH/TEOS, which were the uncharged coatings, compared to the three aminoalkyl-containing coatings that were positively charged ($p \leq 0.05$, GZLM, Pairwise comparison).
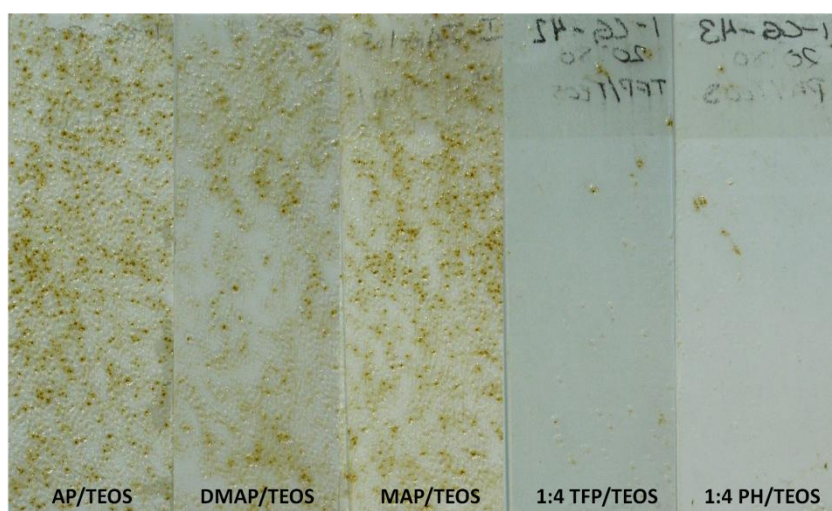
Figure 7.3: Photograph showing *E. crouaniorum* retained on the surfaces after exposure to 8 Pa shear stress.

Statistical analysis of the combined performance of the surface (i.e. analysing together the amount of attached biomass initially attached, and that remaining after exposure to shear stress) revealed four performance groups. The coatings with positively charged surfaces were separated in two groups: MAP/TEOS, which had the highest biomass before and after exposure to shear stress and AP/TEOS and DMAP/TEOS, which had high-intermediate biomass before and after exposure to shear stress ($p \leq 0.05$; RM ANOVA, Post Hoc REGWQ).

The two uncharged coatings had the lowest biomass before and after exposure to shear stress and were significantly different to each other.

7.3.4. Adhesion strength of sporelings of *U. linza* on SET 2 coatings
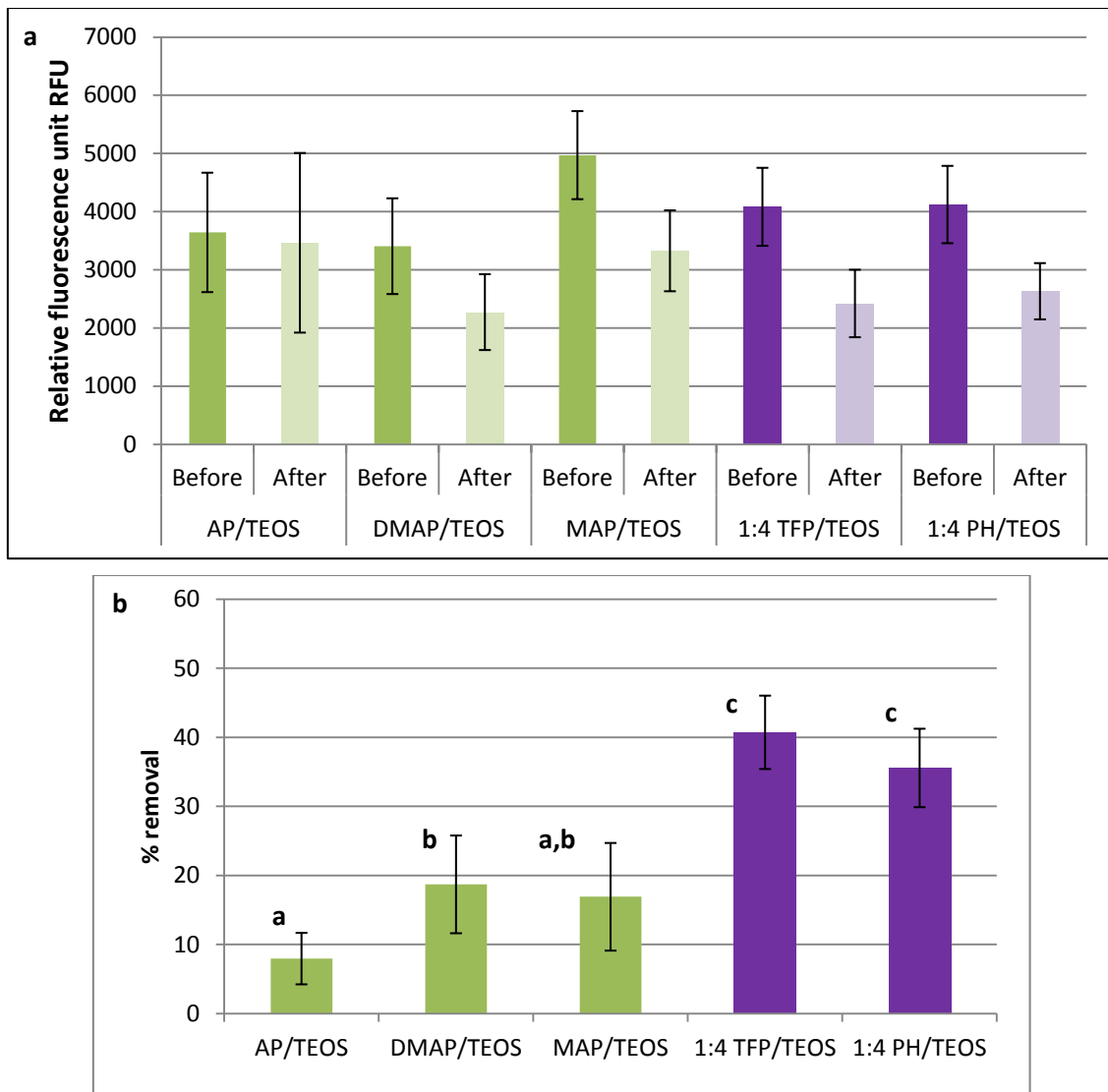
Figure 7.4: Adhesion assays on SET 2 coatings with *U. linza.* a) Biomass of attached sporelings before and after exposure to a wall shear stress of 33 Pa, on 5 different surfaces, after 6 days of incubation at 18°C. Biomass was measured as relative fluorescence units. b) Percentage removal after exposure to 33 Pa shear stress, calculated from data presented in a). Means of 6 replicates ± 2 x SE. Values that are significantly different at $p \leq 0.05$ in GZLM test are indicated by different letters above the bars. The green and the purple colours in the graphs represented respectively the positively charged and the uncharged surfaces.

After 6 days of cultivation, the biomass of sporelings (young plants) on the coatings was not significantly different for all the coatings except for DMAP/TEOS and MAP/TEOS (Fig. 7.4a; $p \leq 0.05$, GZLM, Pairwise comparison). The biomass after exposure to 33 Pa shear stress was significantly different between the surfaces. The adhesion strength on the xerogels was generally relatively high (maximum percentage removal was 41% for 1:4 TFP/TEOS). However, significant differences in percentage removal of sporelings were observed between the xerogel surfaces with positively charged aminopropyl side-chains and uncharged organic side-chains; sporelings on the uncharged surfaces (1:4 TFP/TEOS and 1:4 PH/TEOS) had lower adhesion strength compared to the other surfaces. There was also a significant difference in performance between AP/TEOS and DMAP/TEOS (Fig. 7.4b; $p \leq 0.05$, GZLM, Pairwise comparison).

7.4. Discussion

Previous studies using similar xerogel coatings to those in SET 1, with a wide range of surface energy values, showed various responses regarding the attachment and adhesion strength of different marine fouling organisms, *U. linza*, *N. perminuta* and *B. amphitrite*. Settlement of zoospores of *U. linza* was higher on low surface energy surfaces while the adhesion strength of sporelings was higher on coatings with high surface energy and polarity, except for those containing aminopropyl groups (Bennett et al. 2010). The adhesion strength of *N. perminuta* was also influenced by the surface energy; the higher the surface energy was, the lower the adhesion strength was including on those coatings containing aminoalkyl groups (Finlay et al. 2010). It should be noted that in these publications, surface analyses were performed on pristine coatings. The studies performed at SUNY, described in this Chapter, showed that wettability and surface energy properties of dry surfaces changed following 24h immersion in ASW, the former decreasing and the latter increasing, and we assume that the properties of these coatings after a period of immersion are more likely to be representative of conditions in the bioassays than they would be for dry, pristine coatings. In

fact, if the values for surface energy determined on coatings after immersion are considered against the adhesion data for both algae as reported in Bennett et al. (2010) and Finlay et al. (2010), the general conclusions and trends outlined above do not change (Evariste et al. Submitted to Biofouling). Since *U. linza* and *N. perminuta* clearly respond differently, this set of coatings was therefore of interest to evaluate the effect of wettability/surface energy on attachment and adhesion strength of other fouling organisms such as ectocarpoid algae.

As a result of the earlier studies (Chapters 3 and 6) the starting hypothesis was that the wettability/surface energy would influence the adhesion strength of *E. crouaniorum*. The results presented in this Chapter on SET 1 coatings showed that there was high removal of attached filaments of *E. crouaniorum* from 5 of the 7 coatings tested (PH/TEOS, TFP/TEOS, C18/C8/TEOS, TDF/TEOS and C8/TEOS), which included low surface energy (C18/C8/TEOS, TDF/TEOS), intermediate surface energy (TFP/TEOS, C8/TEOS) and high surface energy (PH/TEOS) surfaces. An influence of the surface energy could be observed, but there was no correlation with adhesion strength. However, adhesion strength was high on the two most hydrophilic coatings. These two coatings, MAP/TEOS and DMAP/TEOS, incorporated two polar aminoalkyl silanes. At the pH of seawater (c. 8.2), the amino groups would be protonated (Detty pers. comm.) and therefore, it was hypothesised that the strong adhesion shown to these two coatings was a consequence of charge rather than surface energy/polarity per se.

To test this hypothesis, Prof. M. Detty therefore constructed the SET 2 coatings in which the proportions of the silanes were tuned to provide materials with similar surface topographies/roughnesses and surface energies following immersion in ASW, but with xerogel side chains that either were neutral or were amine-containing, which could be protonated in ASW to provide a positive charge. The results shown in Figure 7.2 support the revised hypothesis, with stronger adhesion to all three positively charged coatings compared to those that were uncharged. The results obtained were comparable to those previously

obtained for *U. linza* with similar xerogels, where strong adhesion of sporelings to aminopropylated AP/TEOS xerogels was found (Bennett et al. 2010). This was confirmed by the results of tests with *U. linza* on the SET 2 coatings, which showed significantly stronger adhesion of sporelings to the charged surfaces.

The effect of surface charge on settlement/adhesion strength of fouling organisms has not been extensively studied. Previous studies have suggested that surface charge rather than surface energy *per se*, may determine the surface selection and the settlement of cyprids of two different barnacle species (Aldred et al. 2011; Petrone et al. 2011a). Petrone et al. (2011a) showed that the settlement of cyprids was lower on positively charged surfaces. Finlay et al. (2010) assessed the performance of a series of xerogel coatings (similar to SET 1) on the settlement of cyprids. This set of coatings was originally designed to have a range of wettability but in this Chapter, it was demonstrated that these coatings were either positively charged or uncharged. The assay testing the settlement of cyprids on these coatings did not show similar results to those in Petrone et al. (2011a). Moreover, it has been shown that the settlement of zoospores of *U. linza* was higher on surfaces with positively charged functionality (arginine-rich peptide SAMS) (Ederth et al. 2008; Ederth et al. 2009) and quaternised copolymers (Park et al. 2010), while the adhesion of sporelings was also high on the latter surface.

The physicochemical basis of the stronger adhesion of filaments of *E. crouaniorum* and sporelings of *U. linza* to positively charged surfaces may lie in electrostatic interactions between the positively charged amine-containing surfaces and the biological polymers on the surface that may play a role in adhesion. Previous research on adhesives used by brown macroalgae has mainly focussed on the extracellular matrix of zygotes of fucoids where anionic sulphated fucans and alginates appear to play an important role in adhesion to the substratum (Potin and Leblanc 2006 for review). More generally, the cell wall or extracellular matrix of brown algae consists of a relatively small proportion of crystalline cellulosic

microfibrils embedded in an amorphous matrix of anionic polysaccharides, chiefly alginates and fucans (Kloareg and Quatrano 1988). Recently, it has been shown that adhesive secreted by the spores of another brown alga, *Undaria pinnatifida* was composed of anionic polysaccharides (Petrone et al. 2011b). While there has been only a few biochemical studies on the cell wall composition of ectocarpoid algae, the recently released genome sequence for *Ectocarpus siliculosus* supports the existence of the appropriate genes and enzymes for synthesis and modification of sulphated fucans and alginates (Michel et al. 2010). It is known that the cell wall of *U. linza* is mainly composed of ulvan, which is a sulphated glucuronorhamnoxyloglycan, i.e. negatively charged (Ray and Lahaye 1995). While it has not been established that such molecules have adhesive functionality in *U. linza*, their location in the cell wall could provide the basis for non-specific, electrostatic adhesion.

In conclusion, the results obtained in this Chapter demonstrating strong adhesion of *U. linza* and *E. crouaniorum* to positively charged surfaces are potentially explainable through the presence of anionic polysaccharides in the cell walls of these algae. While the primary function of these polysaccharides may not be in specific adhesion processes, their location at the cell surface would contribute to strong, non-specific, electrostatic adhesion to positively charged surfaces. Whilst it has been suggested that xerogel coatings may have some potential value as practical AF/FR coatings (Selvaggio et al. 2009; Bennett et al. 2010) the results of this Chapter suggest that only uncharged compositions should be considered.

The work described in this Chapter has contributed to a paper *(Evariste, E., Gatley, C.M., Detty, M.R., Callow, M.E., Callow, J.A. 2013 The performance of aminoalkyl/fluorocarbon/hydrocarbon-modified xerogel coatings against the marine alga Ectocarpus crouaniorum: relative roles of surface energy and charge. Biofouling 29 (2): 171-184)* (Appendix 15). The paper contains additional information on the surface composition of these coatings determined at SUNY using XPS and AFM.

8. LABORATORY ASSAYS OF ADHESION TO SILICONE MODULUS SERIES

8.1. Introduction

In Chapter 5, initial experiments to test the effect of coating modulus on the adhesion strength of *Ectocarpus crouaniorum* were described. The results were confusing, partly because two series of coatings were tested, with different chemistries, and within each set of three coatings, there was an anomalous coating, which changed in wettability, not just modulus. In both cases, there was low adhesion of the test organisms to the hydrophilic member of each series, whatever the modulus. Furthermore, the results from the two sets of coatings tested gave contradictory results, one showing positive and the other, negative relationships between adhesion strength and modulus. It was therefore decided to explore the effect of modulus more systematically (in both laboratory and field experiments), using a well-characterised set of hydrophobic coatings based on the same chemistry, PDMS, and with varying modulus obtained by using different molecular weights (viscosities) of the polymer (see Table 4.4). The expectation was that the coatings would vary by at least one order of magnitude. However, the range of moduli obtained was only 0.73 to 1.5 MPa.

8.2. Materials and Methods

The silicone test coatings (M1, M2, M3, M4 and M5) and the standard IS700 (Chapters 4.2.2, 4.2.3, 4.3.4 and 4.3.5) were leached for at least 2 months in a 30-liter tank of deionised water recirculated through a carbon filter before the experiment in order to remove residual curing agents (as explained in Chapter 3.2.2). Two algal species were tested: *E. crouaniorum* CCAP 1310/300 and *U. linza,* following the methods explained in Chapters 2 and 3.2. IS900 was not used as standard due to the reasons explained in Chapter 6. Statistical analysis of

the adhesion data is explained in Chapter 2.10, and statistical tables for the whole Chapter are presented in Appendix 7.

8.3. Results

8.3.1. E. crouaniorum

After blending and filtration, the starting inoculum (i.e. the filtrate) for adhesion assays with *E. crouaniorum* consisted of small filaments averaging 8.6 ± 1.2 cells (mean of 50 observations ± 2 x SE).

After 8 days of growth, the amount of unattached filaments was quantified through chlorophyll *a* (chl *a*) determination (Chapter 2.5) and differences were observed between the coatings, despite being inoculated with the same concentration of filaments. There was a trend of increasing amount of unattached filaments in dishes with increasing modulus, with significantly more unattached filaments in coatings M1 and M2 compared with the other test coatings (Table 8.1; p≤0.05, GZLM, Pairwise comparison). The lowest amount of unattached filaments was obtained with IS700.

Table 8.1: Unattached biomass, after 8 days' incubation of test coatings, as measured by chl *a*. Mean of 3 replicates ± SD. Values, which are significantly different at p≤0.05 in GZLM test, are indicated by different letters after the unattached biomass values. The experimental coatings are arranged in order of decreasing modulus (M1=1.5 MPa; M2=1.04 MPa; M3=0.91 MPa; M4=0.85 MPa; M5=0.73 MPa).

Coatings	IS700	M1	M2	M3	M4	M5
Total unattached biomass (µg chl *a*)	0.93 ± 0.87[a]	9 ± 4[b]	6.53 ± 1.68[b,c]	5.2 ± 0.88[c]	5.1 ± 0.6[c]	5 ± 2.31[c]

After measurements of the unattached filaments, the coatings were incubated for six further days (i.e. 14 days in total) before exposure to 8 Pa shear stress. The amount of biomass

attached to the coatings was measured and differences were observed between the coatings before and after the shear stress exposure (Figs. 8.1a/b).

There were differences in initial attached biomass between the coatings after 14 days of growth, and as expected from the unattached filament results (Table 8.1 and Fig. 8.1a). Figure 8.1a showed that the initial biomass on IS700 was two-three times higher than all the test coatings as observed in previous experiments. In addition, differences of initial biomass were observed between the coatings. A trend was observed for the initial attached biomass as it increased with the decrease of modulus. Statistical analyses showed that three significant groups were formed: the coating M1 had the lowest initial biomass (Fig. 8.1a; p≤0.05, GZLM, Pairwise comparison). The coatings M3 and M4 were grouped with the coating M2 by having intermediate initial attached biomass but they were also grouped with M5, which had the highest initial biomass.

Table 8.2: Values of elastic modulus, viscosity and estimated molecular weight of the silicone modulus series. The molecular weight was calculated using the equation developed by Barry (1946), Log η = 1 + 0.0123*$M_n^{1/2}$; with η: viscosity (data provided by the supplier) and Mn: molecular weight. The experimental coatings are arranged in order of decreasing modulus.

Coatings	M1	M2	M3	M4	M5
Modulus (MPa)	1.5	1.04	0.91	0.85	0.73
Viscosity (mPa s^{-1})	72	4000	6000	14000	50000
Estimated molecular weight (kg mol^{-1})	4.858	44.753	51.015	65.425	90.438

The adhesion strength data (Fig. 8.1b) showed that *E. crouaniorum* filaments adhered weakly (i.e. with a minimum of 67 % removal) to all the test coatings compared to IS700, which had only 19 % removal. Statistical analyses showed differences among the adhesion strength of the test coatings. The coatings M1, M2 and M3 had the weakest adhesion to the surfaces, while the coatings M4 and M5, which were also grouped with M2 had the highest adhesion to the surfaces (Fig. 8.1b; p≤0.05, GZLM, Pairwise comparison). Percentage removal of *E. crouaniorum* showed a weak positive correlation with elastic modulus (or conversely a weak negative correlation between modulus and adhesion strength), with an

$R^2=0.5$. A stronger positive correlation was also observed between the adhesion strength of *E. crouaniorum* filaments and the estimated molecular weight of the PDMS in each coating (calculated from viscosity; Table 8.2), with an $R^2=0.61$ (Fig. 8.1c).
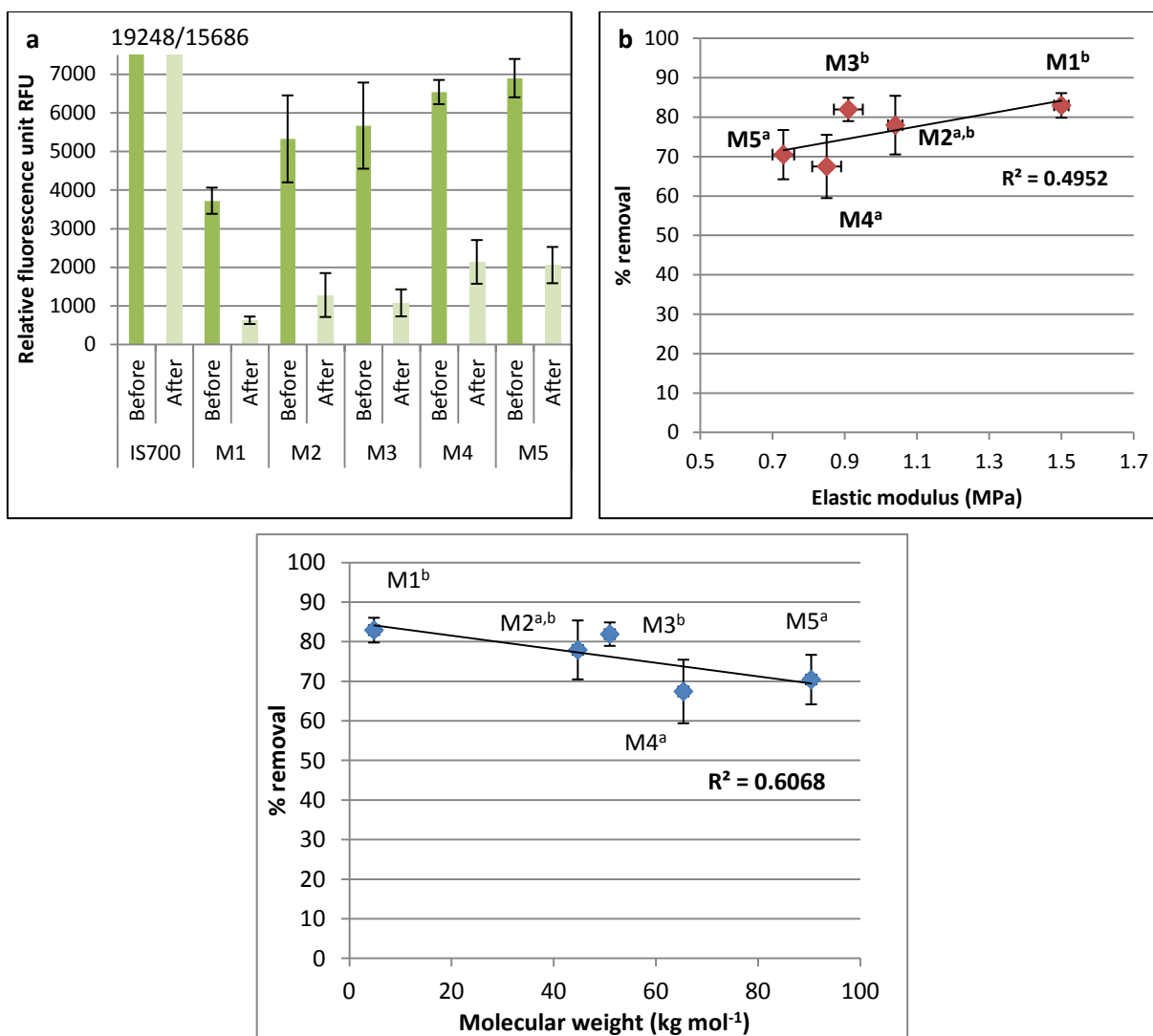
Figure 8.1: Adhesion assays with *E. crouaniorum*. a) Biomass of attached alga before and after exposure to a wall shear stress of 8 Pa, on 6 different surfaces, after incubation for 14 days at 15°C. Biomass was measured as relative fluorescence units. Percentage removal of the test coatings after exposure to shear stress of 8 Pa, calculated from data presented in (a) represented as a function of the elastic modulus (b) and estimated molecular weight (c). Means of nine replicates ± 2 x SE. Values that are significantly different at $p \leq 0.05$ in GZLM test are indicated by different letters above bars. IS700 was not included in the statistical analysis since the purpose was to test the significance of the results in relation to the hypothesis based on the silicone modulus series.

Statistical analysis of the combined performance of the surfaces (i.e. analysing together the amount of biomass before and after exposure to shear stress) revealed four groups. M1, the coating with the highest modulus, had the lowest initial biomass and the lowest adhesion strength of the alga (p≤0.05, RM ANOVA, Post Hoc REGWQ). M3 was grouped with M2 but was also grouped with M4, due to their similar intermediate-high biomass and adhesion strength. The coating M5 was also grouped to M4 due to the high biomass and the lower adhesion strength. These results confirmed the effects of modulus on the attachment and adhesion strength of *E. crouaniorum*; the higher the modulus of coatings was, lower the initial biomass was and lower the adhesion strength was.

8.3.2. *U. linza*

The biomass that developed on the coatings was a consequence of the germination and growth of spores of *U. linza* that adhered during the settlement assay. The coating IS700 had higher biomass of sporelings attached to the surface compared with all the other coatings. Significant differences were observed in the initial biomass of sporelings after 7 days of growth (Fig. 8.2a). The coating M3 was grouped with the coating M1 due to the lower sporeling biomass but was also grouped with the other coatings, which had higher sporeling biomass (Fig. 8.2a; p≤0.05, GZLM, Pairwise comparison). These differences probably reflect variations in the density of spores that settled on the surfaces.
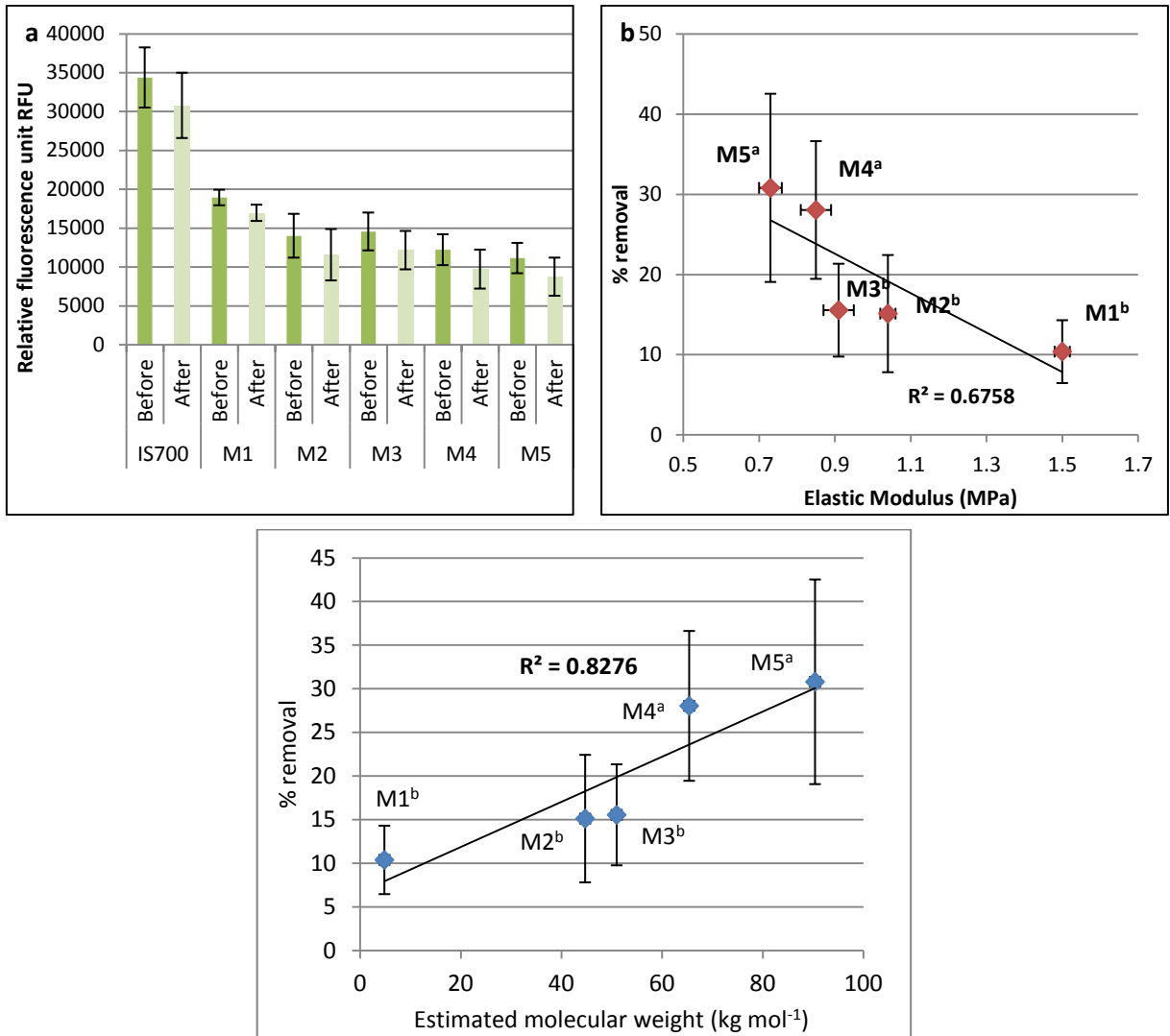
Figure 8.2: Adhesion assays with _U. linza_. a) Biomass of sporelings before and after exposure to a wall shear stress of 50 Pa, on 6 different surfaces, after incubation for 6 days at 18°C. Biomass was measured as relative fluorescence units. Percentage removal of the test coatings after exposure to shear stress of 50 Pa, calculated from data presented in (a) represented as a function of the elastic modulus (b) and estimated molecular weight (c). Means of six replicates ± 2 x SE. Values that are significantly different at p≤0.05 in GZLM test are indicated by different letters above bars. IS700 was not included in the statistical analysis since the purpose was to test the significance of the results in relation to the hypothesis based on the silicone modulus series.

Remaining biomass after the exposure to 50 Pa shear stress showed further differences between the surfaces; with 10-11 % removal, the coatings M1 and IS700 had the highest adhesion strength compared to the other coatings. The adhesion strength of _U. linza_ sporelings was high as the highest % removal was only 31 % on the coating M5, but it was

not possible to use higher shear stress in order to have higher removal as 50 Pa is the highest shear stress of the water channel. Adhesion strength of sporelings was significantly different between the test coatings and two groups were formed. The coatings M1, M2 and M3 were grouped together as they had the highest adhesion strength, while M4 and M5 were grouped together with the lowest adhesion strength (i.e. the highest % removal; Fig. 8.2b; $p \leq 0.05$, GZLM, Pairwise comparison). These results show that increased coating modulus positively influenced the adhesion strength of sporelings (Fig. 8.2b, $R^2=0.68$), i.e. the higher the modulus, the higher the adhesion strength. A stronger negative correlation was observed between the adhesion strength of sporelings and the estimated molecular weight (calculated from the PDMS viscosity; Table 8.2), with an $R^2=0.83$ (Fig. 8.2c).

8.4. Discussion

The attached filaments of *E. crouaniorum* and sporelings of *U. linza* had higher adhesion strength (lower % removal) on IS700 compared to the other coatings (except on M1 for the adhesion strength of *U. linza* sporelings). It is therefore possible to conclude that IS700 was less effective as a fouling-release coating than the modulus series test coatings for both algal species. IS700 is a commercial PDMS-based coating, with similar wettability (102°) as the silicone modulus coatings and similar elastic modulus (1.4 MPa) to M1. The differences between the test coatings and IS700 could be due to the presence of different ingredients added in IS700 such as the pigment and other additives, which could make it less effective than PDMS alone.
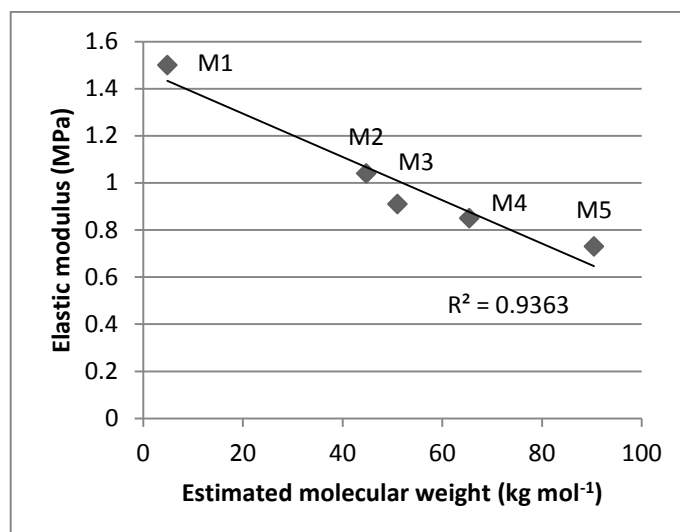
Figure 8.3: Relationship between the elastic modulus and the estimated molecular weight of the silicone modulus coatings.

One of the unusual features of this experiment is that compared to previous experiments (Chapters 3, 5-7), the levels of unattached biomass were extremely high being an order of magnitude greater on the experimental series compared with the PDMS coatings described in Chapter 6. In the case of IS700, the amount of unattached filaments was approximately double that shown in Chapter 6. As all the experiments with *E. crouaniorum* were done using a consistent, cultured source of inoculum, and under identical controlled environments, no clear reason can be advanced to explain why in this experiment there were much higher levels of unattached biomass compared with other experiments. The results with this series of coatings may suggest that the alga cannot attach effectively to these surfaces. Against this, the results for attached biomass after 14 days of growth (see next paragraph) show that the alga did attach well to surfaces to form a substantial biomass.

The test coatings, which were produced from different molecular weights of PDMS to obtain a wide range of moduli, were well-characterised, measuring the wettability/surface energy, roughness and modulus. As expected the modulus was inversely proportional to polymer molecular weight (Fig. 8.3; Brazel and Rosen 2012 referred to the rubber theory). The chain length of the PDMS polymer influences the degree of cross-linking, resulting in differences in

143

the modulus of the coatings without any changes of wettability/surface energy. It was expected that the range of moduli of these test coatings would have been different by at least one order of magnitude, but as explained previously a lower range of moduli was observed for these coatings, from 0.73 to 1.5 MPa.

Brady and Singer (2000) demonstrated that the 'Kendall' model of fracture mechanics suggests that the adhesion strength of a pseudobarnacle, simulating the influence on hard-fouling organisms on elastomeric surfaces is generally proportional to $(\gamma E)^{\frac{1}{2}}$ where γ is the surface energy and E is the elastic modulus, i.e. the harder the coating, the stronger the adhesion. Chaudhury et al. (2005) observed that this relationship was slightly different for soft-fouling organisms showing that the adhesion strength of sporelings of *U. linza* on model PDMS networks was strongly influenced by elastic moduli below approximately 1 MPa being weaker on coatings with moduli of 0.2 and 0.8 MPa compared to coatings with moduli of 2.7 and 9.4 MPa. In this thesis, the starting hypothesis for the experiments on sporelings of *U. linza* was that similar results to those observed by Chaudhury et al. (2005) would be obtained. The results with *U. linza* support this initial hypothesis as the adhesion strength was positively influenced by the modulus in the range 0.73-1.5 MPa; the higher the modulus was, the higher the adhesion strength was. This is entirely consistent with models of fracture mechanics as applied to soft-fouling organisms (Chaudhury et al. 2005).

The initial hypothesis for *E. crouaniorum* was similar to that for sporelings of *U. linza*, as the initial trial experiments using two hydrophobic silicone-based coatings S1 and S2 (Chapter 5), with modulus values of 0.34 and 0.6 MPa showed the anticipated effect of low coating modulus on soft-fouling organisms, i.e. stronger adhesion on the higher modulus coating. Unfortunately, the moduli of the silicone modulus series of coatings tested in the present chapter (0.73-1.5 MPa) did not overlap with those of the S1/S2 coatings used in Chapter 5. Therefore, a direct comparison of effects is impossible, especially as the type of modulus measured was different (storage modulus versus elastic modulus).

The results presented in this Chapter appear to indicate an unexpected effect of modulus on adhesion strength of *E. crouaniorum* - i.e. across the range there was a negative effect of coating modulus on adhesion strength, with greater removal (weaker adhesion) on the higher modulus coatings, although the effect was small, with only approximately a 13 % difference in percentage removal across the series. There is no known theory of fracture mechanics that can account for such a negative effect of modulus and it may be suggested that in addition to modulus, there may be other, uncharacterised differences in the surface and bulk properties of these coatings that affect the adhesion of *E. crouaniorum*. One obvious possibility is surface topography. All the coatings were characterised by profilometry in Chapter 4 as 'smooth' in the micrometer range with Ra roughness of 0.21 μm or less, but it is possible that more sensitive surface analytical techniques such as AFM could reveal variations in a more complex topography to account for these unexpected differences. Another possibility is that changing the molecular weight of the PDMS polymer results in differences in coating mesh size, which would be inversely proportional to molecular weight i.e. the smaller the molecular weight, the higher the modulus, but the lower the mesh size. Mesh size could have an influence on the degree of penetration into the coating of adhesive polymers secreted by the alga, so the higher penetration into the high molecular weight, lower modulus coatings, might be the basis of the slightly stronger adhesion to coatings of low modulus. This is clearly speculative and it would be interesting to examine the protein adsorption properties of these coatings.

9. FIELD ASSAYS OF FOULING PERFORMANCE OF A RANGE OF SILICONE AND FLUOROPOLYMER COATINGS DURING 2010 SEASON

9.1. Introduction

The challenge of finding effective, environmentally friendly antifouling and fouling-release (AF/FR) coatings has led researchers to test their coatings not only in the laboratory but also in the field to assess their effectiveness in the real world. The two situations are different. Whereas laboratory assays present the challenge of a single species, under controlled and defined conditions, coatings in the field are exposed to a whole community of organisms that compete for colonisation of the surfaces. Field assays reveal long-term performance of the test surfaces in the real-world where the surfaces are surrounded by a diverse and dynamic community that is in constant change due to fluctuating environmental factors (physical, biological and chemical) (Benedetti-Cecchi 2000; Thomason et al. 2002).
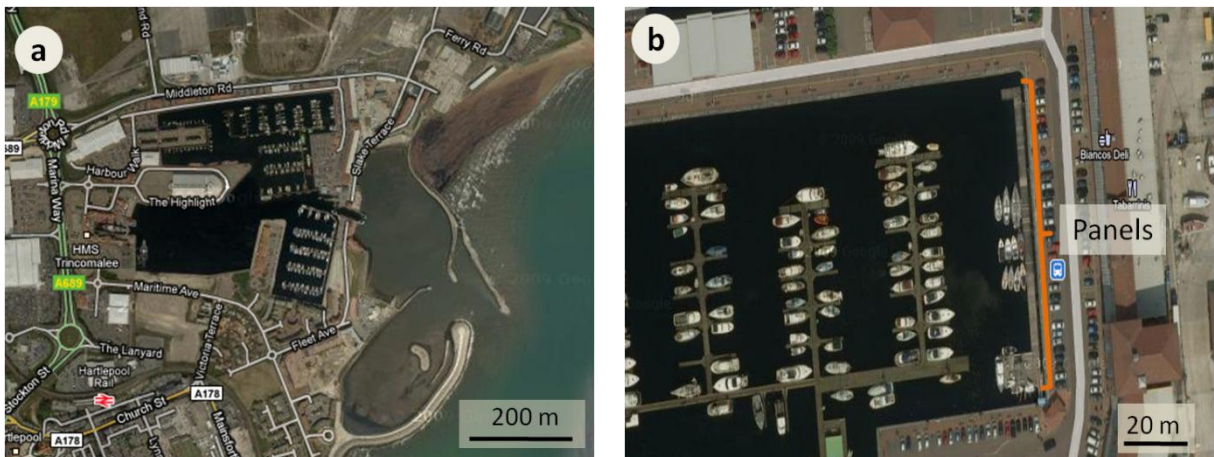
Figure 9.1: Immersion site in Hartlepool Marina. a) General view of Hartlepool Marina. b) Location of the panels (orange line), immersed between the pontoon and the wall. The length of the pontoon was approximately 70 m (from Google Maps).

The main aim of the 2010 field assays reported in this Chapter was to conduct pilot tests that would guide subsequent more detailed field experiments in 2011. For the field assays

reported in this Chapter; two sites were chosen to place several panels with test surfaces in static immersion. Hartlepool Marina (Fig. 9.1) was used as the main site in view of its proximity to the main International Paint laboratories at Gateshead, and Prendergast (2007) observed the presence of ectocarpoid algae on panels over a number of years. Newton Ferrers (Fig. 9.2) was chosen as secondary site due to the presence of test rafts belonging to International Paint in the Yealm estuary.

Three different experiments were performed, two in Hartlepool Marina and one in Newton Ferrers during the spring-summer season of 2010, to assess the performance in the field of the two sets of coatings tested in Chapter 5 (i.e. the three fluoropolymers and the three silicone-based coatings). To assess the performance of the test surfaces on the appearance of organisms, batches of test slides were immersed in Hartlepool Marina on 4th of May 2010 for 4 successive periods of one month (Experiment 1). The purpose of this experiment was to obtain a 'snapshot' of the fouling community (particularly ectocarpoid algae) in relation to any variations in fouling pressure during the spring/summer period. The second experiment also involved immersion of surfaces on May 4th, but the slides were all immersed at the same time, then removed at monthly intervals over four months, allowing the succession of species, and in particular the presence of ectocarpoid algae to be examined in relation to the properties of the surfaces (Experiment 2).

The third experiment, performed on the external side of a raft at Newton Ferrers from the 10th of June 2010 (Fig. 9.3), was smaller as the number of slides of each treatment was limited (Experiment 3). The observation of the diversity, with a particular interest in ectocarpoid algae, was done in two collections (after 43 and 86 days' immersion). Initially, it was decided that there would only be one collection of data for this experiment. However, after 43 days, when the panels were observed, there was an abundance of ectocarpoid algae, so it was decided that only three replicate slides for each treatment would be removed, leaving the

remaining three for further observation approximately 1.5 months later, the 22nd of September (i.e. in total 86 days' immersion).
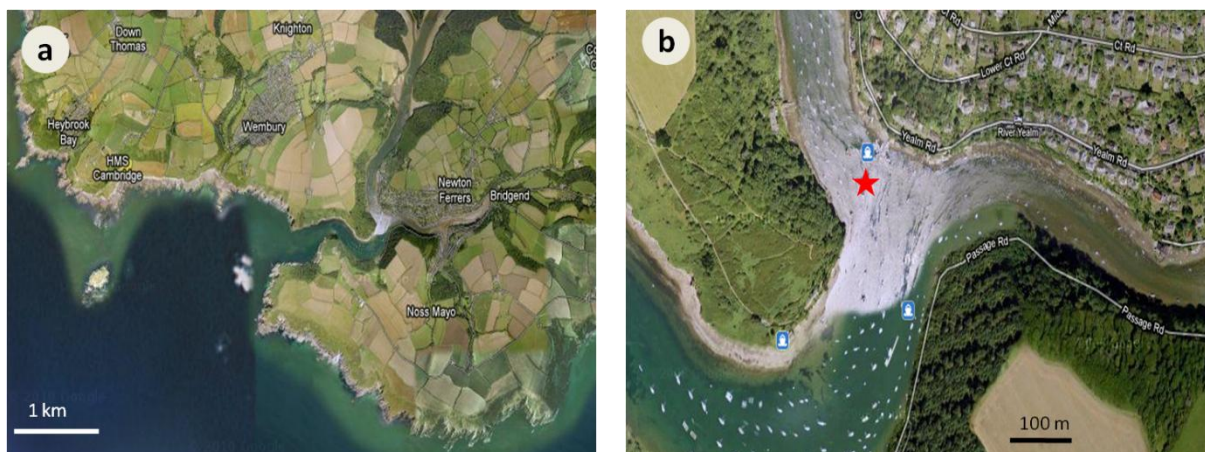
Figure 9.2: Immersion site in Newton Ferrers. a) General view of Newton Ferrers area. b) Location of the panels (represented by the red star), immersed on a raft in the entrance of the estuary (from Google Maps).

9.2. Materials and Methods

9.2.1. Test coatings

Two sets of coatings were tested during these field experiments, the three silicone-based coatings S1, S2 and S3 and the three fluoropolymer coatings mD10, mD10-H and mE10-H (tested in laboratory experiments in Chapter 5). In addition, the two Intersleek coatings IS700 and IS900 were tested as commercial standards and glass slides as negative controls. These surfaces were produced and characterised as described in Chapter 4.

9.2.2. Preparation of the field experiments

To test the performance of the different surfaces, 6-replicate panels measuring 35 cm length by 15 cm width were made in International Paint (Fig. 9.3). Each panel, immersed at 1 m depth and oriented at 45° from a vertical position, contained one slide of each surface (i.e. a total of 9 slides), arranged randomly on the panels (using random calculation from Excel).

The panels immersed in Hartlepool Marina were placed between the pontoon and the wall to avoid boat traffic that could disturb the panels (Fig. 9.1).

The three experiments were performed using 'destructive' techniques as the slides were collected and not placed back in the seawater after observation due to manipulation and observation under the microscope.
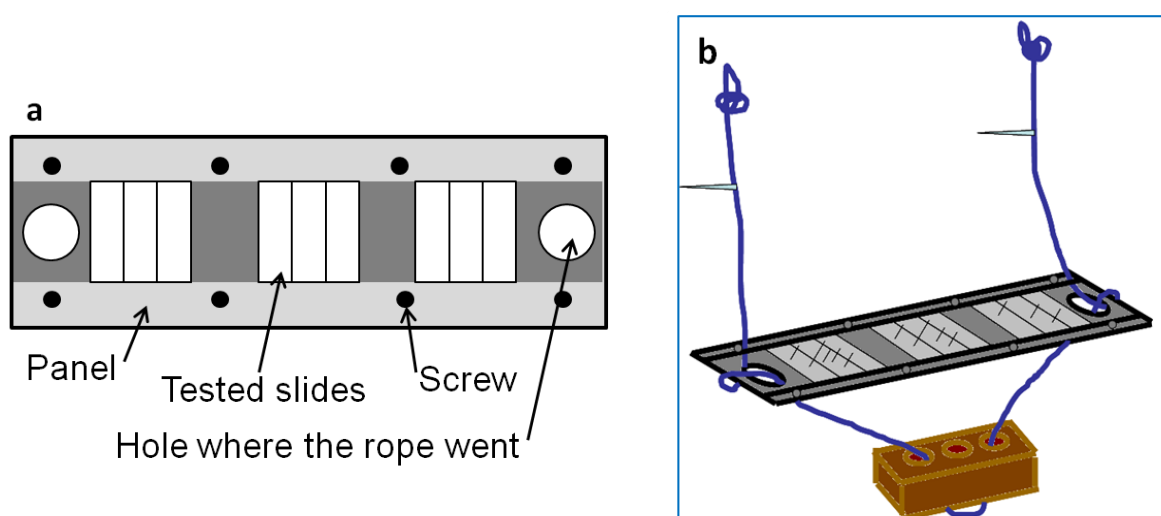
Figure 9.3: Experimental panels, with 9 different surfaces (a), attached with blue ropes on to the pontoon (b). There were light blue cable ties at 1 meter from the panel, which were aligned with the water surface to ensure that all the panels were immersed at 1 meter. The whole panel was oriented at about 45 degrees from a vertical position. The weight allowed the panel to stay in the same position. Figures not to scale.

Percentage cover of all the fouling categories was obtained following the "Phoenix" in-house Experimental Fouling Assessment Record Sheet (standard assessment used by International Paint). It recorded the percentage cover of microfouling (slime, biofilm), weeds (algae), soft-bodied animals (tunicates, hydroids) and hard-bodied animals (worms, barnacles). The percentage cover of ectocarpoid algae was also recorded separately. Statistical analysis of the adhesion data is explained in Chapter 2.10, and statistical tables for the whole Chapter are presented in Appendix 8.

9.3. Results

9.3.1. Experiment 1: Trial experiment on variations in initial surface colonisation at Hartlepool Marina with surfaces of different modulus.

Although four data collections were made, no results are reported for the second data collection as the slides were sent by post and damaged during transport. In that case, for experiments 1 and 2, the results of only three collections are discussed, using the terms: first, second and third data collections. Figure 9.4a shows that for all three collections, the main type of fouling organisms observed on all the surfaces within each successive 1-month period was microfouling, with low amounts of weed and animal fouling (Fig. 9.4a). On most surfaces, the total fouling coverage approached 100% coverage.

During the last data collection (i.e. after 36 days' immersion), the total coverage was significantly lower than the two previous ones ($p \leq 0.05$, GZLM, Pairwise comparison). It was also observed that at the last data collection, IS700 had lower total coverage than all the other surfaces ($p \leq 0.05$, GZLM, Pairwise comparison).

The percentage cover of microfouling decreased with the time of immersion, showing that the accumulation/appearance of microfouling was lower for the 'summer period' (end of July and early September) than for early June (Fig. 9.4b). Only during the last data collection, were differences observed between the surfaces; IS700 had less microfouling (60 %) than mD10, S2, S3 and glass ($p \leq 0.05$, GZLM, Pairwise comparison). No further differences were observed.
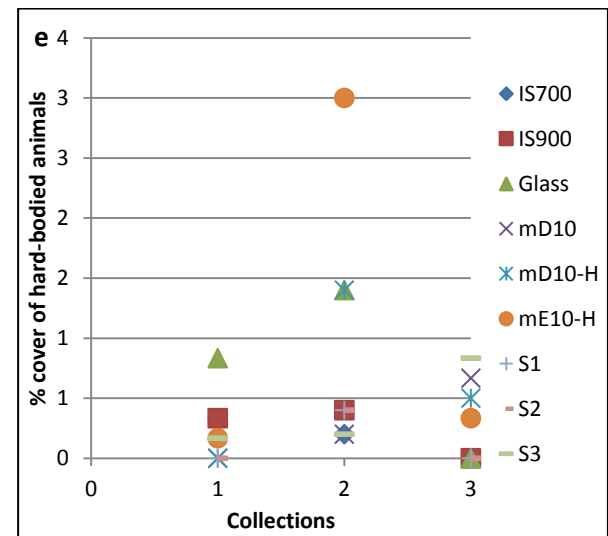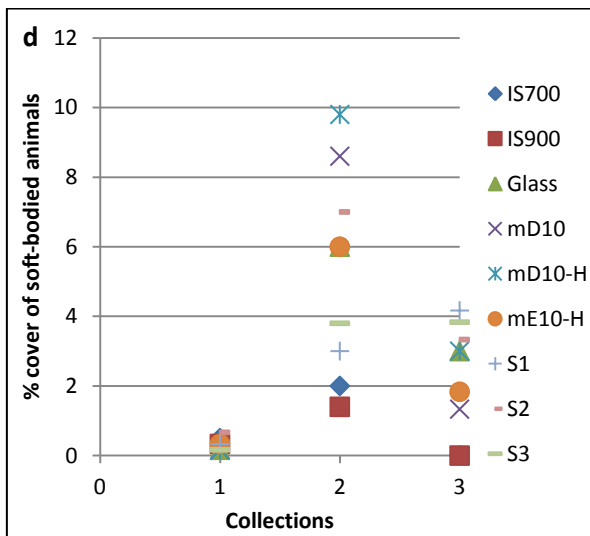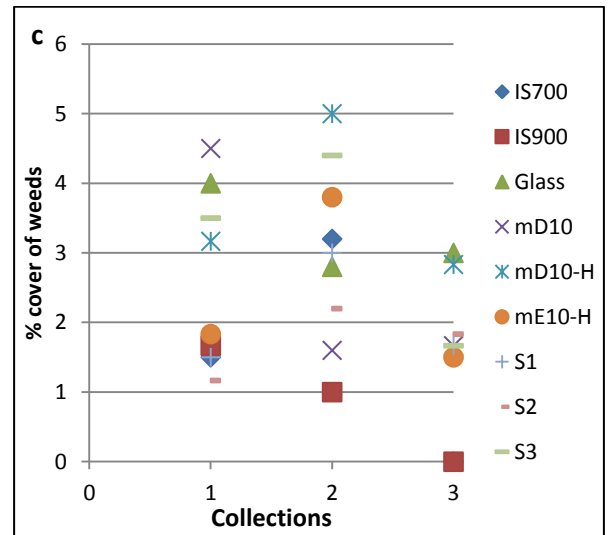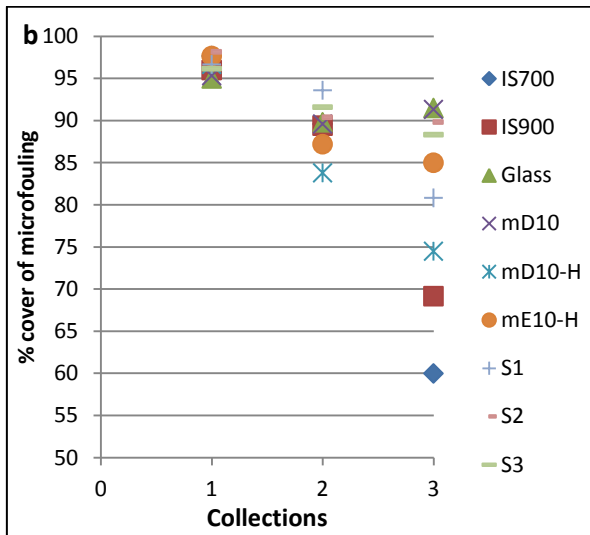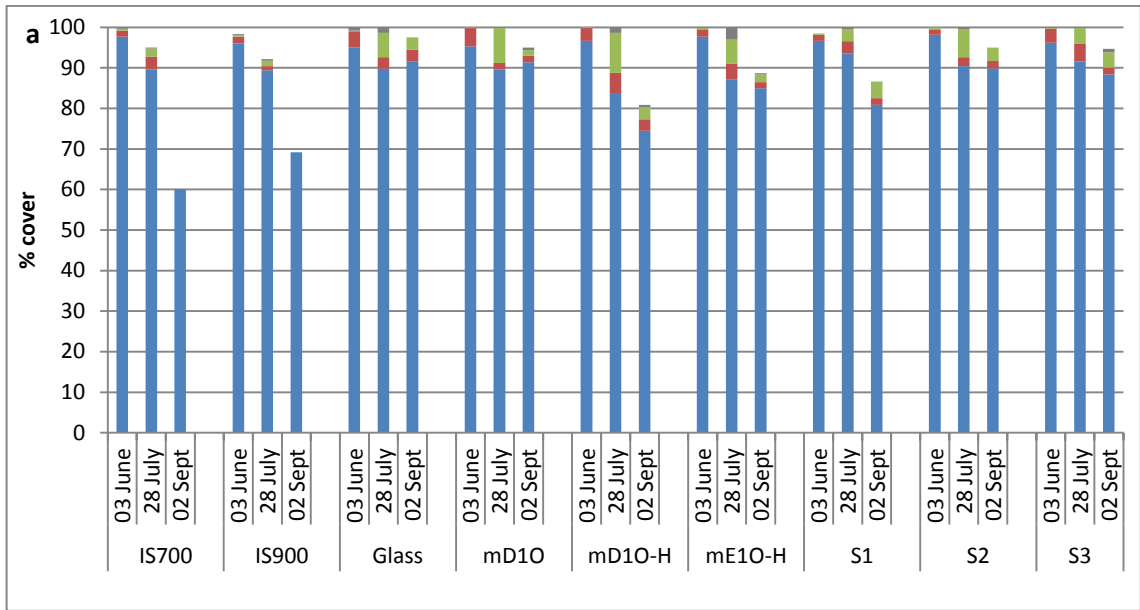
Figure 9.4: Percentage cover observed on 9 different surfaces in Hartlepool Marina after one month's immersion during spring/summer 2010. a) Percentage cover for the 4 fouling categories: microfouling (blue), weeds (red), soft-bodied animals (green) and hard-bodied animals (grey). Figures b, c, d and e represent the percentage cover of one of the fouling categories: microfouling, weeds, soft- and hard-bodied animals, respectively. For each data collection, n=6 for each treatment. Note: the scale is different for each graph. The panels were immersed on the 4th of May, 7th of July and 28th of July and inspected on 3rd of June (collection 1), 28th of July (collection 2) and 2nd of September (collection 3).

The percentage of weeds represented in Figure 9.4c varied slightly between 0 and 5 % for the three collections. However, no significant difference was observed between the surfaces at each collection ($p \leq 0.05$, GZLM, Pairwise comparison).

Figure 9.4d shows the coverage of soft-bodied animals. For the first and third data collections, the coverage was lower than 4 % while for the second one, it was higher with percentage up to 10 % (mostly represented by polyps). However, no significant differences between the surfaces were observed due to high variation between the replicates, except for IS900 that was different from S2 and mD10-H for the second data collection (i.e. after 21 days' immersion) ($p \leq 0.05$, GZLM, Pairwise comparison).

For the coverage of hard-bodied animals, significant differences were observed (Fig. 9.4e). For the second data collection, the coverage on both coatings mE10-H and glass slides was not significantly different but was higher than on the other surfaces ($p \leq 0.05$, GZLM, Pairwise comparison). However, the percentage cover on all the surfaces was lower than 4 % (mostly represented by barnacles) so although statistically significant these differences are relatively minor.
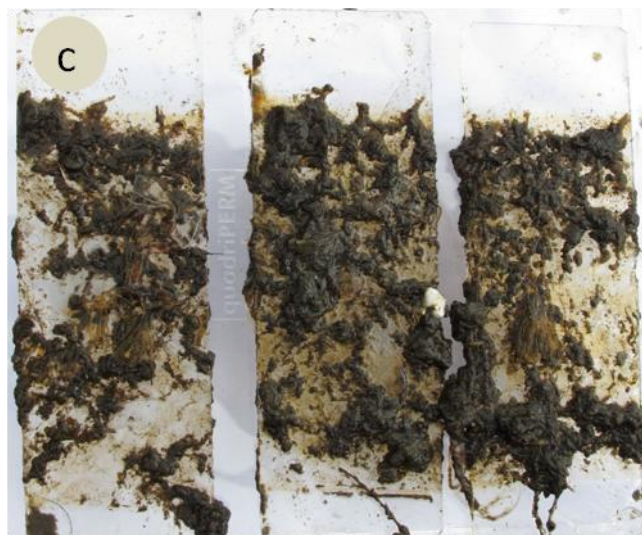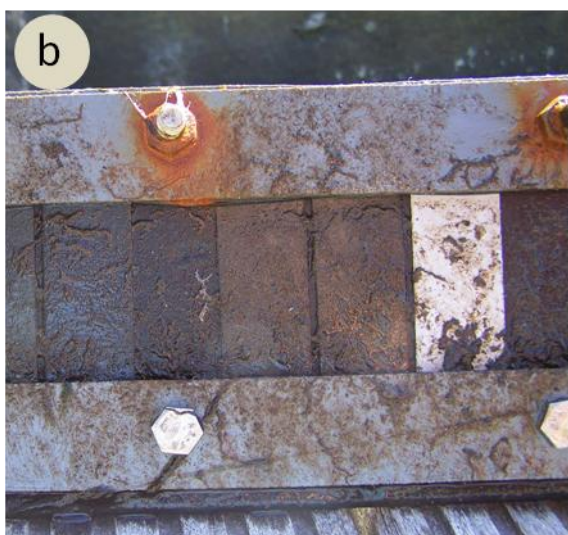
Figure 9.5: Panels immersed in Hartlepool Marina after a month of immersion (a and b) and slides after 3 months' immersion (c). As it is difficult to distinguish the test surfaces, red stars were placed above each slide in Figure a.

For all the data collections, a detailed microscopic observation of the presence of ectocarpoid algae was made and two genera were generally observed, *Hincksia* and *Ectocarpus*. However, only a few filaments were found on the surfaces, due to the high quantity of microfouling and silt making the observations difficult. Because the percentage cover of ectocarpoid algae was lower than 2%, it was not of interest to do further analysis.

9.3.2. Experiment 2: Trial experiment on the 'succession' of organisms at Hartlepool Marina with surfaces of different modulus.

Figure 9.6a shows that, as for Experiment 1, microfouling predominated at all the collections and on all the surfaces, except maybe for the glass surface, which showed reduced microfouling at the last collection (Fig. 9.6b). Figures 9.6c, d and e showed low variation for the different fouling categories (except microfouling), except on the glass slides.

For all the data collections, a particular observation for the presence of ectocarpoid algae was made. Microscopy revealed only a few filaments of *Hincksia* and *Ectocarpus* on the slides (<1 % cover), due to the high quantity of microfouling and silt making observations difficult.

Differences in microfouling coverage were observed between both the data collections and the surfaces (Fig. 9.6b). After 28 days' immersion, the coverage of microfouling on all the surfaces was similar, while differences were observed between the surfaces after 89 days' immersion. Statistical analysis showed that the coverage of microfouling decreased significantly with the length of immersion ($p \leq 0.05$, GZLM, Pairwise comparison). For the whole experiment, the glass surface had a lower coverage than mE10-H, IS700, IS900 and S1 ($p \leq 0.05$, GZLM, Pairwise comparison). When the collections were analysed separately, it was possible to observe further differences. After 89 days' immersion, the coverage on the coatings mD10-H and mD10 was significantly lower than on IS900. In addition, after 119 days, the coverage on glass slides was significantly lower than on all the other surfaces except mD10-H.
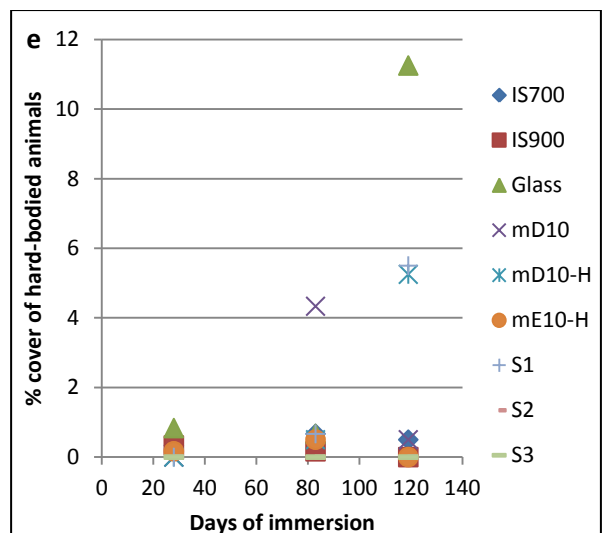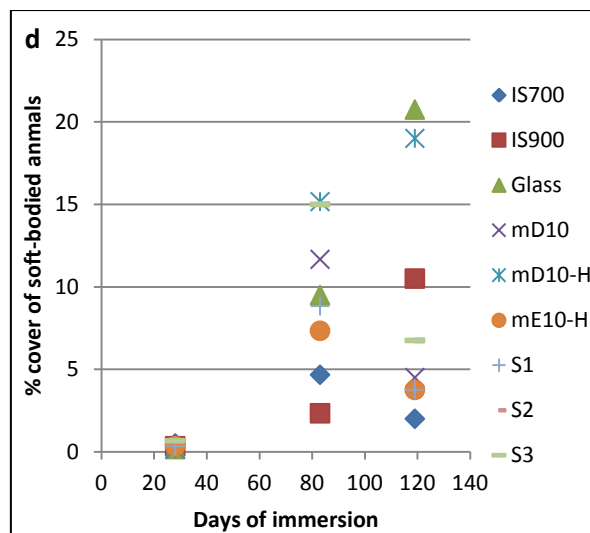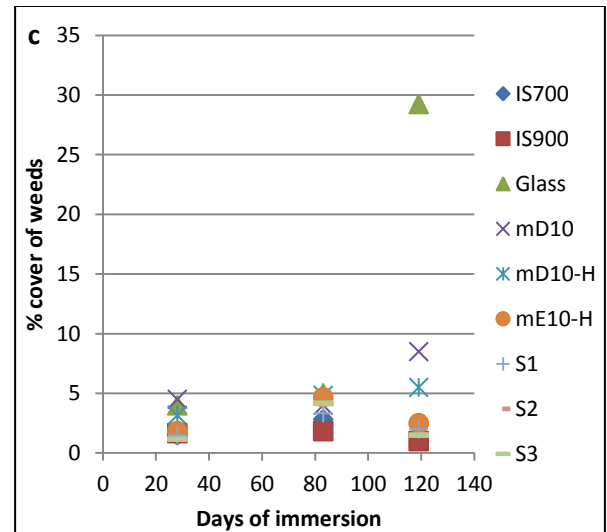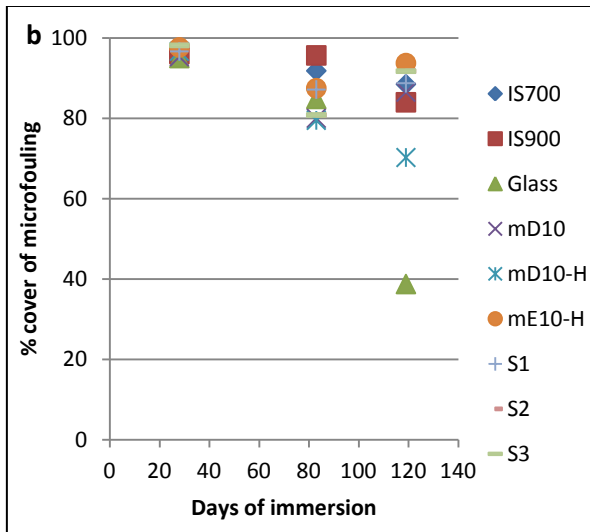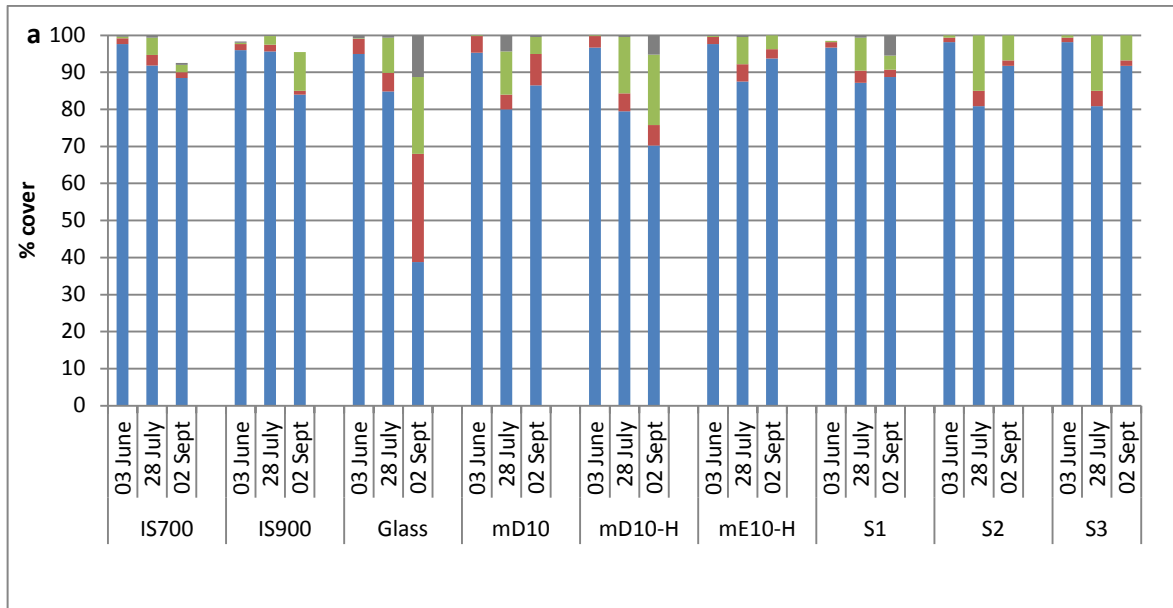
Figure 9.6: Percentage cover observed on 9 different surfaces in Hartlepool Marina after 28, 89 and 119 days' immersion during spring/summer 2010. a) Percentage cover for the 4 fouling categories: microfouling (blue), weeds (red), soft-bodied animals (green) and hard-bodied animals (grey). Figures b, c, d and e represent the percentage cover of one of the fouling categories: microfouling, weeds, soft- and hard-bodied animals, respectively. For each data collection, n=6 for each treatment. Note: the scale is different for each graph. The panels were all immersed on the 4th of May and data collected on the 3rd of June, the 28th of July and the 2nd of September.

The coverage of weeds represented in Figure 9.6c varied between 0 and 10 % for all the surfaces except for the last collection (i.e. 119 days' immersion) and on glass slides, which was around 30 %. No significant difference was observed between the surfaces for the two first data collections. However, data after 119 days' immersion showed that the glass slides had a significantly higher percentage cover than all the other surfaces ($p \leq 0.05$, GZLM, Pairwise comparison).

After 28 days' immersion, almost no soft-bodied animals were observed on the surfaces. Then from 89 days' immersion, soft-bodied animals were present on the surfaces with a percentage between 0 and 22 % (Fig. 9.6d; mostly represented by polyps), and the coating mD10-H had significantly a higher coverage than IS900 and IS700. In addition, after 119 days' immersion, glass and mD10-H had significantly a higher percentage cover than IS700 and mE10-H ($p \leq 0.05$, GZLM, Pairwise comparison).

As for soft-bodied animals, after 28 days' immersion, almost no hard-bodied animals were present on the surfaces. Then from 119 days' immersion, some of the surfaces had a low coverage of hard-bodied animals, up to 11 % (mostly represented by barnacles). However, no significant differences were observed between the surfaces for any of the collections ($p \leq 0.05$, GZLM, Pairwise comparison).

In conclusion, small variations were observed between both the collections and the surfaces. The negative control surface (i.e. glass) had more weeds and soft-bodied animals after 119

days' immersion. The percentage of animal (soft and hard) fouling was greater from 89 days compared to the start, but microfouling was still the dominant fouling category. However, no other important variation was noticed, as for example only few filaments of ectocarpoid algae were observed during the experiment showing no difference between the surfaces.

9.3.3. Experiment 3: Succession of organisms at Newton Ferrers

Figure 9.7 shows that at the Newton Ferrers site, after 43 and 86 days' immersion the percentage cover differed between both the surfaces and the collections. After 43 days' immersion (i.e. 21st of July), most of the surfaces were dominated by microfouling and weeds, while after 86 days (i.e. 22nd of September), soft- and hard-bodied animals were also present at a large coverage.
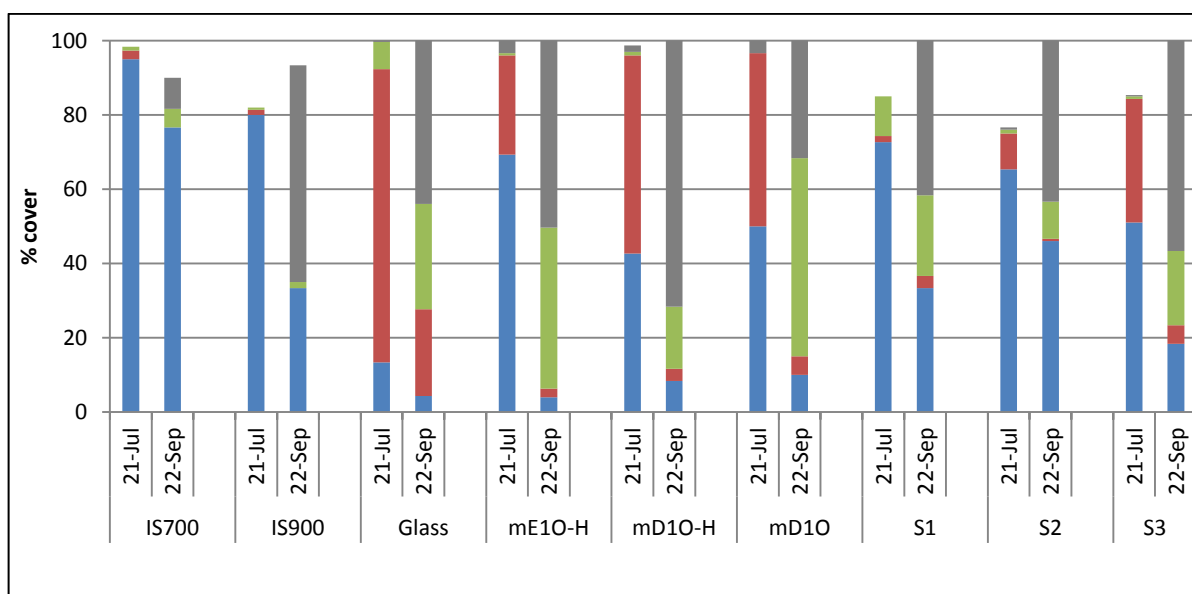
Figure 9.7: Percentage cover observed on 9 different surfaces attached to Newton Ferrers raft after 43 and 86 days' immersion during summer 2010. Percentage cover for the 4 fouling categories: microfouling (blue), weeds (red), soft-bodied animals (green) and hard-bodied animals (grey). The panels were all immersed on the 10th of June and data were collected on the 23rd of July (i.e. 43 days) and the 22nd of September (i.e. 86 days).

For the microfouling coverage, differences between both data collections were observed as the amount of microfouling on the surfaces decreased for the second collection (Fig. 9.8b;

p≤0.05, GZLM, Pairwise comparison). For the whole field experiment, the coverage of microfouling on IS700 was significantly lower than on mD10-H and glass surfaces (p≤0.05, GZLM, Pairwise comparison). In addition, after 43 days' immersion, IS700 had higher coverage than glass, the three fluoropolymers and S2. Glass had a lower coverage of microfouling than IS700, IS900 and S2, as it had high cover of weeds (p≤0.05, GZLM, Pairwise comparison). However, there was no significant difference after 86 days. It is possible to conclude that the coverage of microfouling was not influenced by the coating modulus.
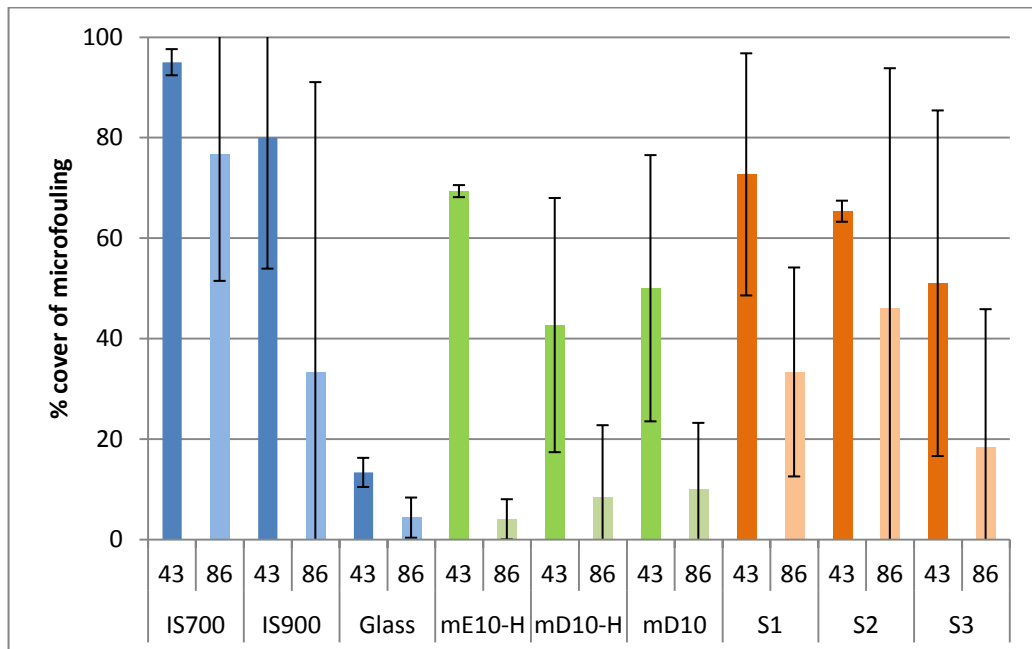
Figure 9.8: Percentage cover of microfouling as a function of days and surfaces. Each bar represents the mean of collected data (n=3; 3 panels x 1 replicate) ± SD.

Differences in percentage cover of weeds were observed between both the data collections and the surfaces. After 43 days' immersion, several surfaces (mD10, mD10-H, mE10-H, S3 and glass) had high coverage of weeds (>26 %) compared to the other surfaces (Fig. 9.9). However, all the surfaces had low coverage after 86 days' immersion except glass, which had 23 % cover. The coverage after 43 days' immersion was not significantly different for the three fluoropolymers due to high variation between the replicates, showing there was no

effect of modulus for this set of coatings (p≤0.05, GZLM, Pairwise comparison). The fluoropolymers were less effective than both Intersleek coatings, while S1 and S2 were similar to them (p≤0.05, GZLM, Pairwise comparison). For the set of silicone-based coatings, S3 had a higher amount of weeds attached to its surface compared to S1 and S2, showing a possible effect of modulus and wettability; the amount of weeds is higher on high modulus and high wettability coatings. However, it is not possible to conclude if the differences of weeds reflect the effect of modulus or wettability or even the combination of both.
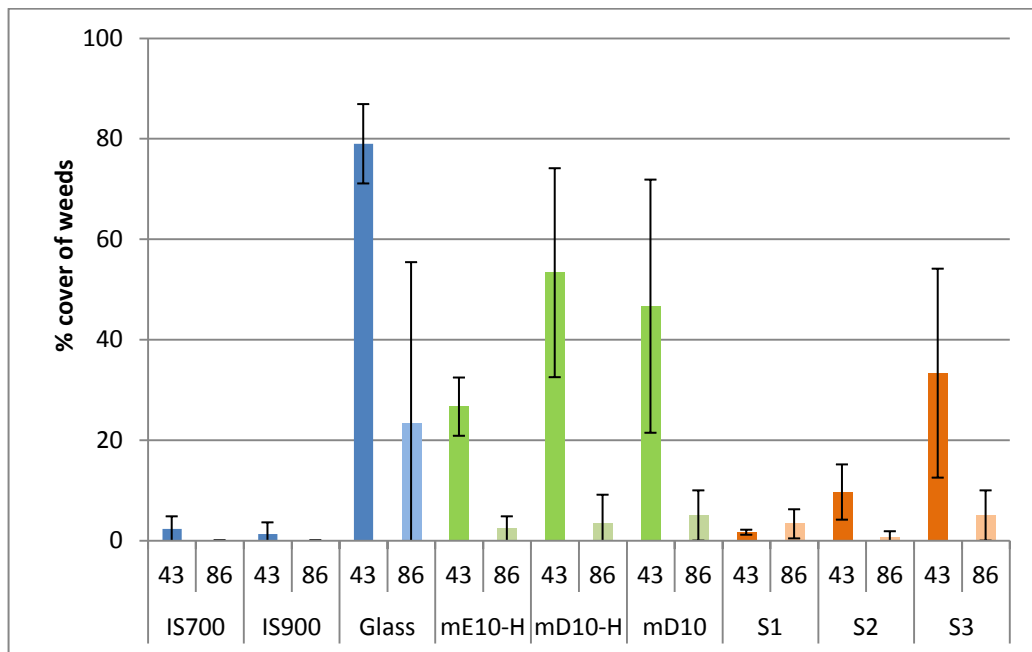
Figure 9.9: Percentage cover of weeds as a function of days and surfaces. Each bar represents the mean of collected data (n=3; 3 panels x 1 replicate) ± SD.
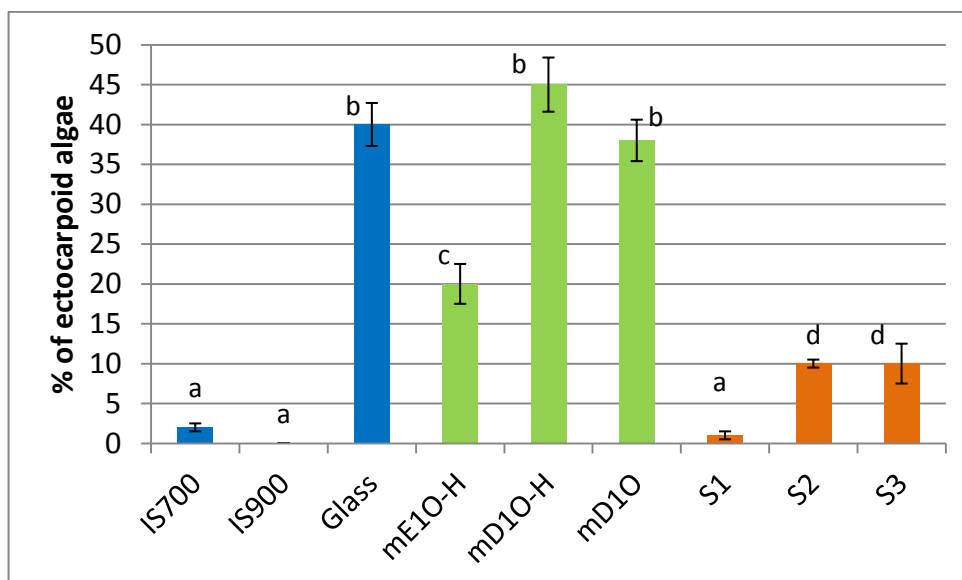
Figure 9.10: Percentage cover of ectocarpoid algae on the 9 different surfaces after 43 days' immersion in Newton Ferrers. Mean of 3 replicates (3 panels x 1 replicate) ± SD. Values, which are significantly different at p≤0.05 in GZLM test are indicated by different letters above the bars.

Figure 9.10 shows the percentage of ectocarpoid algae on nine different surfaces only after 43 days' immersion, as there were no ectocarpoid algae after 86 days. Microscopy revealed both *Hincksia* and *Ectocarpus* on the surfaces, but no differences in surface preferences between the two genera were observed compared to the results obtained for the laboratory experiments (Chapter 5). Figure 9.10 shows that glass slides, mD10 and mD10-H had a higher coverage than the other surfaces. The coating mE10-H had a medium percentage cover followed by S2 and S3, while IS900, IS700 and S1 had almost no ectocarpoid algae. The statistical analysis confirmed that the coverage of ectocarpoid algae was grouped into these four groups (p≤0.05, GZLM, Pairwise comparison). Differences were observed between the two sets of coatings; mE10-H had lower coverage than mD10 and mD10-H, and S1 had lower coverage of ectocarpoid algae than S2 and S3 (p≤0.05, GZLM, Pairwise comparison). For both sets of coatings, the lower coverage of ectocarpoid algae was observed on the coatings with the lowest modulus mE10-H and S1. However, for each set of

coatings, comparison between the coatings was more complicated since there were differences in both modulus and surface energy; coating mE10-H was hydrophilic compared to the two hydrophobic coatings mD10 and mD10-H but S1 and S2 were hydrophobic while S3 was hydrophilic. It is possible to conclude that the modulus positively correlated to the colonisation of ectocarpoid algae for the set of silicone coatings, but it was not possible to draw any conclusions for the fluoropolymer coatings, as it could be one or the combination of both properties that influenced the colonisation of ectocarpoid algae.

The coverage of ectocarpoid algae plotted as a function of modulus (Fig. 9.11) shows a possible positive correlation between these two parameters. However, the correlation was weak (R^2=0.6) and since more than one property changed between these surfaces, the validity of this comparison is questionable.
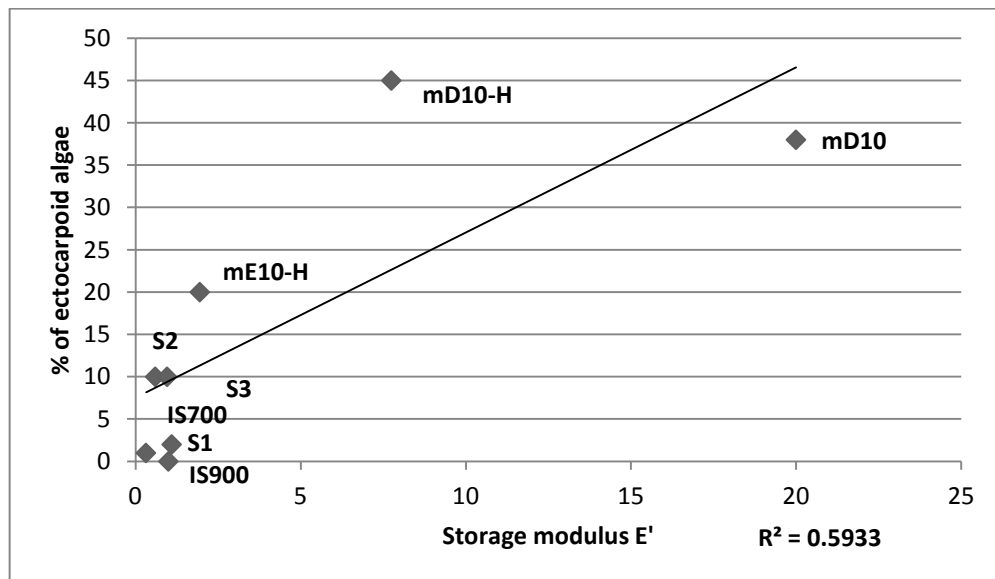
Figure 9.11: Correlation between the percentage of ectocarpoid algae and the storage modulus E' after 43 days' immersion.

In contrast to the microfouling and the weeds, the coverage of soft-bodied animals was low after 43 days' immersion and then increased by day 86 varying between 0 to 54 % cover

according the surfaces (Fig. 9.12; mostly represented by polyps and tunicates). After 86 days, differences were observed between the surfaces (p≤0.05, GZLM, Pairwise comparison). The coatings mD10 and mE10-H, which had a high coverage, were higher than IS900 and the coverage on mD10 was also higher than on IS700 and S2.
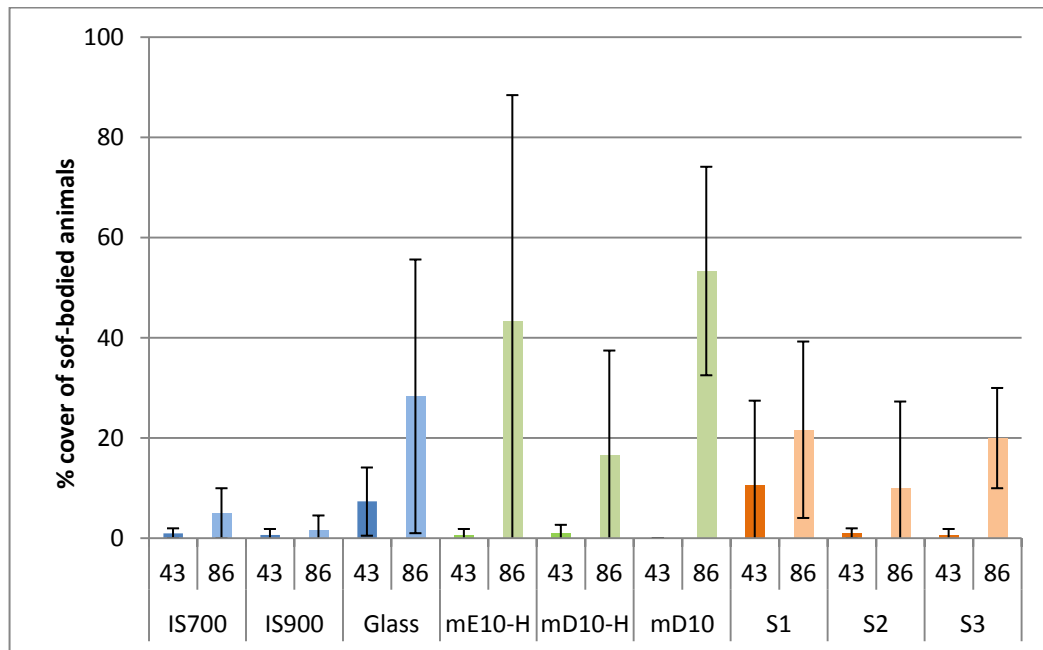
Figure 9.12: Percentage cover of soft-bodied animals as a function of days and surfaces. Each bar represents the mean of collected data (n=3; 3 panels x 1 replicate) ± SD.

After 43 days' immersion, the percentage cover of hard-bodied animals was low and similar between all the surfaces, while after 86 days, the surfaces had a greater percentage cover, except IS700 (Fig. 9.13; mostly represented by barnacles and worms). No significant difference was observed for both collections, as variations between the replicates were high (p≤0.05, GZLM, Pairwise comparison).
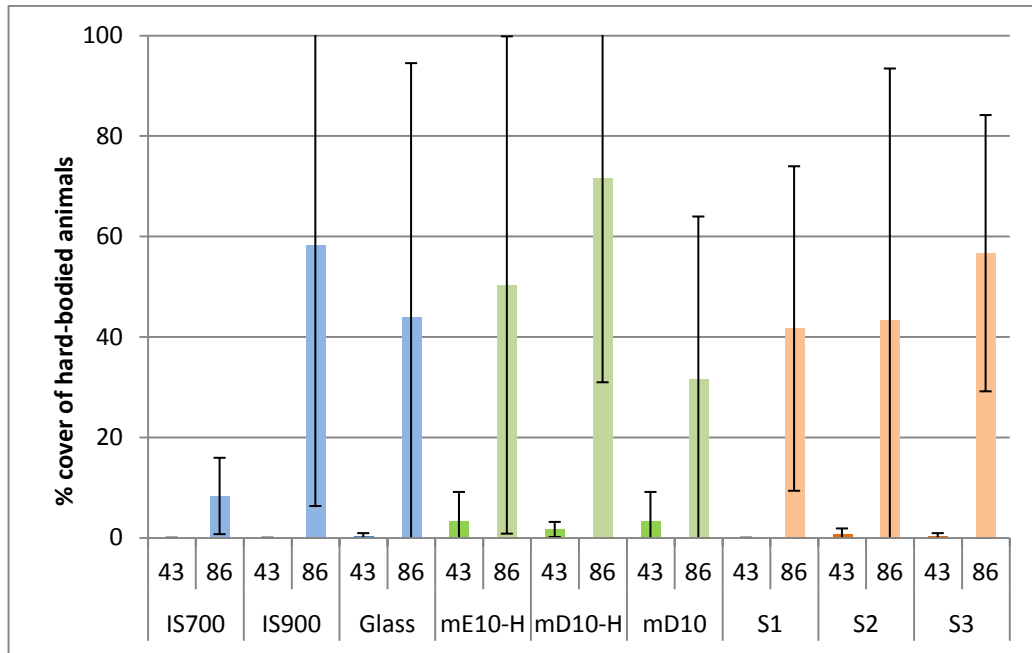
Figure 9.13: Percentage cover of hard-bodied animals as a function of days and surfaces.
Each bar represents the mean of collected data (n=3; 3 panels x 1 replicate) ± SD.

9.4. Discussion

One of the aims of the pilot field experiments described in this Chapter was to compare the results obtained with those in laboratory assays. The laboratory assay assessed the FR performance of the test surfaces on the attachment and adhesion strength of *Ectocarpus crouaniorum*. On the contrary, static field assays basically measure how well surfaces are colonised and there may be little relationship between these two measures of performance. Although as explained by Martinelli et al. (2012b), depending on location, immersed panels might be subjected to water currents and other disturbances (such as grazers and boat traffic), which could expose the surfaces to a low shear stress, thus introducing an element of FR for organisms that do not adhere strongly. Hartlepool Marina being fully enclosed by a sea wall has limited tidal exchange and almost no water current, while the panel raft in Newton Ferrers was placed in the estuary where there are water currents and other disturbances such as boat traffic and tidal flow. Swain et al. (1998) also showed that disturbances such as grazing decrease the colonisation of fouling organisms on surfaces.

Slight differences between both the surfaces and the collections were observed during the experiments performed in Hartlepool Marina. For the first experiment, microfouling was always dominant, with a low percentage of weeds, soft- and hard-bodied animals. No variation in the appearance of organisms was observed at each monthly immersion, except for a slightly higher amount of soft-bodied animals at the second collection (Fig. 9.5). It seems that during this period of time, the same category of fouling organisms attached to the surface without differences between the surfaces, so there was no effect of surface and bulk properties. This was expected since each surface was only immersed for one month, thus allowing little time for the development of macrofoulers. The appearance of fouling categories was not significantly different during the data collections, except for the appearance of microfouling that decreased slightly from the end of spring (start of June) to the "summer period" (end of July and early September). For the second experiment, a higher proportion of weeds, soft- and hard-bodied animals was observed after 89 and 119 days' immersion. However, there was still a high percentage of microfouling (with silt). In retrospect, the location of the panels was not ideal. The panels from the 28 days' immersion were covered by silt and debris, which obscured the biofouling. It appears that much of the general detritus from the marina finished up in that area, which may have impacted the fouling community that developed on the surfaces.

However, the experiment performed in Newton Ferrers was more informative. Only two data collections were done but they showed variations in colonisation between 43 and 86 days' immersion -the first data collection showed that the surfaces were fouled by microfouling and weeds while after 86 days, a larger amount of soft- and hard-bodied animals was present on the surfaces. These results were consistent with previous studies on succession of organisms, which showed that colonisation starts mostly by microfouling and weeds and later soft- and hard-bodied animals colonise the surfaces and grow over the microfouling and the weeds.

The comparison of the coverage for both data collections at Newton Ferrers showed that most of the surfaces did not have the same dominant fouling category. IS700 and IS900 were different, because IS900 had a high percentage cover of hard-bodied animals after 86 days' immersion while IS700 was dominated by microfouling. The three fluoropolymers were also different, as for Hartlepool Marina, the coatings with high modulus and low wettability mD10 and mD10-H, had a high percentage of weeds compared to the coating mE10-H that had low modulus and high wettability after 43 days' immersion. After 86 days, the hardest coating mD10 was colonised by microfouling and soft-bodied animals while mD10-H the coating with intermediate modulus was covered by microfouling and hard-bodied animals. In addition, the three silicone-based coatings were different; for the first collection, the coatings with high wettability and low modulus S1 and S2 were dominated by microfouling while the coating with low wettability and high modulus S3 had a high percentage cover of weeds. However, after 86 days, the two hydrophobic coatings S1 and S2 were different; S1 had a high coverage of hard-bodied animals while S2 had a mixture of microfouling and hard-bodied animals.

The presence of ectocarpoid algae after 43 days' immersion showed that they were present in Newton Ferrers during the period of immersion (i.e. 10th of June to 23rd of July). Differences between the surfaces were observed; both IS700 and IS900 had low percentage cover, the latter being consistent with the laboratory assays (Chapters 3 and 5), which showed that filaments on IS900 had a low adhesion strength. However, in the laboratory assays, ectocarpoid algae attached more strongly to IS700 than to IS900 (Chapters 3 and 5). The differences could be explained by the fact that in the field, ectocarpoid algae are interacting with other organisms; the environmental factors are also important for the adhesion of organisms and could have affected the presence of ectocarpoid algae. In addition, one of the differences between the laboratory and field experiments was that the stage of development that attached to the surfaces was different; while filaments were used

for the laboratory assay, spores most likely attached to the surfaces in the field assays and so their adhesion preferences might be different.

The comparison of the percentage cover of ectocarpoid algae for the three fluoropolymer coatings showed that the data obtained were similar to those from the laboratory assays. In the field, the percentage cover was low for mE10-H, which is similar to the low biomass before and after shear for the laboratory experiment (Chapter 5). The coating mD10-H for laboratory assays and field experiment had high percentage cover, high adhesion strength (Chapter 5). The coatings mD10 and mD10-H had similar and high biomass before the shear stress exposure for the laboratory assays but the percentage removal of mD10 was higher (30 % removal) than mD10-H (8 % removal); the field experiment showed that mD10 had similar percentage cover as mD10-H. As for IS700, these differences could be explained by the environmental factors, the competition with other organisms or the lower shear stress in the field compared to the laboratory.

Environmental disturbances could also explain that the results for percentage cover of ectocarpoid algae for the silicone-based coatings were not consistent with the results obtained in the laboratory (Chapter 5). In the field, S2 and S3 had similar percentage cover (ca. 10%), while S1 had a low percentage cover (ca. 1%) indicating a reduced ability of ectocarpoid algae to colonise the low surface energy S1 surface. However, in the laboratory assays, the lowest initial attachment and lowest adhesion strength of *E. crouaniorum* were shown on the high surface energy/high modulus S3 coating (Chapter 5).

Correlations between properties (wettability, surface energy and modulus) and percentage cover by ectocarpoid algae in the field were observed at Newton Ferrers and a positive but weak correlation (R^2=0.6) was found between the storage modulus and percentage cover of ectocarpoid algae (Fig. 9.11). However, any interpretation of these data must be treated with caution since, as explained above, the range of surfaces tested was heterogeneous with

different chemistries, surface and bulk properties. For this reason, the field experiments in 2011 and 2012 were performed more systematically, with sets of coatings varying in either modulus (Chapter 11) or surface wettability (Chapter 10) but with a common chemistry in each case.

As explained earlier, the field experiments in 2010 were pilot trials intended to inform the more systematic trials in 2011 and 2012. Only one field site was possible for the 2011/12 tests for financial and logistic reasons. Even though abundant ectocarpoid algae were observed at Newton Ferrers, it was decided to immerse the panels in Hartlepool Marina for the 2011/12 field assays. During the same period that the field assay described in this Chapter was performed, International Paint immersed some panels at a different location in Hartlepool Marina and the presence of ectocarpoid algae was observed on their test surfaces in relatively large quantity, showing that they were present in Hartlepool Marina so it was probably just the location used for the experiment described in this Chapter that was not optimal. Another reason for choosing Hartlepool over Newton Ferrers is that it was later decided to measure changes in the wettability of surfaces immersed in the field, in parallel with the fouling observations. Since the instrument used to measure the contact angle was located at International Paint laboratory in Gateshead, the decision was made to focus all further field immersion trials on Hartlepool Marina.

It was also decided to change the design of the panels. The design used for this experiment was useful as it was possible to observe the slides under the microscope, but only three-quarters of the slides were subjected to fouling colonisation making the surface area exposed to organisms relatively small, especially if the edge effects were considered. It would have also been more interesting to have more replicates within the same panels, as even if the panels were placed close to each other, differences of fouling were observed and so by having more replicates within the same panels, the variance of the results may

decrease. All these observations were then taken into account in order to improve the field assay in 2011.

10. FIELD ASSAYS DURING 2011 OF ANTIFOULING PERFORMANCE OF SILICONE 'HYBRID' COATINGS WITH SYSTEMATIC VARIATIONS IN SURFACE ENERGY AND WETTABILITY

10.1. Introduction

Studies have demonstrated the influence of surface energy on the attachment and the adhesion of marine organisms mostly in laboratory bioassays (Chapter 6; e.g. Finlay et al. 2002; Bennett et al. 2010). However, the effect of surface energy observed in laboratory assays might not be borne out in field assays; it is then of importance to perform field assays to compare the results in the field with those in laboratory assays. Unfortunately, only a few studies have compared field and laboratory results. For example, Martinelli et al. (2012b) working with blends of PDMS with a copolymer containing PDMS, PEG and fluoropolymer, showed that the two most effective amphiphilic coatings against adhesion of sporelings of *Ulva linza* and adults of *Balanus amphitrite* in laboratory assays, were also effective against colonisation by hard-bodied animals and weeds in the field.

Previous field experiments studying the effects of wettability and surface energy on the development of fouling organisms showed that wettability might influence the fouling organisms, especially at the start of the immersion. Huggett et al. (2009) showed an influence of the wettability of silane-based coatings on the settlement and recruitment of larvae of *Hydroides elegans*, but only for the 10 first days after immersion. In addition, the silane-based coatings showed no quantitative influence of wettability on the biofilm community (Huggett et al. 2009). Several other field studies with the same set of silyl-based coatings with varying wettability showed that at an early stage of immersion (i.e. around three days), the initial wettability was positively and negatively correlated with the settlement of

barnacles and bryozoans, respectively (Rittschof and Costlow 1989; Roberts et al. 1991). However, after a month of immersion, differences were observed in the coverage of these organisms (and other hard fouling organisms) but no clear correlation was observed with the initial wettability of the silyl-based coatings (Holm et al. 1997). Dexter et al. (1975) studied surfaces with varying surface energy (and varying chemistry) (i.e. glass, polystyrene, polypropylene, nickel and polyvinyl-fluoride) and showed that higher biofilm coverage was observed on high surface energy surfaces (i.e. nickel, which would also contain biocides) compared to lower surface energy surfaces (i.e. polyvinyl-fluoride) after 7 and 14 days' immersion. Lakshmi et al. (2012) showed there was a positive correlation between the density and the attachment of bacteria and surface energy of test surfaces (i.e. PDMS, silicone rubber, polypropylene) after one day's immersion, but not after few days' immersion. However, both Dexter et al. (1975) and Lakshmi et al. (2012) used test surfaces that were heterogeneous with different chemistries (and probably different moduli and topography), so any interpretation of the data obtained in these studies has to be treated with caution.

Changes of surface wettability following immersion have been observed in several studies (e.g. Martinelli et al. 2012a) using the captive bubble method (Chapter 2) and could affect the attachment and adhesion of fouling organisms. These changes could be due to several mechanisms such as surface reconstruction (Hu and Tsai 1996; Krishnan et al. 2006a; Magin et al. 2011; Sundaram et al. 2011), formation of a conditioning film (Thome et al. 2012) and hydration of the surface (Rosenhahn et al. 2010 for review). These seven previously cited studies immersed the surfaces in sterile artificial seawater (ASW) or in MilliQ water. However, only few studies have observed the changes in wettability under field conditions (Rittschof and Costlow 1989). Accumulation of conditioning macromolecules, bacteria, diatoms and other marine organisms can also change surface wettability. The formation of a conditioning layer occurs within seconds of immersion (Jain and Bhosle 2009)

whereas colonisation by bacteria and other unicells starts within minutes to hours of immersion (Callow and Callow 2006).

In an attempt to differentiate between changes in wettability caused by physical/chemical changes to the surface (such as reconstruction and hydration), from those caused by surface conditioning and fouling, in parallel with the studies on the development of marine fouling, underwater contact angles (using the captive bubble technique (Chapter 2)) were measured for the same coatings after different periods of immersion in either sterile ASW, or in natural seawater under field conditions. The comparison between ASW and field immersion appears to be a unique feature of the present study and provides an extra dimension to the study of the effects of coating properties in the field. Unfortunately, the measurement of changes in wettability after immersion could only be carried out over a 10-day period since after that time the level of fouling prevented accurate measurement of the contact angles.

The silicone 'hybrid' coatings tested for this field assay were previously assessed in laboratory assays in Chapter 6. A negative correlation was observed between the adhesion strength of sporelings of *U. linza* and the wettability/surface energy (except for the most hydrophilic coating H10). However, no clear correlation was observed for *E. crouaniorum*, as the lowest adhesion strength was obtained with both the highest surface energy coatings (H7 and H10) and the lowest surface energy coating (H), while the highest adhesion strength of *E. crouaniorum* was observed with H2 (with a surface energy of 29.4 mN m^{-1}). In order to compare the performance of the test coatings in the laboratory with those in the field, panels were immersed under static conditions in Hartlepool Marina on the 28th of March 2011. At the same time, changes of wettability were observed after immersion in sterile ASW and in Hartlepool Marina using the captive bubble method.

Despite the high coverage of microfouling and silting on the test surfaces during the field experiments in 2010, Hartlepool Marina was still chosen to be the field site as the equipment

to measure the wettability changes was close to the site and for other reasons explained in Chapter 9. However, the location of the panels was changed; they were placed close to the location where International Paint immersed their panels and where ectocarpoid algae had previously been observed (Fig. 10.1). The aims of the experiment were (a) to observe the appearance and the succession of the different fouling categories, especially ectocarpoid algae, in order to see if there were differences between both the surfaces and the fouling organisms, (b) to correlate any differences in colonisation with the surface properties of the coatings, using an assessment method, which was non-destructive.
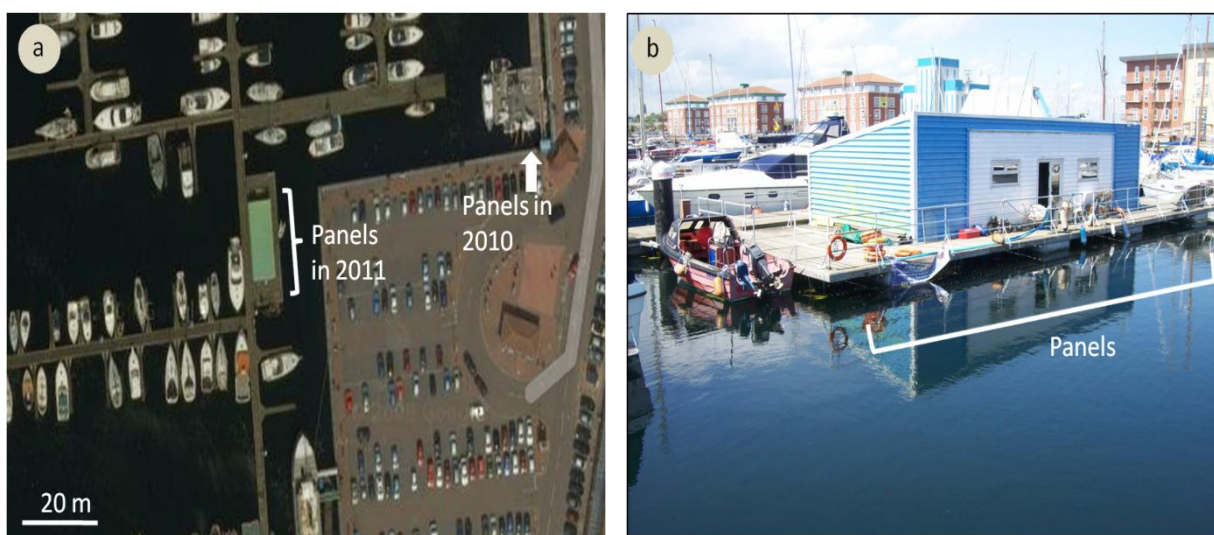
Figure 10.1: Immersion sites in Hartlepool Marina for the field experiments in 2010 (a) and 2011 (a and b).

10.2. Materials and Methods

10.2.1. Test surfaces

The test coatings were the six silicone 'hybrid' coatings with varying wettabilities (64° to 101°), tested in laboratory assays in Chapter 6. IS900 and IS700 were used as commercial standard coatings and a commercial tie coat as a negative control surface (i.e. the tie coat had no antifouling properties and was therefore expected to foul heavily). The composition

and characterisation of these surfaces was described in Chapter 4, except for the tie coat, which has not been characterised.

10.2.2. Changes in surface wettability for immersed surfaces

Three-replicate slides of each surface were immersed on the 28th of March 2011 in either sterile ASW or in Hartlepool Marina. For the sterile ASW treatment, the slides put in slide boxes (without the lid) were placed in a small container that was filled with sterile autoclaved ASW, located in the biological laboratory of International Paint (i.e. 18°C). For the slides immersed in Hartlepool Marina, they were placed into "open-slide boxes" (Fig. 10.2) to allow seawater to flow through the boxes and to make the slide collections easier. Slides were collected on days 1, 3, 7 and 10 (until the 7th of April); and for each collection, an "open-slide box" immersed in Hartlepool Marina was recovered and placed into a coolbox containing natural seawater to facilitate the transport to International Paint laboratory. The following day, the wettability of each surface in both treatments was measured using the underwater contact angle method (Chapter 2).

Slides were also observed by transmitted light microscopy to observe the diatoms and other fouling organisms, but to facilitate the microscopic observations on the two Intersleek coatings and to be able to observe bacteria, the surfaces were stained using DAPI (4′, 6-diamidino-2-phenylindole), a fluorescent DNA stain (0.1 μg ml^{-1} (in MilliQ water), 5 min in darkness) before observation under the UV microscope.
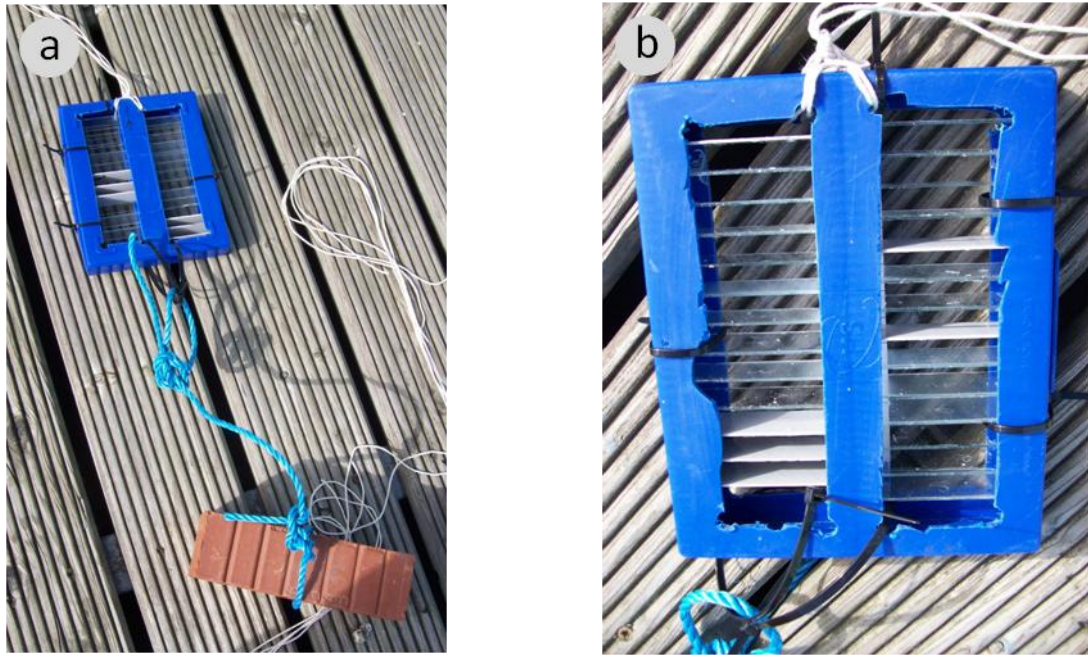
Figure 10.2: "Open-slide box". The slides were placed in the slide box (b) attached to a brick to maintain it in place (a). The boxes were immersed at 50 cm depth.

10.2.3. Static field immersion experiment

The coatings were applied as explained in Chapter 4 but to larger glass slides (75 x 50 mm, Corning) to provide a larger surface area for fouling colonisation with reduced edge effects. Coated surfaces were glued to wooden panels, measuring 60 x 60 cm using Epiglass adhesive.

Before gluing the test surfaces, the three-replicate panels were protected with two layers of anti-corrosive paint (applied by a technician at International Paint) and a grey Veridian tie coat (acrylic; International Paint) was applied. A top coat of IS900 (red; same composition as grey IS900 (Chapter 4) except that Part A was red) was applied by brush between the test surfaces glued on the panels.

On each panel, eight surfaces were placed: six experimental coatings (H, H1, H2, H3, H7 and H10), IS900 (grey) as commercial standard and the tie coat used for the test coatings

(unpigmented Veridian (Chapter 4)) as negative control (Fig. 10.3). The coating IS700 was not used, as the design of the panels could not accommodate another treatment. The panel design was of 7 rows x 8 columns. The surfaces were randomly distributed (using Excel program) on the first row of the panels (with different distribution for each panel). For each subsequent row, the corresponding slide position was moved one place to the right. The experimental design thus allowed an analysis of the influence of surface depth on the incidence of fouling.

The three-replicate panels were immersed on the 28th of March 2011 and the data were collected after 23, 37, 43, 61, 80, 98 and 157 days. The panels were maintained vertically and in the same position by a weight attached to the bottom of each panel and by two ropes attached to the pontoon. Percentage cover of all the fouling categories was obtained following the 'Phoenix' in-house Experimental Fouling Assessment Record Sheet (International Paint assessment sheet), which recorded the percentage cover of microfouling, weeds, soft- and hard-bodied animals. The percentage cover of ectocarpoid algae was also recorded separately and samples were taken using forceps for subsequent microscopic examination to determine which genera were present.

Figure 10.3: Panel before immersion. Each panel was labelled in order to recognize them during the inspection. The panels were attached to a weight in order to be in vertical position. Two ropes were attached to the pontoons to keep the panel in the same position during the field experiment.

10.2.4.   Statistical analysis of field data: Generalized estimating equations

Statistics were performed as described in Chapter 2.10 and statistical tables for the whole Chapter are presented in Appendix 9.

10.3. Results

10.3.1.   Changes in surface wettability for surfaces immersed in sterile ASW and in Hartlepool Marina

The wettability of surfaces immersed for 10 days in sterile ASW and natural seawater (Hartlepool Marina) was measured at five different periods: days 0 (i.e. pristine surfaces freshly immersed in MilliQ water), 1, 3, 7 and 10 using the underwater contact angle method (Fig. 10.4). The surfaces were immersed in MilliQ water and the underwater contact angle measurements were done within minutes after immersion. The experiment was ended after 10 days, as the accumulation of microfouling on the surfaces immersed in Hartlepool Marina made the reliable measurements of contact angles difficult.

The data obtained at day 0, which were measured within a few minutes after immersion in MilliQ water, were already described and explained in Chapter 4. A narrower range of wettabilities was observed using the underwater method compared to the static water contact angle measurements on dry coatings in air and as expected, the increase of PEO content in the blend increased the wettability. While the more hydrophobic coatings H and H1 were less hydrophobic when measured by captive bubble, the other coatings became more hydrophobic, decreasing the range of wettability overall.
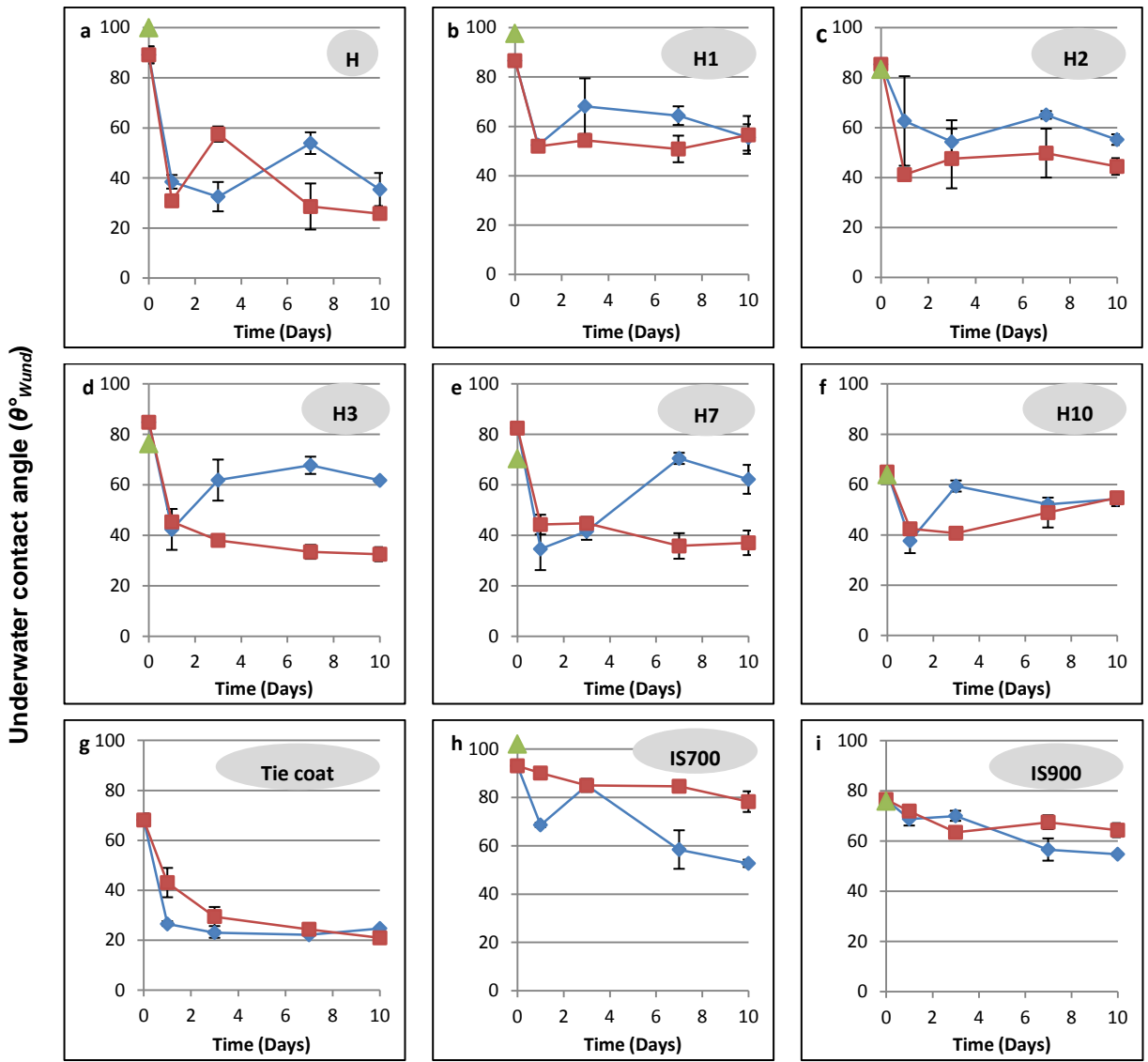
Figure 10.4: Underwater contact angles of 9 different surfaces after immersion in seawater: H (a), H1 (b), H2 (c), H3 (d), H7 (e), H10 (f), Tie coat (g), IS700 (h) and IS900 (i). The angle that was measured was the water-side angle of the captive air bubble, i.e. θ^{o}_{wund}, as described in Chapter 2. The blue and red lines represent the data obtained after immersion in seawater in Hartlepool Marina and in sterile ASW, respectively. The green triangles represent the water contact angles in air of a dry coating, following the static contact angle method in air (Chapter 2.9.1.1), except for the tie coat as it was not measured. Mean of three replicates ± SD.

The changes of wettability following immersion were different between the two treatments (i.e. sterile ASW and natural seawater). After one day's immersion in sterile ASW, all the surfaces became more hydrophilic, but the decrease of contact angles was different between

177

the surfaces. For example, H the most hydrophobic coating had the highest decrease of contact angles dropping from 89° to 31° (a decrease of 65%) after one day's immersion in sterile ASW (Fig. 10.4a) while H10 had the lowest decrease of contact angles dropping from 66° to 42° (a decrease of 36%; Fig. 10.4f). Meanwhile, IS900 and IS700 had only a low decrease of contact angles (lower than 8%; Figs. 10.4h/i). Following the high decrease of contact angles after one day's immersion in sterile ASW, the contact angles of the test surfaces were relatively stable with slight decrease or increase between day 1 and day 10, except for day 3, the coating H was more hydrophobic (from 31° to 58°) but returned to 29° at day 7.

As for the surfaces immersed in sterile ASW, the underwater contact angles of surfaces immersed in Hartlepool Marina decreased after one day's immersion. Coating H had the highest decrease of contact angles (from 89° to 38° (a decrease of 57%); Fig. 10.4a) while H2 had the lowest (from 85° to 62.6° (a decrease of 26%); Fig. 10.4f). No clear pattern to the changes observed between 1 and 10 days' immersion was found, it could be due to differences in the adhesion of microfouling (or biofilm) and other organisms on the surfaces. However, the changes were smaller in magnitude than those obtained after one day's immersion. The wettability of the tie coat and H2 was relatively stable during the experiment with less than 10° differences. The contact angles of IS700 and IS900 decreased in general with the length of immersion; the difference was lower than 15° for IS900 (between 1 and 10 days) but higher than 30° for IS700. Coatings H3, H7 and H10 became in general more hydrophobic with the length of immersion while H and H1 were variable (i.e. both increasing and decreasing during the experiment). However, it was observed that the coatings H, H1, H2, H10, IS900 and the tie coat after 10 days' immersion had relatively similar contact angles to those in sterile ASW.
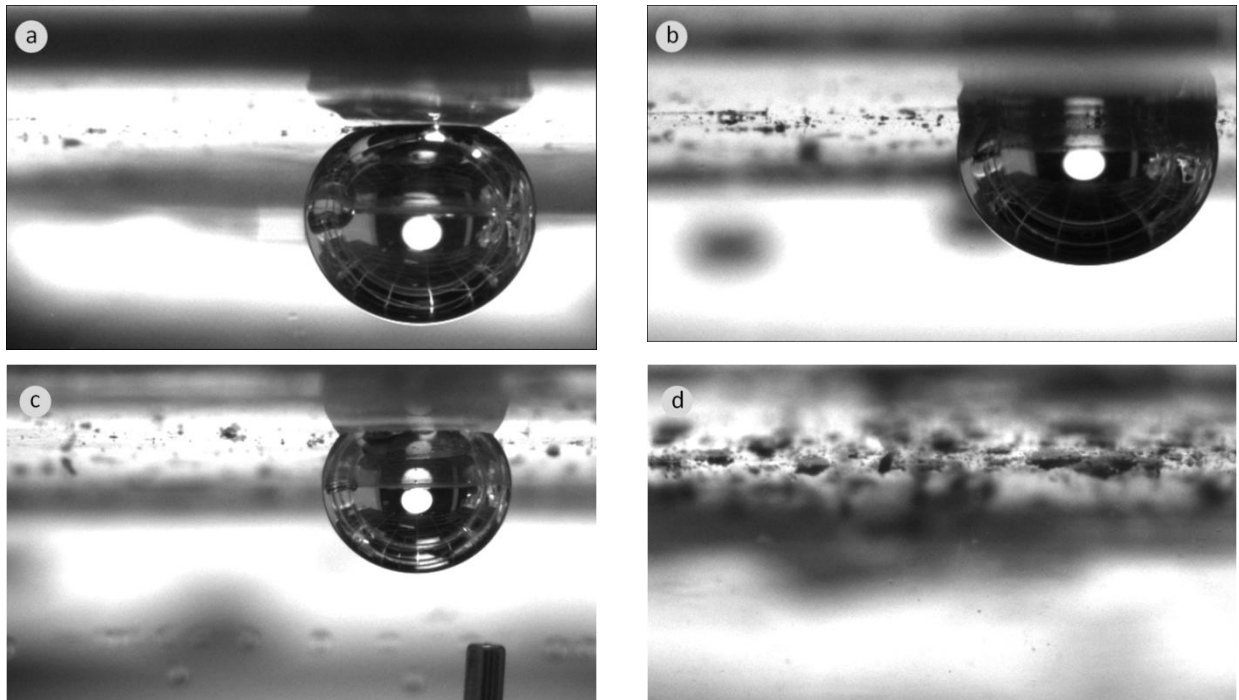
Figure 10.5: Views of surfaces during the underwater contact angle measurements, showing the increase of fouling on the surfaces submerged in Hartlepool Marina: day 1 (a), day 3 (b), day 7 (c) and day 10 (d). The images were taken while the underwater contact angles were measured on the tie coat (a) and H10 (b-d) and Figures a, b and c show the bubbles. The figures show that with the length of immersion the surfaces had more detritus and fouling organisms attached to the surfaces. The contact angles (water-side) were at day 0, 26.5° for the tie coat and 59.4° and 52.1° for H10 respectively at day 3, 7.

Microscope observations were performed after 3, 7 and 10 days. After 3 days, it was possible to observe some detritus on the surfaces immersed in Hartlepool Marina and also some small agglomerations of bacteria under UV microscope. After 7 and 10 days' immersion, a biofilm consisting of diatoms, small animals and detritus was observed on all coatings under transmitted light microscope (Figs. 10.5 and 10.6) and some bacteria were observed under UV microscope. The biofilm appeared to be more extensive on the tie coat. No bacteria were observed on the surfaces immersed in sterile ASW.
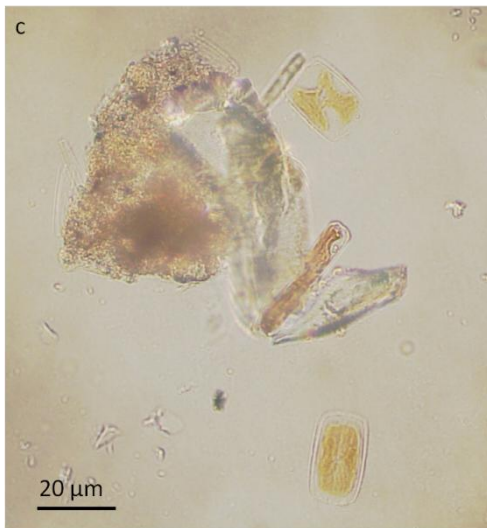
Figure 10.6: Visual appearance of slides on test surfaces in the open slide boxes, after 7 days (a and b) and representative microscope images of the surface biofilm on H2 after 7 days (c) and H1 after 10 days (d) showing presence of diatoms and agglomerations of detritus. No images of bacteria observed under UV microscope have been shown, as the staining was too weak.

10.3.2. Comparisons between different determinations of surface wettability
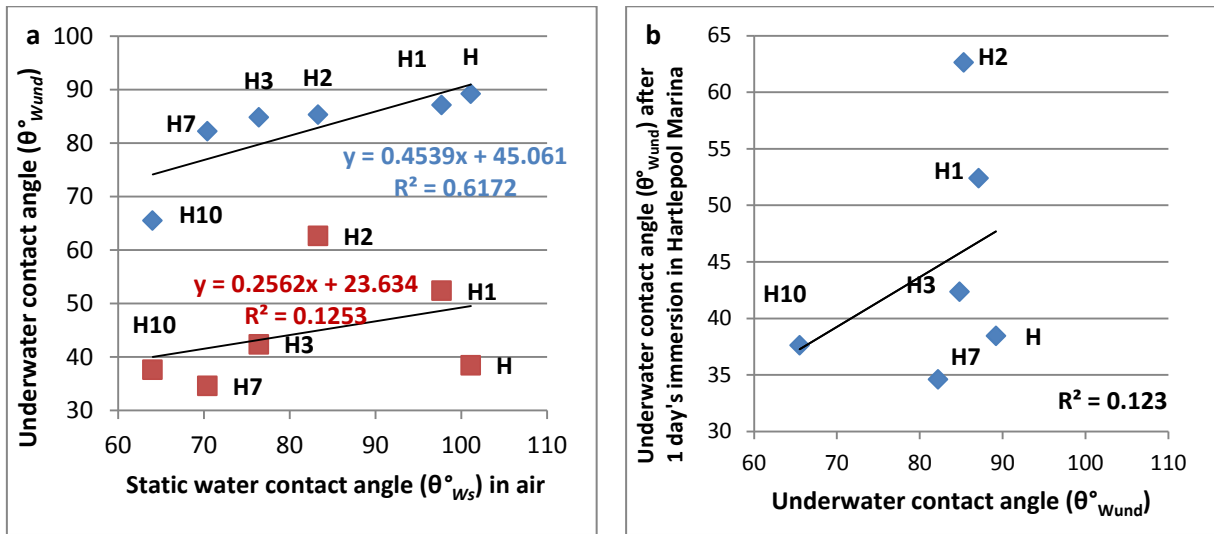
Figure 10.7: Correlations between three surface properties. a) Correlations between the initial surface wettability as determined by static water contact angle in air and underwater contact angles determined at T=0 (blue points) and after 1 day's immersion in Hartlepool Marina (red points). b) Correlation between underwater contact angles at T=0 and after immersion for 1 day in Hartlepool Marina.

Figure 10.7 showed that the water contact angles determined for dry coatings and for coatings freshly immersed in MilliQ water were not strongly correlated (blue data points, R^2=0.6). The range of values for the underwater contact angle method was reduced compared with contact angle determinations in air. In theory, the wettability values of an inert, non-reconstructing surface using the two methods should be similar. The fact that they are not demonstrates either that the two methods are not exactly measuring the same physico-chemical properties, or that even a short immersion (a few minutes until the measurements could be taken) is sufficient to cause some surface changes. Nevertheless, the underwater contact angle method still demonstrates that there was a gradient of wettability. However, the comparison between water contact angles determined for dry coatings and for coatings after 1 day's immersion in Hartlepool Marina demonstrated a weak correlation (Fig. 10.7a, red data points, R^2=0.1). This presumably reflects the effect of the

longer immersion time on surface changes and/or surface conditioning. The former is more likely since the changes after immersion in ASW for 1 day were similar (for most coatings) to those observed in Hartlepool Marina.

Figure 10.7b compares wettabilities at T=0 (i.e. freshly immersed in MilliQ water) and T=1 day, using the same, underwater contact angle, method. There was a weak correlation between the two determinations (R^2=0.1).

One of the objectives of the studies described in this Chapter was to try to determine the effect of coating wettability on coating performance in the field. As the comparisons described above showed, it is difficult to select which measure of wettability should be used to determine these effects. It may be argued that the most meaningful comparison should be based upon the properties of coatings as perceived by the fouling organisms, i.e. after immersion in Hartlepool Marina. For the silicone 'hybrid' coatings, the change in wettability after immersion is greatest after the first day's immersion in Hartlepool Marina (Fig. 10.4). After that, for some coatings, the underwater contact angle was fairly stable; for others, there were some fluctuations. It clearly is impossible to select a single time point between 1 and 10 days that totally captures these variations for all the experimental coatings. It could also be argued that at the later time points, the measurement of wettability is more likely to be influenced by the presence of the developing biofilm and associated fouling, rather than the inherent coating properties. For all these reasons, as a practical compromise, it was decided to use the underwater contact angle values after 1 day's immersion in Hartlepool Marina, as the main basis of comparison with the degree of fouling. In addition, for comparability with the literature, it was decided to make correlations with initial surface wettability of non-immersed, pristine coatings, and with contact angle hysteresis determined from the dynamic contact angle measurements described in Chapter 4, which were also made on non-immersed, pristine coatings.

10.3.3. General observations of the percentage fouling

Seven data inspections were done between the 23rd and the 157th days' immersion –i.e. between the 20th April and 5th September 2011. After 98 days' immersion, filamentous brown algae –i.e. ectocarpoid algae- were no longer present on the test surfaces. Since the focus of the experiment was the observation of colonisation by ectocarpoid algae, a decision was made to perform one last inspection two months later.

Figure 10.8 shows the percentage cover of the four categories of fouling organisms (microfouling, weeds, soft- and hard-bodied animals) for each coating on one panel (7 replicates; data shown for the other 2 panels in Appendix 10). The effects of the coatings, replication, time of immersion and depth (row) were determined for all the fouling categories using generalized estimated equations GEEs as statistical analysis (Chapter 2; data were significantly different when $p<0.05$).

Variations were observed in total fouling –i.e. differences in percentage cover in all four fouling categories (Fig. 10.8; Appendix 10 for the other panel results). A high total fouling coverage was observed from 43 days' immersion (>60-70 %) on most of the test surfaces (Fig. 10.8; Appendix 11 for pictures of the boards). Differences in fouling coverage were also observed between the surfaces and inspections.

After 43 days' immersion, microfouling coverage was high –i.e. between 60 and 80 % cover- on all the coatings except on the tie coat, which had high coverage at 23 days. As other fouling categories appeared, the percentage cover of microfouling decreased (Fig. 10.8).
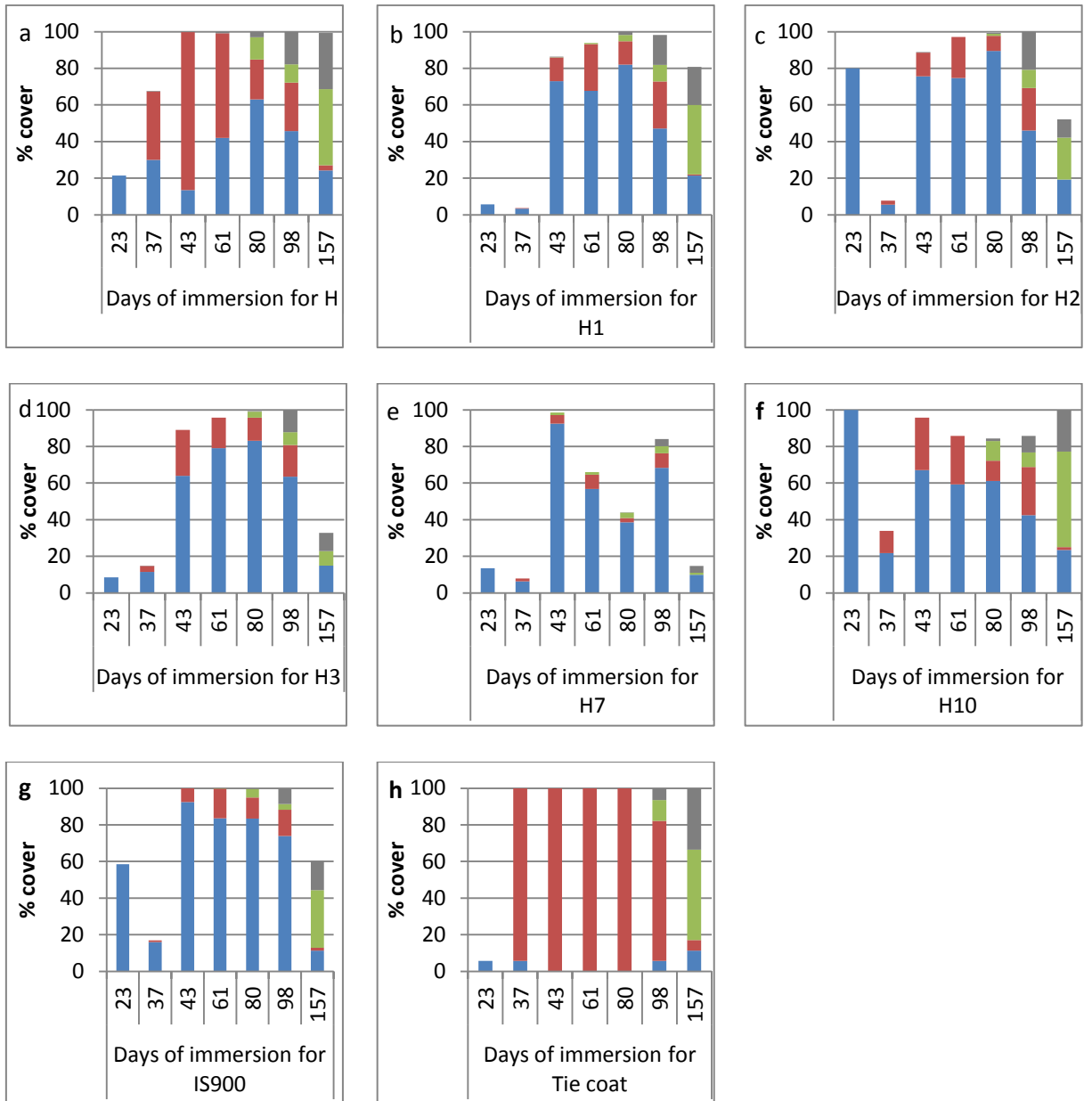
Figure 10.8: Percentage cover observed on 8 different test surfaces attached to Panel 1, immersed in Hartlepool Marina during 157 days of immersion. Percentage cover for the 4 fouling categories: microfouling (blue), weeds (red), soft-bodied animals (green) and hard-bodied animals (grey). For each graph, the axis x represents the length of immersion (i.e. day of immersion) for each coating. Mean of 7 replicates.

Weeds were present on the tie coat (a standard surface, which is known to be fouled readily) after 37 days' immersion and on the other surfaces after 43 days (Fig. 10.8). Between 43 and 98 days, the coverage of weeds was around 10-20% and was relatively constant on all the

surfaces. At the last inspection at 157 days, only a small coverage of weeds was observed. The weed category was composed of brown filamentous algae –i.e. ectocarpoid algae- until 98 days when other types of brown algae (such as *Chorda filum*), red algae (such as *Gracilaria* sp.) and small tufts of green algae were present.

Soft- and hard-bodied animals appeared after 37-43 days' immersion, and had a rapid growth from 80 days' immersion. After 157 days' immersion, their coverage was still increasing and they were growing over the weeds.

10.3.3.1. Analysis of the total percentage cover

Figure 10.9a shows total percentage cover for all surfaces; at the two first inspections, the total coverage was relatively low (around 20-30 %), then increased reaching a plateau close to 100 % from 43 days to 98 days before decreasing to approximately 70 % at 157 days.
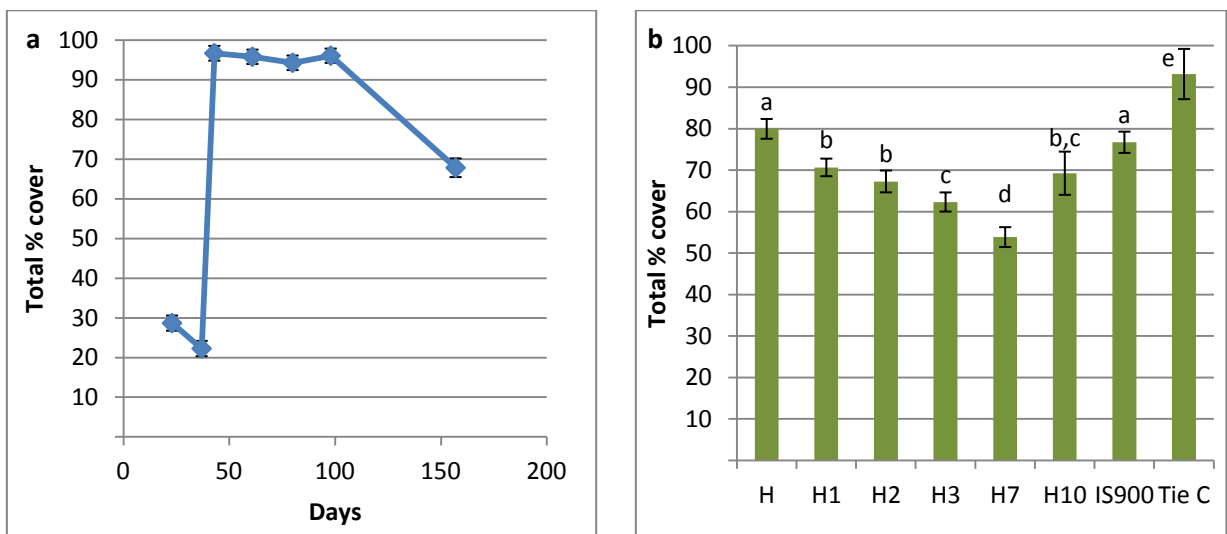
Figure 10.9: Total percentage cover as a function of immersion days of the panels (a) and as a function of each surface (b). a) Each data point represents at each inspection day the mean of all collected data regrouping the replicates, surface and panels together (n=168; 7 replicates x 8 surfaces x 3 panels) ± 2 x SE. b) Each bar represents the mean of all the collected data for a surface averaged over the whole experiment (n= 147; 7 replicates x 7 inspections x 3 panels) ± 2 x SE. Tie C= Tie coat. Values that are significantly different at p≤0.05 in GEEs are indicated by different letters above the bars in Figure b.

Significant differences for the total fouling coverage were observed between the surfaces (Fig. 10.9b). Coating H7 had significantly the lowest total coverage throughout whole experiment, followed by H3 and H10 (Fig. 10.9b). The highest total coverage was observed on the tie coat with 92 % cover. The coverage on all the other surfaces was around 60-80 % and the surfaces were separated in two groups as shown in Figure 10.9b; H and IS900 were grouped together followed by H1, H2 and H10 grouped together with slightly lower coverage.

10.3.3.2. Analysis of the percentage cover of microfouling

As shown in Figure 10.10a, the percentage cover of microfouling increased rapidly until it reached a maximum between 43 and 80 days, then it decreased from 98 days' immersion. This pattern was observed for all the surfaces except for the tie coat, which had a high coverage after 23 days' immersion, then a low percentage cover for the rest of the experiment. The decrease of percentage cover of microfouling was linked to the appearance of weeds, soft- and hard-bodied animal fouling.

Statistical analysis showed that tie coat had significantly the lowest percentage cover while IS900 had significantly the highest (Fig. 10.10b). There were no significant differences in coverage between any of the silicone 'hybrid' coatings, except the coverage on H that was significantly lower than on H1 and H10.
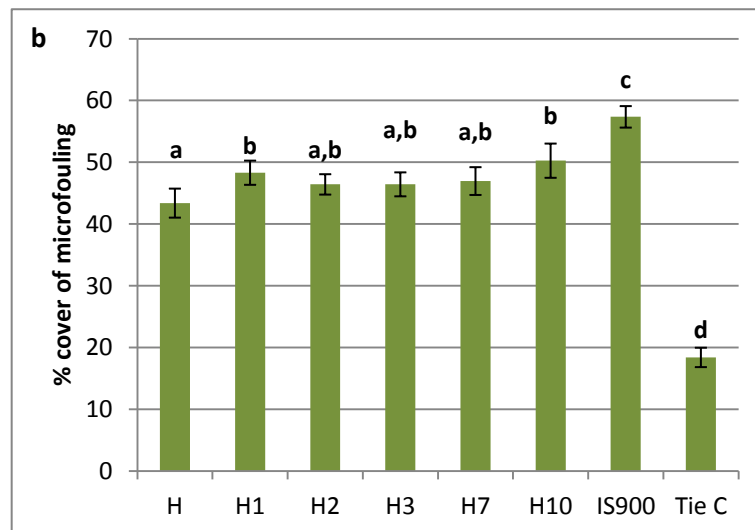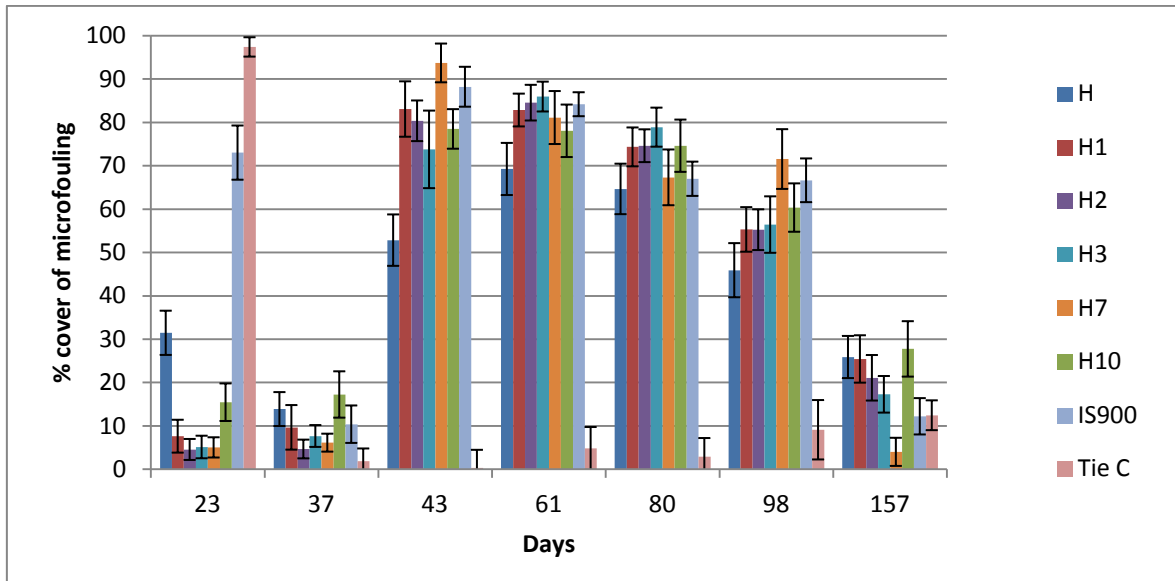
Figure 10.10: Percentage cover of microfouling as a function of immersion days and surfaces (a) and as a function of each surface averaged over the whole experiment (b). Each bar represents the mean of collected data (for a: n= 21: 7 replicates x 1 inspection x 3 panels; for b: n= 147: 7 replicates x 7 inspections x 3 panels) ± 2 x SE. Tie C = Tie coat. Values that are significantly different at p≤0.05 in GEEs are indicated by different letters above the bars in Figure b.

10.3.3.3. Analysis of percentage cover of weeds with particular reference to ectocarpoid algae
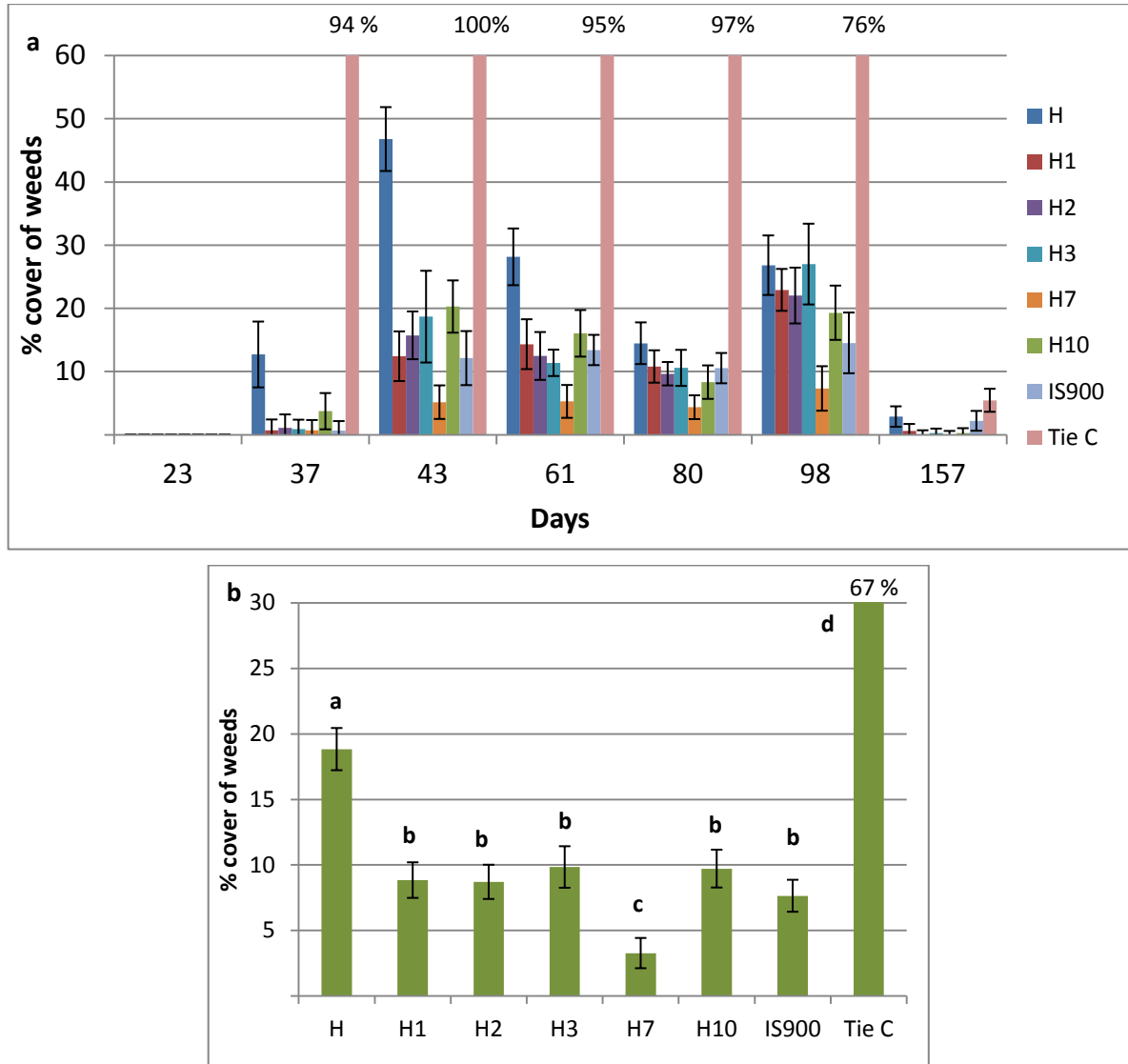
Figure 10.11: Percentage cover of weeds as a function of days and surfaces (a) and as a function of each surface averaged over the whole experiment (b). Each bar represents the mean of collected data (for a: n= 21: 7 replicates x 1 inspection x 3 panels; for b: n= 147: 7 replicates x 7 inspections x 3 panels) ± 2 x SE. Tie C= tie coat. Values that are significantly different at p≤0.05 in GEEs are indicated by different letters above the bars in Figure b.

Throughout the experiment, two peaks of weed coverage were observed, particularly visible on H (Fig. 10.11a) the first at 43 days mainly composed of ectocarpoid algae, and the

second at 98 days, composed of other brown algae such as *Chorda filum*, some red algae and some filaments of green algae such as *Ulva*. These variations might be due to the competition with other fouling organisms such as barnacles and to grazing animals. During the last survey (i.e. after 157 days' immersion), only a few algae were observed.

Statistical analysis showed that the tie coat had significantly higher weed coverage at all the inspections. However, there were significant differences between the coatings; H had significantly the highest weed coverage while coating H7 had the lowest (Fig. 10.11b). With a percentage cover around 10 %, the other coatings were not significantly different to each other.

Ectocarpoid algae

The two genera, *Ectocarpus* and *Hincksia,* were observed on most of the surfaces during the field assay, while *Pilayella* was observed only on few occasions. Ectocarpoid algae increased quickly at the start of the field trial and reached a maximum at 43 days' immersion before decreasing and disappearing after 98 days' immersion (Fig. 10.12a). Statistical analysis showed that the tie coat had significantly the highest coverage with 57 % while IS900 had similar coverage to the silicone 'hybrid' coatings except H and H7 (Fig. 10.12b). Coating H7 had significantly the lowest coverage, while H had the highest of the silicone 'hybrid' coatings with 15 %. All the percentage covers of the other coatings were not significantly different.
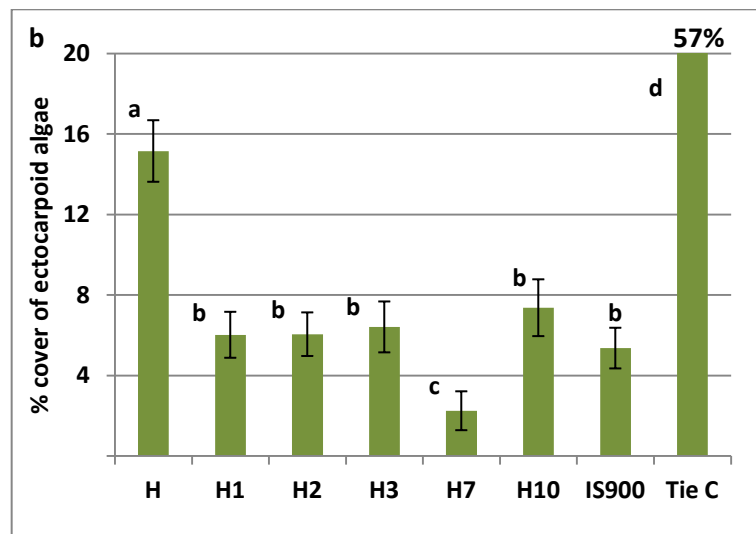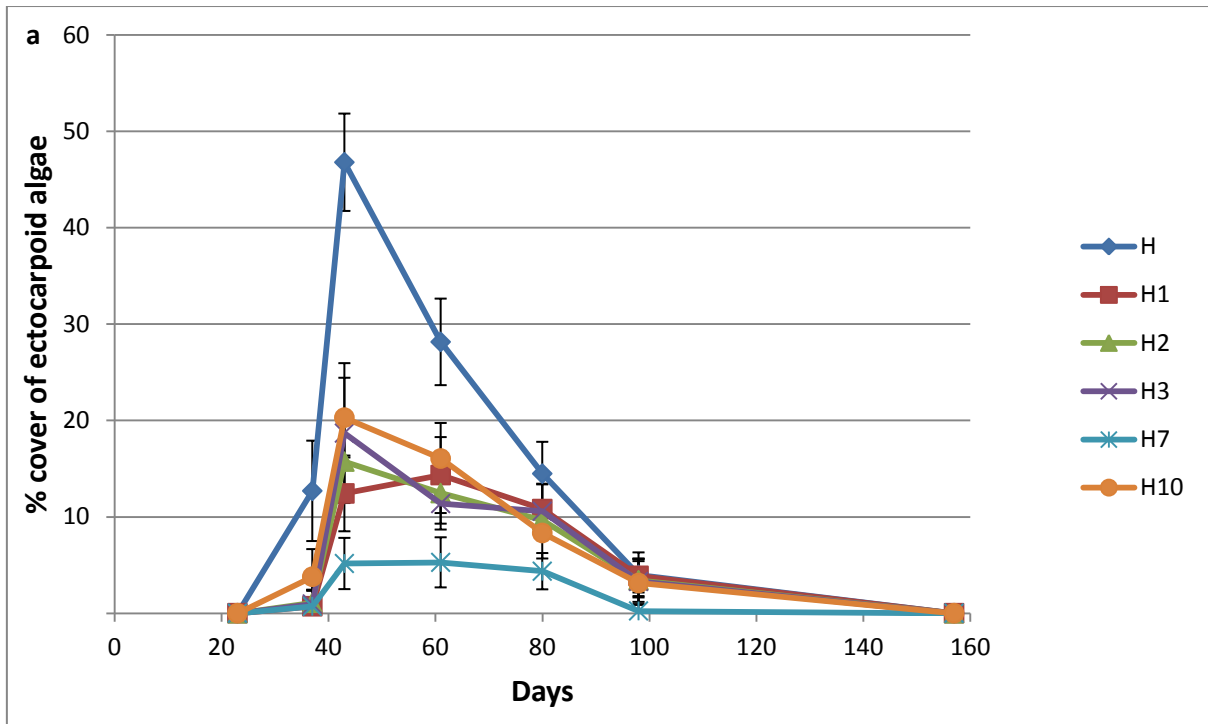
Figure 10.12: Percentage cover of ectocarpoid algae as a function of immersion days and silicone 'hybrid' coatings (a) and as a function of each surface averaged over the whole experiment (b). Each bar/dot represents the mean for one coating for one inspection (for a: n= 21: 7 replicates x 1 inspection x 3 panels; for b: n= 147: 7 replicates x 7 inspections x 3 panels) ± 2 x SE. Tie C= tie coat. Values that are significantly different at p≤0.05 in GEEs are indicated by different letters above the bars in Figure b.

10.3.3.4. Analysis of the percentage cover of soft-bodied animals
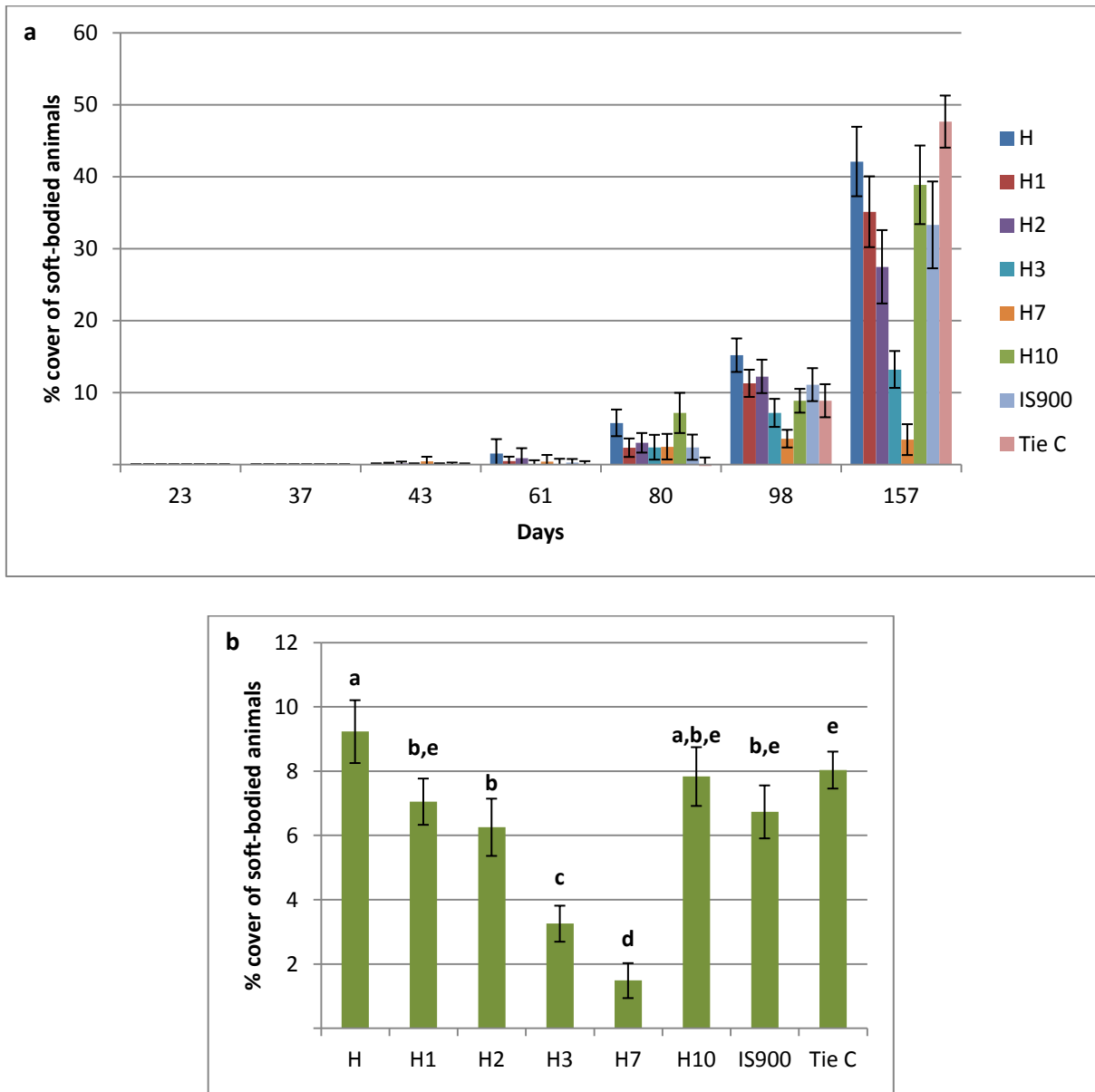
Figure 10.13: Percentage cover of soft-bodied animals as a function of immersion days and surfaces (a) and as a function of each surface averaged over the whole experiment (b). Each bar represents the mean of collected data (for a: n= 21: 7 replicates x 1 inspection x 3 panels; for b: n= 147: 7 replicates x 7 inspections x 3 panels) ± 2 x SE. Tie C=tie coat. Values that are significantly different at p≤0.05 in GEEs are indicated by different letters above the bars in Figure b.

The first visible colonisation of soft-bodied animals was observed after 43 days (mostly represented by tunicates and polyps). However, until 80 days, the coverage was relatively

low, and then it increased quickly, up to 30 % after 157 days' immersion (Fig. 10.13a). If the panels were left immersed longer, soft-bodied animal fouling might have increased even more.

The coverage of soft-bodied animals was different between the surfaces (Fig. 10.13b). Coating H7 had significantly the lowest coverage, followed by H3. The other surfaces were similar except for the coverage on H, which was higher than on H1, H2 and IS900; and the coverage on H2, which was lower than on the tie coat (Fig. 10.13b).

10.3.3.5. Analysis of the percentage cover of hard-bodied animals

The first observation of hard-bodied animals was at 37 days' immersion (mostly represented by barnacles). However, as for the soft-bodied animals, coverage was relatively low until 80 days, and then it increased quickly, up to 20 % after 157 days' immersion (Fig. 10.14a). As for soft-bodied animals, if the panels had been immersed longer the amount of hard-bodied animal fouling might have further increased. Differences in the percentage cover of hard-bodied animals were observed between the surfaces (Fig. 10.14b). Coating H7 had significantly the lowest coverage, followed by H3, while H had the highest. The other surfaces were grouped together except for the coverage on H1, which was higher than on H10.
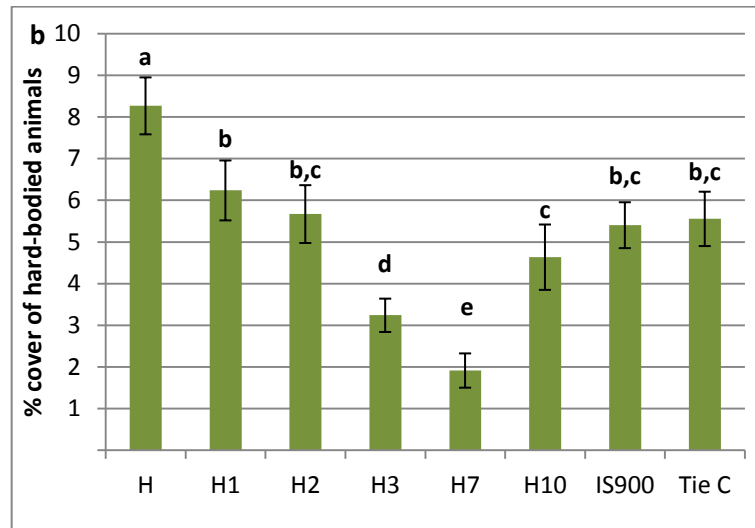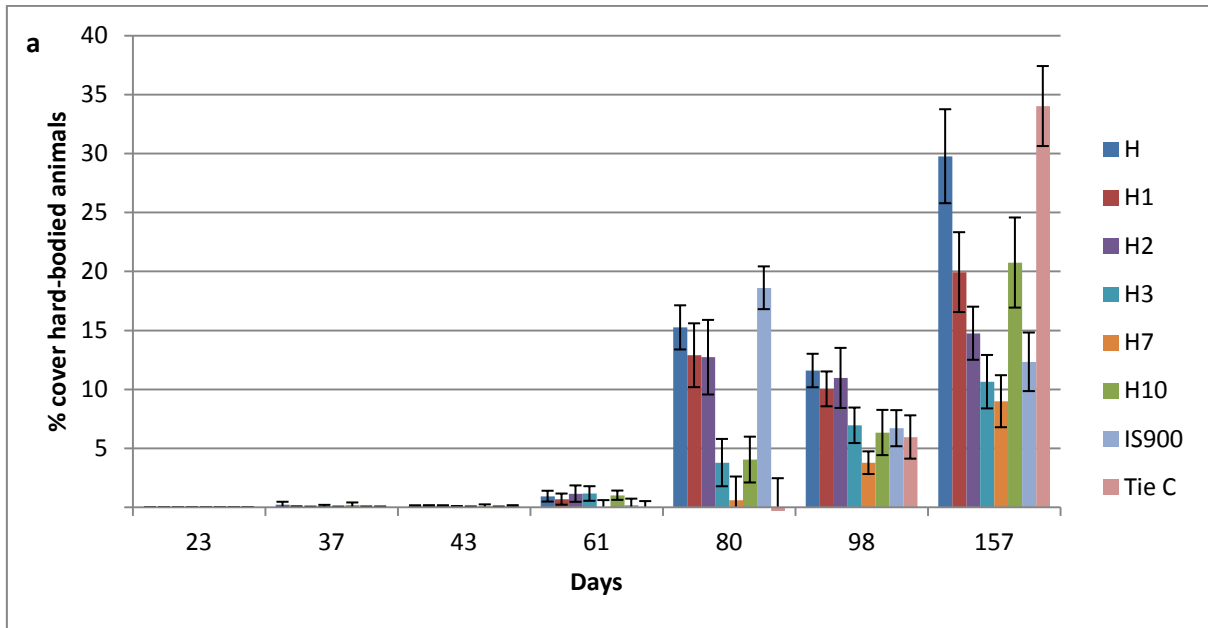
Figure 10.14: Percentage cover of hard-bodied animals as a function of immersion days and surfaces (a) and as a function of each surface averaged over the whole experiment (b). Each bar represents the mean of collected data (for a: n= 21: 7 replicates x 1 inspection x 3 panels; for b: n= 147: 7 replicates x 7 inspections x 3 panels) ± 2 x SE. Tie C=tie coat. Values that are significantly different at p≤0.05 in GEEs are indicated by different letters above the bars in Figure b.

10.3.3.6. Effects of 'replicates' and depth observed in the field assay

Even if the main interest of the field assay was to observe the influence of surface properties on the appearance of fouling organisms on test surfaces, the results obtained allowed the

influence of panel-replicates and depth to be observed by studying the results between panels and rows, respectively.

Differences were observed between the panels for the different fouling categories but they were minimal (<7% difference). It still showed that even though the panels were in adjacent positions on the pontoon and at the same depth, the results show that external factors slightly influenced the fouling appearance.

An effect of depth was observed for all the fouling categories except the total % cover, but the differences were minor (<3%) for the animal fouling. However, slightly higher differences were observed for the other categories of fouling. It was observed that the deeper the surfaces were immersed, higher coverage of microfouling was present (rows 6-7: 48-49%, other rows: 42-44 %). For the weeds and ectocarpoid algae, row 4 had a higher coverage than other rows (row 4: 21% and rows 1 and 7:15% for the weeds; row 4: 17% and the other rows:11-14% for the ectocarpoid algae).

10.3.3.7. Relationship between fouling cover and surface wettability for the silicone hybrid coatings

As explained earlier, the % cover of the different fouling categories was correlated to three measures of surface wettability for the six silicone 'hybrid' coatings, viz. initial static contact angle in air, contact angle hysteresis and underwater contact angle after 1 day's immersion in Hartlepool Marina.

The total % cover did not show any strong correlation to any these three measures of surface wettability (Fig. 10.15). However, for the static contact angle in air, it was observed that H10 was not following the same trend as the other coatings and by excluding this coating, it was possible to observe a strong correlation between the coverage of total fouling and static water contact angle in air (R^2=0.89; Fig. 10.15a). By linking the % covers of the different

coatings together (Fig. 10.15a), a similar relationship was observed to the one between the % removal of *U. linza* and the static contact angle observed in Chapter 6 (Fig. 6.3b), as the colonisation would be inversely linked to the % removal.
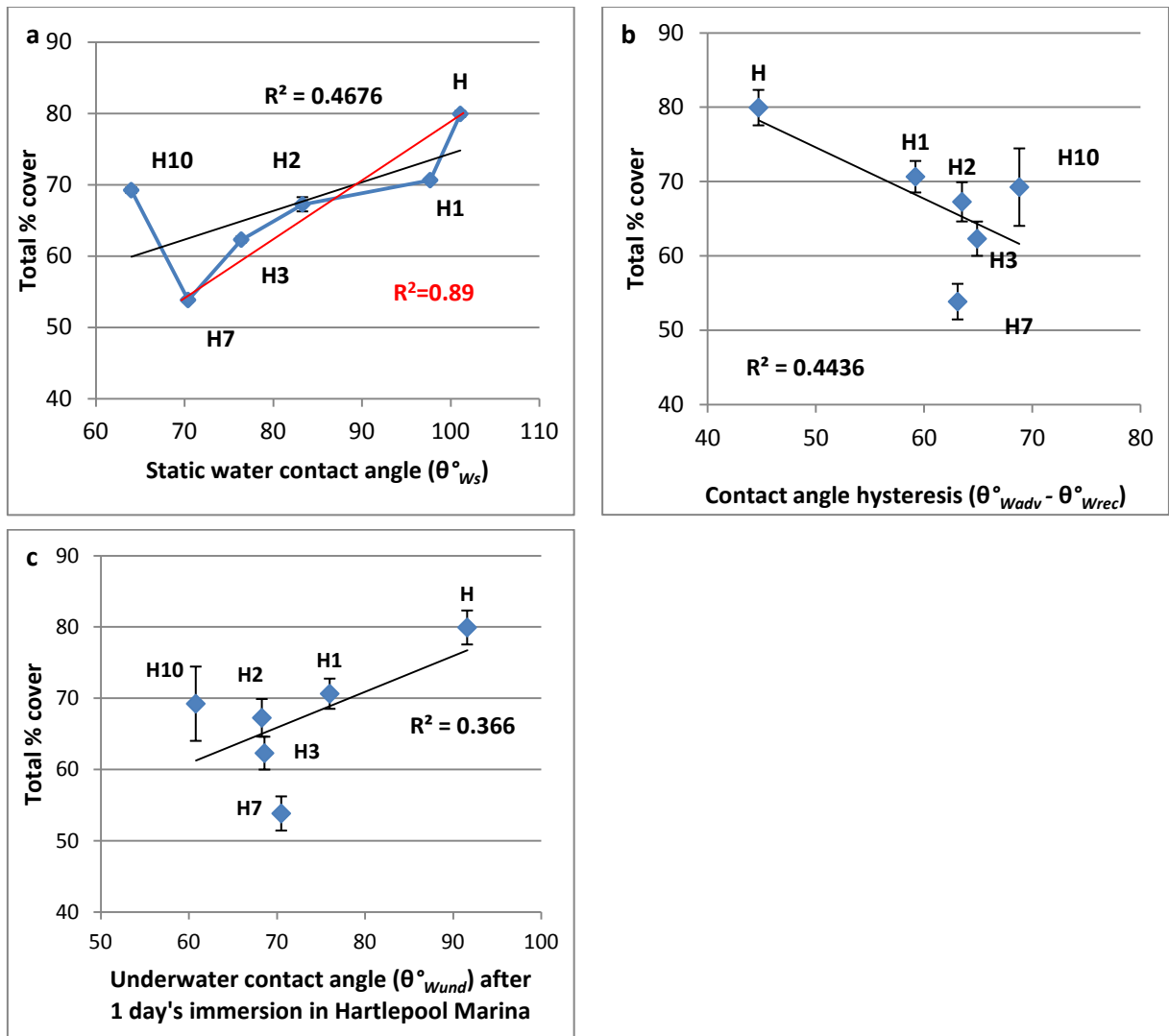
Figure 10.15: Correlations between total % cover averaged over the whole experiment and surface properties of the silicone 'hybrid' coatings: the initial static contact angle in air (a), the contact angle hysteresis (b) and the underwater contact angle after 1 day's immersion in Hartlepool Marina (c). Each point represents the mean of all the collected data for a surface (n= 147; 7 replicates x 7 inspections x 3 panels) ± 2 x SE. Linear trend lines and R^2 correlations are shown for all data points (black) and for all points excluding H10 (red).

No strong correlation was observed between the percentage cover of microfouling and the static water contact angle in air (R^2=0.38; Fig. 10.16a). However, stronger positive and

negative correlations were observed between the % cover and either the contact angle hysteresis and underwater contact angle after one day's immersion in Hartlepool Marina, respectively (R^2=0.66-0.67; Figs. 10.16b/c).
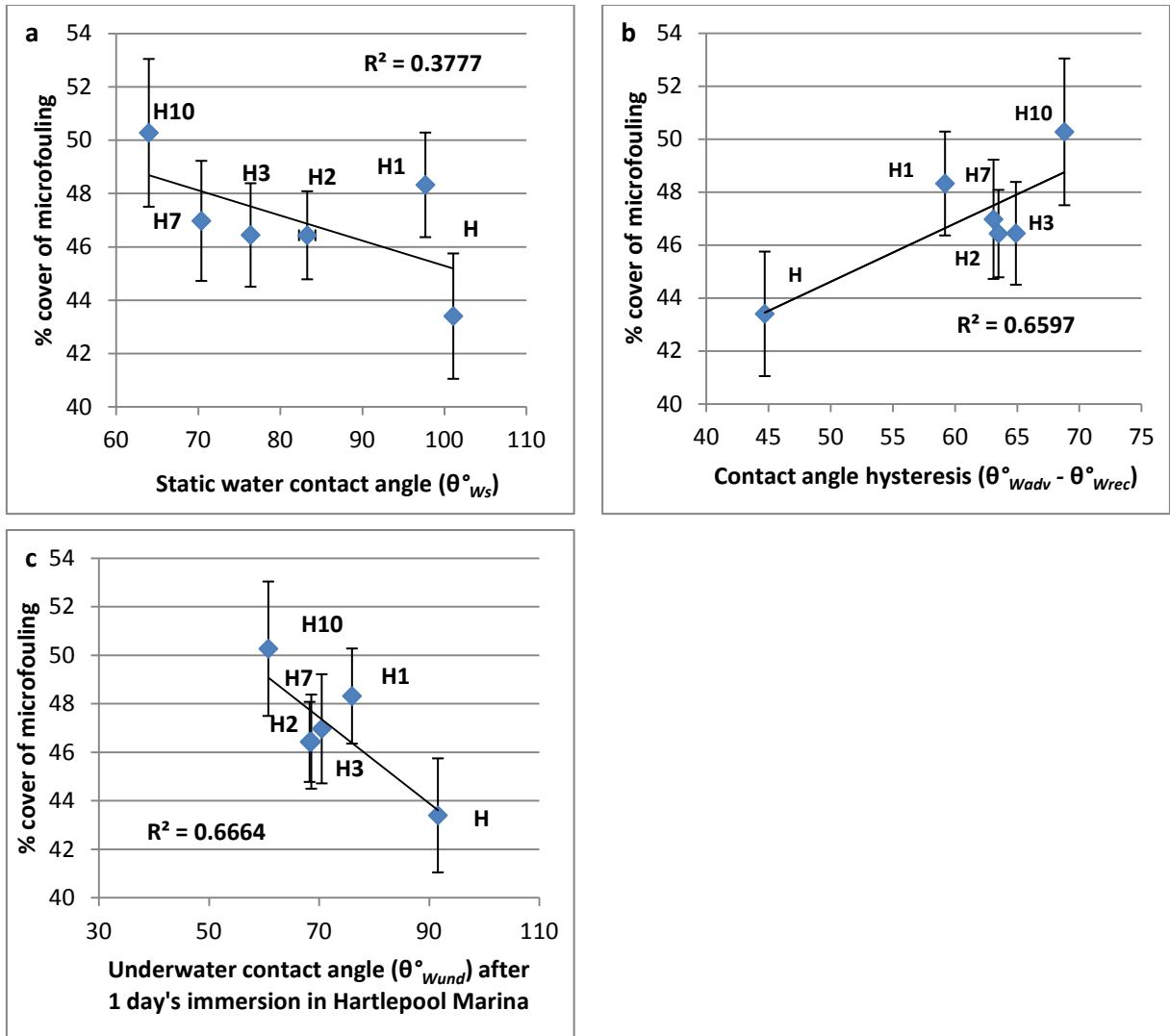
Figure 10.16: Correlations between the % cover of microfouling averaged over the whole experiment and surface properties of the silicone 'hybrid' coatings: the initial static contact angle in air (a), the contact angle hysteresis (b) and the underwater contact angle after 1 day's immersion in Hartlepool Marina (c). Each point represents the mean of all the collected data for a surface (n= 147; 7 replicates x 7 inspections x 3 panels) ± 2 x SE. Linear trend lines and R^2 correlations are shown for all data points.

While no strong correlation was observed between the % cover of weeds and either static contact angle in air and underwater contact angle after 1 day's immersion in Hartlepool Marina ($R^2 < 0.4$; Figs. 10.16b/c), a weak negative correlation was observed between the % cover of weeds and the contact angle hysteresis ($R^2 = 0.59$; Fig. 10.17b).
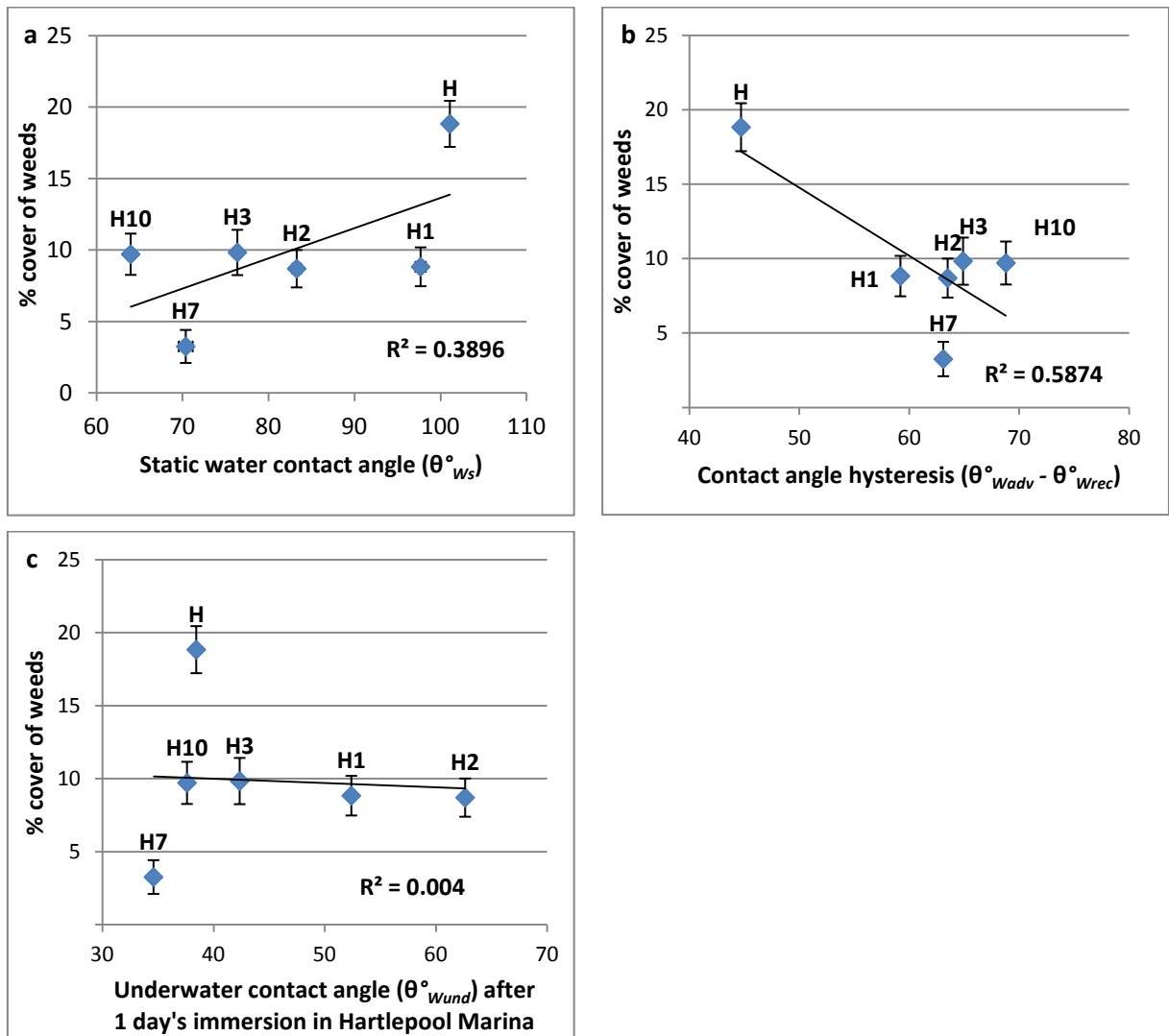
Figure 10.17: Correlations between the % cover of weeds averaged over the whole experiment and surface properties of the silicone 'hybrid' coatings: the initial static contact angle in air (a), the contact angle hysteresis (b) and the underwater contact angle after 1 day's immersion in Hartlepool Marina (c). Each point represents the mean of all the collected data for a surface (n= 147; 7 replicates x 7 inspections x 3 panels) ± 2 x SE. Linear trend lines and R^2 correlations are shown for all data points.
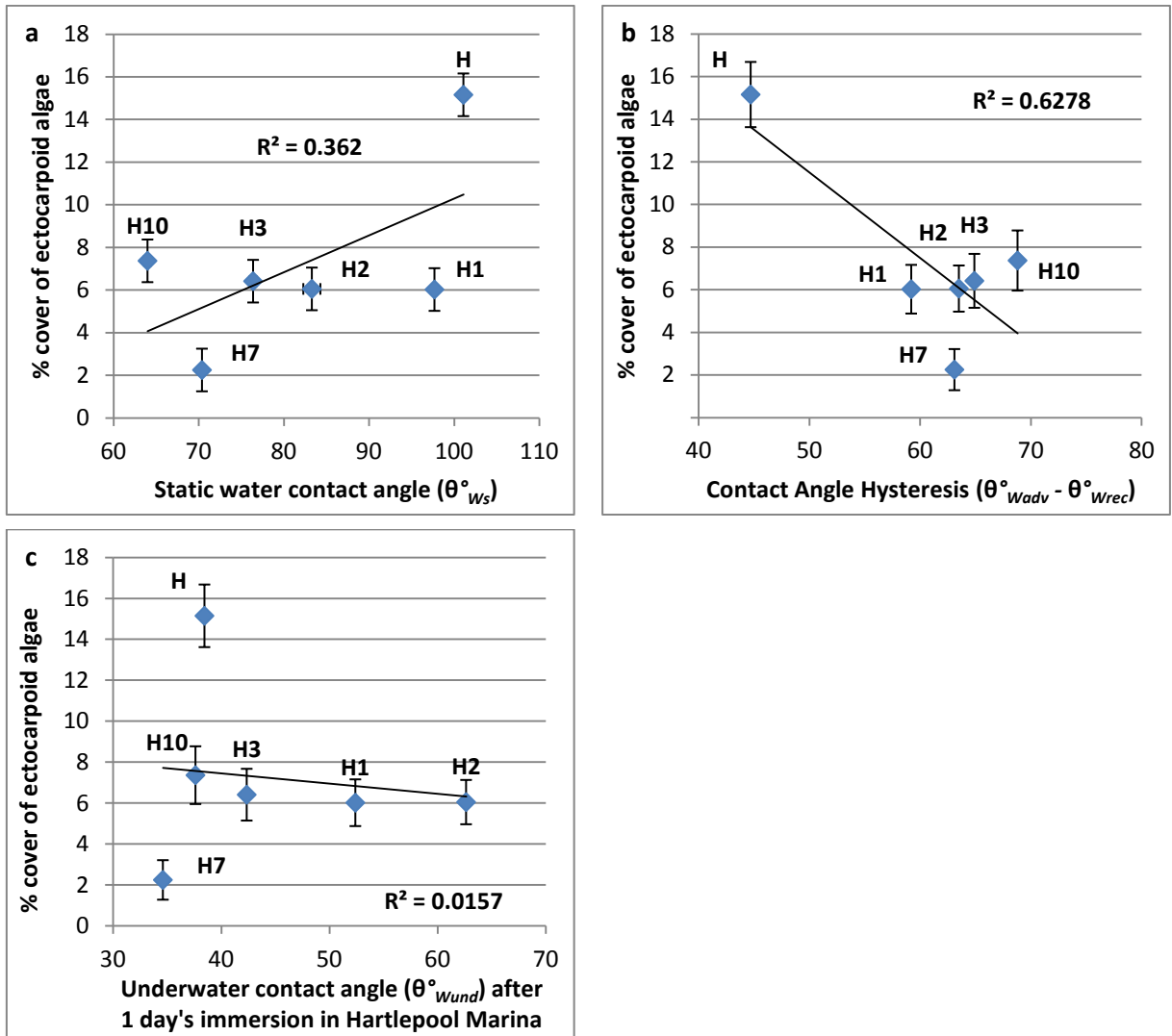
Figure 10.18: Correlations between the % cover of ectocarpoid algae averaged over the whole experiment and surface properties of the coatings: the initial static contact angle in air (a), the contact angle hysteresis (b) and the underwater contact angle after 1 day's immersion in Hartlepool Marina (c). Each point represents the mean of all the collected data for a surface (n= 147; 7 replicates x 7 inspections x 3 panels) ± 2 x SE. Linear trend lines and R^2 correlations are shown for all data points.

Only weak correlations were observed between the presence of ectocarpoid algae and either the static contact angle in air or the underwater contact angle after one day's immersion in Hartlepool Marina ($R^2 < 0.4$; Figs. 10.18a/c). However, a stronger negative correlation was observed between the % cover of ectocarpoid algae and the contact angle hysteresis ($R^2 = 0.63$; Fig. 10.18b).

The % cover of soft-bodied animals was not correlated to the three surface properties represented in Figures 10.19 (R^2<0.3). However, if the coating H10 was excluded from the correlation as it was not following the same trend as the other coatings, a positive correlation was observed between the static contact angle in air and the % cover of soft-bodied animals (R^2=0.91; Fig. 10.19a). As for the total % cover, by linking the % cover of the different coatings together, a similar relationship to the one observed in Chapter 6 (Fig. 6.3b) between the % removal of *U. linza* and static contact angle was observed, as the colonisation would be inversely linked to the % removal.
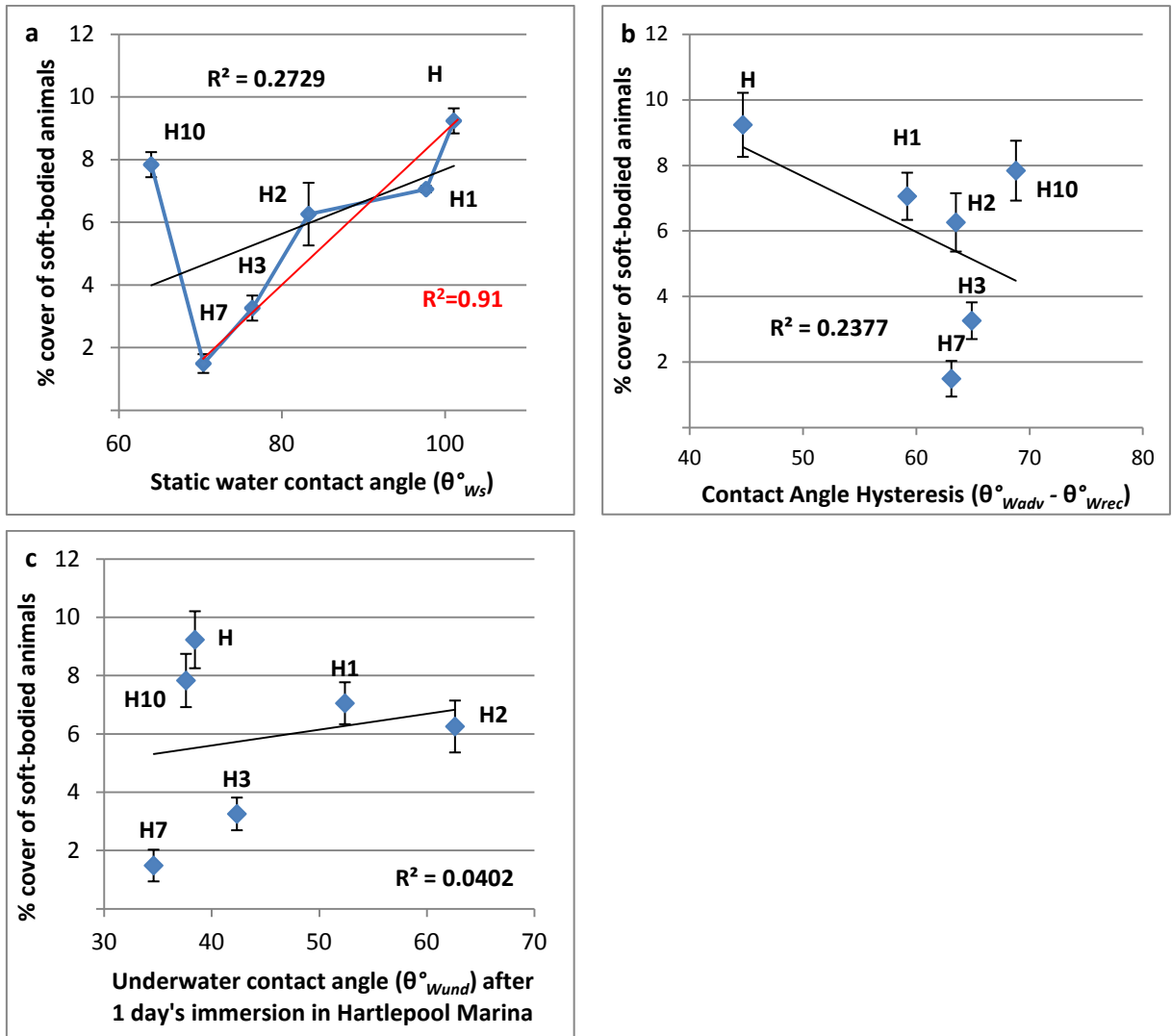
Figure 10.19: Correlations between the % cover of soft-bodied animals averaged over the whole experiment and surface properties of the silicone 'hybrid' coatings: the initial static contact angle in air (a), the contact angle hysteresis (b) and the underwater contact angle after 1 day's immersion in Hartlepool Marina (c). Each point represents the mean of all the collected data for a surface (n= 147; 7 replicates x 7 inspections x 3 panels) $\pm$ 2 x SE. Linear trend lines and R^2 correlations are shown for all data points (black) and for all points excluding H10 (red).

While no correlation was observed between the % cover of hard-bodied animals and underwater contact angle after one day's immersion in Hartlepool Marina (R^2=0.1; Fig. 10.20c), stronger positive and negative correlations were observed with the static contact angle in air and contact angle hysteresis, respectively (R^2=0.54-0.65; Figs. 10.20a/b). As for the % cover of soft-bodied animals, by linking the % cover of the different coatings together (Fig. 10.20a), a similar relationship to the one observed in Chapter 6 (Fig. 6.3b) between the

% removal of *U. linza* and static contact angle was observed, as the colonisation would be inversely linked to the % removal.
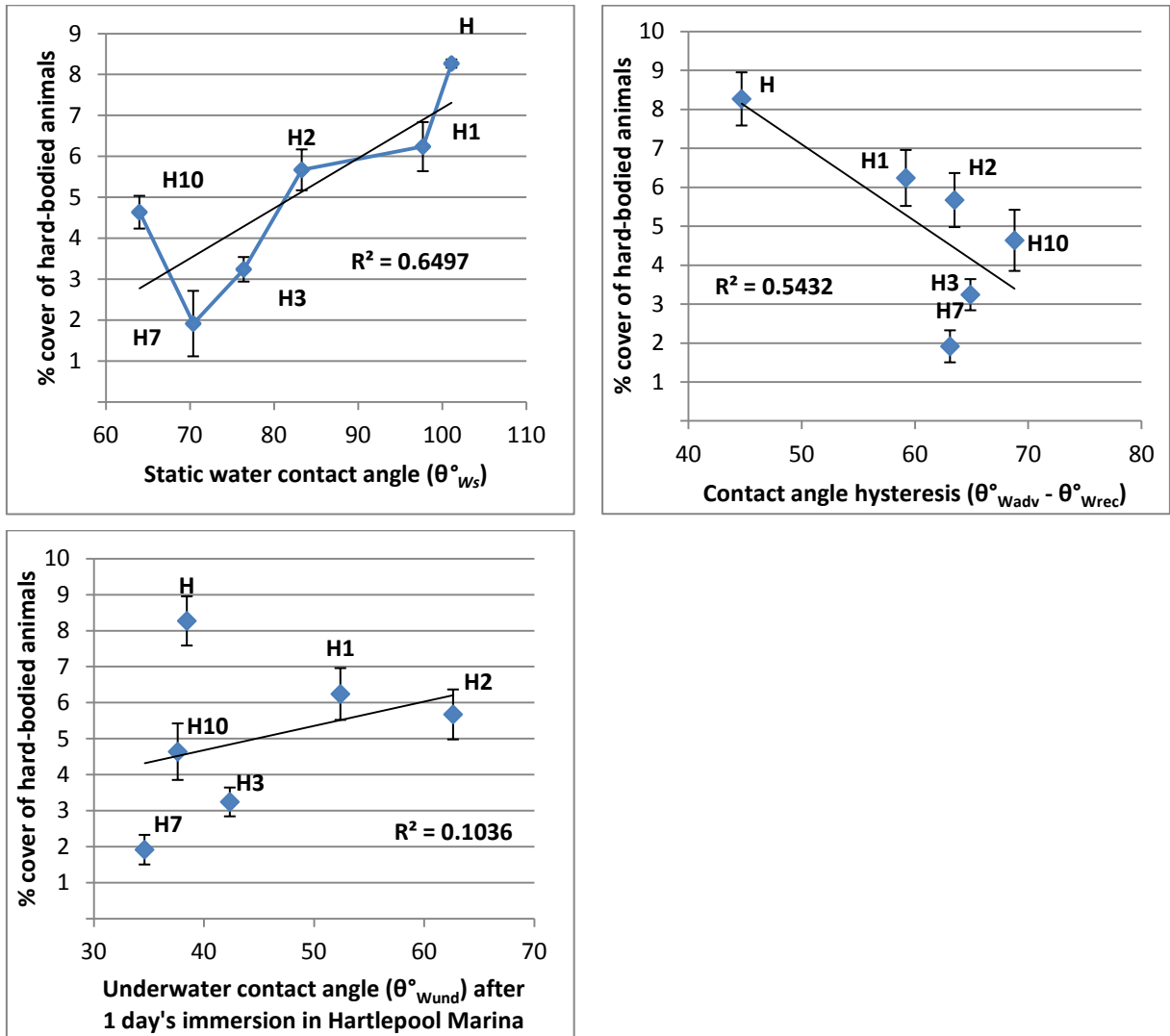
Figure 10.20: Correlations between the % cover of hard-bodied animals averaged over the whole experiment and surface properties of the silicone 'hybrid' coatings: the initial static contact angle in air (a), the contact angle hysteresis (b) and the underwater contact angle after 1 day's immersion in Hartlepool Marina (c). Each point represents the mean of all the collected data for a surface (n= 147; 7 replicates x 7 inspections x 3 panels) ± 2 x SE. Linear trend lines and R^2 correlations are shown for all data points.

10.4. Discussion

This Chapter presents the results of field experiments performed during the spring-summer season of 2011, testing the performance of well-characterised coatings made from the blending of PDMS and PDMS-PEO copolymers. By mixing different ratios of these two copolymers, a series of coatings having a graduated range of initial wettability/surface energy was produced (as shown in Chapter 4). It has been demonstrated in Chapter 4 that the wettability and related properties (surface energy and its components) were the measured parameters that varied among these coatings as they have similar modulus and roughness. These coatings formed then a good series to investigate the effects of wettability on the colonisation of fouling organisms.

It has been shown in previous studies that surfaces change quickly after immersion due to for example surface reorganisation and formation of a conditioning film and so the wettability would vary and influence the results of the field assay (Sundaram et al. 2011; Thome et al. 2012). In order to observe the changes of wettability of immersed surfaces (in sterile ASW and in natural seawater), the underwater contact angles were measured during a period of 10 days.

The wettability values of dry and freshly immersed (in MilliQ water) surfaces were different, as it has been demonstrated previously for other surfaces (Zhang et al. 1989; Maldonado-Codina and Morgan 2007). It is highly possible that these differences were due to a rapid surface reorganisation since the coatings, except H, were amphiphilic in nature containing hydrophilic PEO blocks and hydrophobic PDMS blocks. Previous experiments testing amphiphilic coatings also showed that coatings became more hydrophilic after immersion (Krishnan et al. 2006a; Sundaram et al. 2011; Martinelli et al. 2012a). However, H the most hydrophobic coating, which contained only PDMS, had the highest decrease of contact angle after one day's immersion, while IS700, which also contained only PDMS as polymer, had barely any changes of wettability (<10°) after 1 day, showing that IS700 was more stable

than H. It is possible that other properties or other mechanisms changed the wettability such as the conditioning film produced by the absorption of macromolecules (Thome et al. 2012), or even the presence of the curing agent on the surface of the test coatings. It is likely that the changes in wettability on immersion are due to contributions from more than one of these effects.

After the first day of immersion, the wettability values showed that there was no clear pattern to explain the wettability changes, some coatings had a relatively stable wettability while others were subjected to fluctuations. The microscope observations showed that a biofilm (i.e. bacteria and diatoms) and associated fouling were developed on the surfaces immersed in Hartlepool Marina, especially from 7 days. The fact that no qualitative differences of the fouling organisms attached to the coatings were observed between the experimental coatings suggests that during the 10 first days' immersion, the fouling community was not influenced by the surface wettability. However, it was possible that the species of bacteria were different between the surfaces. In addition, it is likely possible that the wettability values from 7 days in Hartlepool Marina were due to the presence of fouling organisms rather than the properties of the surfaces. As the surfaces immersed at Hartlepool Marina were less hydrophilic than the surfaces in sterile ASW, it is possible to suggest that it was due to the presence of the biofilm formed in natural seawater (Hartlepool Marina).

The results obtained during the static field experiment showed that the different factors (i.e. coatings (or surface properties), days of immersion, panels and rows) that were analysed influenced the colonisation of the different fouling organisms (i.e. % cover). Each category of fouling organisms appeared at different periods and their cover evolved differently. As shown for a number of previous field experiments (Bailey-Brock 1989; Benedetti-Cecchi 2000; Prendergast 2007), microfouling was the first category that was visible by eye, followed by weeds. Then later – around 43 days' immersion for this experiment- soft- and hard-bodied animals were visible. However, these data have to be taken with caution, it does not mean

that algal spores and animal larvae were not present from the first days of immersion, but that their growth took longer than the microfouling to be visible.

As expected, the silicone 'hybrid' coatings were in general more effective as antifouling coatings than the tie coat (i.e. for the total fouling, coverage of weeds and ectocarpoid algae). The performance of the commercial amphiphilic coating IS900 was relatively similar to the performance of most of the silicone 'hybrid' coatings, except for the microfouling colonisation; coating H had higher coverage than IS900 for the coverage of weeds, ectocarpoid algae and animal fouling. In addition, IS900 was less effective than H7 for the coverage of weeds and ectocarpoid algae and also more effective than both H3 and H7 for the coverage of animal fouling. The comparison of the test coatings showed that coating H7 was the most effective due to the lowest percentage cover for all fouling categories except microfouling, while coating H was the least effective coating of the silicone 'hybrid' coatings.

One of the aims of the underwater contact angle measurements during 10 days' immersion in seawater was to evaluate the influence of wettability on the coating performance in the field, viz. colonisation of fouling organisms. It was then decided to compare the % cover of fouling organisms to three surface properties: initial surface wettability and contact angle hysteresis of dry coatings and wettability of coatings after one day's immersion in Hartlepool Marina.

Differences of fouling coverage between the coatings showed that the structure of the biofouling communities (i.e. the % covers of the fouling categories) was partly influenced by the measured surface properties. An influence of the initial static contact angle in air was only observed on the % cover of the hard-bodied animals (R^2=0.65). Coating H10 did not follow the same trend as the other coatings for the correlations between the static contact angle in air and total fouling and % cover of soft-bodied animals and so by excluding H10 from the correlations, more positive correlations were observed between static contact angle

in air and the % cover of total fouling and soft-bodied animals (R^2=0.89-0.91). It was already observed that H10 had an anomalous performance for the adhesion strength of *U. linza* (Chapter 6; Fig. 6.3). This could be due to other, unmeasured surface properties such as a sub-optimal patterning of surface domains produced by the segregation of hydrophilic and hydrophobic chains, as proposed in Chapter 6.

Further correlations were observed; negative correlations were observed between the contact angle hysteresis and the coverage of weeds, ectocarpoid algae and hard-bodied animals (R^2>0.5), while % cover of microfouling was positively and negatively correlated with the contact angle hysteresis (R^2=0.66) and the underwater contact angle after one day's immersion (R^2=0.67), respectively. These correlations showed that wettability from pristine and immersed surfaces influenced the colonisation of fouling organisms. However, as the correlations were not perfectly linear or did not include all the coatings, it is possible to conclude that the colonisation of surfaces is more complex and does not depend only on the measured surface properties.

Significant but minor differences between the panels were observed for all fouling categories except for hard-bodied animals, showing that external factors slightly influenced the colonisation of the test surfaces. Seawater and environmental parameters such as salinity, pH, light and temperature are known to affect colonisation by fouling organisms. However, the panels were close to each other, so no such variations of these parameters could have affected the community. It is possible the biological interactions such as competition, predation and physical disturbances could have influenced the fouling community, as demonstrated by Swain et al. (1998). In addition, populations of marine organisms are often characterised by variable recruitment patterns that seem unpredictable in time and space (e.g. Jernakoff 1983; Roughgarden et al. 1988; Vadas et al. 1992), which could explain the variations between the panels.

In addition, an effect of depth was observed for all four fouling categories, but the differences for the animal fouling were relatively minimal. However, the analyses showed that coverage of microfouling was higher with the increase of depth and that the coverage of weeds was higher in the middle of the panels (i.e. row 4) compared to the rows on the edges, showing that at this depth, the light might have been optimum for the settlement of spores, which are known to be phototactic (Fletcher and Callow 1992 for review; Greer and Amsler 2002 and 2004).

The laboratory assays described in Chapter 6 assessed the fouling-release performance of the silicone 'hybrid' coatings on the adhesion of ectocarpoid algae and showed no clear correlation between the adhesion strength of *E. crouaniorum* and the measured surface properties. The field assay described in this Chapter essentially assessed the performance of the same coatings on the colonisation of fouling organisms. However, it was possible to observe that the laboratory results partly predicted the results obtained in the field assay; the coating H7 was for both types of experiments the most effective coating. However, the fouling coverage gave different results on the performance of the other coatings compared to the laboratory experiments.

Summary of the results:

- The wettability values obtained for the dry and freshly immersed (in MilliQ water) surfaces showed either that the two methods measure slightly different aspects of surface wettability, or that in few minutes of immersion needed to measure the underwater contact angle, a surface reorganisation happened.
- The surfaces became more hydrophilic after 24 h immersion in sterile ASW showing a surface reorganisation and possibly the effect of conditioning film due to the absorption of macromolecules present in the ASW.

- The surfaces in Hartlepool Marina were in general more hydrophobic than those immersed in sterile ASW, suggesting that the biofilm formed in natural seawater made the surfaces more hydrophobic.

- Each category of fouling organism appeared at different periods and their cover evolved differently.

- The silicone 'hybrid' coatings were in general more effective than the commercial standard amphiphilic coating IS900.

- H7 was the most effective antifouling coating while H was the least effective of the silicone 'hybrid' coatings.

- Positive correlations were observed between the initial contact angle and the total fouling and animal fouling.

- A negative correlation was observed between the contact angle hysteresis and the coverage of weeds, ectocarpoid algae and hard-bodied animals, while a positive correlation was observed for the microfouling coverage.

- A negative correlation was observed between the microfouling coverage and the contact angle after one day's immersion in Hartlepool Marina.

- Laboratory assays partly predicted the results obtained with the field assay; H7 was the most effective coating in both situations.

11. FIELD ASSAYS OF ANTIFOULING PERFORMANCE OF SILICONE COATINGS WITH A RANGE OF MODULUS DURING 2012 SEASON

11.1. Introduction

As explained in the two previous Chapters, field experiments evaluate the performance of test coatings in a natural environment allowing comparison with the results obtained in laboratory assays. In Chapter 8, a systematic series of hydrophobic coatings with varying modulus produced from different molecular weights of PDMS (viscosity from 72 to 50000 mPa s^{-1}) was tested to observe the effect of modulus on the adhesion strength of two algae, *Ectocarpus crouaniorum* and *Ulva linza.* The results obtained in Chapter 8 showed that the modulus influenced slightly the adhesion strength of these two algae, with different relationship to the modulus depending on the alga. The adhesion strength of *U. linza* was positively correlated with the elastic modulus (and to the molecular weight of PDMS), as observed previously by Chaudhury et al. (2005). However, the attachment and adhesion strength of *E. crouaniorum* filaments was negatively correlated with modulus. The aims of this field experiment were (a) to observe the appearance and the succession of the different fouling organisms, especially ectocarpoid algae, in order to see if there were differences between the surfaces and also between the fouling organisms on the different surfaces, (b) to correlate any difference in colonisation with the bulk properties of the coatings. It is the first study to assess colonisation in the field with a systematic series of coating with a range of modulus. This experiment was performed in Hartlepool Marina, following the same protocol as Chapter 10.

11.2. Materials and Methods

11.2.1. Coatings

The test coatings were five silicone-based coatings (M1, M2, M3, M4 and M5) with varying moduli, from 0.73 to 1.5 MPa. IS900 was used as commercial standard coating and a commercial tie coat as a negative control surface (i.e. the tie coat had no antifouling properties and was therefore expected to foul heavily). The composition and characterisation of these surfaces was described in Chapter 4.

11.2.2. Static field immersion experiment

Figure 11.1: Panel before immersion. The panels were attached to a weight in order to be in vertical position. Two ropes were attached to the pontoons to keep the panel in the same position during the field experiment.

The experiment was done following the method designed in Chapter 10. The panel design was of 7 rows x 7 columns (Fig. 11.1). The three-replicate panels were immersed on the 13th March 2012, and the data were collected after 20, 39, 47, 60 and 83 days. Percentage covers of all the fouling categories were obtained following the 'Phoenix' in-house Experimental Fouling Assessment Record Sheet. The percentage of ectocarpoid algae was

also recorded separately and samples were taken using forceps for subsequent microscopic examination to determine which genera were present.

11.2.3. Statistical analysis of the field data: Generalized estimating equations

It was explained in Chapter 2.10 and statistical tables for the whole Chapter are presented in Appendix 12.

11.3. Results

11.3.1. General observation of the percentage fouling

Five data inspections were done between the 20th and the 83rd days' immersion –i.e. between the 13rd of March and 5th of July 2012. Only a few algae were visible during the whole experiment and as the animal fouling started to have a relatively high coverage, it was assumed that no more algae would grow on the surfaces during the summer season, and it was then decided to stop the experiment and to analyse the results obtained.

Figure 11.2 shows the percentage cover of the four categories of fouling organisms (microfouling, weeds, soft- and hard-bodied animals) for each coating on one panel (7 replicates, data shown for the other 2 panels in Appendix 13). The effects of the coatings, replication, time of immersion and depth (row) were determined for all the fouling categories using generalized estimated equations GEEs as statistical analysis (Chapter 2; data were significantly different when $p<0.05$).

Variations between the surfaces and the inspections were observed in total fouling –i.e. differences in percentage cover in all four fouling categories- and also in percentage cover of different fouling categories (Fig. 11.2; Appendix 13). It was observed that from 60 days' immersion the total fouling reached 100 % cover for almost all of the test coatings.
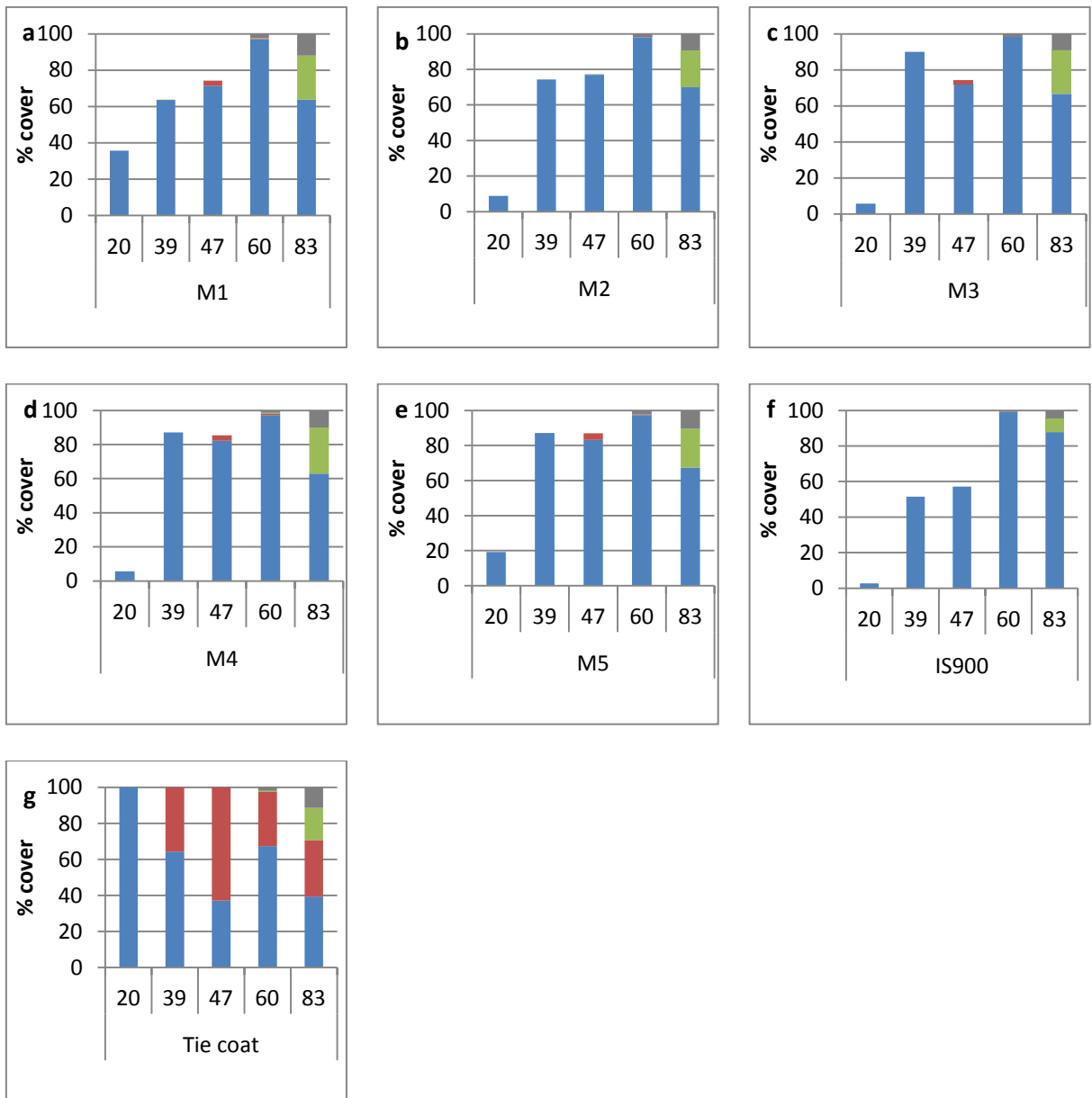
Figure 11.2: Percentage cover observed on 7 different test surfaces attached to Panel 2, immersed in Hartlepool Marina during 83 days' immersion. Percentage cover for the 4 fouling categories: microfouling (blue), weeds (red), soft-bodied animals (green) and hard-bodied animals (grey). For each graph, the axis x represents the length of immersion for each coating. Mean of 7 replicates.

The coverage of microfouling was also different between the panels; it was relatively low during the three first inspections on panels 1 and 2, while on panel 3, microfouling was

already covering the majority of the surfaces at the second inspection. The presence of the other fouling categories (weeds, soft- and hard-bodied animals) appeared after 47-60 days' immersion.

11.3.2. Analysis of the total percentage cover

Figure 11.3a shows total percentage cover for all surfaces. At the first inspection the total coverage was relatively low (around 20%), then increased linearly until 60 days' immersion, and for the two last inspections, the coverage reached a plateau close to 100 %.

Significant differences for the total fouling coverage were observed between the surfaces (Fig. 11.3b). As expected, the tie coat, which had no antifouling properties, had significantly the highest total coverage. All the other surfaces were grouped together, except M1 that had significantly a higher coverage. No strong linear correlation was observed between the total % cover and the elastic modulus, the viscosity and the estimated molecular weight of PDMS (Figs. 10.3c-e). However, as M1 had a higher coverage than the other test coatings, a positive effect of the elastic modulus was observed with the total % cover, with an increase in fouling when the elastic modulus was >1 MPa.

In addition, a red curve was drawn in Figure 11.3c showing a possible correlation between total % cover and elastic modulus with low coverage for M3 (i.e. 0.91 MPa) and higher coverage for M5 and M1 the softest and hardest coatings.
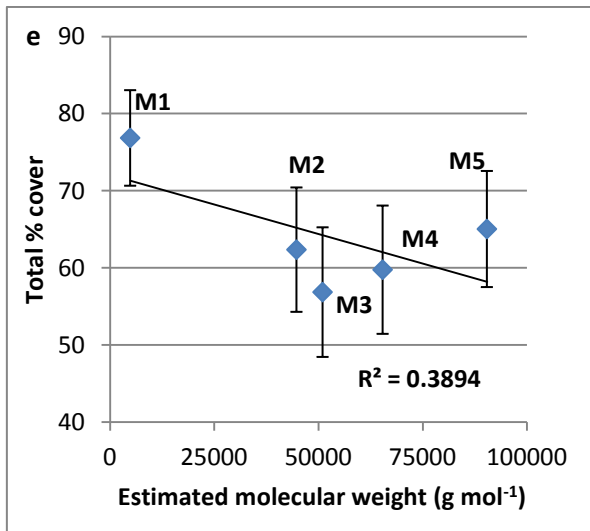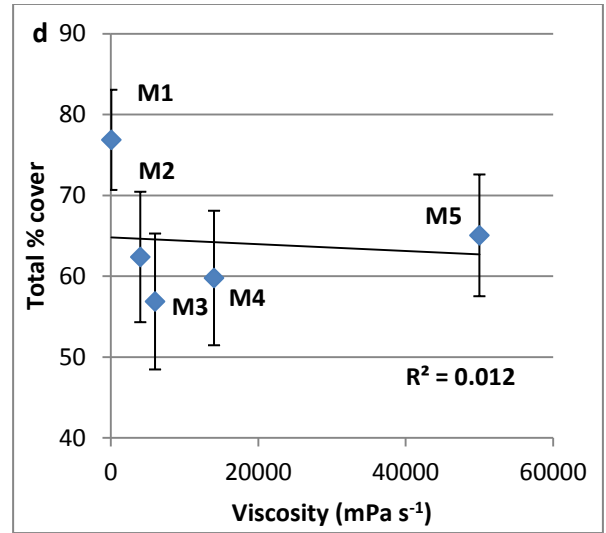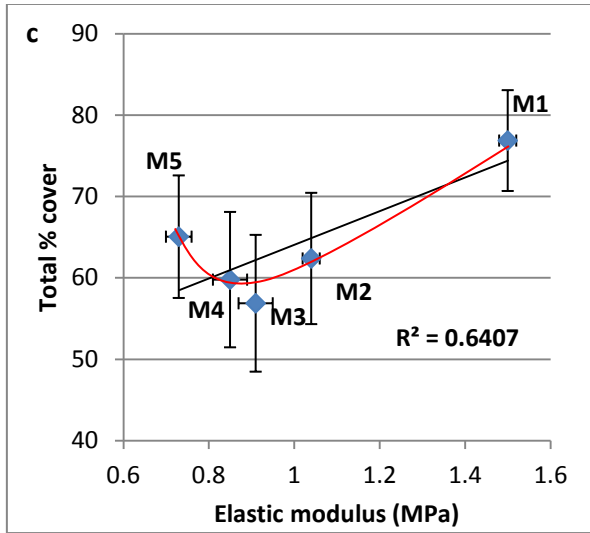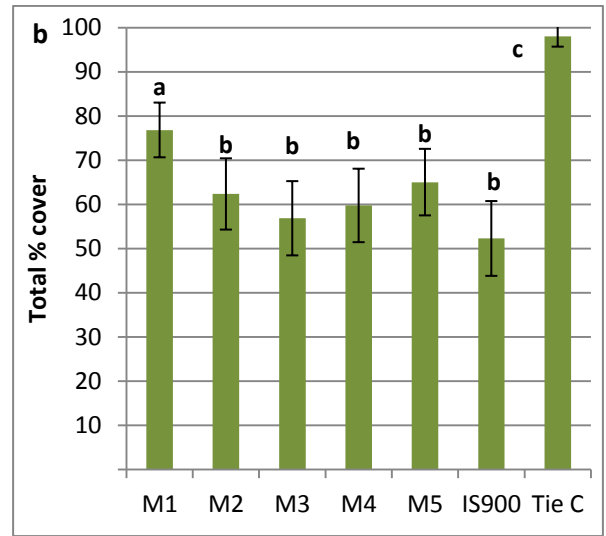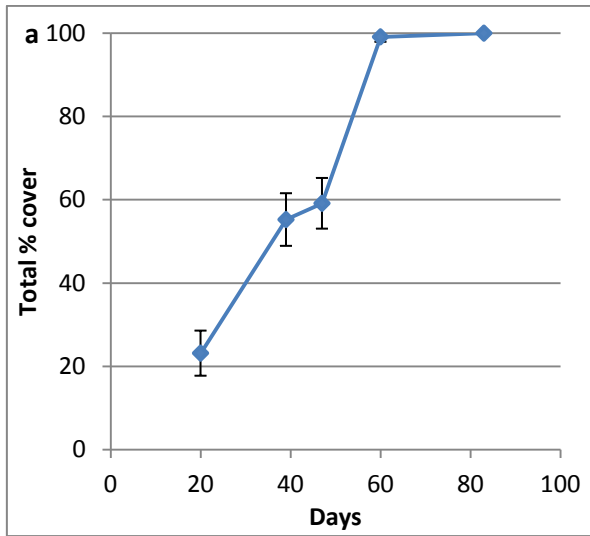
Figure 11.3: Total percentage cover as a function of immersion days of the panels (a) and as a function of each surface averaged over the whole experiment (b) and correlations between the total % cover and properties of the silicone 'modulus' coatings: elastic modulus (c), viscosity (d) and estimated molecular weight (e). a) Each data point represents the mean of all collected data (n=147) at each inspection day (7 surfaces x 7 replicates x 3 panels) ± 2 x SE. Figures b-e, each bar/points represents the mean of all the collected data for a surface (n= 105; 7 replicates x 5 inspections x 3 panels) ± 2 x SE. Tie C= tie coat. In Figure b, the experimental coatings are arranged in order of decreasing modulus (M1=1.5 MPa; M2=1.04 MPa; M3=0.91 MPa; M4=0.85 MPa; M5=0.73 MPa). Values that are significantly different at p≤0.05 in GEEs are indicated by different letters above the bars in Figure b. Linear trend lines and R^2 correlations are shown for all data points in Figures c-e and the curve in red shows the effect of high modulus on the total % cover in Figure c.

11.3.3. Analysis of the percentage cover of microfouling

As shown in Figure 11.4a, the percentage cover of microfouling increased until 60 days' immersion reaching approximately 100 % cover for most of the surfaces and after 83 days' immersion, the coverage decreased to 70 % as the animal coverage increased. This pattern was observed for all the surfaces except for the tie coat, which had a microfouling coverage of 36 % after 20 days' immersion, then a variable coverage due to an appearance of weeds and then of animal fouling.

Statistical analysis showed that tie coat and M1 had significantly the highest percentage cover compared to the other surfaces, which were grouped together (Figs. 11.4a/b). Although no strong linear correlations were observed between the microfouling coverage and the elastic modulus, the viscosity and the estimated molecular weight of PDMS (Figs. 11.4b-d), a positive effect of modulus was observed on the microfouling coverage, as when the elastic modulus was higher than 1 MPa, the coverage of microfouling was higher.

In addition, a red curve was drawn in Figure 11.4b showing a possible correlation between microfouling coverage and elastic modulus, as for total % cover, with the highest coverage on the softest and hardest coatings (M5 and M1).
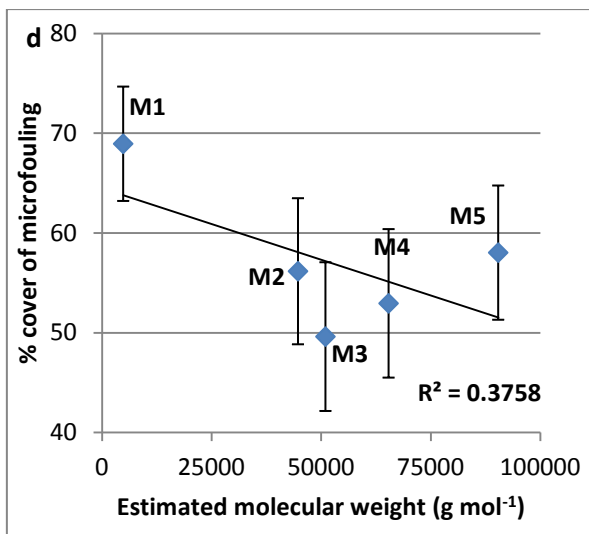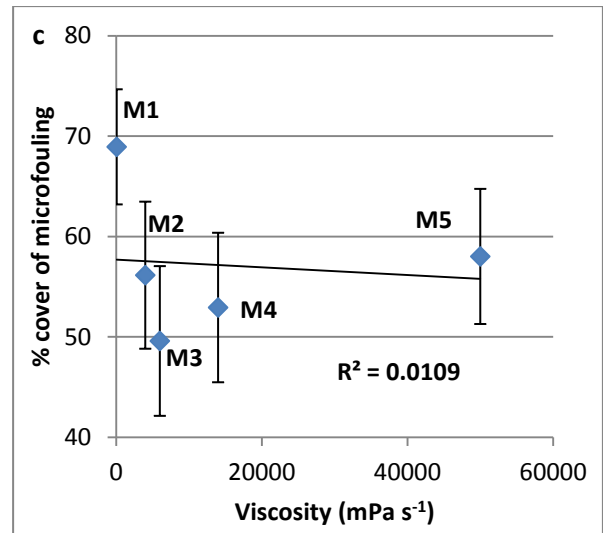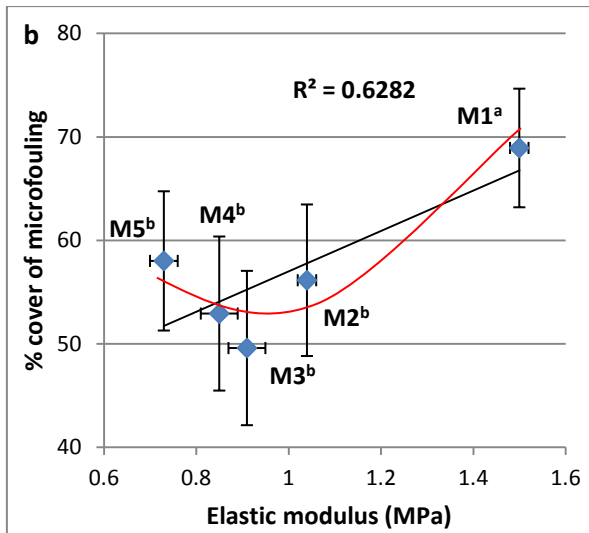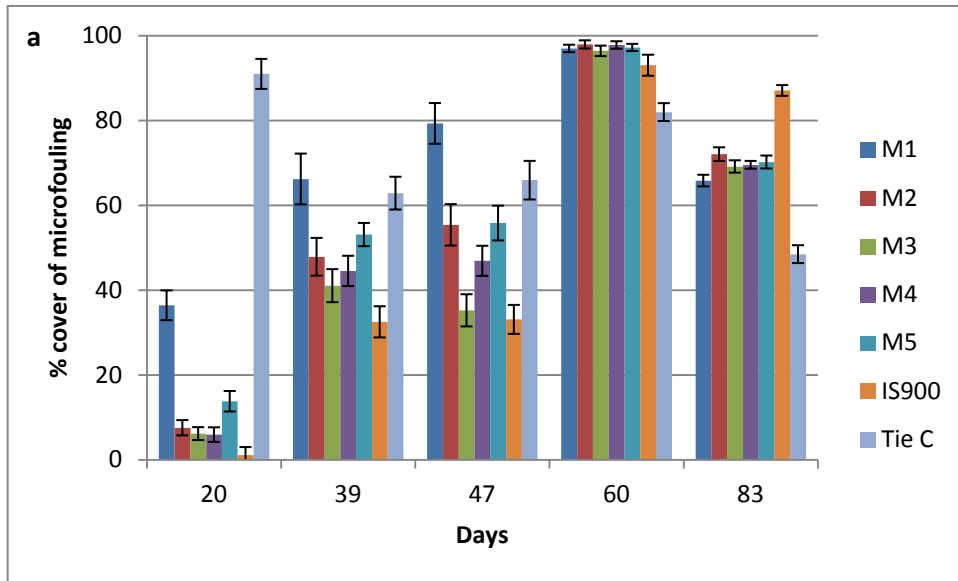
Figure 11.4: Percentage cover of microfouling as a function of immersion days and surfaces (a) and correlations between the % cover of microfouling averaged over the whole experiment and properties of the silicone 'modulus' coatings: the elastic modulus (b), viscosity (c) and estimated molecular weight (d). Each bar/dot represents the mean of collected data (for a (n= 21): 7 replicates x 1 inspection x 3 panels; for b-d (n= 105): 7 replicates x 5 inspections x 3 panels) ± 2 x SE. Tie C = Tie coat. Values that are significantly different at p≤0.05 in GEEs are indicated by different letters above the bars in Figure b. Linear trend lines and R^2 correlations are shown for all data points in Figures b-d and the curve in red shows the effect of high modulus on the % cover of microfouling in Figure b.

11.3.4. Analysis of percentage cover of weeds with particular reference to ectocarpoid algae

Throughout the experiment, almost no biomass of weeds was observed except on the tie coat (Fig. 11.5). Most of the weeds identified were ectocarpoid algae, but some filaments of *Ulva* were also visible. Differences were observed between the inspections of data; at first, after 20 days' immersion, no weeds were observed, then for the 2nd and 3rd inspections, the mean of weed coverage was around 5 % and for the last inspection the coverage was around 2-3 %.

The statistical analysis showed that the tie coat had significantly higher weed coverage at all the inspections compared to the other surfaces, which were grouped together. As weed coverage was not different between the test coatings, it is possible to conclude that the modulus (but also viscosity and estimated molecular weight) did not influence the weed coverage. However, the results have to be taken with caution as the mean coverage of the test species for whole experiment was lower than 1 %, so it is possible that during a field assay with higher coverage of weeds, differences would have been visible (the graphs representing the % cover of weeds as a function of modulus, viscosity and estimated molecular weight were not shown as the % cover was lower than 1 %).
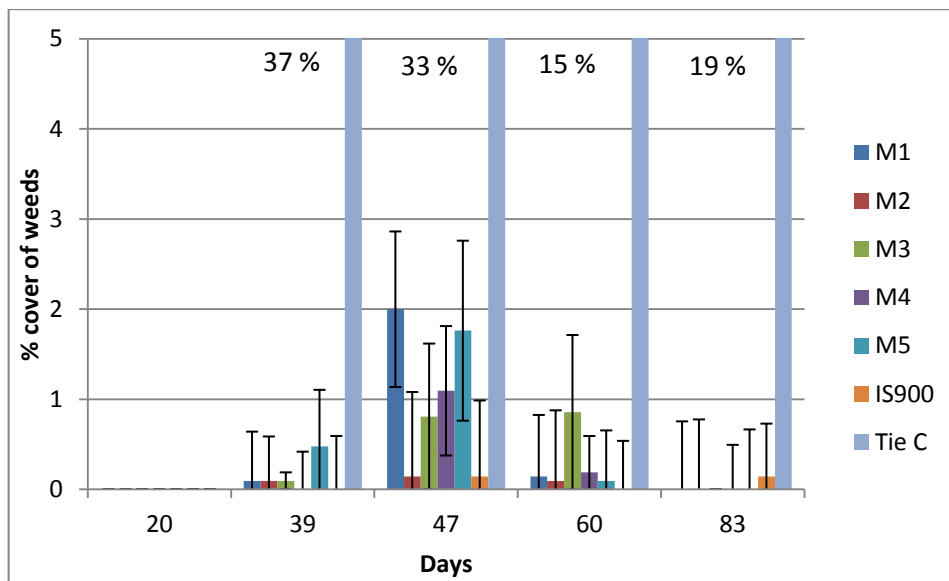
Figure 11.5: Percentage cover of weeds as a function of days and surfaces. Each bar represents the mean of collected data (for a (n=21): 7 replicates x 1 inspection x 3 panels) ± 2 x SE. Tie C= tie coat.

Ectocarpoid algae

The two genera, *Ectocarpus* and *Hincksia,* were observed on the surfaces fouled with weeds. No ectocarpoid algae were observed after 20 days' immersion, then a low coverage was observed for the two following inspections (with 5 % cover) and an even lower coverage was observed from 60 days (with less than 2 % cover). No difference was observed between the surfaces expect for tie coat, which had the highest coverage of ectocarpoid algae during the experiment (Fig. 11.6). The results showed that the modulus (but also viscosity and estimated molecular weight) did not influence the presence of ectocarpoid algae (graph not represented as percentage cover low), but as for the weeds, differences between the coatings might have been visible if there had been a higher coverage on the surfaces.
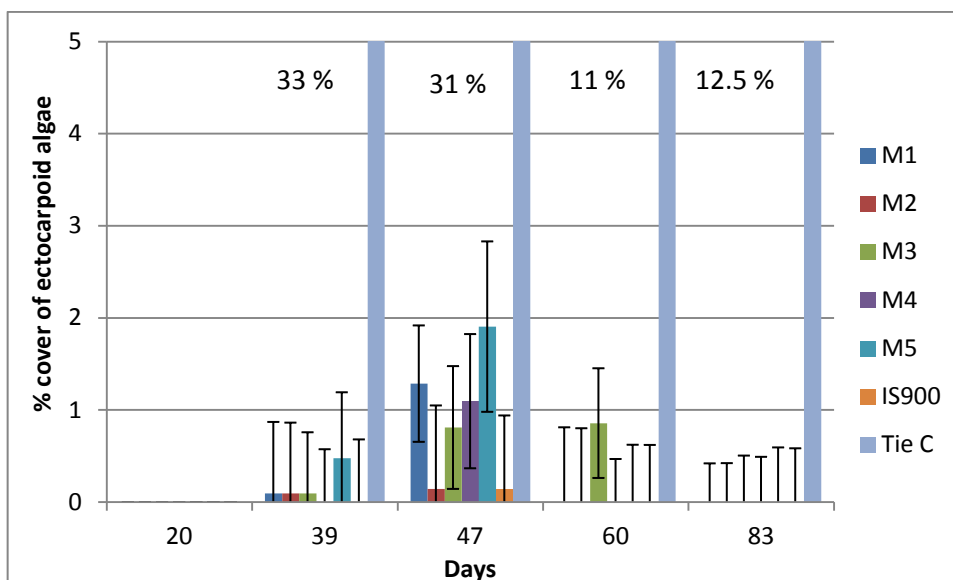
Figure 11.6: Percentage cover of ectocarpoid algae as a function of days of immersion and surfaces. Each bars represents the mean for one surface for one inspection (n=21; 7 replicates x 3 panels) ± 2 x SE.

11.3.5. Analysis of the percentage cover of soft-bodied animals

The first visible colonisation of soft-bodied animals (mostly represented by polyps) was observed after 39 days. However, until 83 days, the coverage was relatively low; only for the last inspection a high percentage cover was visible on the surfaces (Fig. 11.7a). If the panels were left immersed longer, soft-bodied animal fouling might have increased even more. The coverage of soft-bodied animals was significantly lower on IS900 compared to the other surfaces, which grouped together. After 83 days' immersion, the coverage on surfaces was between 20-25%; M2 had lower coverage than M1 and M3, but no further differences were observed. The results showed that modulus (but also viscosity and estimated molecular weight) did not influence the coverage of soft-bodied animals (Figs. 11.7b-d; $R^2<0.3$).
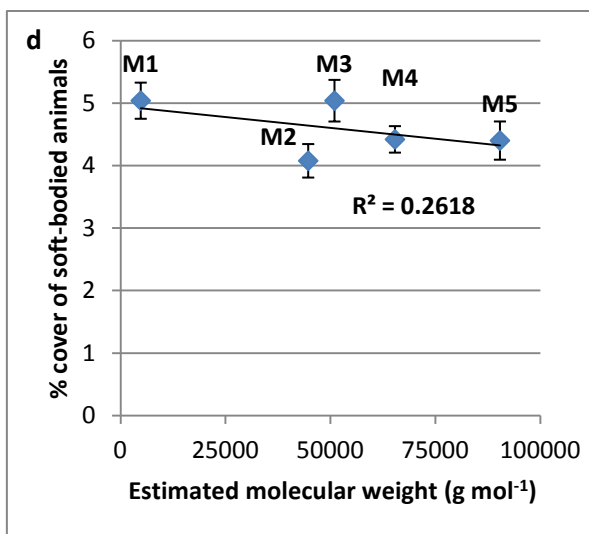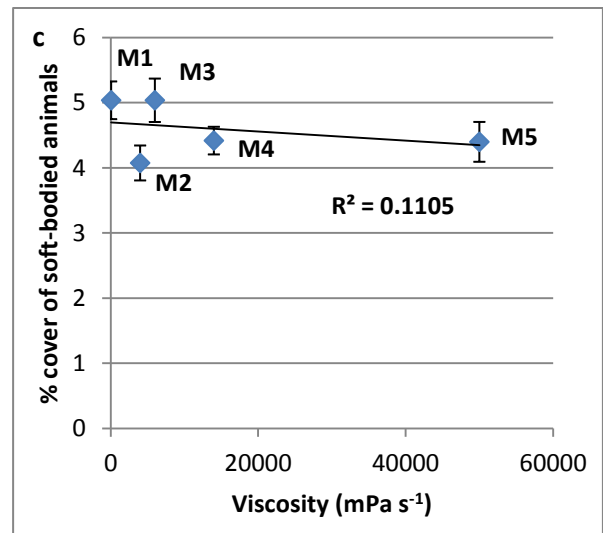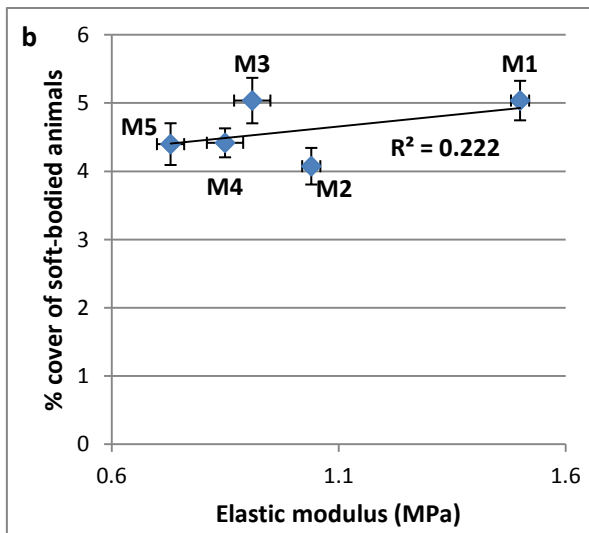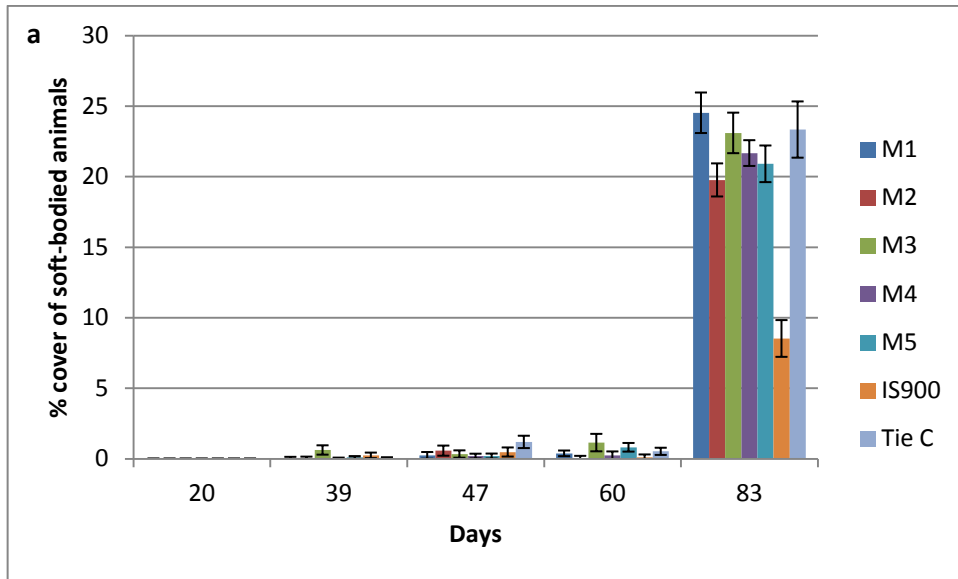
Figure 11.7: Percentage cover of soft-bodied animals as a function of immersion days and surfaces (a) and correlation between the % cover of soft-bodied animals averaged over the whole experiment and properties of silicone 'modulus' coatings: the elastic modulus (b), viscosity (c) and estimated molecular weight (d). Each bar/dot represents the mean of collected data (for a (n=21): 7 replicates x 1 inspection x 3 panels; for b-d (n=105): 7 replicates x 5 inspections x 3 panels) ± 2 x SE. Tie C=tie coat. Linear trend lines and R^2 correlations are shown for all data points in Figures b-d.

11.3.6.   Analysis of the percentage cover of hard-bodied animals

The first observation of hard-bodied animals (mostly tubeworms and a few barnacles) was made after 39 days' immersion. However, as for the soft-bodied animals, coverage was relatively low until 83 days and if the panels had been immersed longer, the amount of hard-bodied animal fouling might have increased further (Fig. 11.8a).

Differences in percentage cover of hard-bodied animals were observed between the surfaces (Fig. 11.8a). Coating IS900 had significantly the lowest coverage; M3 was significantly lower than M1 and tie coat. No further differences were observed between the surfaces, but the differences between minimal and maximal were not higher than 3% cover, so the results have to be taken with caution. In addition, after 83 days' immersion, M3 had lower coverage of hard-bodied animals than M1 and M5 (Fig. 11.8a). These results show that despite small differences, no effect of modulus (but also viscosity and estimated molecular weight) was observed on the colonisation by hard-bodied animals (Figs. 11.8b-d, R^2<0.5).
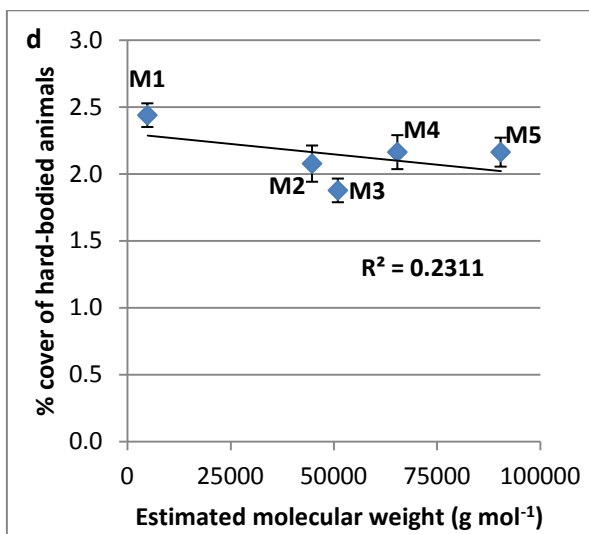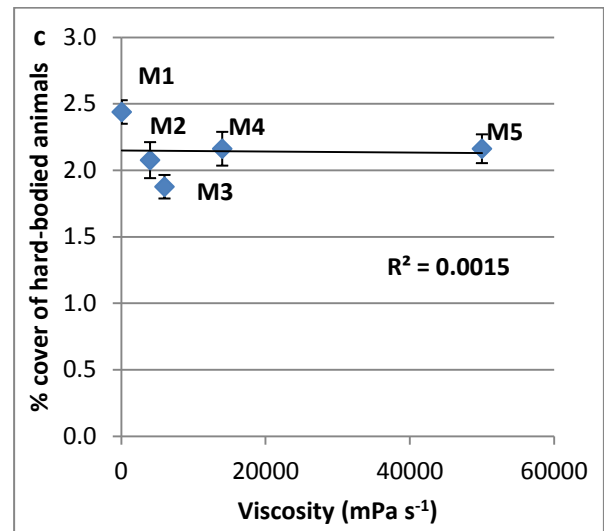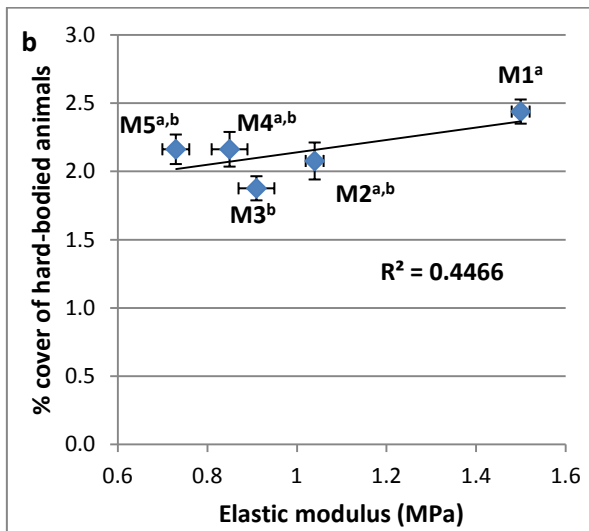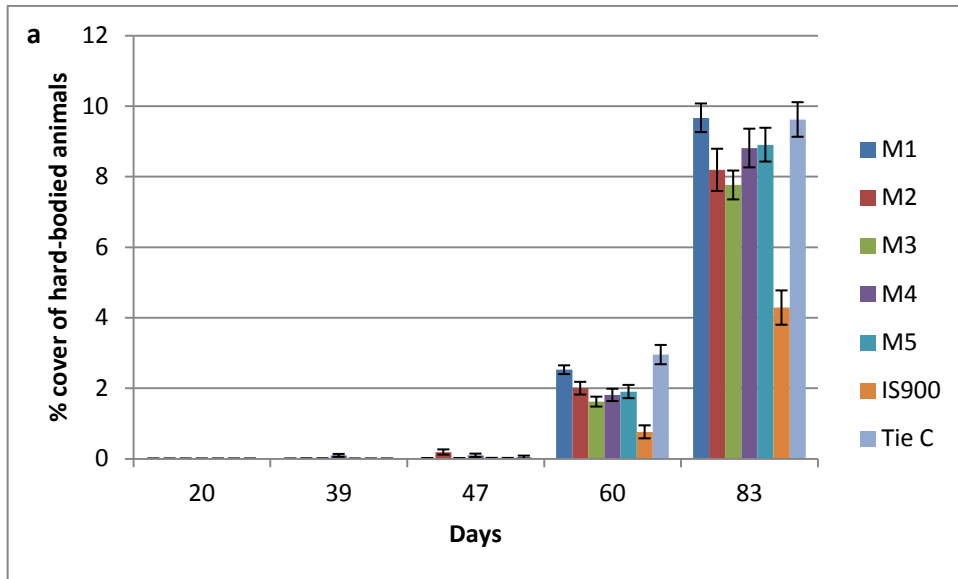
Figure 11.8: Percentage cover of hard-bodied animals as a function of immersion days and surfaces averaged over the whole experiment (a) and correlation between the % cover and the elastic modulus (b), viscosity (c) and estimated molecular weight (d). Each bar/dot represents the mean of collected data (for a (n=21): 7 replicates x 1 inspection x 3 panels; for b-d (n=105): 7 replicates x 5 inspections x 3 panels) ± 2 x SE. Tie C=tie coat. Values that are significantly different at p≤0.05 in GEEs are indicated by different letters above the bars in Figure b. Linear trend lines and R^2 correlations are shown for all data points in Figures b-d.

11.3.7. Effects of 'replicates' and depth observed in the field assay

Even though the main interest of the field assay was to observe the influence of modulus on the appearance of fouling organisms on test surfaces, the results obtained also allowed the observation of the influence of panel-replicates and depth by studying the results between panels and rows, respectively.

Differences of total % cover were observed between the three panels, but they were minor for all the categories of fouling except for the total % cover and the coverage of microfouling. Panel 2 had 10 to 15 % cover higher than the two other panels. However, no major differences were observed on the effect of depth for any of the fouling categories.

11.4. Discussion

The series of coatings tested in this Chapter was made from different molecular weights of PDMS in order to obtain a range of modulus without changing the wettability. These coatings were hydrophobic (i.e. 100°) and had a range of moduli from 0.73 to 1.5 MPa; they had similar thickness (i.e. >200 µm) and roughness (i.e. <0.2 µm). Even if the range of modulus was lower than expected, these coatings represented a good systematic series to test the effect of modulus.

The field assay, which was performed in Hartlepool Marina, was the first study to assess the performance of a systematic series of coatings with varying modulus on the colonisation of

fouling organisms. At first, the surfaces were colonised by microfouling and then a low percentage of weeds (<5%). After 60-83 days' immersion, the coverage of animal fouling was relatively high (>20% and 10% for soft- and hard-bodied animals, respectively). These results were consistent with previous studies on succession of organisms (Bailey-Brock 1989; Benedetti-Cecchi 2000).

Differences between the surfaces were observed; as expected the tie coat, which did not contain any antifouling properties, had higher total % cover and weed coverage, showing that the tie coat was less effective than the other test surfaces. However, no differences were observed between the silicone modulus series except for the total coverage and the microfouling coverage, M1 had higher total % cover and microfouling coverage than the other test coatings. These results showed that the modulus, and the associated parameters of viscosity and estimated molecular weight, influenced the coverage of total fouling and microfouling; the coverage was higher when the elastic modulus was higher than 1 MPa. The coverage of weeds, ectocarpoid algae and animals was not influenced by the elastic modulus and the associated parameters of viscosity and estimated molecular weight. In addition, small differences were observed for the animal fouling (soft and hard), IS900 had lower coverage of animal fouling than the test coatings after 83 days' immersion, showing that IS900 was more effective than the experimental silicones for these fouling categories. It is possible that with the use of a water jet or some water flow, differences in adhesion strength would have been visible.

The laboratory assays described in Chapter 8 assessed the fouling-release performance of the same series of silicone coatings with a range of modulus on the adhesion of ectocarpoid algae and showed that the increase of elastic modulus increased the adhesion strength of *E. crouaniorum*. The field assay described in this Chapter essentially assessed the performance of the same coatings on the colonisation of fouling organisms. Unfortunately, as almost no

ectocarpoid algae colonised the surfaces during the field assay, it was not possible to compare both experiments.

12.   General Discussion

12.1. Aims and objectives of the project

The origin of this project was that International Paint had observed that ectocarpoid algae, known as fouling organisms for many years, had become more common colonisers of submerged surfaces protected with non-biocidal coatings. It was considered by the company that this problem needed some fundamental research so they funded a PhD project at the University of Birmingham, the outcomes of which are represented in this thesis. **The main aim** of the project was defined as the development of a laboratory-scale adhesion bioassay for ectocarpoid algae, and the application of the developed methodology to study the influence of specific physico-chemical parameters on the attachment and adhesion strength of these brown algae. A secondary aim was then to explore whether the results from the laboratory studies were reflected in field-based experiments.

To achieve these aims a number of **specific objectives** were set:

- To acquire isolates of a range of ectocarpoid algae and to culture these on a large enough scale to provide a readily available source of inoculum for adhesion bioassays.

- To develop a reproducible laboratory bioassay for attachment and adhesion of ectocarpoid algae to test surfaces and to demonstrate the ability of the bioassay to distinguish between standard test materials with different surface properties.

- To prepare, or acquire test coatings designed to provide systematic variations in a range of surface and bulk properties (wettability, modulus, charge) known to influence the adhesion of marine fouling organisms and to characterise these properties through appropriate analytical techniques.

- To apply the developed laboratory adhesion bioassay to these test coatings to determine which surface and bulk properties are relevant to the adhesion of ectocarpoid algae.

- To compare the performance of these test coatings on the adhesion strength of ectocarpoid algae with those on the adhesion strength of *Ulva linza*, the only macroalga that has been previously used in laboratory-based adhesion assays.

- To assess the performance of the same test coatings in field immersion assays and to compare the results with the laboratory assays.

- To explore the influence of immersion on the surface wettability of coatings under laboratory and field conditions.

The next two sections of this discussion describe how these aims and objectives were fulfilled through an analysis of the technical achievements and novel outcomes.

12.2. Technical achievements

A novel bioassay was developed to assess the performance of test surfaces with ectocarpoid algae.

A novel bioassay was developed to assess the performance of non-biocidal FR surfaces on the adhesion of ectocarpoid algae (Chapter 3; Appendix 14). Prior to this work were no published examples in the literature reporting the use of a quantitative adhesion assay for these algae. Hall and Baker (1985) studied the colonisation and growth of *Ectocarpus siliculosus* on copper-nickel plates incubating in cultures of the alga. It was observed that colonisation proceeded from spores rather than mature plants. No attempt was made to characterise the adhesion strength of attached algae. While at the start of this project the

possibility of developing an adhesion assay using spores as the initial source of inoculum was considered, it was soon realised that this was an impractical route because of the quantity of spores that would be required. Previous studies on spore behaviour of ectocarpoid algae were able to obtain spore concentrations of approx. 6×10^4 per ml (Iken et al. 2001; Greer and Amsler 2002; Greer and Amsler 2004). A simple calculation shows that this is too low to form the basis of a quantitative adhesion bioassay. For example, the routine quantitative bioassay used extensively in Birmingham to assess the adhesion strength of the green macroalga *U. linza* in relation to coating/surface properties, is based on the colonisation of coatings deposited on glass microscope slides, by motile spores synchronously released from fertile fronds of the alga collected from the field; approximately a litre of spores at a concentration of 1×10^6 per ml is required to assess the performance of 8-10 test surfaces (with 9 replicates). While it may have been theoretically possible to develop an alternative assay format for use with smaller volumes and concentrations of ectocarpoid spores, such as a multiwell plate format, the deposition of coatings in multiwell plates was not considered to be appropriate by International Paint. In addition, measurement of adhesion strength in the calibrated water channel would not have been possible with a multiwell plate format. In view of these considerations, the starting point of the new bioassay using ectocarpoid algae was based on the colonisation of surfaces by small fragments of vegetative filaments, obtained by blending the cultured algae. The multicellular filaments attached to the surfaces by producing prostrate filaments and the adhesion strength of the biomass attached after 14 days' growth was then assessed by applying a hydrodynamic shear stress.

This new bioassay fulfilled all the requirements for a good laboratory bioassay as the cultures used provided a sufficient amount of starting inoculum (filaments) to test several surfaces in one experiment using nine replicates. It uses cultured ectocarpoid algae, which are good models for bioassays as they have a small size and a rapid growth, they are easy to culture

and at relatively low cost. Chapter 3 and the following Chapters showed that the results obtained with this bioassay were consistent and reproducible. In addition, the protocol is easy to perform and to repeat under the same conditions (temperature, medium, species). This bioassay was also validated as it was not only possible to measure the adhesion strength of cultivated species but also the adhesion strength of wild, uncultivated mixture of ectocarpoid algae and the results observed using the wild mixture were similar to those obtained with both cultivated *Ectocarpus* spp. tested (Chapter 3). The development of the assay and its use to test standard surfaces is described in the published paper Evariste et al. (2012). Apart from the protocol developed for *U. linza*, it is the only other published protocol to assess the performance of FR surfaces against macroalgae.

Generalized linear modelling (GZLM) with pairwise comparisons was used to assess coating performance (i.e. biomass before exposure to shear stress and % removal) as it gives flexibility over a classical ANOVA to account for a non-normal distribution of the response variable. In addition to the GZLM test, repeated-measures analysis of variance (RM ANOVA) was used to assess combined performance of the test surfaces using together the amount of attached biomass before and that was remaining after the exposure to shear stress.

Field isolates of ectocarpoid algae were brought into uni-algal culture on a large scale

In addition to the three cultured species of *Ectocarpus* acquired from SAMS, it was considered important to compare the adhesion properties of these cultivated species with fresh isolates of ectocarpoid algae made from the field. Therefore, a number of samples of ectocarpoid algae were collected from FR coatings on raft panels at International Paint's laboratory in Newton Ferrers and from boats moored in Hartlepool Marina. The samples were brought into uni-algal culture and the various genera and/or species were identified

using standard morphological criteria. From this bank of isolates, two isolates, one *Ectocarpus* sp*.* and one *Hincksia* sp*.,* were selected for large-scale culture to provide sufficient biomass for comparative adhesion assays on standard surfaces and to compare two genera of ectocarpoid algae.

Experimental coatings with systematic differences in surface or bulk properties were produced and characterised

1. The range of surfaces tested in consideration of the effects of surface/bulk properties wettability and modulus on fouling settlement and adhesion was expanded beyond published studies and standard test materials.

To test systematically the effects of surface wettability, a series of silicone 'hybrid' coatings was produced, based on formulations proposed by International Paint, with different blended ratios of PDMS polymer and PDMS-PEO copolymer (Chapter 4.3.2). The combination of the hydrophobic and hydrophilic components creates the property of amphiphilicity, which is a feature of both the commercial Intersleek 900, and a number of recent experimental coating designs (Finnie and Williams 2010). This well-characterised series of coatings provided a good test to determine the influence of wettability on the adhesion of organisms since modulus was constant across the range (i.e. approx. 1 MPa) and all surfaces had Ra roughness values in the sub-micron range (<0.3 µm; Table 4.9). It was the first series of silicone-based amphiphilic coatings with such a range of wettability to be documented and tested against fouling organisms.

To test the effects of modulus, a systematic series of five silicone-based coatings was produced from different molecular weights of PDMS, to give a range of elastic modulus from 0.73 to 1.5 MPa (Chapter 4). However, the range obtained was smaller than that anticipated from the wide spread in viscosity/molecular weight of PDMS used. Being silicone-based, all the test coatings were hydrophobic, with similar water contact angles, ca. 100° and similar

surface energies (~23 mN m^{-1}). This series of coatings was innovative as only a few papers relate the production of a systematic series of FR coatings with varying modulus and similar wettability and chemistry (Chaudhury et al. 2005; Kaffashi et al. 2012).

2. **Different analytical techniques were used to measure the surface properties to obtain information on the surface heterogeneity of these coatings**

In general, to study the surface properties, the wettability/surface energy is measured with either static contact angle in air or dynamic contact angle. However, for the silicone 'hybrid' coatings, in addition to these two methods, underwater contact angles were measured before and after 1-month leaching in deionised water and after immersion in ASW and natural seawater during 10 days. Although previous studies have observed the underwater contact angles of coatings after immersion in deionised water or ASW (Hu and Tsai 1996; Magin et al. 2011; Sundaram et al. 2011; Martinelli et al. 2012a), the work described in this thesis is the first to compare the wettability changes of surfaces immersed in sterile ASW and natural seawater for a period of 10 days and to correlate these changes to the colonisation of fouling organisms.

The comparative performance of experimental coatings was tested in both laboratory and field assays

An innovative part of this project was that it brought the opportunity to assess the performance of most of the test surfaces in the laboratory and in the field. Only a few previous studies have reported both types of assays (e.g. Rittschof and Costlow 1989; Huggett et al. 2009; Martinelli et al. 2012b). By investigating both types of assay, further information on the performance of the surfaces was obtained as laboratory assays assess the performance of test surfaces against a single species under controlled and defined conditions, while field assays, by exposing the surfaces to a marine community reveal long-term performance of these surfaces in the natural environment.

12.3. Novel outcomes of the research

The novel adhesion assay was used to characterise the adhesion preferences of ectocarpoid algae

1. Two different morphotypes of ectocarpoid algae with different adhesion properties were observed

During this study, two morphological variants ("morphotypes") of ectocarpoid algae were observed. The first morphotype, termed 'normal' has both prostrate and erect filaments in equal quantity, whilst the second 'star' morphotype had more erect filaments than prostrate filaments. While both morphotypes were observed on test coatings before exposure to shear stress, only the normal morphotype (but in lower quantity than before the exposure to a shear stress) was generally present on the surfaces after exposure to shear stress. It is assumed that due to the lower amount of prostrate filaments, which are the structures of the organism that adhere to the surfaces, the star morphotype had lower adhesion strength than the normal one.

2. Not all ectocarpoid algae show the same adhesion preferences

While both cultivated *E. crouaniorum* and *Ectocarpus* sp. showed similar adhesion strength preferences on standard surfaces (i.e. low adhesion to Nexterion glass and IS900 and high/medium adhesion to IS700 and T2), the adhesion strength of *Hincksia secunda* on the same surfaces was different (i.e. low adhesion to IS700, IS900 and T2 and high adhesion to Nexterion glass; Chapter 3). It is thus possible to conclude that the adhesion preferences of one species do not represent the preferences of the whole Ectocarpaceae.

However, the experiment with the mixed, uncultivated mixture of ectocarpoid algae, which may more accurately reflect the fouling potential of ectocarpoid algae in the wild, showed similar results to those of the cultured *Ectocarpus*. These results suggest that the adhesion preferences obtained from the bioassay based on cultured *Ectocarpus* are broadly representative of the population of wild ectocarpoid algae if *Ectocarpus* is the dominant genus.

3. Not all macroalgae show the same adhesion preferences

The adhesion of filaments of *E. crouaniorum* and sporelings of *U. linza* was tested on silicone 'hybrid' coatings with a range of wettability (Chapter 6) and on the silicone 'modulus' series with a range of modulus (Chapter 8). For both sets of coatings the trends in adhesion strength in relation to coating properties was different. For the silicone 'hybrid' coatings, the results with *U. linza* were similar to other studies made with other (non-silicone) sets of coatings (Akesso et al. 2009a and 2009b; Bennett et al. 2010); the sporelings of *U. linza* adhered more strongly to hydrophilic than hydrophobic coatings, except for the most hydrophilic coating H10 composed of only PDMS-PEO copolymer. However, the results obtained with *E. crouaniorum* were different; no linear correlation, but a more complex relationship was observed between total surface energy and adhesion strength of *E. crouaniorum*. Low adhesion strength was observed for the filaments attached on the two most hydrophilic coatings with a total surface energy between 35.7 and 40.6 mN m^{-1} (i.e. H7 (30% PDMS-70% PDMS-PEO) and H10 (100% PDMS-PEO)) and also the most hydrophobic coating H with a total surface energy of 23.3 mN m^{-1}.

For the silicone 'modulus' series, *U. linza* followed the models of fracture mechanics as applied to soft-fouling organisms (Chaudhury et al. 2005), showing that the adhesion strength of sporelings was positively influenced by the modulus in the range 0.73-1.5 MPa,

as the higher the modulus was, the higher the adhesion strength was. However, the adhesion strength of *E. crouaniorum* was negatively correlated to the modulus, so weaker adhesion on the higher modulus was found, however, the effect was relatively small (13 % difference). As no known theory of fracture mechanics can explain these results, alternative explanations are required. One possibility is that the PDMS chain length could influence the degree of penetration of the adhesive of *E. crouaniorum*, so higher penetration into the high molecular weight, lower modulus coatings might be the basis of the slightly stronger adhesion to coatings of low modulus.

4. ***E. crouaniorum* and *U. linza* adhere strongly to coatings with a net positive surface charge**

Chapter 7 described the experiments assessing the performance of two sets of xerogel coatings on the adhesion strength of *E. crouaniorum.* SET 1, which was a similar set to those tested in Bennett et al. (2010; Finlay et al. 2010), had a range of wettability from 49° to 107.9°. Despite having similar surface properties to the silicone 'hybrid' coatings (Chapter 6), the results of the adhesion strength of *E. crouaniorum* were different, even though they both showed an influence of wettability on adhesion strength. The results of SET 1 of the xerogel coatings indicated that the adhesion strength might be a consequence of charge rather than surface energy/polarity per se for these coatings. The results obtained by testing SET 2, which was composed of coatings either positively charged or uncharged confirmed these observations showing a stronger adhesion of *E. crouaniorum* on the positively charged coatings. The adhesion strength of sporelings of *U. linza* was similar to those of *E. crouaniorum* with a stronger adhesion on positively charged xerogel coatings. These relationships have not been previously documented. These results could be explained by the presence of anionic polysaccharides in the cell walls of the algae, which might contribute to strong, non-specific, electrostatic adhesion to positively charged surfaces. The results also

showed that to produce effective FR coatings against soft-fouling organisms, only uncharged xerogel coatings should be considered.

Colonisation of fouling organisms is influenced by surface and bulk properties in the field

1. Colonisation of fouling organisms is complex and unpredictable

Field assays were performed every year during this study in order to assess the performance of the test coatings in the real world. Compared to the laboratory assays where environmental and biological factors are controlled, the field assays exposed the coatings to an uncontrolled environment with dynamic fouling community and environmental factors that change continually (temperature, salinity, light). Although the field assays described in Chapters 10/11 were performed in the same location in Hartlepool Marina and in similar period of the year (end of spring-summer), the colonisation of IS900 and the tie coat was different in the two years. While in 2011 (Chapter 10) IS900 had from 43 days' immersion between 5-10 % of weeds on its surfaces, in 2012 (Chapter 11) no algae were observed during the whole experiment. For the tie coat, Chapter 10 showed that from 37 days, the surfaces were mostly covered by algae (close to 100%), while in 2011 no more than 40-60% of weed coverage was observed. In addition, in 2011 the hard-bodied animals were essentially composed of barnacles (Chapter 10), while in 2012 tubeworms (from the genus S*pirorbis*) were the dominant type of hard-bodied animals (Chapter 11). It could also be observed that variation of colonisation of fouling was observed during the same year, as significant differences were observed between the panels (Chapters 10/11). These results showed that although the observation of the colonisation of surfaces by fouling organisms in the real environment is essential to assess the performance of test surfaces, it is a complex experiment, in which most of the parameters cannot be controlled or even measured.

2. Colonisation was influenced by the surface properties of the coatings.

As there were differences in percentage cover between the test coatings in the silicone 'hybrid' series, it is possible to conclude that the colonisation of fouling organisms was influenced by the surface properties of these coatings. Relationships were observed between % coverage of all fouling categories and the measured surface properties (initial static contact angle, contact angle hysteresis and underwater contact angle after 1 day's immersion in Hartlepool Marina). Negative correlations were observed between the contact angle hysteresis and the coverage of weeds, ectocarpoid algae and hard-bodied animals. Both positive and negative correlations were observed between the % cover of microfouling and the contact angle hysteresis and the underwater contact angle after one day's immersion, respectively. In addition, positive correlations were observed between initial contact angle in air and % cover of hard-bodied animals, total fouling and soft-bodied animals. However, for the two last fouling categories, the correlations were only observed by excluding H10, the most hydrophilic coating composed of only PDMS-PEO copolymer, as it did not follow the trend observed with the other coatings. These different relationships between the measured surface properties and the % coverage of the different categories showed that the wettability of pristine and immersed surfaces influenced the colonisation of fouling organisms, and furthermore, colonisation is more complex than a simple relationship with one surface property as the fouling categories do not depend on only one measured surface property.

3. The modulus of silicone-based coatings influenced the colonisation of microfouling

No previous studies have documented a field assay testing a systematic series of coatings with varying modulus. Chapter 11 showed that no significant differences were observed between the test coatings except for M1 the hardest coatings that had higher total and

microfouling % cover. These results showed that when the coatings had higher elastic modulus (>1 MPa), a higher colonisation of microfouling and total fouling was observed. However, no effect of the modulus and the associated parameters (viscosity and estimated molecular weight) was observed on the colonisation of the weeds, ectocarpoid algae and animal fouling.

An optimal surface energy for reduced adhesion and surface colonisation was detected for the silicone 'hybrid' coatings

For the silicone 'hybrid' coatings, analysing the results obtained in the laboratory for the two test algae and in the field for all the fouling categories (except microfouling coverage), it is possible to conclude that the coating H7 composed of 70 % PDMS-PEO and 30 % PDMS, with a surface energy of 35.7 mN m^{-1}, had optimal properties to decrease the adhesion strength of both macroalgae and the lowest colonisation of fouling organisms in general. Therefore, it is possible to conclude that laboratory assays partly presented in Chapter 10 predicted the results obtained with the field assay, as H7 was the most effective coating for both types of experiments.

Exploration of the surface wettability of the silicone 'hybrid' series of coatings.

1. The test coatings showed changing wettabilities under different immersion treatments

Silicone 'hybrid' coatings were amphiphilic (except H) and this type of coating is known to have heterogeneous surfaces at a micro- or nano-scale. Therefore, to investigate the surface heterogeneity of these experimental coatings, several analytical techniques were used: static

contact angle in air (before and after 1-month leaching in deionised water), dynamic contact angle, underwater contact angle (before and after 1-month leaching in deionised water) and underwater contact angle of surfaces immersed in ASW and natural seawater. The results obtained with these different methods confirmed that the surfaces were not inert; a possible examination is there was a reorganisation of PEO and PDMS chains, bringing more PEO to the surface, making the surfaces more hydrophilic. However, the coating H, which contained only PDMS polymer, also showed changes in wettability; these changes could be due to surface conditioning and/or to the presence of the curing agent on the surface of the test coating.

For example, the contact angle hysteresis (obtained from the dynamic contact angle measurements) progressively increased as the proportion of PEO in the coatings increased as previously observed by Cho et al. (2012), who studied different amphiphilic coatings made of PEG and mixed hydrocarbon. Additional information on the surface properties was obtained by following the changes of wettability of surfaces immersed in deionised water and in seawater (i.e. sterile ASW and natural seawater). The surfaces were more hydrophilic after 1-month leaching (except H, the most hydrophobic coating containing no PEO, underwater contact angle method) and after one day's immersion in seawater, suggesting again a surface reorganisation and possibly the effect of a conditioning film.

2. **The underwater contact angle method and static contact angle method in air gave different values for wettability**

The wettability values of the silicone 'hybrid' coatings obtained for the dry and freshly immersed (in distilled water) surfaces showed either that the two methods measure slightly different aspects of surface wettability, or that in the few minutes of immersion needed to measure the underwater contact angle, a surface change happened (such as a surface reorganisation), as the range of wettability was narrower with the underwater contact angle method.

3. **Differences were observed between underwater contact angles of surfaces immersed in ASW and natural seawater**

Wettability of test surfaces was lower for surfaces immersed in Hartlepool Marina than in sterile ASW after 10 days' immersion. The differences observed between these treatments could be due to various factors. It is possible that the presence of a biofilm (i.e. bacteria and diatoms) and associated fouling in the natural seawater would make the surface less hydrophilic. Previous papers measured the wettability of a biofilm, and even if the data obtained were in contradiction for *Cobetia marina*, it was observed that each bacterial biofilm has a different wettability. Akesso et al. (2009b) showed that *Cobetia marina* attached to a membrane filter were hydrophilic (i.e. <15°) while *Marinobacter hydrocarbonoclasticus* were hydrophobic (i.e. 81.5°), using static contact angle in air on a dry bacterial lawn. However, Mitik-Dineva et al. (2009) showed that *C. marina* had a wettability of 75° on glass surfaces (for a dry bacterial lawn). Mitik-Dineva et al. (2009) also showed that other species of bacteria could be either hydrophilic or hydrophobic. However, in the field, the biofilm is composed of a mixture of bacteria and diatoms. The diversity of the biofilm attached to the surfaces had not been identified and so it is not possible to determine its contribution on the changes of surface wettability.

In addition, conditioning films change the wettability of immersed surfaces (Thome et al. 2012) and as the macromolecules present in natural seawater and ASW should be different, it is possible that the conditioning film of the surfaces immersed in sterile ASW and natural seawater would also be different. For example, a large amount of hydrocarbon, which was observed on the surface of the seawater in Hartlepool Marina, could influence the wettability of the surfaces. It is likely that the wettability changes on immersed surfaces are due to contributions from more than one of these effects. Such observations have never been

reported previously and bring further information for the evolution of wettability of the coatings after immersion in seawater.

General conclusions on the colonisation, attachment and adhesion strength of ectocarpoid algae

During this project, the performance of different sets of coatings was assessed against two algae and the natural environment. The results showed that ectocarpoid algae have different adhesion preferences to *U. linza*, the 'model' species used extensively as a reference for soft-fouling organisms in laboratory assays. Therefore, it is possible to conclude that several species of macroalgae should be used to assess the performance of AF/FR coatings on soft-fouling organisms to down-select the best coatings that had the low adhesion strength for these different species.

This study showed that the attachment and adhesion strength of *E. crouaniorum* were influenced by different bulk and surface properties such as chemistry, wettability, charge and modulus. With the two series of coatings varying in wettability (silicone 'hybrid' coatings and SET 1 xerogels), it was observed that the behaviour of *E. crouaniorum* was different; it could be due to the chemistry, the surface charge or other unmeasured parameters. In addition, uncharged xerogel coatings were more effective than positively charged xerogel coatings to decrease the adhesion strength of *E. crouaniorum* and *U. linza*. Moreover, although the adhesion strength of *U. linza* showed a positive correlation with the elastic modulus, an opposite correlation was observed with *E. crouaniorum* (Chapter 8).

In addition, all the test coatings (except xerogel coatings) were tested in field and showed different results to those in laboratory. However, the field results confirmed that H7 had an optimal composition to have lower colonisation of ectocarpoid algae and other fouling

organisms, correlations were observed between the % cover of fouling categories and the measured surface properties, showing that colonisation was complex.

12.4. Potential areas for future work

In Chapter 3, the adhesion of several ectocarpoid algae was tested on standard surfaces showing differences between the genera. It would be interesting to observe if it would also be the case for the other sets of test coatings.

Would the relationship between the adhesion of other fouling organisms and the experimental surfaces tested during this project be similar to those obtained for ectocarpoid algae and *U. linza*? During this project, the performance of test surfaces was assessed in the laboratory against ectocarpoid algae and *U. linza* showing different relationships between the adhesion strength of the organisms and the surface and bulk properties. However, the fouling community is not only composed of these organisms; there are many others such as diatoms, bacteria and barnacles. Therefore, it is of importance to test more fouling organisms. It would specially be interesting to observe if other fouling organisms would also have low adhesion strength on H7, one of the most hydrophilic coatings from the silicone 'hybrid' series (Chapter 6), which showed low adhesion strength of both *E. crouaniorum* and *U. linza*, which generally has different adhesion preferences. The results obtained during the field assay would suggest that would be the case as H7 was the most effective coating for all fouling categories (except for microfouling, Chapter 10).

Field experiments were performed during this study, and improvements were done in the design and analyses after the first field assay, but further improvements could have been done to obtain further information on the performance of the test coatings. Due to logistic reasons, only one field site was used from 2011 to assess the performance of the test surfaces, but it would have been interesting to assess the performance of the coatings at other field sites (in England or in other part of the world); the performance of the coatings

might have been different as the biological and environmental factors would be different. In addition, the test coatings were produced as FR coatings but the field assay tested only their performance against colonisation and not their FR performance, as the coatings were not exposed to a shear stress during the field assay. **If the coatings were exposed to a shear stress using for example a water jet, would the results have been similar to those obtained in Chapters 10-11?** The performance of the coatings could have been observed in longer field assays, such as one or two years and so further information on their performance would have been observed. **Would ectocarpoid algae reappear during the year?** It could be possible as during the winter the amount of fouling biomass of the surfaces is in general lower.

It was observed during the experiments that microfouling colonised within a month the test surfaces. However, the biofilm formed by the microfouling had different thickness between the surfaces, which was not taken into account with the 'Phoenix' in-house Experimental Fouling Assessment Record Sheet. Dobretsov and Thomason (2011) showed that the thickness as well as the percentage cover and the diversity of a biofilm present on the surfaces provide further information on the performance of the test surfaces. It would be interesting to measure the biofilm thickness and try to correlate these data with the surface properties.

The results obtained for the adhesion strength of *E. crouaniorum* on the silicone 'hybrid' coatings were not fully explained by the surface properties measured (static contact angle, underwater contact angle and contact angle hysteresis). As it was suggested in the Discussion of Chapter 6, it would be interesting to do further measurements using AFM and XPS to obtain more information on the topography, the composition and the reorganisation of the surfaces (with measurements before and after immersion in ASW). In addition, for the silicone 'hybrid' coatings, more information would have been obtained on the surface properties of immersed coatings if the surface energy could have been measured using

underwater contact angle method. However, this would have required the use of a second liquid. Octane, the second liquid previously used in literature (e.g. Hu and Tsai 1996; Magin et al. 2011) could not be used as it penetrates and swells silicone-based coatings. Although some experiments were done in this project to find a liquid that would replace octane, the results were inconclusive; therefore, it would be interesting to continue the search.

To explore the influence of modulus on the adhesion of marine species, especially ectocarpoid algae, a systematic series of coatings with a bigger range of modulus than that studied in Chapter 8, such as the systematic series of PDMS coatings, described by Kaffashi et al. (2012) with varying elastic modulus from 0.47 to 25.72 MPa, would bring further information on these relationships. In addition, to obtain further information on the relationship between adhesion of ectocarpoid algae and modulus, it would be interesting to assess the performance of a series of hydrophilic coatings with varying modulus, as the silicone modulus coatings were all hydrophobic.

In Chapter 7, it was observed that the filaments of *E. crouaniorum* and sporelings of *U. linza* had lower adhesion strength on hydrophilic xerogel coatings with neutral side chains than on positively charged hydrophilic coatings. **What would be the adhesion strength of both algae on negatively charged coatings?** It could also be interesting to investigate if these adhesion preferences would also be visible on hydrophobic coatings and on silicone or fluoropolymer coatings. In addition, these coatings have been only tested in the laboratory. **Would the results be similar if the coatings were tested in the field?**

Is the adhesion strength of ectocarpoid algae influenced by the thickness of the coatings? Chaudhury et al. (2005) showed that the thickness of the PDMS coatings positively influenced the adhesion strength of sporelings of *U. linza* when the coating film was lower than 100 μm of thickness. However, the adhesion behaviour of ectocarpoid algae

and *U. linza* was in general completely different; it is therefore possible that the coating thickness would not have the same effect on the adhesion of ectocarpoid algae.

APPENDIX 1: RECIPE OF ½-STRENGTH PROVASOLI MEDIUM

Recipe from CCAP (www.ccap.ac.uk)

Stocks	**per litre**
(1) PII trace metals	
Na_2 EDTA	1.0 g
H_3BO_3	1.12 g
$MnSO_4.H_2O$	0.12 g
$ZnSO_4.7H_2O$	0.022 g
$CoSO_4.7H_2O$	0.005 g
(2) IronEDTA	
$Fe(NH_4)_2(SO_4)_2.6H_2O$	0.7 g
Na_2 EDTA	0.6 g

Medium	**Stock**	**per litre medium**
Na_2 ßglycero $PO_4.5H_2O$	50 g l^{-1}	8.0 ml
$NaNO_3$	35 g l^{-1}	110 ml
IronEDTA (2)		100 ml
Vitamin B12	0.01 g l^{-1}	8.75 ml
Thiamine	0.5 g l^{-1}	8.0 ml
Biotin	0.005 g l^{-1}	8.0 ml
PII trace metals (1)		200 ml

To prepare final medium, dispense the above into 10 ml aliquots and sterilise by autoclaving. Finally, to use add 10 ml per litre to sterile 30 ppt filtered seawater (pH=8.1).

APPENDIX 2: ULVA CULTURE MEDIUM

Provasoli's ES enriched seawater from Starr and Zeikus (1987)

1. Add 5 g Tris buffer (tris(hydroxymethyl)aminomethane)
2. Add 3.5 g Sodium nitrate ($NaNO_3$)
3. Add 500 mg β-glycerolphosphate disodium salt pentahydrate ($C_3H_7Na_2O_6P.5H_2O$)
4. Add 250 ml of PII metals[1]
5. Add 250 ml of Fe stock[2]
6. Make up to 1 L with distilled water, pH to 7.8 using hydrochloric acid.
7. Autoclave
8. Add 1 ml of biotin, thiamine and cyanocobalamin solution[3]
9. Make to 2% solution in seawater (20 ml stock per liter of seawater)
10. If above pH 8.2, add concentrate HCl (1-2 drops at a time), if below add NaOH (several drops).

[1]**PII metals**

500 ml distilled water

500 mg Na_2EDTA (ethylenediaminetetraacetic acid disodium salt dehydrate)

570 mg Boric acid (H_3BO_3)

24.5 mg Iron (III) chloride hexahydrate ($FeCl_3.6H_2O$)

82 mg Manganese (II) sulphate monohydrate ($MnSO_4.H_2O$)

11.2 mg Zinc sulphate heptahydrate ($ZnSO_4.7H_2O$)

2.4 mg Cobalt (II) sulphate heptahydrate ($CoSO_3.7H_2O$)

[2]**Fe stock**

500 ml distilled water

351 mg Ammonium iron (II) sulphate hexahydrate ($Fe(NH_4)_2(SO_4)_2.6H_2O$)

300 mg Na_2EDTA (ethylenediaminetetraacetic acid disodium salt dehydrate)

[3]**Biotin, Thiamine and Cyanocobalamin solution**

100 ml distilled water

5 mg Biotin (vitamin B_7)

500 mg Thiamine hydrochloride (vitamin B_1)

10 mg Cyanocobalamin (vitamin B_{12})

APPENDIX 3: STATISTICAL TABLES FOR CHAPTER 3

- *Ectocarpus crouaniorum*

RM ANOVA

Source	SS	df	MS	F	p-values
Intercept	4,23E+08	1	4,23E+08	697,3	2.5E-22
Coatings	2,07E+08	3	6,91E+07	113,9	1.7E-16
Error	1,82E+07	32	6,07E+05		

Appendix 3.1: RM ANOVA table.

Pairwise comparisons after GZLM

(I) Coatings	(J) Coatings	Before exposure to shear stress			After exposure to shear stress		
		Mean Difference (I-J)	df	p-values	Mean Difference (I-J)	df	p-values
IS700	IS900	468.5	1	0.145	-34.8	1	8.9E-06
	Nexterion	2229.2	1	1.7E-17	-13.5	1	0.064
	T2	-3114.6	1	6.4E-09	18.5	1	0.035
IS900	IS700	-468.5	1	0.145	34.8	1	8.9E-06
	Nexterion	1760.7	1	6.5E-14	21.3	1	0.01
	T2	-3583.0	1	8.9E-12	53.3	1	4.7E-11
Nexterion	IS700	-2229.2	1	1.7E-17	13.5	1	0.064
	IS900	-1760.7	1	6.5E-14	-21.3	1	0.01
	T2	-5343.8	1	0.0E+00	32	1	1.6E-04
T2	IS700	3114.6	1	6.4E-09	-18.5	1	0.035
	IS900	3583.0	1	8.9E-12	-53.3	1	4.7E-11
	Nexterion	5343.8	1	0.0E+00	-32	1	1.6E-04

Appendix 3.2: Table of the Pairwise comparison data obtained after GZLM analysis, before and after exposure to shear stress. Before and after exposure, the probability distribution was tweddie and normal, respectively and the link function was identity for both. The Grey cells represent the significant comparisons.

- *Ectocarpus sp.*

RM ANOVA

Source	SS	df	MS	F	p-values
Intercept	1.94E+09	1	1.94E+09	726.15	1.4E-23
Coatings	7.61E+08	3	2.54E+08	95.22	4.9E-16
Error	8.53E+07	32	2.67E+06		

Appendix 3.3: RM ANOVA table.

Pairwise comparisons after GZLM

(I) Coatings	(J) Coatings	Before exposure to shear stress			After exposure to shear stress		
		Mean Difference (I-J)	df	p-values	Mean Difference (I-J)	df	p-values
IS700	IS900	1743.1	1	0.052	-27.1	1	0.006
	Nexterion	13681.3	1	0	8.6	1	0.344
	T2	9183.8	1	0	44.2	1	5.7E-06
IS900	IS700	-1743.1	1	0.052	27.1	1	0.006
	Nexterion	11938.2	1	0	35.7	1	3.4E-04
	T2	7440.8	1	0	71.3	1	2.5E-14
Nexterion	IS700	-13681.3	1	0	-8.6	1	0.344
	IS900	-11938.2	1	0	-35.7	1	3.5E-04
	T2	-4497.5	1	1.52E-08	35.6	1	3.4E-04
T2	IS700	-9183.8	1	0	-44.2	1	5.7E-06
	IS900	-7440.8	1	0	-71.3	1	2.5E-14
	Nexterion	4497.5	1	1.52E-08	-35.6	1	3.4E-04

Appendix 3.4: Table of the Pairwise comparison data obtained after GZLM analysis, before and after exposure to shear stress. Before and after exposure, the probability distribution was normal and the link function was identity. The Grey cells represent the significant comparisons.

- *Hincksia secunda*

RM ANOVA

Source	SS	df	MS	F	p-values
Intercept	7.84E+08	1	7.84E+08	539.7	1.3E-21
Coatings	4.61E+07	3	1.54E+07	10.6	5.5E-05
Error	4.65E+07	32	1.45E+06		

Appendix 3.5: RM ANOVA table.

Pairwise comparisons after GZLM

(I) Coatings	(J) Coatings	Before exposure to shear stress			After exposure to shear stress		
		Mean Difference (I-J)	df	p-values	Mean Difference (I-J)	df	p-values
IS700	IS900	3312.7	1	1.43E-09	-5.7	1	0.679
	Nexterion	3554.6	1	8.48E-11	71.8	1	1.58E-12
	T2	3751.2	1	7.37E-12	24.4	1	0.087
IS900	IS700	-3312.7	1	1.43E-09	5.7	1	0.679
	Nexterion	241.9	1	1.000	77.5	1	3.18E-13
	T2	438.5	1	1.000	30.1	1	0.047
Nexterion	IS700	-3554.6	1	8.48E-11	-71.8	1	1.58E-12
	IS900	-241.9	1	1.000	-77.5	1	3.18E-13
	T2	196.6	1	1.000	-47.4	1	6.72E-09
T2	IS700	-3751.2	1	7.37E-12	-24.4	1	0.087
	IS900	-438.5	1	1.000	-30.1	1	0.047
	Nexterion	-196.6	1	1.000	47.4	1	6.72E-09

Appendix 3.6: Table of the Pairwise comparison data obtained after GZLM analysis, before and after exposure to shear stress. Before and after exposure, the probability distribution was normal and tweedie, respectively and the link function was identity and log, respectively. The Grey cells represent the significant comparisons.

- Mixture of uncultivated 'wild' ectocarpoid algae

RM ANOVA

Source	SS	df	MS	F	p-values
Intercept	1.07E+09	1	1.07E+09	286.1	1.6E-17
coating	1.77E+08	3	5.89E+07	15.7	1.9E-06
Error	1.20E+08	32	3.75E+06		

Appendix 3.7: RM ANOVA table.

Pairwise comparisons after GZLM

		Before exposure to shear stress			After exposure to shear stress		
(I) coatings	(J) coatings	Mean Difference (I-J)	df	p-values	Mean Difference (I-J)	df	p-values
IS900	IS700	1734.2	1	0.071	22.79	1	0.157
	Nexterion	5630.0	1	5.3E-11	16.06	1	0.321
	T2	4857.2	1	2E-08	37.41	1	0.002
IS700	IS900	-1734.2	1	0.071	-22.79	1	0.157
	Nexterion	3895.8	1	9.3E-06	-6.74	1	0.500
	T2	3123.1	1	4.6E-04	14.62	1	0.271
Nexterion	IS900	-5630.0	1	5.3E-11	-16.06	1	0.321
	IS700	-3895.8	1	9.3E-06	6.74	1	0.500
	T2	-772.7	1	0.349	21.35	1	0.096
T2	IS900	-4857.2	1	2E-08	-37.41	1	0.002
	IS700	-3123.1	1	4.6E-04	-14.62	1	0.271
	Nexterion	772.7	1	0.349	-21.35	1	0.096

Appendix 3.8: Table of the Pairwise comparison data obtained after GZLM analysis, before and after exposure to shear stress. Before and after exposure, the probability distribution was normal and tweedie, respectively and the link function was identity and log, respectively. The Grey cells represent the significant comparisons.

- *Ulva linza*

Pairwise comparisons after GZLM

(I) Coatings	(J) Coatings	Before exposure to shear stress			After exposure to shear stress		
		Mean Difference (I-J)	df	p-values	Mean Difference (I-J)	df	p-values
IS700	IS900	-348.8	1	0.712	-32.6	1	1.23E-09
	Nexterion	8818.9	1	0	39.0	1	2.83E-13
	T2	7821.4	1	0	21.9	1	5.46E-05
IS900	IS700	348.8	1	0.712	32.6	1	1.23E-09
	Nexterion	9167.7	1	0	71.6	1	0
	T2	8170.3	1	0	54.4	1	0
Nexterion	IS700	-8818.9	1	0	-39.0	1	2.83E-13
	IS900	-9167.7	1	0	-71.6	1	0
	T2	-997.5	1	0.013	-17.1	1	0.001
T2	IS700	-7821.4	1	0	-21.9	1	5.46E-05
	IS900	-8170.3	1	0	-54.4	1	0
	Nexterion	997.5	1	0.013	17.1	1	0.001

Appendix 3.9: Table for the Pairwise comparison data obtained after GZLM analysis, before and after exposure to shear stress. Before and after exposure, the probability distribution was tweedie and normal, respectively and the link function was identity, respectively. The Grey cells represent the significant comparisons.

APPENDIX 4: STATISTICAL TABLES FOR CHAPTER 5

- Fluropolymer coatings
  - *E. crouaniorum*

RM ANOVA

Source	SS	df	MS	F	p-values
Intercept	1.05E+09	1	1.05E+09	618.1	6.1E-26
Coatings	3.54E+08	4	8.86E+07	52.0	2.6E-15
Error	6.82E+07	40	1.71E+06		

Appendix 4.1: RM ANOVA table.

		Before exposure to shear stress			After exposure to shear stress		
(I) Coatings	(J) Coatings	Mean Difference (I-J)	df	p-values	Mean Difference (I-J)	df	p-values
IS700	IS900	2285.6	1	0.004	-51.3	1	5.9E-12
	mD10-H	3747.0	1	1E-07	-.5	1	0.943
	mD1O	5441.8	1	9.8E-18	-25.3	1	0.002
	mE10-H	6328.7	1	0	-31.4	1	8.4E-05
IS900	IS700	-2285.6	1	0.004	51.3	1	5.9E-12
	mD10-H	1461.4	1	0.010	50.8	1	9E-12
	mD1O	3156.2	1	2.2E-09	26.0	1	0.002
	mE10-H	4043.1	1	1.5E-16	19.9	1	0.016
mD1O	IS700	-5441.8	1	9.8E-18	25.3	1	0.002
	IS900	-3156.2	1	2.2E-09	-26.0	1	0.002
	mD10-H	-1694.8	1	3.2E-04	24.8	1	0.002
	mE10-H	886.9	1	0.006	-6.1	1	0.789
mD10-H	IS700	-3747.0	1	1E-07	.5	1	0.943
	IS900	-1461.4	1	0.010	-50.8	1	9E-12
	mD1O	1694.8	1	3.2E-04	-24.8	1	0.002
	mE10-H	2581.7	1	5E-10	-30.9	1	1E-04
mE10-H	IS700	-6328.7	1	0	31.4	1	8.4E-05
	IS900	-4043.1	1	1.5E-16	-19.9	1	0.016
	mD10-H	-2581.7	1	5E-10	30.9	1	1E-04
	mD1O	-886.9	1	0.006	6.1	1	0.789

Appendix 4.2: Table of the Pairwise comparison data obtained after GZLM analysis, before and after exposure to shear stress. Before and after exposure, the probability distribution was tweedie and normal, respectively and the link function was identity. The Grey cells represent the significant comparisons.

➢ *U.linza*

(I) Coatings	(J) Coatings	Before exposure to shear stress			After exposure to shear stress		
		Mean Difference (I-J)	df	p-values	Mean Difference (I-J)	df	p-values
IS700	IS900	-912.0	1	0.618	-69.5	1	0
	mD1O	7114.5	1	0	16.9	1	2.7E-14
	mD1O-H	6659.0	1	0.000	17.4	1	7E-15
	mE1O-H	6101.3	1	5E-17	-75.6	1	0
IS900	IS700	912.0	1	0.618	69.5	1	0
	mD1O	8026.6	1	0	86.4	1	0
	mD1O-H	7571.0	1	0	86.9	1	0
	mE1O-H	7013.3	1	0	-6.1	1	0.010
mD1O	IS700	-7114.5	1	0	-16.9	1	2.7E-14
	IS900	-8026.6	1	0	-86.4	1	0
	mD1O-H	-455.5	1	0.867	.4	1	0.838
	mE1O-H	-1013.2	1	0.618	-92.5	1	0
mD1O-H	IS700	-6659.0	1	0	-17.4	1	7E-15
	IS900	-7571.0	1	0	-86.9	1	0
	mD1O	455.5	1	0.867	-.4	1	0.838
	mE1O-H	-557.7	1	0.867	-93.0	1	0
mE1O-H	IS700	-6101.3	1	5E-17	75.6	1	0
	IS900	-7013.3	1	0	6.1	1	0.010
	mD1O	1013.2	1	0.618	92.5	1	0
	mD1O-H	557.7	1	0.867	93.0	1	0

Appendix 4.3: Table of the Pairwise comparison data obtained after GZLM analysis, before and after exposure to shear stress. Before and after exposure, the probability distribution was normal and the link function was identity. The Grey cells represent the significant comparisons.

- Silicone coatings
  - *E. crouaniorum*

RM ANOVA

Source	SS	df	MS	F	p-values
Intercept	1.09E+09	1	1.09E+09	536.8	8.6E-25
Coatings	3.12E+08	4	7.81E+07	38.4	3.4E-13
Error	8.14E+07	40	2.03E+06		

Appendix 4.4: RM ANOVA table.

(I) Coatings	(J) Coatings	Before exposure to shear stress			After exposure to shear stress		
		Mean Difference (I-J)	df	p-values	Mean Difference (I-J)	df	p-values
S1	S3	1107.5	1	0.082	-17.9	1	0.004
	IS700	-4700.3	1	4E-17	27.6	1	3.5E-06
	IS900	-2414.7	1	5.1E-05	-23.7	1	8E-05
	S2	-247.3	1	0.648	33.6	1	8.8E-09
S2	S3	1354.8	1	0.037	-51.5	1	0
	IS700	-4453.0	1	1.8E-15	-6.0	1	0.556
	IS900	-2167.4	1	2.6E-04	-57.4	1	0
	S1	247.3	1	0.648	-33.6	1	8.8E-09
S3	IS700	-5807.8	1	0	45.5	1	2E-15
	IS900	-3522.2	1	5.8E-10	-5.8	1	0.556
	S1	-1107.5	1	0.082	17.9	1	0.004
	S2	-1354.8	1	0.037	51.5	1	0
IS700	HSE	5807.8	1	0	-45.5	1	2E-15
	IS900	2285.6	1	1.3E-04	-51.3	1	4.3E-19
	S1	4700.3	1	4E-17	-27.6	1	3.5E-06
	S2	4453.0	1	1.8E-15	6.0	1	0.556
IS900	S3	3522.2	1	5.8E-10	5.8	1	0.556
	IS700	-2285.6	1	1.3E-04	51.3	1	4.3E-19
	S1	2414.7	1	5.1E-05	23.7	1	8E-05
	S2	2167.4	1	2.6E-04	57.4	1	0

Appendix 4.5: Table of the Pairwise comparison data obtained after GZLM analysis, before and after exposure to shear stress. Before and after exposure, the probability distribution was normal and the link function was identity. The Grey cells represent the significant comparisons.

➢ *U. linza*

(I) Coatings	(J) Coatings	Before exposure to shear stress			After exposure to shear stress		
		Mean Difference (I-J)	df	p-values	Mean Difference (I-J)	df	p-values
S1	S3	-2277.4	1	7.8E-06	-8.0	1	0.253
	IS700	-7407.0	1	0	-77.5	1	1.7E-08
	IS900	-8319.1	1	0	5.1	1	0.253
	S2	459.2	1	0.509	1.4	1	0.662
S2	S3	-2736.6	1	3.1E-08	8.0	1	0.253
	IS700	-7866.3	1	0	-69.5	1	1.2E-06
	IS900	-8778.3	1	0	13.1	1	0.007
	S1	-459.2	1	0.509	9.4	1	0.153
S3	IS700	-5129.7	1	1.0E-13	77.5	1	1.7E-08
	IS900	-6041.7	1	0	69.5	1	1.2E-06
	S1	2277.4	1	7.8E-06	82.6	1	1.1E-09
	S2	2736.6	1	3.1E-08	78.9	1	8.5E-09
IS700	S3	5129.7	1	1.0E-13	-5.1	1	0.253
	IS900	-912.0	1	0.509	-13.1	1	0.007
	S1	7407.0	1	0	-82.6	1	1.1E-09
	S2	7866.3	1	0	-3.7	1	0.281
IS900	S3	6041.7	1	0	-1.4	1	0.662
	IS700	912.0	1	0.509	-9.4	1	0.153
	S1	8319.1	1	0	-78.9	1	8.5E-09
	S2	8778.3	1	0	3.7	1	0.281

Appendix 4.6: Table of the Pairwise comparison data obtained after GZLM analysis, before and after exposure to shear stress. Before and after exposure, the probability distribution was normal and tweedie, respectively and the link function was identity and log, respectively. The Grey cells represent the significant comparisons.

APPENDIX 5: STATISTICAL TABLES FOR CHAPTER 6

- *E. crouaniorum*

RM ANOVA

Source	SS	df	MS	F	p-values
Intercept	6.60E+08	1	6.60E+08	1625.1	1.1E-38
Coatings	3.91E+07	5	7.83E+06	19.3	1.8E-10
Error	1.95E+07	48	4.06E+05		

Appendix 5.1: RM ANOVA table.

(I) Coatings	(J) Coatings	Before exposure to shear stress			After exposure to shear stress		
		Mean Difference (I-J)	df	p-values	Mean Difference (I-J)	df	p-values
H	H1	-1289.1	1	3.5E-05	15.0	1	3.2E-03
	H10	-2587.5	1	7.6E-19	-13.8	1	0.03
	H2	-870.8	1	0.01	28.8	1	6.8E-12
	H3	-2427.0	1	1.1E-16	14.8	1	3.2E-03
	H7	-2673.6	1	0	-12.1	1	0.049
H1	H	1289.1	1	3.5E-05	-15.0	1	3.2E-03
	H10	-1298.4	1	3.4E-05	-28.8	1	1.3E-08
	H2	418.4	1	0.55	13.8	1	6.2E-04
	H3	-1137.9	1	3.3E-04	-.2	1	1.00
	H7	-1384.5	1	8.4E-06	-27.1	1	7.0E-08
H2	H	870.8	1	0.01	-28.8	1	6.8E-12
	H1	-418.4	1	0.55	-13.8	1	6.2E-04
	H10	-1716.7	1	1.3E-08	-42.6	1	0
	H3	-1556.3	1	3.5E-07	-14.0	1	5.7E-04
	H7	-1802.9	1	2.0E-09	-40.9	1	0
H3	H	2427.0	1	1.1E-16	-14.8	1	3.2E-03
	H1	1137.9	1	3.3E-04	.2	1	1.00
	H10	-160.5	1	1.000	-28.6	1	1.6E-08
	H2	1556.3	1	3.5E-07	14.0	1	5.7E-04
	H7	-246.6	1	1.000	-26.9	1	8.4E-08
H7	H	2673.6	1	0	12.1	1	0.049
	H1	1384.5	1	8.4E-06	27.1	1	7.0E-08
	H10	86.1	1	1.000	-1.7	1	1.00
	H2	1802.9	1	2.0E-09	40.9	1	0
	H3	246.6	1	1.000	26.9	1	8.4E-08
H10	H	2587.5	1	7.6E-19	13.8	1	0.03
	H1	1298.4	1	3.4E-05	28.8	1	1.3E-08
	H2	1716.7	1	1.3E-08	42.6	1	0
	H3	160.5	1	1.000	28.6	1	1.6E-08

	H7	-86.1	1	1.000	1.7	1	1.00

Appendix 5.2: Table of the Pairwise comparison data obtained after GZLM analysis, before and after exposure to shear stress. Before and after exposure, the probability distribution was normal and tweedie, respectively and the link function was identity. The Grey cells represent the significant comparisons.

- *U. Linza*

		Before exposure to shear stress			After exposure to shear stress		
(I) Coatings	(J) Coatings	Mean Difference (I-J)	df	p-values	Mean Difference (I-J)	df	p-values
H	H1	-3288.2	1	0	-4.4	1	0.5
	H10	-3151.4	1	0	-15.6	1	5.4E-04
	H2	-2695.6	1	0	-25.3	1	2.3E-09
	H3	-3099.3	1	0	-21.9	1	3.5E-07
	H7	-2831.6	1	0	-50.0	1	0
H1	H	3288.2	1	0	4.4	1	0.540
	H10	136.8	1	1.00	-11.2	1	0.025
	H2	592.6	1	0.365	-20.9	1	1.2E-06
	H3	188.9	1	1.00	-17.5	1	7.8E-05
	H7	456.5	1	0.943	-45.6	1	0
H2	H	2695.6	1	0	25.3	1	2.3E-09
	H1	-592.6	1	0.365	20.9	1	1.2E-06
	H10	-455.8	1	0.943	9.7	1	0.059
	H3	-403.7	1	1.00	3.4	1	0.540
	H7	-136.1	1	1.00	-24.7	1	5.6E-09
H3	H	3099.3	1	0	21.9	1	3.5E-07
	H1	-188.9	1	1.00	17.5	1	7.8E-05
	H10	-52.1	1	1.00	6.3	1	0.343
	H2	403.7	1	1.00	-3.4	1	0.540
	H7	267.6	1	1.00	-28.1	1	2.0E-11
H7	H	2831.6	1	0	50.0	1	0
	H1	-456.5	1	0.943	45.6	1	0
	H10	-319.7	1	1.00	34.4	1	7.5E-17
	H2	136.1	1	1.00	24.7	1	5.6E-09
	H3	-267.6	1	1.00	28.1	1	2.0E-11
H10	H	3151.4	1	0	15.6	1	5.4E-04
	H1	-136.8	1	1.00	11.2	1	0.025
	H2	455.8	1	0.943	-9.7	1	0.06
	H3	52.1	1	1.00	-6.3	1	0.343
	H7	319.7	1	1.00	-34.4	1	7.5E-17

Appendix 5.3: Table for the Pairwise comparison data obtained after GZLM analysis, before and after exposure to shear stress. Before and after exposure, the probability distribution was tweedie

and normal, respectively and the link function was log and identity, respectively. The Grey cells represent the significant comparisons.

APPENDIX 6: STATISTICAL TABLES FOR CHAPTER 7

- SET 1
  - *E. crouaniorum*

RM ANOVA

Source	SS	df	MS	F	p-values
Intercept	3.93E+08	1	3.93E+08	1112.4	1.2E-38
Coatings	7.95E+07	6	1.32E+07	37.5	6.9E-18
Error	1.98E+07	56	3.53E+05		

Appendix 6.1: RM ANOVA table.

(I) Coatings	(J) Coatings	Before exposure to shear stress			After exposure to shear stress		
		Mean Difference (I-J)	df	p-values	Mean Difference (I-J)	df	p-values
A	B	-370.3	1	1.00	4.9	1	0.959
	C	844.9	1	0.011	-75.0	1	0
	D	863.4	1	0.009	-76.6	1	0
	E	927.5	1	3.1E-03	-60.2	1	0
	F	544.8	1	0.450	-68.7	1	0
	G	568.5	1	0.381	-73.1	1	0
B	A	370.3	1	1.00	-4.9	1	0.959
	C	1215.2	1	1.3E-04	-79.9	1	0
	D	1233.7	1	9.1E-05	-81.5	1	0
	E	1297.8	1	2.4E-05	-65.1	1	0
	F	915.1	1	0.016	-73.6	1	0
	G	938.7	1	0.012	-78.0	1	0
C	A	-844.9	1	0.011	75.0	1	0
	B	-1215.2	1	1.3E-04	79.9	1	0
	D	18.4	1	1.00	-1.6	1	1.00
	E	82.6	1	1.00	14.8	1	8.4E-04
	F	-300.2	1	1.00	6.3	1	0.559
	G	-276.5	1	1.00	1.9	1	1.00
D	A	-863.4	1	0.009	76.6	1	0
	B	-1233.7	1	9.1E-05	81.5	1	0
	C	-18.4	1	1.00	1.6	1	1.00
	E	64.2	1	1.00	16.4	1	1.4E-04
	F	-318.6	1	1.00	7.9	1	0.246
	G	-294.9	1	1.00	3.5	1	1.00
E	A	-927.5	1	3.1E-03	60.2	1	0
	B	-1297.8	1	2.4E-05	65.1	1	0
	C	-82.6	1	1.00	-14.8	1	8.4E-04
	D	-64.2	1	1.00	-16.4	1	1.4E-04
	F	-382.8	1	0.876	-8.5	1	0.193

	G	-359.1	1	0.982	-12.9	1	0.005
F	A	-544.8	1	0.450	68.7	1	0
	B	-915.1	1	0.016	73.6	1	0
	C	300.2	1	1.00	-6.3	1	0.559
	D	318.6	1	1.00	-7.9	1	0.246
	E	382.8	1	0.876	8.5	1	0.193
	G	23.7	1	1.00	-4.4	1	0.959
G	A	-568.5	1	0.381	73.1	1	0
	B	-938.7	1	0.012	78.0	1	0
	C	276.5	1	1.00	-1.9	1	1.00
	D	294.9	1	1.00	-3.5	1	1.00
	E	359.1	1	0.982	12.9	1	0.005
	F	-23.7	1	1.00	4.4	1	0.959

Appendix 6.2: Table of the Pairwise comparison data obtained after GZLM analysis, before and after exposure to shear stress. Before and after exposure, the probability distribution was normal and the link function was identity. The Grey cells represent the significant comparisons.

- SET 2
  - *E. crouaniorum*

RM ANOVA

Source	SS	df	MS	F	p-values
Intercept	2.80E+09	1	2.80E+09	1960.8	1.3E-35
Coatings	8.04E+08	4	2.01E+08	140.9	5.2E-23
Error	5.70E+07	40	1.43E+06		

Appendix 6.3: RM ANOVA table.

(I) Coatings	(J) Coatings	Before exposure to shear stress			After exposure to shear stress		
		Mean Difference (I-J)	df	p-values	Mean Difference (I-J)	df	p-values
AP/TEOS	DMAP/TEOS	-1439.2	1	7.9E-04	-20.3	1	7.9E-04
	1:4 TFP/TEOS	6162.2	1	0	-59.5	1	0
	1:4 PH/TEOS	2259.8	1	1.1E-07	-85.8	1	0
	MAP/TEOS	-1767.9	1	4E-05	-2.8	1	0.624
DMAP/TEOS	AP/TEOS	1439.2	1	7.9E-04	20.3	1	7.9E-04
	1:4 TFP/TEOS	7601.4	1	0	-39.1	1	1.1E-11
	1:4 PH/TEOS	3699.1	1	5.4E-19	-65.5	1	0
	MAP/TEOS	-328.6	1	0.419	17.5	1	4.6E-03
MAP/TEOS	AP/TEOS	1767.9	1	4E-05	2.8	1	0.624
	DMAP/TEOS	328.6	1	0.419	-17.5	1	4.6E-03
	1:4 TFP/TEOS	7930.0	1	0	-56.6	1	0
	1:4 PH/TEOS	4027.7	1	0	-83.0	1	0
1:4 TFP/TEOS	AP/TEOS	-6162.2	1	0	59.5	1	0

	DMAP/TEOS	-7601.4	1	0	39.1	1	1.1E-11
	1:4 PH/TEOS	-3902.3	1	0	-26.3	1	9.1E-06
	MAP/TEOS	-7930.0	1	0	56.6	1	0
1:4 PH/TEOS	AP/TEOS	-2259.8	1	1.1E-07	85.8	1	0
	DMAP/TEOS	-3699.1	1	5.4E-19	65.5	1	0
	1:4 TFP/TEOS	3902.3	1	0	26.3	1	9.1E-06
	MAP/TEOS	-4027.7	1	0	83.0	1	0

Appendix 6.4: Table for the Pairwise comparison data obtained after GZLM analysis, before and after exposure to shear stress. Before and after exposure, the probability distribution was normal and the link function was identity. The Grey cells represent the significant comparisons.

- *U. linza*

		Before exposure to shear stress			After exposure to shear stress		
(I) Coatings	(J) Coatings	Mean Difference (I-J)	df	p-values	Mean Difference (I-J)	df	p-values
AP/TEOS	DMAP/TEOS	236.8	1	1.00	-10.7	1	0.035
	1:4 TFP/TEOS	-440.3	1	1.00	-32.8	1	3.8E-18
	1:4 PH/TEOS	-479.3	1	1.00	-27.6	1	4.2E-13
	MAP/TEOS	-1328.2	1	0.095	-9.0	1	0.138
DMAP/TEOS	AP/TEOS	-236.8	1	1.00	10.7	1	0.035
	1:4 TFP/TEOS	-677.1	1	0.813	-22.0	1	6.0E-07
	1:4 PH/TEOS	-716.1	1	0.813	-16.9	1	1.9E-04
	MAP/TEOS	-1565.0	1	0.021	1.8	1	0.711
MAP/TEOS	AP/TEOS	1328.2	1	0.095	9.0	1	0.138
	DMAP/TEOS	1565.0	1	0.021	-1.8	1	0.711
	1:4 TFP/TEOS	887.9	1	0.813	-23.8	1	7.6E-07
	1:4 PH/TEOS	848.9	1	0.813	-18.7	1	1.9E-04
1:4 TFP/TEOS	AP/TEOS	440.3	1	1.00	32.8	1	3.8E-18
	DMAP/TEOS	677.1	1	0.813	22.0	1	6.0E-07
	1:4 PH/TEOS	-39.0	1	1.00	5.2	1	0.318
	MAP/TEOS	-887.9	1	0.813	23.8	1	7.6E-07
1:4 PH/TEOS	AP/TEOS	479.3	1	1.00	27.6	1	4.2E-13
	DMAP/TEOS	716.1	1	0.813	16.9	1	1.9E-04
	1:4 TFP/TEOS	39.0	1	1.00	-5.2	1	0.318
	MAP/TEOS	-848.9	1	0.813	18.7	1	1.9E-04

Appendix 6.4: Table for the Pairwise comparison data obtained after GZLM analysis, before and after exposure to shear stress. Before and after exposure, the probability distribution was gamma and normal, respectively and the link function was log and identity, respectively. The Grey cells represent the significant comparisons.

APPENDIX 7: STATISTICAL TABLES FOR CHAPTER 8

- *E. crouaniorum*

RM ANOVA

Source	SS	df	MS	F	p-values
Intercept	1.12E+09	1	1.12E+09	779.2	7.6E-28
Coatings	6.24E+07	4	1.56E+07	10.8	4.8E-06
Error	5.76E+07	40	1.44E+06		

Appendix 7.1: RM ANOVA table.

(I) Coatings	(J) Coatings	Before exposure to shear stress			After exposure to shear stress		
		Mean Difference (I-J)	df	p-values	Mean Difference (I-J)	df	p-values
M1	M2	-1602.1	1	0.016	5.0	1	0.870
	M3	-1945.5	1	1.7E-03	1.0	1	0.978
	M4	-2815.0	1	7.3E-07	15.5	1	1.3E-03
	M5	-3175.7	1	1.4E-08	12.5	1	0.017
M2	M1	1602.1	1	0.016	-5.0	1	0.870
	M3	-343.4	1	0.983	-4.0	1	0.978
	M4	-1212.9	1	0.095	10.5	1	0.058
	M5	-1573.6	1	0.016	7.5	1	0.323
M3	M1	1945.5	1	1.7E-03	-1.0	1	0.978
	M2	343.4	1	0.983	4.0	1	0.978
	M4	-869.4	1	0.292	14.5	1	3.2E-03
	M5	-1230.1	1	0.095	11.5	1	0.033
M4	M1	2815.0	1	7.3E-07	-15.5	1	1.3E-03
	M2	1212.9	1	0.095	-10.5	1	0.058
	M3	869.4	1	0.292	-14.5	1	3.2E-03
	M5	-360.7	1	0.983	-3.0	1	0.978
M5	M1	3175.7	1	1.4E-08	-12.5	1	0.017
	M2	1573.6	1	0.016	-7.5	1	0.323
	M3	1230.1	1	0.095	-11.5	1	0.033
	M4	360.7	1	0.983	3.0	1	0.978

Appendix 7.2: Table of the Pairwise comparison data obtained after GZLM analysis, before and after exposure to shear stress. Before and after exposure, the probability distribution was normal and the link function was identity. The Grey cells represent the significant comparisons.

- *U. linza*

(I) Coatings	(J) Coatings	Before exposure to shear stress			After exposure to shear stress		
		Mean Difference (I-J)	df	p-values	Mean Difference (I-J)	df	p-values
M1	M2	4920.9	1	0.033	-4.7	1	0.400
	M3	4371.0	1	0.076	-5.2	1	0.400
	M4	6718.9	1	0.001	-17.8	1	0.001
	M5	7795.8	1	5.6E-05	-20.3	1	1.3E-04
M2	M1	-4920.9	1	0.033	4.7	1	0.400
	M3	-549.9	1	1.000	-.5	1	1.000
	M4	1798.1	1	0.885	-13.1	1	0.033
	M5	2874.9	1	0.470	-15.6	1	0.013
M3	M1	-4371.0	1	0.076	5.2	1	0.400
	M2	549.9	1	1.000	.5	1	1.000
	M4	2348.0	1	0.686	-12.6	1	0.041
	M5	3424.8	1	0.277	-15.1	1	0.017
M4	M1	-6718.9	1	0.001	17.8	1	0.001
	M2	-1798.1	1	0.885	13.1	1	0.033
	M3	-2348.0	1	0.686	12.6	1	0.041
	M5	1076.8	1	1.000	-2.5	1	1.000
M5	M1	-7795.8	1	5.6E-05	20.3	1	1.3E-04
	M2	-2874.9	1	0.470	15.6	1	0.013
	M3	-3424.8	1	0.277	15.1	1	0.017
	M4	-1076.8	1	1.000	2.5	1	1.000

Appendix 7.3: Table of the Pairwise comparison data obtained after GZLM analysis, before and after exposure to shear stress. Before and after exposure, the probability distribution was normal and tweedie, respectively and the link function was identity and log, respectively. The Grey cells represent the significant comparisons.

APPENDIX 8: STATISTICAL TABLES FOR CHAPTER 9

- **Experiment 1: Trial experiment on variations in initial surface colonisation at Hartlepool Marina with surfaces of different modulus.**

	Source	(Intercept)	Surfaces	Collections	Surfaces * Collections
Total % cover	Wald Chi-Square	16258.86	31.41	84.79	59.52
	df	1	8	2	16
	p-values	0	1.2E-04	0	6.3E-07
% cover of microfouling	Wald Chi-Square	9653.81	9.05	51.61	48.14
	df	1	8	2	16
	p-values	0	0.34	6.19E-12	4.52E-05
% cover of weeds	Wald Chi-Square	160.94	19.02	20.89	6.171
	df	1	8	2	16
	p-values	0	0.02	2.90E-5	0.99
% cover of soft-bodied animals	Wald Chi-Square	97.61	18.45	91.03	22.05
	df	1	8	2	16
	p-values	0	0.02	0	0.14
% cover of hard-bodied animals	Wald Chi-Square	15.58	16.29	7.20	28.79
	df	1	8	2	16
	p-values	7.90E-05	0.04	0.03	0.03

Appendix 8.1: Table of the test model effect of the GZLM analysis. The Grey cells represent the significant comparisons.

		Total % cover			% cover of soft-bodied animals			% cover of hard-bodied animals		
(I) Surfaces	(J) Surfaces	Mean Difference (I-J)	df	p-values	Mean Difference (I-J)	df	p-values	Mean Difference (I-J)	df	p-values
mD10	mD10-H	4.72	1	1.00	-1.72	1	1.00	1.33	1	0.17
	mE10-H	2.11	1	1.00	1.22	1	1.00	1.33	1	0.17
	Glass	-0.83	1	1.00	0.17	1	1.00	1.17	1	0.42
	IS700	11.67	1	0.01	2.67	1	1.00	1.33	1	0.17
	IS900	9.17	1	0.11	3.50	1	1.00	1.50	1	0.06
	S1	3.28	1	1.00	-0.06	1	1.00	1.44	1	0.08
	S2	0.00	1	1.00	-1.94	1	1.00	1.67	1	0.02
	S3	0.11	1	1.00	0.61	1	1.00	1.22	1	0.32
mD10-H	mD10	-4.72	1	1.00	1.72	1	1.00	-1.33	1	0.17
	mE10-H	-2.61	1	1.00	2.94	1	1.00	0.00	1	1.00
	Glass	-5.56	1	1.00	1.89	1	1.00	-0.17	1	1.00
	IS700	6.94	1	0.70	4.39	1	0.29	0.00	1	1.00

	IS900	4.44	1	1.00	5.22	1	0.06	0.17	1	1.00
	S1	-1.44	1	1.00	1.67	1	1.00	0.11	1	1.00
	S2	-4.72	1	1.00	-0.22	1	1.00	0.33	1	1.00
	S3	-4.61	1	1.00	2.33	1	1.00	-0.11	1	1.00
mE10-H	mD10	-2.11	1	1.00	-1.22	1	1.00	-1.33	1	0.17
	mD10-H	2.61	1	1.00	-2.94	1	1.00	0.00	1	1.00
	Glass	-2.94	1	1.00	-1.06	1	1.00	-0.17	1	1.00
	IS700	9.56	1	0.08	1.44	1	1.00	0.00	1	1.00
	IS900	7.06	1	0.66	2.28	1	1.00	0.17	1	1.00
	S1	1.17	1	1.00	-1.28	1	1.00	0.11	1	1.00
	S2	-2.11	1	1.00	-3.17	1	1.00	0.33	1	1.00
	S3	-2.00	1	1.00	-0.61	1	1.00	-0.11	1	1.00
Glass	mD10	0.83	1	1.00	-0.17	1	1.00	-1.17	1	0.42
	mD10-H	5.56	1	1.00	-1.89	1	1.00	0.17	1	1.00
	mE10-H	2.94	1	1.00	1.06	1	1.00	0.17	1	1.00
	IS700	12.50	1	2.75E-03	2.50	1	1.00	0.17	1	1.00
	IS900	10.00	1	0.05	3.33	1	1.00	0.33	1	1.00
	S1	4.11	1	1.00	-0.22	1	1.00	0.28	1	1.00
	S2	0.83	1	1.00	-2.11	1	1.00	0.50	1	1.00
	S3	0.94	1	1.00	0.44	1	1.00	0.06	1	1.00
IS700	mD10	-11.67	1	0.01	-2.67	1	1.00	-1.33	1	0.17
	mD10-H	-6.94	1	0.70	-4.39	1	0.29	0.00	1	1.00
	mE10-H	-9.56	1	0.08	-1.44	1	1.00	0.00	1	1.00
	Glass	-12.50	1	2.75E-03	-2.50	1	1.00	-0.17	1	1.00
	IS900	-2.50	1	1.00	0.83	1	1.00	0.17	1	1.00
	S1	-8.39	1	0.21	-2.72	1	1.00	0.11	1	1.00
	S2	-11.67	1	0.01	-4.61	1	0.20	0.33	1	1.00
	S3	-11.56	1	0.01	-2.06	1	1.00	-0.11	1	1.00
IS900	mD10	-9.17	1	0.11	-3.50	1	1.00	-1.50	1	0.06
	mD10-H	-4.44	1	1.00	-5.22	1	0.06	-0.17	1	1.00
	mE10-H	-7.06	1	0.66	-2.28	1	1.00	-0.17	1	1.00
	Glass	-10.00	1	0.05	-3.33	1	1.00	-0.33	1	1.00
	IS700	2.50	1	1.00	-0.83	1	1.00	-0.17	1	1.00
	S1	-5.89	1	1.00	-3.56	1	1.00	-0.06	1	1.00
	S2	-9.17	1	0.11	-5.44	1	0.04	0.17	1	1.00
	S3	-9.06	1	0.12	-2.89	1	1.00	-0.28	1	1.00
S1	mD10	-3.28	1	1.00	0.06	1	1.00	-1.44	1	0.08
	mD10-H	1.44	1	1.00	-1.67	1	1.00	-0.11	1	1.00
	mE10-H	-1.17	1	1.00	1.28	1	1.00	-0.11	1	1.00
	Glass	-4.11	1	1.00	0.22	1	1.00	-0.28	1	1.00
	IS700	8.39	1	0.21	2.72	1	1.00	-0.11	1	1.00
	IS900	5.89	1	1.00	3.56	1	1.00	0.06	1	1.00
	S2	-3.28	1	1.00	-1.89	1	1.00	0.22	1	1.00

	S3	-3.17	1	1.00	0.67	1	1.00	-0.22	1	1.00
S2	mD10	0.00	1	1.00	1.94	1	1.00	-1.67	1	0.02
	mD10-H	4.72	1	1.00	0.22	1	1.00	-0.33	1	1.00
	mE10-H	2.11	1	1.00	3.17	1	1.00	-0.33	1	1.00
	Glass	-0.83	1	1.00	2.11	1	1.00	-0.50	1	1.00
	IS700	11.67	1	0.01	4.61	1	0.20	-0.33	1	1.00
	IS900	9.17	1	0.11	5.44	1	0.04	-0.17	1	1.00
	S1	3.28	1	1.00	1.89	1	1.00	-0.22	1	1.00
	S3	0.11	1	1.00	2.56	1	1.00	-0.44	1	1.00
S3	mD10	-0.11	1	1.00	-0.61	1	1.00	-1.22	1	0.32
	mD10-H	4.61	1	1.00	-2.33	1	1.00	0.11	1	1.00
	mE10-H	2.00	1	1.00	0.61	1	1.00	0.11	1	1.00
	Glass	-0.94	1	1.00	-0.44	1	1.00	-0.06	1	1.00
	IS700	11.56	1	0.01	2.06	1	1.00	0.11	1	1.00
	IS900	9.06	1	0.12	2.89	1	1.00	0.28	1	1.00
	S1	3.17	1	1.00	-0.67	1	1.00	0.22	1	1.00
	S2	-0.11	1	1.00	-2.56	1	1.00	0.44	1	1.00

Appendix 8.2: Table of the Pairwise comparison data comparing the surfaces between each other, obtained after GZLM analysis. The % cover for each surface was the mean of all the data collection made in Hartlepool Marina. The probability distribution was normal and the link function was identity. The Grey cells represent the significant comparisons. Microfouling and weeds were not represented in this table, as the surfaces were not significantly different for these fouling categories as shown in Appendix 11.1.

	(I) Collections	1		2		3	
	(J) Collections	2	3	1	3	1	2
Total % cover	Mean Difference (I-J)	-0.35	14.37	0.35	14.72	-14.37	-14.72
	df	1	1	1	1	1	1
	p-values	0.85	6.66E-15	0.85	2.00E-15	6.66E-15	2.00E-15
% cover of microfouling	Mean Difference (I-J)	10.48	15.43	-10.48	4.94	-15.43	-4.94
	df	1	1	1	1	1	1
	p-values	3.51E-06	5.98E-12	3.51E-06	0.02	5.98E-12	0.02
% cover of weeds	Mean Difference (I-J)	-1.39	0.96	1.39	2.35	-0.96	-2.35
	df	1	1	1	1	1	1
	p-values	0.01	0.06	0.01	1.63E-05	0.06	1.63E-05
% cover of soft-bodied animals	Mean Difference (I-J)	-8.78	-1.96	8.78	6.81	1.96	-6.81
	df	1	1	1	1	1	1
	p-values	0	0.04	0	3.41E-12	0.04	3.41E-12
% cover of hard-bodied animals	Mean Difference (I-J)	-0.67	-0.06	0.67	0.61	0.06	-0.61
	df	1	1	1	1	1	1
	p-values	0.047	0.840	0.047	0.053	0.840	0.053

Appendix 8.3: Table of the Pairwise comparison data comparing the data collection between each other, obtained after GZLM analysis. The % cover for each data collection was the mean of all the % covers of all the fouling categories made in Hartlepool Marina. The probability distribution was normal and the link function was identity.

- **Experiment 2: Experiment 2: Trial experiment on the 'succession' of organisms at Hartlepool Marina with surfaces of different modulus.**

	Source	(Intercept)	Surfaces	Collections	Surfaces * Collections
Total % cover	Wald Chi-Square	62344.85	20.96	1.68	10.88
	df	1	8	2	16
	p-values	0	0.01	0.43	0.82
% cover of microfouling	Wald Chi-Square	10521.82	45.07	63.67	68.75
	df	1	8	2	16
	p-values	0	3.57E-07	1.49E-14	1.65E-08
% cover of weeds	Wald Chi-Square	34.92	20.85	8.47	27.04
	df	1	8	2	16
	p-values	3.44E-09	0.01	0.01	0.04
% cover of soft-bodied animals	Wald Chi-Square	80.02	23.28	43.24	30.72
	df	1	8	2	16
	p-values	0	3.03E-03	4.07E-10	0.01
% cover of hard-bodied animals	Wald Chi-Square	20.68	24.55	13.94	35.42
	df	1	8	2	16
	p-values	5.44E-06	1.85E-03	9.41E-04	3.48E-03

Appendix 8.4: Table of the test model effect of the GZLM analysis. The Grey cells represent the significant comparisons.

(I) Surfaces	(J) Surfaces	Total % cover			% cover of microfouling			% cover of weeds			% cover of soft-bodied animals			% cover of hard-bodied animals		
		Mean Difference (I-J)	df	p-values	Mean Difference (I-J)	df	p-values	Mean Difference (I-J)	df	p-values	Mean Difference (I-J)	df	p-values	Mean Difference (I-J)	df	p-values
Glass	IS700	4.17	1	0.40	-17.41	1	6.63E-05	9.95	1	0.049	7.47	1	0.04	4.15	1	0.01
	IS900	4.66	1	0.20	-15.28	1	9.32E-04	10.79	1	0.02	4.89	1	0.87	4.25	1	0.01
	mD10	0.00	1	1.00	-15.96	1	4.20E-04	7.15	1	0.66	4.55	1	1.00	4.26	1	0.01
	mD10-H	0.00	1	1.00	-9.06	1	0.35	7.46	1	0.52	-0.68	1	1.00	2.28	1	1.00
	mE10-H	0.00	1	1.00	-18.36	1	1.83E-05	9.31	1	0.09	5.61	1	0.44	3.44	1	0.10
	S1	0.50	1	1.00	-18.49	1	1.56E-05	9.85	1	0.05	6.61	1	0.13	2.53	1	0.90
	S2	0.00	1	1.00	-18.92	1	8.59E-06	10.39	1	0.03	4.17	1	1.00	4.36	1	0.01
	S3	0.00	1	1.00	-12.82	1	0.01	4.13	1	1.00	4.73	1	0.96	3.96	1	0.02
IS700	Glass	-4.17	1	0.40	17.41	1	6.63E-05	-9.95	1	0.049	-7.47	1	0.04	-4.15	1	0.01
	IS900	0.49	1	1.00	2.12	1	1.00	0.84	1	1.00	-2.58	1	1.00	0.10	1	1.00
	mD10	-4.17	1	0.40	1.44	1	1.00	-2.80	1	1.00	-2.92	1	1.00	0.11	1	1.00
	mD10-H	-4.17	1	0.40	8.35	1	0.57	-2.49	1	1.00	-8.16	1	0.01	-1.87	1	1.00
	mE10-H	-4.17	1	0.40	-0.95	1	1.00	-0.64	1	1.00	-1.86	1	1.00	-0.71	1	1.00
	S1	-3.67	1	0.67	-1.08	1	1.00	-0.10	1	1.00	-0.86	1	1.00	-1.62	1	1.00
	S2	-4.17	1	0.40	-1.52	1	1.00	0.44	1	1.00	-3.31	1	1.00	0.21	1	1.00
	S3	-4.17	1	0.40	4.58	1	1.00	-5.82	1	1.00	-2.74	1	1.00	-0.19	1	1.00
IS900	Glass	-4.66	1	0.20	15.28	1	9.32E-04	-10.79	1	0.02	-4.89	1	0.87	-4.25	1	0.01
	IS700	-0.49	1	1.00	-2.12	1	1.00	-0.84	1	1.00	2.58	1	1.00	-0.10	1	1.00
	mD10	-4.66	1	0.20	-0.68	1	1.00	-3.64	1	1.00	-0.34	1	1.00	0.01	1	1.00
	mD10-H	-4.66	1	0.20	6.23	1	1.00	-3.33	1	1.00	-5.58	1	0.44	-1.97	1	1.00
	mE10-H	-4.66	1	0.20	-3.07	1	1.00	-1.49	1	1.00	0.72	1	1.00	-0.81	1	1.00
	S1	-4.16	1	0.40	-3.21	1	1.00	-0.94	1	1.00	1.72	1	1.00	-1.72	1	1.00
	S2	-4.66	1	0.20	-3.64	1	1.00	-0.40	1	1.00	-0.73	1	1.00	0.11	1	1.00
	S3	-4.66	1	0.20	2.46	1	1.00	-6.66	1	0.95	-0.16	1	1.00	-0.29	1	1.00
mD10	Glass	0.00	1	1.00	15.96	1	4.20E-04	-7.15	1	0.66	-4.55	1	1.00	-4.26	1	0.01

	IS700	4.17	1	0.40	-1.44	1	1.00	2.80	1	1.00	2.92	1	1.00	-0.11	1	1.00
	IS900	4.66	1	0.20	0.68	1	1.00	3.64	1	1.00	0.34	1	1.00	-0.01	1	1.00
	mD10-H	0.00	1	1.00	6.91	1	1.00	0.31	1	1.00	-5.23	1	0.62	-1.98	1	1.00
	mE10-H	0.00	1	1.00	-2.39	1	1.00	2.16	1	1.00	1.06	1	1.00	-0.82	1	1.00
	S1	0.50	1	1.00	-2.53	1	1.00	2.70	1	1.00	2.06	1	1.00	-1.73	1	1.00
	S2	0.00	1	1.00	-2.96	1	1.00	3.24	1	1.00	-0.38	1	1.00	0.10	1	1.00
	S3	0.00	1	1.00	3.14	1	1.00	-3.02	1	1.00	0.18	1	1.00	-0.31	1	1.00
mD10-H	Glass	0.00	1	1.00	9.06	1	0.35	-7.46	1	0.52	0.68	1	1.00	-2.28	1	1.00
	IS700	4.17	1	0.40	-8.35	1	0.57	2.49	1	1.00	8.16	1	0.01	1.87	1	1.00
	IS900	4.66	1	0.20	-6.23	1	1.00	3.33	1	1.00	5.58	1	0.44	1.97	1	1.00
	mD10	0.00	1	1.00	-6.91	1	1.00	-0.31	1	1.00	5.23	1	0.62	1.98	1	1.00
	mE10-H	0.00	1	1.00	-9.30	1	0.30	1.84	1	1.00	6.29	1	0.19	1.16	1	1.00
	S1	0.50	1	1.00	-9.43	1	0.28	2.39	1	1.00	7.29	1	0.048	0.25	1	1.00
	S2	0.00	1	1.00	-9.87	1	0.20	2.93	1	1.00	4.85	1	0.88	2.08	1	1.00
	S3	0.00	1	1.00	-3.77	1	1.00	-3.33	1	1.00	5.42	1	0.52	1.68	1	1.00
mE10-H	Glass	0.00	1	1.00	18.36	1	1.83E-05	-9.31	1	0.09	-5.61	1	0.44	-3.44	1	0.10
	IS700	4.17	1	0.40	0.95	1	1.00	0.64	1	1.00	1.86	1	1.00	0.71	1	1.00
	IS900	4.66	1	0.20	3.07	1	1.00	1.49	1	1.00	-0.72	1	1.00	0.81	1	1.00
	mD10	0.00	1	1.00	2.39	1	1.00	-2.16	1	1.00	-1.06	1	1.00	0.82	1	1.00
	mD10-H	0.00	1	1.00	9.30	1	0.30	-1.84	1	1.00	-6.29	1	0.19	-1.16	1	1.00
	S1	0.50	1	1.00	-0.13	1	1.00	0.54	1	1.00	1.00	1	1.00	-0.91	1	1.00
	S2	0.00	1	1.00	-0.57	1	1.00	1.09	1	1.00	-1.44	1	1.00	0.92	1	1.00
	S3	0.00	1	1.00	5.53	1	1.00	-5.17	1	1.00	-0.88	1	1.00	0.52	1	1.00
S1	Glass	-0.50	1	1.00	18.49	1	1.56E-05	-9.85	1	0.05	-6.61	1	0.13	-2.53	1	0.90
	IS700	3.67	1	0.67	1.08	1	1.00	0.10	1	1.00	0.86	1	1.00	1.62	1	1.00
	IS900	4.16	1	0.40	3.21	1	1.00	0.94	1	1.00	-1.72	1	1.00	1.72	1	1.00
	mD10	-0.50	1	1.00	2.53	1	1.00	-2.70	1	1.00	-2.06	1	1.00	1.73	1	1.00
	mD10-H	-0.50	1	1.00	9.43	1	0.28	-2.39	1	1.00	-7.29	1	0.048	-0.25	1	1.00
	mE10-H	-0.50	1	1.00	0.13	1	1.00	-0.54	1	1.00	-1.00	1	1.00	0.91	1	1.00

268

	S2	-0.50	1	1.00	-0.43	1	1.00	0.54	1	1.00	-2.44	1	1.00	1.83	1	1.00
	S3	-0.50	1	1.00	5.67	1	1.00	-5.72	1	1.00	-1.88	1	1.00	1.43	1	1.00
S2	Glass	0.00	1	1.00	18.92	1	8.59E-06	-10.39	1	0.03	-4.17	1	1.00	-4.36	1	0.01
	IS700	4.17	1	0.40	1.52	1	1.00	-0.44	1	1.00	3.31	1	1.00	-0.21	1	1.00
	IS900	4.66	1	0.20	3.64	1	1.00	0.40	1	1.00	0.73	1	1.00	-0.11	1	1.00
	mD10	0.00	1	1.00	2.96	1	1.00	-3.24	1	1.00	0.38	1	1.00	-0.10	1	1.00
	mD10-H	0.00	1	1.00	9.87	1	0.20	-2.93	1	1.00	-4.85	1	0.88	-2.08	1	1.00
	mE10-H	0.00	1	1.00	0.57	1	1.00	-1.09	1	1.00	1.44	1	1.00	-0.92	1	1.00
	S1	0.50	1	1.00	0.43	1	1.00	-0.54	1	1.00	2.44	1	1.00	-1.83	1	1.00
	S3	0.00	1	1.00	6.10	1	1.00	-6.26	1	1.00	0.57	1	1.00	-0.41	1	1.00
S3	Glass	0.00	1	1.00	12.82	1	0.01	-4.13	1	1.00	-4.73	1	0.96	-3.96	1	0.02
	IS700	4.17	1	0.40	-4.58	1	1.00	5.82	1	1.00	2.74	1	1.00	0.19	1	1.00
	IS900	4.66	1	0.20	-2.46	1	1.00	6.66	1	0.95	0.16	1	1.00	0.29	1	1.00
	mD10	0.00	1	1.00	-3.14	1	1.00	3.02	1	1.00	-0.18	1	1.00	0.31	1	1.00
	mD10-H	0.00	1	1.00	3.77	1	1.00	3.33	1	1.00	-5.42	1	0.52	-1.68	1	1.00
	mE10-H	0.00	1	1.00	-5.53	1	1.00	5.17	1	1.00	0.88	1	1.00	-0.52	1	1.00
	S1	0.50	1	1.00	-5.67	1	1.00	5.72	1	1.00	1.88	1	1.00	-1.43	1	1.00
	S2	0.00	1	1.00	-6.10	1	1.00	6.26	1	1.00	-0.57	1	1.00	0.41	1	1.00

Appendix 8.5: Table of the Pairwise comparison data comparing the surfaces between each other, obtained after GZLM analysis. The % cover for each surface was the mean of all the data collection made in Hartlepool Marina. The probability distribution was normal and the link function was identity. The Grey cells represent the significant comparisons.

	(I) Collections	1		2		3	
	(J) Collections	2	3	1	3	1	2
% cover of microfouling	Mean Difference (I-J)	7.15	16.98	-7.15	9.83	-16.98	-9.83
	df	1	1	1	1	1	1
	p-values	3.44E-04	4.33E-15	3.44E-04	1.76E-05	4.33E-15	1.76E-05
% cover of weeds	Mean Difference (I-J)	-0.46	-4.96	0.46	-4.50	4.96	4.50
	df	1	1	1	1	1	1
	p-values	0.79	0.02	0.79	0.03	0.02	0.03
% cover of soft-bodied animals	Mean Difference (I-J)	-4.97	-8.55	4.97	-3.57	8.55	3.57
	df	1	1	1	1	1	1
	p-values	1.33E-04	3.84E-10	1.33E-04	0.01	3.84E-10	0.01
% cover of hard-bodied animals	Mean Difference (I-J)	-0.64	-2.49	0.64	-1.85	2.49	1.85
	df	1	1	1	1	1	1
	p-values	0.31	6.96E-04	0.31	0.02	6.96E-04	0.02

Appendix 8.6: Table of the Pairwise comparison data comparing the data collection between each other, obtained after GZLM analysis. The % cover for each data collection was the mean of all the % covers of all the fouling categories made in Hartlepool Marina. The probability distribution was normal and the link function was identity. Total % cover was not represented in this table, as the surfaces were not significantly different for these fouling categories as shown in Appendix 11.4.

- **Experiment 3: Succession of organisms at Newton Ferrers**

	Source	(Intercept)	Surfaces	Collections	Surfaces * Collections
Total % cover	Wald Chi-Square	7249.51	18.26	8.16	18.29
	df	1	8	1	8
	p-values	0	0.02	4.29E-03	0.02
% cover of microfouling	Wald Chi-Square	231.25	56.11	35.94	7.98
	df	1	8	1	8
	p-values	0	2.69E-09	2.04E-09	0.44
% cover of weeds	Wald Chi-Square	143.23	131.54	72.29	56.61
	df	1	8	1	8
	p-values	0	0	0	2.14E-09
% cover of soft-bodied animals	Wald Chi-Square	47.24	21.16	29.76	21.06
	df	1	8	1	8
	p-values	6.27E-12	0.01	4.88E-08	0.01
% cover of hard-bodied animals	Wald Chi-Square	51.91	7.15	47.19	6.94
	df	1	8	1	8
	p-values	5.81E-13	0.52	6.43E-12	0.54

Appendix 8.7: Table of the test model effect of the GZLM analysis. The Grey cells represent the significant comparisons.

(I) Surfaces	(J) Surfaces	Total % cover			% cover of microfouling			% cover of weeds			% cover of soft-bodied animals		
		Mean Difference (I-J)	df	p-values	Mean Difference (I-J)	df	p-values	Mean Difference (I-J)	df	p-values	Mean Difference (I-J)	df	p-values
Glass	IS700	5.83	1	1.00	-77.00	1	4.87E-09	50.00	1	0	14.83	1	1.00
	IS900	12.33	1	0.33	-47.83	1	2.06E-03	50.50	1	0	16.67	1	0.88
	mD10	0.00	1	1.00	-21.17	1	1.00	25.33	1	4.01E-04	-8.83	1	1.00
	mD10-H	0.67	1	1.00	-16.67	1	1.00	22.83	1	2.08E-03	9.00	1	1.00
	mE10-H	0.00	1	1.00	-27.83	1	0.47	36.67	1	1.17E-08	-4.17	1	1.00
	S1	7.50	1	1.00	-44.17	1	0.01	48.67	1	3.77E-15	1.67	1	1.00
	S2	11.67	1	0.45	-46.83	1	2.82E-03	46.00	1	1.21E-13	12.33	1	1.00
	S3	7.33	1	1.00	-25.83	1	0.62	32.00	1	1.39E-06	7.50	1	1.00
IS700	Glass	-5.83	1	1.00	77.00	1	4.87E-09	-50.00	1	0	-14.83	1	1.00
	IS900	6.50	1	1.00	29.17	1	0.36	0.50	1	1.00	1.83	1	1.00
	mD10	-5.83	1	1.00	55.83	1	1.10E-04	-24.67	1	6.19E-04	-23.67	1	0.07
	mD10-H	-5.17	1	1.00	60.33	1	1.71E-05	-27.17	1	9.89E-05	-5.83	1	1.00
	mE10-H	-5.83	1	1.00	49.17	1	1.32E-03	-13.33	1	0.32	-19.00	1	0.42
	S1	1.67	1	1.00	32.83	1	0.17	-1.33	1	1.00	-13.17	1	1.00
	S2	5.83	1	1.00	30.17	1	0.31	-4.00	1	1.00	-2.50	1	1.00
	S3	1.50	1	1.00	51.17	1	6.54E-04	-18.00	1	0.04	-7.33	1	1.00
IS900	Glass	-12.33	1	0.33	47.83	1	2.06E-03	-50.50	1	0	-16.67	1	0.88
	IS700	-6.50	1	1.00	-29.17	1	0.36	-0.50	1	1.00	-1.83	1	1.00
	mD10	-12.33	1	0.33	26.67	1	0.55	-25.17	1	4.39E-04	-25.50	1	0.03
	mD10-H	-11.67	1	0.45	31.17	1	0.25	-27.67	1	6.74E-05	-7.67	1	1.00
	mE10-H	-12.33	1	0.33	20.00	1	1.00	-13.83	1	0.29	-20.83	1	0.21
	S1	-4.83	1	1.00	3.67	1	1.00	-1.83	1	1.00	-15.00	1	1.00
	S2	-0.67	1	1.00	1.00	1	1.00	-4.50	1	1.00	-4.33	1	1.00
	S3	-5.00	1	1.00	22.00	1	1.00	-18.50	1	0.03	-9.17	1	1.00
mD10	Glass	0.00	1	1.00	21.17	1	1.00	-25.33	1	4.01E-04	8.83	1	1.00

	IS700	5.83	1	1.00	-55.83	1	1.10E-04	24.67	1	6.19E-04	23.67	1	0.07
	IS900	12.33	1	0.33	-26.67	1	0.55	25.17	1	4.39E-04	25.50	1	0.03
	mD10-H	0.67	1	1.00	4.50	1	1.00	-2.50	1	1.00	17.83	1	0.61
	mE10-H	0.00	1	1.00	-6.67	1	1.00	11.33	1	0.63	4.67	1	1.00
	S1	7.50	1	1.00	-23.00	1	0.99	23.33	1	1.59E-03	10.50	1	1.00
	S2	11.67	1	0.45	-25.67	1	0.62	20.67	1	0.01	21.17	1	0.19
	S3	7.33	1	1.00	-4.67	1	1.00	6.67	1	1.00	16.33	1	0.92
mD10-H	Glass	-0.67	1	1.00	16.67	1	1.00	-22.83	1	2.08E-03	-9.00	1	1.00
	IS700	5.17	1	1.00	-60.33	1	1.71E-05	27.17	1	9.89E-05	5.83	1	1.00
	IS900	11.67	1	0.45	-31.17	1	0.25	27.67	1	6.74E-05	7.67	1	1.00
	mD10	-0.67	1	1.00	-4.50	1	1.00	2.50	1	1.00	-17.83	1	0.61
	mE10-H	-0.67	1	1.00	-11.17	1	1.00	13.83	1	0.29	-13.17	1	1.00
	S1	6.83	1	1.00	-27.50	1	0.48	25.83	1	2.81E-04	-7.33	1	1.00
	S2	11.00	1	0.58	-30.17	1	0.31	23.17	1	1.72E-03	3.33	1	1.00
	S3	6.67	1	1.00	-9.17	1	1.00	9.17	1	1.00	-1.50	1	1.00
mE10-H	Glass	0.00	1	1.00	27.83	1	0.47	-36.67	1	1.17E-08	4.17	1	1.00
	IS700	5.83	1	1.00	-49.17	1	1.32E-03	13.33	1	0.32	19.00	1	0.42
	IS900	12.33	1	0.33	-20.00	1	1.00	13.83	1	0.29	20.83	1	0.21
	mD10	0.00	1	1.00	6.67	1	1.00	-11.33	1	0.63	-4.67	1	1.00
	mD10-H	0.67	1	1.00	11.17	1	1.00	-13.83	1	0.29	13.17	1	1.00
	S1	7.50	1	1.00	-16.33	1	1.00	12.00	1	0.52	5.83	1	1.00
	S2	11.67	1	0.45	-19.00	1	1.00	9.33	1	1.00	16.50	1	0.90
	S3	7.33	1	1.00	2.00	1	1.00	-4.67	1	1.00	11.67	1	1.00
S1	Glass	-7.50	1	1.00	44.17	1	0.01	-48.67	1	3.77E-15	-1.67	1	1.00
	IS700	-1.67	1	1.00	-32.83	1	0.17	1.33	1	1.00	13.17	1	1.00
	IS900	4.83	1	1.00	-3.67	1	1.00	1.83	1	1.00	15.00	1	1.00
	mD10	-7.50	1	1.00	23.00	1	0.99	-23.33	1	1.59E-03	-10.50	1	1.00
	mD10-H	-6.83	1	1.00	27.50	1	0.48	-25.83	1	2.81E-04	7.33	1	1.00
	mE10-H	-7.50	1	1.00	16.33	1	1.00	-12.00	1	0.52	-5.83	1	1.00

	S2	4.17	1	1.00	-2.67	1	1.00	-2.67	1	1.00	10.67	1	1.00
	S3	-0.17	1	1.00	18.33	1	1.00	-16.67	1	0.08	5.83	1	1.00
S2	Glass	-11.67	1	0.45	46.83	1	2.82E-03	-46.00	1	1.21E-13	-12.33	1	1.00
	IS700	-5.83	1	1.00	-30.17	1	0.31	4.00	1	1.00	2.50	1	1.00
	IS900	0.67	1	1.00	-1.00	1	1.00	4.50	1	1.00	4.33	1	1.00
	mD10	-11.67	1	0.45	25.67	1	0.62	-20.67	1	0.01	-21.17	1	0.19
	mD10-H	-11.00	1	0.58	30.17	1	0.31	-23.17	1	1.72E-03	-3.33	1	1.00
	mE10-H	-11.67	1	0.45	19.00	1	1.00	-9.33	1	1.00	-16.50	1	0.90
	S1	-4.17	1	1.00	2.67	1	1.00	2.67	1	1.00	-10.67	1	1.00
	S3	-4.33	1	1.00	21.00	1	1.00	-14.00	1	0.28	-4.83	1	1.00
S3	Glass	-7.33	1	1.00	25.83	1	0.62	-32.00	1	1.39E-06	-7.50	1	1.00
	IS700	-1.50	1	1.00	-51.17	1	6.54E-04	18.00	1	0.04	7.33	1	1.00
	IS900	5.00	1	1.00	-22.00	1	1.00	18.50	1	0.03	9.17	1	1.00
	mD10	-7.33	1	1.00	4.67	1	1.00	-6.67	1	1.00	-16.33	1	0.92
	mD10-H	-6.67	1	1.00	9.17	1	1.00	-9.17	1	1.00	1.50	1	1.00
	mE10-H	-7.33	1	1.00	-2.00	1	1.00	4.67	1	1.00	-11.67	1	1.00
	S1	0.17	1	1.00	-18.33	1	1.00	16.67	1	0.08	-5.83	1	1.00
	S2	4.33	1	1.00	-21.00	1	1.00	14.00	1	0.28	4.83	1	1.00

Appendix 8.8: Table of the Pairwise comparison data comparing the surfaces between each other, obtained after GZLM analysis. The % cover for each surface was the mean of all the data collection made in Newton Ferrers. The probability distribution was normal and the link function was identity. The Grey cells represent the significant comparisons. Percentage cover of hard-bodied animals was not represented in this table, as the surfaces were not significantly different for these fouling categories as shown in Appendix 11.7.

	(I) Collections	1
	(J) Collections	2
Total % cover	Mean Difference (I-J)	-6.37
	df	1.000
	p-values	4.29E-03
% cover of microfouling	Mean Difference (I-J)	33.89
	df	1
	p-values	2.04E-09
% cover of weeds	Mean Difference (I-J)	23.44
	df	1
	p-values	0
% cover of soft-bodied animals	Mean Difference (I-J)	-19.67
	df	1
	p-values	4.88E-08
% cover of hard-bodied animals	Mean Difference (I-J)	-44.04
	df	1
	p-values	6.43E-12

Appendix 8.9: Table of the Pairwise comparison data comparing the data collection between each other, obtained after GZLM analysis. The % cover for each data collection was the mean of all the % covers of all the fouling categories made in Newton Ferrers. The probability distribution was normal and the link function was identity.

APPENDIX 9: STATISTICAL TABLES FOR CHAPTER 10

	Source	(Intercept)	Panel	Row	Surfaces	Day	Panel * Row	Panel * Surfaces	Panel * Day	Surfaces * Day	Panel * Surfaces * Day	Panel * Row * Day
total % cover	Wald Chi-Square	13002.80	7.77	22.72	343.99	5337.91	7.56	83.79	182.26	3080.05	671.59	225.06
	df	1	2	6	7	6	12	14	12	42	84	72
	p-values	0	0.02	8.94E-04	0	0	0.82	5.57E-12	0	0	0	1.17E-17
% cover of microfouling	Wald Chi-Square	14496.32	19.99	62.10	1322.44	5053.11	54.84	74.25	157.90	9519.08	994.69	484.83
	df	1	2	6	7	6	12	14	36	42	84	72
	p-values	0	4.57E-05	1.68E-11	0	0	1.94E-07	3.25E-10	3.32E-17	0	0	0
% cover of weeds	Wald Chi-Square	4139.46	109.90	62.20	3711.96	4234.34	217.14	85.67	4852.33	116.30	783.38	277.26
	df	1	2	6	7	6	12	42	42	14	84	84
	p-values	0	0	1.61E-11	0	0	0	8.05E-05	0	0	0	0
% cover of ectocarpoid algae	Wald Chi-Square	3185.65	130.52	46.97	2950.66	3289.80	39.61	118.58	234.57	4188.52	217.35	179.91
	df	1	2	6	7	6	12	14	10	35	60	70
	p-values	0	0	1.90E-08	0	0	8.35E-05	1.19E-18	0	0	1.08E-19	1.26E-11
% cover of soft-bodied animals	Wald Chi-Square	2019.60	32.07	23.92	458.29	2508.15	10.06	51.43	76.16	1351.27	177.02	131.09
	df	1	2	6	7	5	12	14	10	35	60	70
	p-values	0	1.09E-07	5.40E-04	0	0	0.61	3.50E-06	2.82E-12	0	1.76E-13	1.35E-05
% cover of hard-bodied animals	Wald Chi-Square	2049.22	16.16	54.03	347.55	2170.83	54.64	31.68	367.57	840.37	800.94	387.98
	df	1	2	6	7	6	12	14	12	42	84	72
	p-values	0	3.10E-04	7.28E-10	0	0	2.10E-07	4.45E-03	0	0	0	0

Appendix 9.1: Table of the test model effect of the GEEs analysis. The Grey cells represent the significant comparisons.

(I) Surface	(J) Surface	Total % cover			% cover of microfouling			% cover of weeds			% cover of ectocarpoid algae			% cover of soft-bodied animals			% cover of hard-bodied animals		
		Mean Difference (I-J)	df	p-values	Mean Difference (I-J)	df	p-values	Mean Difference (I-J)	df	p-values	Mean Difference (I-J)	df	p-values	Mean Difference (I-J)	df	p-values	Mean Difference (I-J)	df	p-values
H	H1	9.29	1	2.08E-07	-1.96	1	1.00	10.00	1	0	9.13	1	0	2.18	1	0.01	2.03	1	5.43E-04
	H2	12.68	1	8.41E-11	0.08	1	1.00	10.13	1	0	9.10	1	0	2.98	1	9.63E-05	2.60	1	3.01E-06
	H3	17.64	1	0	1.02	1	1.00	9.00	1	1.37E-13	8.74	1	3.09E-16	5.97	1	0	5.03	1	0
	H7	26.10	1	0	-2.35	1	1.00	15.57	1	0	12.91	1	0	7.74	1	0	6.35	1	0
	H10	10.70	1	2.57E-03	-3.35	1	1.00	9.12	1	4.26E-15	7.79	1	2.90E-12	1.40	1	0.33	3.63	1	2.87E-10
	IS900	3.23	1	0.21	-24.87	1	0	11.19	1	0	9.79	1	0	2.50	1	2.31E-03	2.86	1	3.96E-09
	Tie coat	-13.23	1	9.17E-04	7.94	1	1.69E-03	-47.91	1	0	-41.71	1	0	1.20	1	0.33	2.71	1	4.44E-07
H1	H	-9.29	1	2.08E-07	1.96	1	1.00	-10.00	1	0	-9.13	1	0	-2.18	1	0.01	-2.03	1	5.43E-04
	H2	3.38	1	0.21	2.04	1	1.00	0.13	1	1.00	-0.03	1	1.00	0.80	1	0.90	0.57	1	1.00
	H3	8.34	1	4.27E-06	2.98	1	1.00	-1.00	1	1.00	-0.39	1	1.00	3.80	1	5.13E-15	3.00	1	1.09E-11
	H7	16.80	1	0	-0.39	1	1.00	5.57	1	2.17E-08	3.77	1	1.54E-05	5.57	1	0	4.32	1	0
	H10	1.40	1	1.00	-1.39	1	1.00	-0.88	1	1.00	-1.35	1	1.00	-0.78	1	0.90	1.60	1	0.03
	IS900	-6.06	1	2.67E-03	-22.92	1	0	1.20	1	1.00	0.66	1	1.00	0.32	1	1.00	0.83	1	0.59
	Tie coat	-22.52	1	2.22E-10	9.89	1	2.58E-07	-57.91	1	0	-50.84	1	0	-0.98	1	0.32	0.68	1	0.86
H2	H	-12.68	1	8.41E-11	-0.08	1	1.00	-10.13	1	0	-9.10	1	0	-2.98	1	9.63E-05	-2.60	1	3.01E-06
	H1	-3.38	1	0.21	-2.04	1	1.00	-0.13	1	1.00	0.03	1	1.00	-0.80	1	0.90	-0.57	1	1.00
	H3	4.96	1	0.04	0.94	1	1.00	-1.13	1	1.00	-0.36	1	1.00	3.00	1	4.51E-07	2.43	1	4.13E-08
	H7	13.42	1	6.72E-12	-2.43	1	1.00	5.44	1	7.46E-09	3.80	1	2.83E-06	4.77	1	2.73E-17	3.76	1	3.74E-18
	H10	-1.98	1	1.00	-3.43	1	1.00	-1.01	1	1.00	-1.32	1	1.00	-1.58	1	0.15	1.03	1	0.42
	IS900	-9.44	1	5.14E-06	-24.96	1	0	1.06	1	1.00	0.69	1	1.00	-0.48	1	1.00	0.27	1	1.00
	Tie coat	-25.90	1	8.05E-13	7.85	1	1.53E-04	-58.04	1	0	-50.81	1	0	-1.78	1	0.01	0.12	1	1.00
H3	H	-17.64	1	0	-1.02	1	1.00	-9.00	1	1.37E-13	-8.74	1	3.09E-16	-5.97	1	0	-5.03	1	0
	H1	-8.34	1	4.27E-06	-2.98	1	1.00	1.00	1	1.00	0.39	1	1.00	-3.80	1	5.13E-15	-3.00	1	1.09E-11

	H2	-4.96	1	0.04	-0.94	1	1.00	1.13	1	1.00	0.36	1	1.00	-3.00	1	4.51E-07	-2.43	1	4.13E-08
	H7	8.46	1	4.63E-06	-3.37	1	1.00	6.57	1	1.28E-10	4.17	1	8.72E-07	1.77	1	1.39E-04	1.33	1	6.49E-05
	H10	-6.94	1	0.07	-4.37	1	0.88	0.12	1	1.00	-0.95	1	1.00	-4.58	1	8.34E-16	-1.40	1	0.02
	IS900	-14.40	1	7.38E-15	-25.90	1	0	2.20	1	0.31	1.05	1	1.00	-3.48	1	1.06E-10	-2.16	1	7.15E-08
	Tie coat	-30.86	1	1.25E-18	6.91	1	4.32E-03	-56.91	1	0	-50.45	1	0	-4.78	1	0	-2.31	1	0
H7	H	-26.10	1	0	2.35	1	1.00	-15.57	1	0	-12.91	1	0	-7.74	1	0	-6.35	1	0
	H1	-16.80	1	0	0.39	1	1.00	-5.57	1	2.17E-08	-3.77	1	1.54E-05	-5.57	1	0	-4.32	1	0
	H2	-13.42	1	6.72E-12	2.43	1	1.00	-5.44	1	7.46E-09	-3.80	1	2.83E-06	-4.77	1	2.73E-17	-3.76	1	2.03E-08
	H3	-8.46	1	4.63E-06	3.37	1	1.00	-6.57	1	1.28E-10	-4.17	1	8.72E-07	-1.77	1	1.39E-04	-1.33	1	6.49E-05
	H10	-15.40	1	3.05E-06	-1.00	1	1.00	-6.45	1	1.51E-10	-5.12	1	7.22E-08	-6.35	1	0	-2.72	1	0
	IS900	-22.86	1	0	-22.53	1	0	-4.38	1	2.15E-06	-3.11	1	1.46E-04	-5.25	1	0	-3.49	1	3.74E-18
	Tie coat	-39.32	1	0	10.28	1	1.39E-09	-63.48	1	0	-54.61	1	0	-6.55	1	0	-3.64	1	1.30E-18
H10	H	-10.70	1	2.57E-03	3.35	1	1.00	-9.12	1	4.26E-15	-7.79	1	2.90E-12	-1.40	1	0.33	-3.63	1	2.87E-10
	H1	-1.40	1	1.00	1.39	1	1.00	0.88	1	1.00	1.35	1	1.00	0.78	1	0.90	-1.60	1	0.03
	H2	1.98	1	1.00	3.43	1	1.00	1.01	1	1.00	1.32	1	1.00	1.58	1	0.15	-1.03	1	0.42
	H3	6.94	1	0.07	4.37	1	0.88	-0.12	1	1.00	0.95	1	1.00	4.58	1	8.34E-16	1.40	1	0.02
	H7	15.40	1	3.05E-06	1.00	1	1.00	6.45	1	1.51E-10	5.12	1	7.22E-08	6.35	1	0	2.72	1	2.03E-08
	IS900	-7.46	1	0.07	-21.52	1	0	2.07	1	0.31	2.01	1	0.25	1.10	1	0.49	-0.77	1	0.63
	Tie coat	-23.92	1	1.35E-07	11.29	1	1.08E-07	-57.03	1	0	-49.49	1	0	-0.20	1	1.00	-0.92	1	0.59
IS900	H	-3.23	1	0.21	24.87	1	0	-11.19	1	0	-9.79	1	0	-2.50	1	2.31E-03	-2.86	1	3.96E-09
	H1	6.06	1	2.67E-03	22.92	1	0	-1.20	1	1.00	-0.66	1	1.00	-0.32	1	1.00	-0.83	1	0.59
	H2	9.44	1	5.14E-06	24.96	1	0	-1.06	1	1.00	-0.69	1	1.00	0.48	1	1.00	-0.27	1	0.63
	H3	14.40	1	7.38E-15	25.90	1	0	-2.20	1	0.31	-1.05	1	1.00	3.48	1	1.06E-10	2.16	1	9.65E-09
	H7	22.86	1	0	22.53	1	0	4.38	1	2.15E-06	3.11	1	1.46E-04	5.25	1	0	3.49	1	0
	H10	7.46	1	0.07	21.52	1	0	-2.07	1	0.31	-2.01	1	0.25	-1.10	1	0.49	0.77	1	1.00
	Tie coat	-16.46	1	1.25E-06	32.81	1	0	-59.11	1	0	-51.50	1	0	-1.30	1	0.12	-0.15	1	1.00
Tie coat	H	13.23	1	9.17E-04	-7.94	1	1.69E-03	47.91	1	0	41.71	1	0	-1.20	1	0.33	-2.71	1	4.44E-07
	H1	22.52	1	2.22E-10	-9.89	1	2.58E-07	57.91	1	0	50.84	1	0	0.98	1	0.32	-0.68	1	0.86

|																		
H2	25.90	1	8.05E-13	-7.85	1	1.53E-04	58.04	1	0	50.81	1	0	1.78	1	0.01	-0.12	1	0.59
H3	30.86	1	1.25E-18	-6.91	1	4.32E-03	56.91	1	0	50.45	1	0	4.78	1	0	2.31	1	7.15E-08
H7	39.32	1	0	-10.28	1	1.39E-09	63.48	1	0	54.61	1	0	6.55	1	0	3.64	1	1.30E-18
H10	23.92	1	1.35E-07	-11.29	1	1.08E-07	57.03	1	0	49.49	1	0	0.20	1	1.00	0.92	1	1.00
IS900	16.46	1	1.25E-06	-32.81	1	0	59.11	1	0	51.50	1	0	1.30	1	0.12	0.15	1	1.00

Appendix 9.8: Table of the Pairwise comparison data comparing the surfaces between each other, obtained after GEEs analysis. The % cover for each surface was the mean of all the data collection made in Hartlepool Marina. The probability distribution was normal and the link function was identity. The Grey cells represent the significant comparisons.

(I) days of immersion	(J) days of immersion	Total % cover			% cover of microfouling			% cover of weeds			% cover of ectocarpoid algae			% cover of soft-bodied animals			% cover of hard-bodied animals		
		Mean Difference (I-J)	df	p-values	Mean Difference (I-J)	df	p-values	Mean Difference (I-J)	df	p-values	Mean Difference (I-J)	df	p-values	Mean Difference (I-J)	df	p-values	Mean Difference (I-J)	df	p-values
23	37	6.40	1	1.56E-10	21.02	1	0	-14.33	1	0	-14.39	1	0	0.00	1	.	-0.06	1	0.02
	43	-68.00	1	0	-38.88	1	0	-28.86	1	0	-28.86	1	0	-0.10	1	0.13	-0.06	1	1.94E-03
	61	-67.11	1	0	-41.38	1	0	-24.47	1	0	-24.47	1	0	-0.45	1	0.06	-0.66	1	2.63E-10
	80	-65.60	1	0	-33.08	1	0	-20.77	1	0	-20.77	1	0	-3.18	1	0	-8.34	1	0
	98	-67.38	1	0	-22.60	1	0	-26.97	1	0	-3.80	1	6.84E-15	-9.79	1	0	-7.80	1	0
	157	-39.16	1	0	11.70	1	0	-1.46	1	4.43E-11	0.00	1	1.00	-30.14	1	0	-18.90	1	0
37	23	-6.40	1	1.56E-10	-21.02	1	0	14.33	1	0	14.39	1	0	0.00	1	.	0.06	1	0.02
	43	-74.40	1	0	-59.89	1	0	-14.53	1	0	-14.47	1	0	-0.10	1	0.13	0.00	1	0.83
	61	-73.52	1	0	-62.39	1	0	-10.14	1	0	-10.08	1	0	-0.45	1	0.06	-0.59	1	1.55E-08
	80	-72.01	1	0	-54.09	1	0	-6.44	1	0	-6.38	1	0	-3.18	1	0	-8.28	1	0
	98	-73.79	1	0	-43.62	1	0	-12.63	1	0	10.59	1	0	-9.79	1	0	-7.73	1	0
	157	-45.56	1	0	-9.32	1	5.85E-18	12.87	1	0	14.39	1	0	-30.14	1	0	-18.84	1	0
43	23	68.00	1	0	38.88	1	0	28.86	1	0	28.86	1	0	0.10	1	0.13	0.06	1	1.94E-03
	37	74.40	1	0	59.89	1	0	14.53	1	0	14.47	1	0	0.10	1	0.13	0.00	1	0.83
	61	0.89	1	1.00	-2.50	1	0.06	4.39	1	2.69E-05	4.39	1	1.80E-05	-0.35	1	0.13	-0.60	1	1.58E-08
	80	2.40	1	0.07	5.80	1	1.27E-05	8.09	1	0	8.09	1	0	-3.07	1	0	-8.28	1	0
	98	0.62	1	1.00	16.28	1	0	1.89	1	0.13	25.06	1	0	-9.68	1	0	-7.74	1	0
	157	28.85	1	0	50.58	1	0	27.40	1	0	28.86	1	0	-30.04	1	0	-18.84	1	0
61	23	67.11	1	0	41.38	1	0	24.47	1	0	24.47	1	0	0.45	1	0.06	0.66	1	2.63E-10
	37	73.52	1	0	62.39	1	0	10.14	1	0	10.08	1	0	0.45	1	0.06	0.59	1	1.55E-08
	43	-0.89	1	1.00	2.50	1	0.06	-4.39	1	2.69E-05	-4.39	1	1.80E-05	0.35	1	0.13	0.60	1	1.58E-08
	80	1.51	1	0.04	8.30	1	5.69E-18	3.70	1	1.04E-08	3.70	1	7.77E-09	-2.73	1	3.53E-12	-7.68	1	0
	98	-0.27	1	1.00	18.77	1	0	-2.50	1	0.03	20.67	1	0	-9.34	1	0	-7.14	1	0
	157	27.96	1	0	53.07	1	0	23.01	1	0	24.47	1	0	-29.69	1	0	-18.24	1	0
80	23	65.60	1	0	33.08	1	0	20.77	1	0	20.77	1	0	3.18	1	0	8.34	1	0

	37	72.01	1	0	54.09	1	0	6.44	1	0	6.38	1	0	3.18	1	0	8.28	1	0
	43	-2.40	1	0.07	-5.80	1	1.27E-05	-8.09	1	0	-8.09	1	0	3.07	1	0	8.28	1	0
	61	-1.51	1	0.04	-8.30	1	5.69E-18	-3.70	1	1.04E-08	-3.70	1	7.77E-09	2.73	1	3.53E-12	7.68	1	0
	98	-1.78	1	4.35E-03	10.47	1	9.90E-17	-6.20	1	7.69E-10	16.97	1	0	-6.61	1	0	0.55	1	0.60
	157	26.45	1	0	44.77	1	0	19.31	1	0	20.77	1	0	-26.96	1	0	-10.56	1	0
98	23	67.38	1	0	22.60	1	0	26.97	1	0	3.80	1	6.84E-15	9.79	1	0	7.80	1	0
	37	73.79	1	0	43.62	1	0	12.63	1	0	-10.59	1	0	9.79	1	0	7.73	1	0
	43	-0.62	1	1.00	-16.28	1	0	-1.89	1	0.13	-25.06	1	0	9.68	1	0	7.74	1	0
	61	0.27	1	1.00	-18.77	1	0	2.50	1	0.03	-20.67	1	0	9.34	1	0	7.14	1	0
	80	1.78	1	4.35E-03	-10.47	1	9.90E-17	6.20	1	7.69E-10	-16.97	1	0	6.61	1	0	-0.55	1	0.60
	157	28.23	1	0	34.30	1	0	25.51	1	0	3.80	1	6.84E-15	-20.35	1	0	-11.11	1	0
157	23	39.16	1	0	-11.70	1	0	1.46	1	4.43E-11	0.00	1	1.00	30.14	1	0	18.90	1	0
	37	45.56	1	0	9.32	1	5.85E-18	-12.87	1	0	-14.39	1	0	30.14	1	0	18.84	1	0
	43	-28.85	1	0	-50.58	1	0	-27.40	1	0	-28.86	1	0	30.04	1	0	18.84	1	0
	61	-27.96	1	0	-53.07	1	0	-23.01	1	0	-24.47	1	0	29.69	1	0	18.24	1	0
	80	-26.45	1	0	-44.77	1	0	-19.31	1	0	-20.77	1	0	26.96	1	0	10.56	1	0
	98	-28.23	1	0	-34.30	1	0	-25.51	1	0	-3.80	1	6.84E-15	20.35	1	0	11.11	1	0

Appendix 9.3: Table of the Pairwise comparison data comparing the days of immersion between each other, obtained after GEEs analysis. The % cover for each day of immersion was the mean of all the % covers of all the fouling categories made in Hartlepool Marina. The probability distribution was normal and the link function was identity.
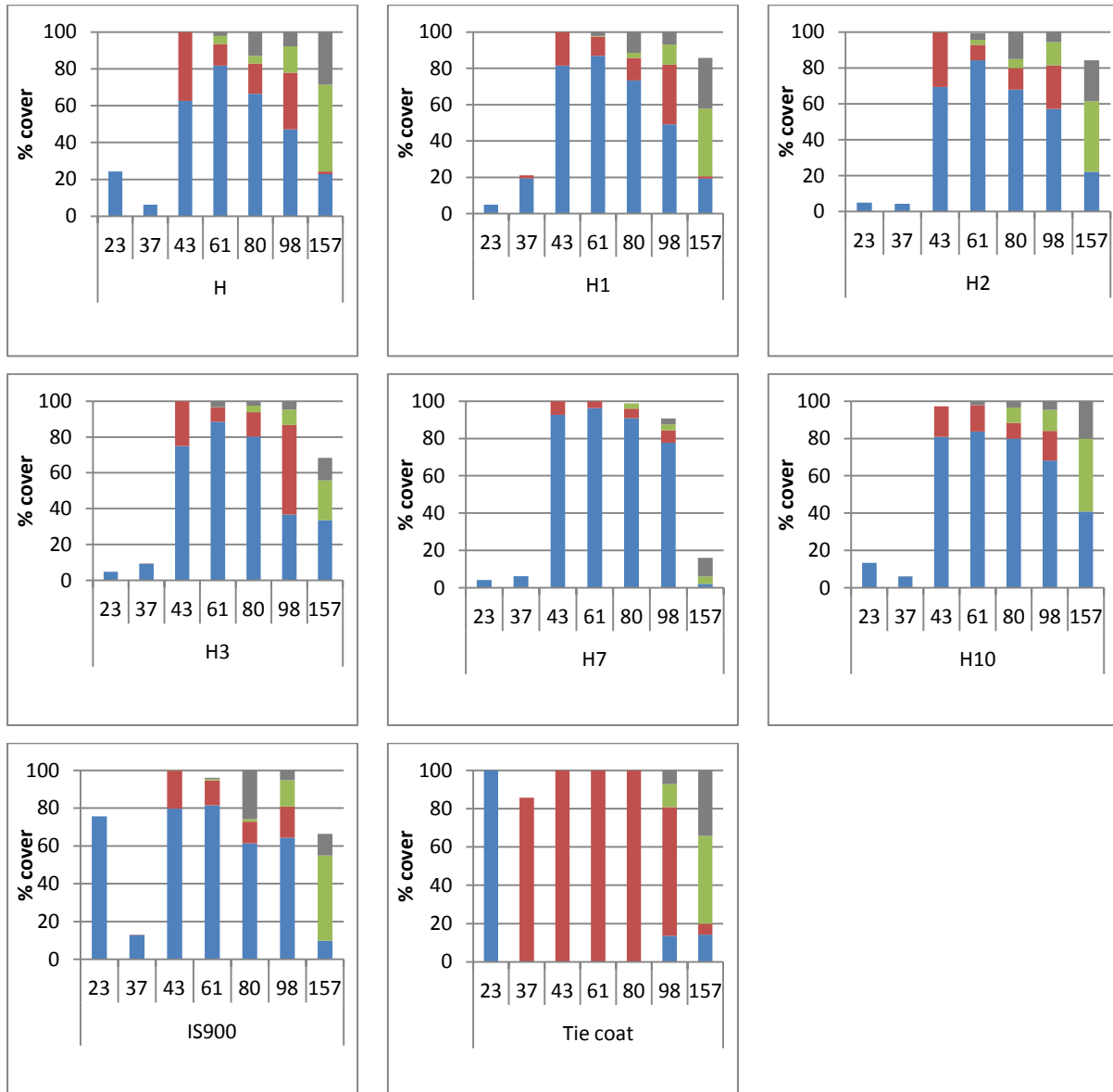
Appendix 10.1: Percentage cover observed on 8 different test surfaces attached to Panel 2, immersed in Hartlepool Marina during 157 days of immersion. Percentage cover for the 4 fouling categories: microfouling (blue), weeds (red), soft-bodied animals (green) and hard-bodied animals (grey). For each graph, the axis x represents the length of immersion for each coating. Mean of 7 replicates.
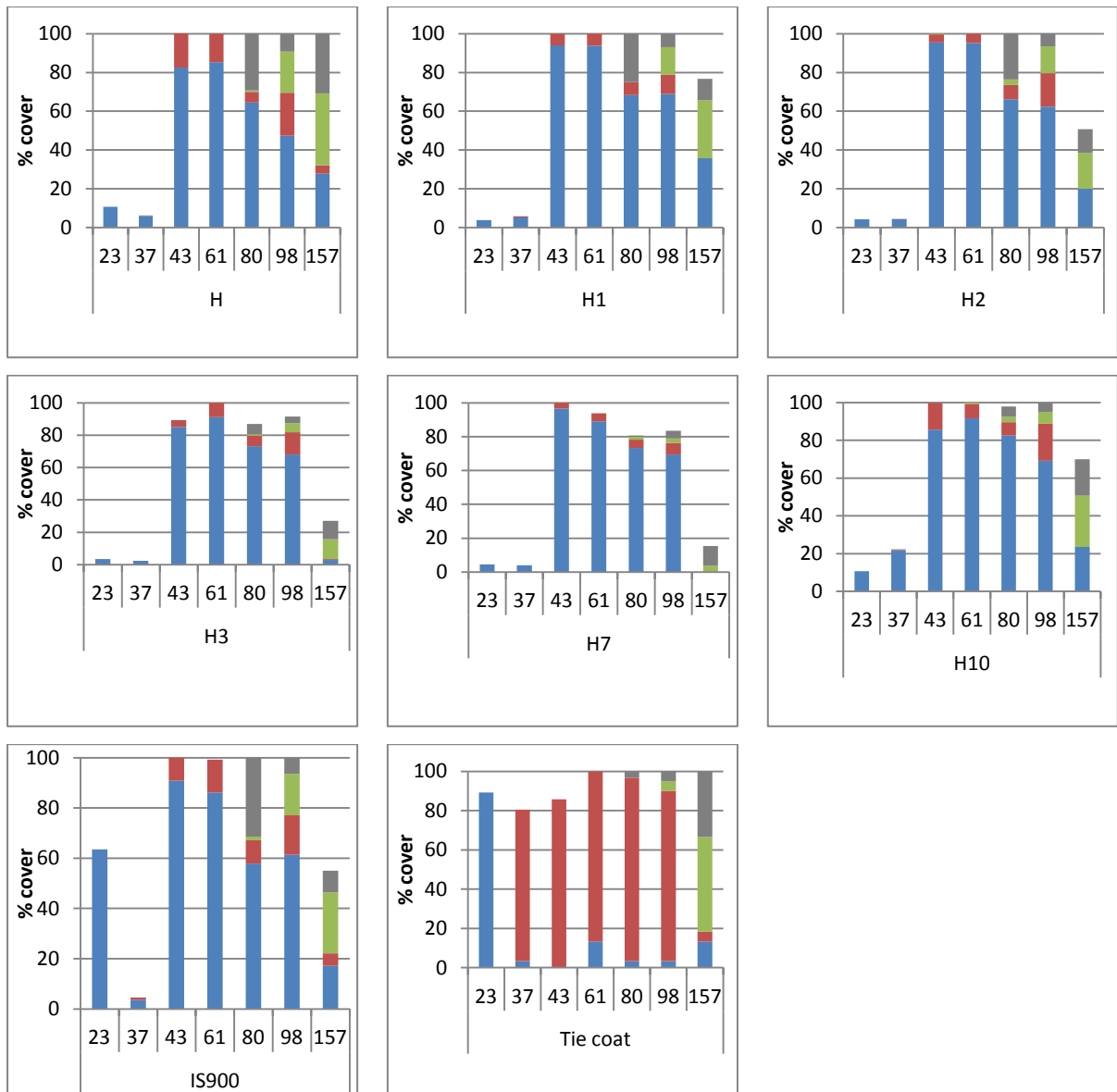
Appendix 10.2: Percentage cover observed on 8 different test surfaces attached to Panel 3, immersed in Hartlepool Marina during 157 days of immersion. Percentage cover for the 4 fouling categories: microfouling (blue), weeds (red), soft-bodied animals (green) and hard-bodied animals (grey). For each graph, the axis x represents the length of immersion for each coating. Mean of 7 replicates.

APPENDIX 11: IMAGES ON PANELS

Appendix 11.1: Images of the panels containing silicone 'hybrid' coatings, IS900 and tie coat after 43 days' immersion.

APPENDIX 12: STATISTICAL TABLES FOR CHAPTER 11

	Source	(Intercept)	Panel	Row	Surfaces	Day	Panel * Row	Panel * Surfaces	Panel * Day	Surfaces * Day	Panel * Row * Day	Panel * Surfaces * Day
total % cover	Wald Chi-Square	.	122.00	0.00	844.78	0.00	54.18	89.61	227.64	1147.82	155.06	232.61
	df	.	2	2	6	2	12	12	7	24	42	43
	p-values	.	0	1.00	0	1.00	2.54E-07	5.88E-14	0	0	7.23E-15	0
% cover of microfouling	Wald Chi-Square	7792.41	57.91	21.46	129.04	5412.01	42.84	86.90	229.87	1047.06	196.23	226.57
	df	1	2	6	6	4	12	12	8	24	48	48
	p-values	0	2.66E-13	1.52E-03	0	0	2.40E-05	1.96E-13	0	0	5.42E-20	0
% cover of weeds	Wald Chi-Square	156.28	27.73	11.47	184.84	322.87	17.06	32.78	81.24	443.90	40.69	115.37
	df	1	2	6	6	4	12	12	8	24	48	48
	p-values	0	9.50E-07	0.07	0	0	0.15	1.05E-03	2.75E-14	0	0.76	1.79E-07
% cover of ectocarpoid algae	Wald Chi-Square	122.38	20.41	10.71	144.76	163.59	15.17	23.97	127.49	209.72	51.27	162.56
	df	1	2	6	6	4	12	12	8	24	48	48
	p-values	0	3.71E-05	0.10	0	0	0.23	0.02	0	0	0.35	2.28E-14
% cover of soft-bodied animals	Wald Chi-Square	1334.96	9.93	32.15	89.69	1553.24	22.05	31.11	37.69	125.55	81.64	92.12
	df	1	2	6	6	4	12	12	8	24	48	48
	p-values	0	0.01	1.53E-05	3.52E-17	0	0.04	1.90E-03	8.59E-06	9.84E-16	1.76E-03	1.33E-04
% cover of hard-bodied animals	Wald Chi-Square	2464.89	17.02	66.29	178.45	2546.61	20.25	30.65	84.32	281.81	62.24	103.32
	df	1	2	6	6	4	12	12	7	24	42	42
	p-values	0	2.01E-04	2.35E-12	0	0	0.06	2.22E-03	1.80E-15	0	0.02	4.42E-07

Appendix 12.1: Table of the test model effect of the GEEs analysis. The Grey cells represent the significant comparisons.

(I) Surfaces	(J) Surfaces	Total % cover			% cover of microfouling			% cover of weeds			% cover of ectocarpoid algae			% cover of soft-bodied animals			% cover of hard-bodied animals		
		Mean Difference (I-J)	df	p-values	Mean Difference (I-J)	df	p-values	Mean Difference (I-J)	df	p-values	Mean Difference (I-J)	df	p-values	Mean Difference (I-J)	df	p-values	Mean Difference (I-J)	df	p-values
M1	M2	14.49	1	2.92E-06	12.78	1	1.64E-04	0.38	1	1.00	0.23	1	1.00	0.96	1	0.22	0.36	1	0.28
	M3	19.99	1	2.14E-12	19.33	1	8.71E-12	0.10	1	1.00	-0.08	1	1.00	0.00	1	1.00	0.56	1	1.00E-04
	M4	17.09	1	2.85E-08	16.00	1	1.06E-07	0.19	1	1.00	0.06	1	1.00	0.62	1	1.00	0.28	1	0.45
	M5	11.81	1	2.84E-04	10.91	1	8.66E-04	-0.02	1	1.00	-0.20	1	1.00	0.64	1	1.00	0.28	1	0.39
	IS900	24.56	1	2.09E-15	19.57	1	2.43E-10	0.39	1	1.00	0.25	1	1.00	3.17	1	6.54E-14	1.43	1	0
	Tie coat	-21.23	1	1.03E-13	-1.10	1	1.00	-20.08	1	0	-17.43	1	0	0.03	1	1.00	-0.09	1	1.00
M2	M1	-14.49	1	2.92E-06	-12.78	1	1.64E-04	-0.38	1	1.00	-0.23	1	1.00	-0.96	1	0.22	-0.36	1	0.28
	M3	5.50	1	0.02	6.55	1	0.02	-0.29	1	1.00	-0.30	1	1.00	-0.96	1	0.34	0.20	1	1.00
	M4	2.60	1	0.38	3.22	1	0.62	-0.19	1	1.00	-0.17	1	1.00	-0.34	1	1.00	-0.09	1	1.00
	M5	-2.68	1	0.38	-1.87	1	1.00	-0.40	1	1.00	-0.43	1	1.00	-0.32	1	1.00	-0.09	1	1.00
	IS900	10.08	1	4.85E-05	6.79	1	0.04	0.01	1	1.00	0.02	1	1.00	2.21	1	1.84E-07	1.07	1	6.24E-10
	Tie coat	-35.71	1	0	-13.88	1	1.69E-06	-20.46	1	0	-17.66	1	0	-0.93	1	0.85	-0.45	1	0.15
M3	M1	-19.99	1	2.14E-12	-19.33	1	8.71E-12	-0.10	1	1.00	0.08	1	1.00	0.00	1	1.00	-0.56	1	1.00E-04

	M2	-5.50	1	0.02	-6.55	1	0.02	0.29	1	1.00	0.30	1	1.00	0.96	1	0.34	-0.20	1	1.00
	M4	-2.90	1	0.38	-3.33	1	0.50	0.10	1	1.00	0.13	1	1.00	0.62	1	1.00	-0.29	1	0.45
	M5	-8.18	1	1.49E-04	-8.42	1	1.64E-04	-0.11	1	1.00	-0.12	1	1.00	0.64	1	1.00	-0.29	1	0.37
	IS900	4.57	1	0.11	0.24	1	1.00	0.30	1	1.00	0.32	1	1.00	3.17	1	5.93E-12	0.87	1	6.26E-11
	Tie coat	-41.22	1	0	-20.43	1	3.42E-17	-20.17	1	0	-17.35	1	0	0.03	1	1.00	-0.65	1	9.76E-05
M4	M1	-17.09	1	2.85E-08	-16.00	1	1.06E-07	-0.19	1	1.00	-0.06	1	1.00	-0.62	1	1.00	-0.28	1	0.45
	M2	-2.60	1	0.38	-3.22	1	0.62	0.19	1	1.00	0.17	1	1.00	0.34	1	1.00	0.09	1	1.00
	M3	2.90	1	0.38	3.33	1	0.50	-0.10	1	1.00	-0.13	1	1.00	-0.62	1	1.00	0.29	1	0.45
	M5	-5.28	1	0.06	-5.09	1	0.09	-0.21	1	1.00	-0.26	1	1.00	0.02	1	1.00	0.00	1	1.00
	IS900	7.48	1	0.01	3.57	1	0.54	0.20	1	1.00	0.19	1	1.00	2.55	1	6.42E-12	1.15	1	1.54E-12
	Tie coat	-38.31	1	0	-17.10	1	3.36E-11	-20.27	1	0	-17.49	1	0	-0.59	1	1.00	-0.36	1	0.33
M5	M1	-11.81	1	2.84E-04	-10.91	1	8.66E-04	0.02	1	1.00	0.20	1	1.00	-0.64	1	1.00	-0.28	1	0.39
	M2	2.68	1	0.38	1.87	1	1.00	0.40	1	1.00	0.43	1	1.00	0.32	1	1.00	0.09	1	1.00
	M3	8.18	1	1.49E-04	8.42	1	1.64E-04	0.11	1	1.00	0.12	1	1.00	-0.64	1	1.00	0.29	1	0.37
	M4	5.28	1	0.06	5.09	1	0.09	0.21	1	1.00	0.26	1	1.00	-0.02	1	1.00	0.00	1	1.00
	IS900	12.75	1	1.92E-07	8.66	1	1.06E-03	0.41	1	1.00	0.45	1	1.00	2.53	1	1.63E-08	1.15	1	2.61E-15
	Tie coat	-33.04	1	0	-12.01	1	1.12E-05	-20.06	1	0	-17.23	1	0	-0.61	1	1.00	-0.36	1	0.25

IS900	M1	-24.56	1	2.09E-15	-19.57	1	2.43E-10	-0.39	1	1.00	-0.25	1	1.00	-3.17	1	6.54E-14	-1.43	1	0
	M2	-10.08	1	4.85E-05	-6.79	1	0.04	-0.01	1	1.00	-0.02	1	1.00	-2.21	1	1.84E-07	-1.07	1	6.24E-10
	M3	-4.57	1	0.11	-0.24	1	1.00	-0.30	1	1.00	-0.32	1	1.00	-3.17	1	5.93E-12	-0.87	1	6.26E-11
	M4	-7.48	1	0.01	-3.57	1	0.54	-0.20	1	1.00	-0.19	1	1.00	-2.55	1	6.42E-12	-1.15	1	1.54E-12
	M5	-12.75	1	1.92E-07	-8.66	1	1.06E-03	-0.41	1	1.00	-0.45	1	1.00	-2.53	1	1.63E-08	-1.15	1	2.61E-15
	Tie coat	-45.79	1	0	-20.67	1	2.49E-14	-20.47	1	0	-17.68	1	0	-3.14	1	1.52E-08	-1.51	1	0
Tie coat	M1	21.23	1	1.03E-13	1.10	1	1.00	20.08	1	0	17.43	1	0	-0.03	1	1.00	0.09	1	1.00
	M2	35.71	1	0	13.88	1	1.69E-06	20.46	1	0	17.66	1	0	0.93	1	0.85	0.45	1	0.15
	M3	41.22	1	0	20.43	1	3.42E-17	20.17	1	0	17.35	1	0	-0.03	1	1.00	0.65	1	9.76E-05
	M4	38.31	1	0	17.10	1	3.36E-11	20.27	1	0	17.49	1	0	0.59	1	1.00	0.36	1	0.33
	M5	33.04	1	0	12.01	1	1.12E-05	20.06	1	0	17.23	1	0	0.61	1	1.00	0.36	1	0.25
	IS900	45.79	1	0	20.67	1	2.49E-14	20.47	1	0	17.68	1	0	3.14	1	1.52E-08	1.51	1	0

Appendix 12.2: Table of the Pairwise comparison data comparing the surfaces between each other, obtained after GEEs analysis. The % cover for each surface was the mean of all the data collection made in Hartlepool Marina. The probability distribution was normal and the link function was identity. The Grey cells represent the significant comparisons.

(I) day of immersion	(J) day of immersion	% cover of microfouling			% cover of weeds			% cover of ectocarpoid algae			% cover of soft-bodied animals			% cover of hard-bodied animals		
		Mean Difference (I-J)	df	p-values	Mean Difference (I-J)	df	p-values	Mean Difference (I-J)	df	p-values	Mean Difference (I-J)	df	p-values	Mean Difference (I-J)	df	p-values
20	39	-26.58	1	0	-5.35	1	0	-4.87	1	0	-0.15	1	0.05	-0.01	1	0.06
	47	-29.94	1	0	-5.54	1	0	-5.24	1	0	-0.46	1	2.54E-04	-0.05	1	0.01
	60	-71.30	1	0	-2.27	1	6.99E-09	-1.74	1	1.23E-04	-0.46	1	1.07E-03	-1.94	1	0
	83	-45.74	1	0	-2.67	1	1.18E-09	-1.79	1	2.84E-07	-20.26	1	0	-8.18	1	0
39	20	26.58	1	0	5.35	1	0	4.87	1	0	0.15	1	0.05	0.01	1	0.06
	47	-3.36	1	0.02	-0.20	1	0.68	-0.37	1	0.73	-0.31	1	0.04	-0.03	1	0.06
	60	-44.72	1	0	3.07	1	4.73E-14	3.13	1	1.76E-10	-0.31	1	0.07	-1.93	1	0
	83	-19.16	1	0	2.67	1	1.46E-07	3.08	1	4.49E-08	-20.11	1	0	-8.16	1	0
47	20	29.94	1	0	5.54	1	0	5.24	1	0	0.46	1	2.54E-04	0.05	1	0.01
	39	3.36	1	0.02	0.20	1	0.68	0.37	1	0.73	0.31	1	0.04	0.03	1	0.06
	60	-41.36	1	0	3.27	1	2.09E-16	3.50	1	2.74E-15	0.00	1	1.00	-1.89	1	0
	83	-15.80	1	0	2.87	1	8.95E-09	3.46	1	1.60E-13	-19.80	1	0	-8.13	1	0
60	20	71.30	1	0	2.27	1	6.99E-09	1.74	1	1.23E-04	0.46	1	1.07E-03	1.94	1	0
	39	44.72	1	0	-3.07	1	4.73E-14	-3.13	1	1.76E-10	0.31	1	0.07	1.93	1	0
	47	41.36	1	0	-3.27	1	2.09E-16	-3.50	1	2.74E-15	0.00	1	1.00	1.89	1	0
	83	25.56	1	0	-0.40	1	0.39	-0.05	1	0.93	-19.80	1	0	-6.24	1	0
83	20	45.74	1	0	2.67	1	1.18E-09	1.79	1	2.84E-07	20.26	1	0	8.18	1	0
	39	19.16	1	0	-2.67	1	1.46E-07	-3.08	1	4.49E-08	20.11	1	0	8.16	1	0
	47	15.80	1	0	-2.87	1	8.95E-09	-3.46	1	1.60E-13	19.80	1	0	8.13	1	0
	60	-25.56	1	0	0.40	1	0.39	0.05	1	0.93	19.80	1	0	6.24	1	0

Appendix 12.3: Table of the Pairwise comparison data comparing the days of immersion between each other, obtained after GEEs analysis. The % cover for each day of immersion was the mean of all the % covers of all the fouling categories made in Hartlepool Marina. The probability distribution was

normal and the link function was identity. Total % cover was not represented in this table, as the surfaces were not significantly different for these fouling categories as shown in Appendix 11.7.
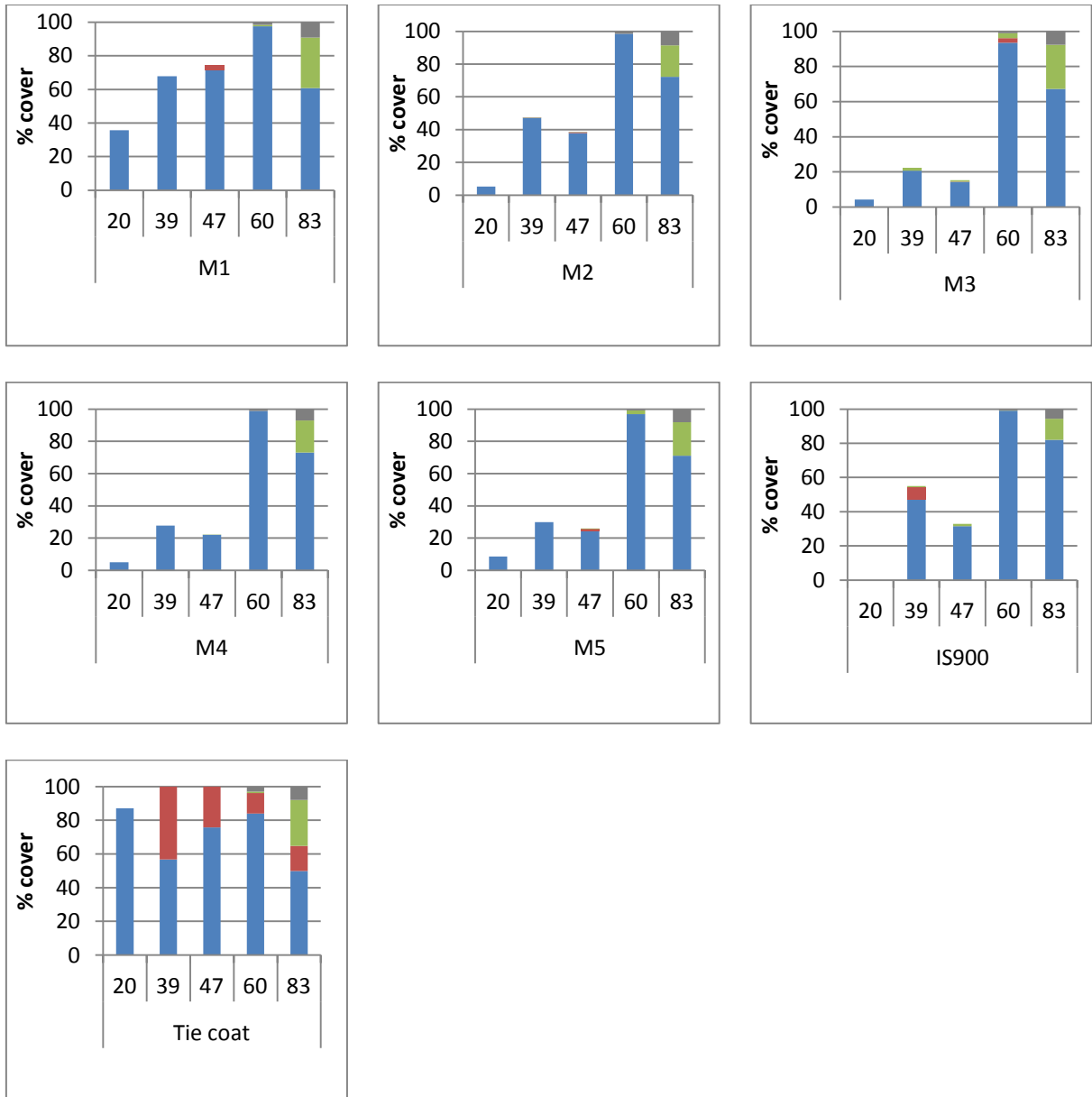
Appendix 13.1: Percentage cover observed on 7 different test surfaces attached to Panel 1, immersed in Hartlepool Marina during 83 days of immersion. Percentage cover for the 4 fouling categories: microfouling (blue), weeds (red), soft-bodied animals (green) and hard-bodied animals (grey). For each graph, the axis x represents the length of immersion for each coating. Mean of 7 replicates.
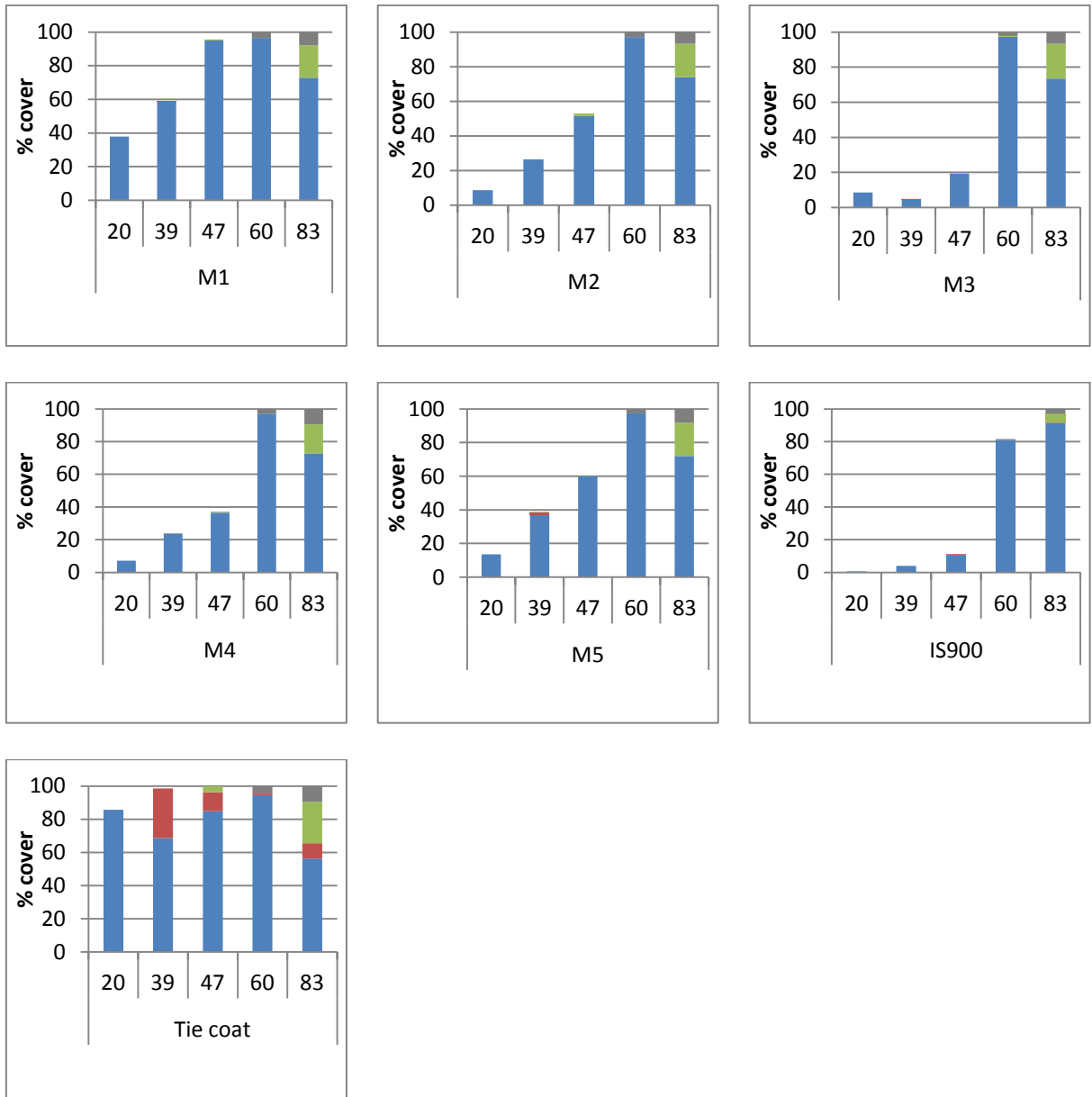
Appendix 13.2: Percentage cover observed on 7 different test surfaces attached to Panel 3, immersed in Hartlepool Marina during 83 days of immersion. Percentage cover for the 4 fouling categories: microfouling (blue), weeds (red), soft-bodied animals (green) and hard-bodied animals (grey). For each graph, the axis x represents the length of immersion for each coating. Mean of 7 replicates.

APPENDIX 14: METHOD PAPER

Evariste E, Gachon CMM, Callow ME, Callow JA. 2012. Development and characteristics of an adhesion bioassay for ectocarpoid algae. Biofouling 28: 15-27.

APPENDIX 15: XEROGEL PAPER

Evariste E, Gatley CM, Detty MR, Callow ME, Callow JA. 2013. The performance of aminoalkyl/fluorocarbon/hydrocarbon-modified xerogel coatings against the marine alga *Ectocarpus crouaniorum*: Relative roles of surface energy and charge. Biofouling 29(2): 171-184.

References

Abarzua S, Jakubowski S. 1995. Biotechnological investigation for the prevention of biofouling. I. Biological and biochemical principles for the prevention of biofouling. Mar Ecol Prog Ser 123: 301-312.

Akesso L, Navabpour P, DTeer, Pettitt ME, Callow ME, Liu C, Su X, Wang S, Zhao Q, Donik C, Kocijan A, Jenko M, Callow JA. 2009a. Deposition parameters to improve the fouling-release properties of thin siloxane coatings prepared by PACVD. Appl Surf Sci 255: 6508-6514.

Akesso L, Pettitt ME, Callow JA, Callow ME, Stallard J, Teer D, Liu C, Wang S, Zhao Q, D'Souza F, Willemsen PR, Donnelly GT, Donik C, Kocijan A, Jenko M, Jones LA, Guinaldo PC. 2009b. The potential of nano-structured silicon oxide type coatings deposited by PACVD for control of aquatic biofouling. Biofouling 25: 55-67.

Aldred N, Ekblad T, Andersson O, Liedberg B, Clare AS. 2011. Real-time quantification of microscale bioadhesion events in situ using imaging surface plasmon resonance (iSPR). ACS Appl Mater Interfaces 3: 2085-2091.

Aldred N, Ista LK, Callow ME, Callow JA, Lopez GP, Clare AS. 2006. Mussel (*Mytilus edulis*) byssus deposition in response to variations in surface wettability. J R Soc Interface 3: 37-43.

Aldred N, Li G, Gao Y, Clare AS, Jiang S. 2010. Modulation of barnacle (*Balanus amphitrite* Darwin) cyprid settlement behavior by sulfobetaine and carboxybetaine methacrylate polymer coatings. Biofouling 26: 673-683.

Amin SA, Green DH, Hart MC, Küpper FC, Sunda WG, Carrano CJ. 2009. Photolysis of iron-siderophore chelates promotes bacterial-algal mutualism. Proceedings of the National Academy of Sciences 106: 17071-17076.

Anderson C, Atlar M, Callow M, Candries M, Milne A, Townsin RL. 2003. The development of foul-release coatings for seagoing vessels Proceedings of IMarEST - Part B4 - Journal of Marine Design and Operations 4: 11-23.

Anderson CD and Hunter JE. 2000. Whither antifouling paints after TBT? NAV 2000 International Conference on Ship and Shipping Research, 13th Congress, Paper 3.7. Venice, Italy, 19-22 September 2000.

Baier RE, DePalma VA. 1971. The relation of the internal surface of grafts to thrombosis. In: Ed. Dale WA. Management of occlusive arterial disease. Year book medical publishers, Chicago. pp. 147-163

Bailey-Brock JH. 1989. Fouling community development on an artificial reef in Hawaiian waters. B Mar Sci 44: 580-591.

Baker JRJ. 1971. Studies on the ship fouling alga *Ectocarpus*. University of Leeds.

Baker JRJ, Evans LV. 1973. The ship-fouling alga *Ectocarpus* I. Ultrastructure and cytochemistry of plurilocular reproductive stages. Protoplasma 77: 1-13.

Baldauf SL. 2003. The deep roots of eukaryotes. Science 300: 1703-1706.

Baldauf SL. 2008. An overview of the phylogeny and diversity of eukaryotes. J Syst Evol 46: 263-273.

Banerjee I, Pangule RC, Kane RS. 2011. Antifouling Coatings: Recent Developments in the Design of Surfaces That Prevent Fouling by Proteins, Bacteria, and Marine Organisms. Adv Mat 23(6): 690–718.

Barry AJ. 1946. Viscometric investigation of dimethylsiloxane polymers. J Appl Phys 17: 1020-1024.

Barry SC, Hayes KR, Hewitt CL, Behrens HL, Dragsund E, Bakke SM. 2008. Ballast water risk assessment: principles, processes, and methods. ICES J Mar Sci 65: 121-131.

Baum C, Meyer W, Stelzer R, Fleischer LG, Siebers D. 2002. Average nanorough skin surface of the pilot whale (*Globicephala melas*, Delphinidae): Considerations on the self-cleaning abilities based on nanoroughness. Mar Biol 140: 653-657.

Bechert DW, Bruse M, Hage W. 2000. Experiments with three-dimensional riblets as an idealized model of shark skin. Exp Fluids 28: 403-412.

Benedetti-Cecchi L. 2000. Predicting direct and indirect interactions during succession in a mid-littoral rocky shore assemblage. Ecol Monogr 70: 45-72.

Bennett SM, Finlay JA, Gunari N, Wells DD, Meyer AE, Walker GC, Callow ME, Callow JA, Bright FV, Detty MR. 2010. The role of surface energy and water wettability in aminoalkyl/fluorocarbon/hydrocarbon-modified xerogel surfaces in the control of marine biofouling. Biofouling 26: 235 - 246.

Berglin M, Lönn N, Gatenholm P. 2003. Coating modulus and barnacle bioadhesion. Biofouling 19: 63 - 69.

Berntsson KM, Jonsson PR, Lejhall M, Gatenholm P. 2000. Analysis of behavioural rejection of micro-textured surfaces and implications for recruitment by the barnacle *Balanus improvisus*. J Exp Mar Biol Ecol 251: 59-83.

Bowen J, Pettitt ME, Kendall K, Leggett GJ, Preece JA, Callow ME, Callow JA. 2007. The influence of surface lubricity on the adhesion of *Navicula perminuta* and *Ulva linza* to alkanethiol self-assembled monolayers. J R Soc Interface 4: 473-477.

Brady RF, Singer IL. 2000. Mechanical factors favoring release from fouling release coatings. Biofouling 15: 73-81.

Brazel C, Rosen S. 2012. Fundamental Principles of Polymeric Materials, 3rd Edition.

Briand J-F. 2009. Marine antifouling laboratory bioassays: an overview of their diversity. Biofouling 25: 297-311.

Callow JA, Callow ME. 2005. The spore adhesive system of *Ulva*. Phycologia 44: 35.

Callow JA, Callow ME. 2006. Biofilms. In: Eds Fusetani N, Clare A. Antifouling Compounds. Progress in Molecular and Subcellular Biology, Sub-series Marine Molecular Biotechnology. Springer-Verlag, Berlin, Heidleberg

Callow JA, Callow ME. 2011. Trends in the development of environmentally friendly fouling-resistant marine coatings. Nature Comms 2: 244.

Callow JA, Callow ME, Ista LK, Lopez G, Chaudhury MK. 2005. The influence of surface energy on wetting behaviour of the spore adhesive of marine alga *Ulva linza* (synonym *Enteromorpha linza*). J R Soc Interface 2: 319-325.

Callow ME. 1996. Ship-fouling: The problem and method of control. *Biodeterioration Abstracts* 10: 411-421.

Callow ME, Callow JA. 2002. Marine biofouling: A sticky problem. Biologist 49: 1-5.

Callow ME, Callow JA. 2006. Biofilms. In Fusetani, N and Clare, AS (Eds), Antifouling Compounds. Progress in Molecular and Subcellular Biology, Sub-series Marine Molecular Biotechnology. Springer-Verlag, Berlin, Heidleberg.

Callow ME, Callow JA, Ista LK, Coleman SE, Nolasco AC, Lopez GP. 2000. Use of self-assembled monolayers of different wettabilities to study surface selection and primary adhesion processes of green algal (*Enteromorpha*) zoospores. Appl Environ Microbiol 66: 3249-3254.

Callow ME, Callow JA, Pickett-Heaps JD, Wetherbee R. 1997. Primary adhesion of *Enteromorpha* (Chlorophyta, Ulvales) propagules: quantitative settlement studies and video microscopy. J Phycol 33: 938-947.

Callow ME, Jennings AR, Brennan AB, Seegert CE, Gibson A, Wilson L, Feinberg A, Baney R, Callow JA. 2002. Microtopographic cues for settlement of zoospores of the green fouling alga *Enteromorpha*. Biofouling 18: 229 - 236.

Cao X, Pettit ME, Conlan SL, Wagner W, Ho AD, Clare AS, Callow JA, Callow ME, Grunze M, Rosenhahn A. 2009. Resistance of polysaccharide coatings to proteins,hematopoietic cells, and marine organisms. Biomacromolecules 10: 907-915.

Cardinal A. 1964. Etude sur les Ectocarpacées de la Manche. Nova Hedwigia (Beih) 15: 1-86.

Carman ML, Estes TG, Feinberg AW, Schumacher JF, Wilkerson W, Wilson LH, Callow ME, Callow JA, Brennan AB. 2006. Engineered antifouling microtopographies - correlating wettability with cell attachment. Biofouling 22: 11-21.

Chambers LD, Stokes KR, Walsh FC, Wood RJK. 2006. Modern approaches to marine antifouling coatings. Surf Coat Tech 201: 3642–3652.

Charrier B, Coelho SM, Bail AL, Tonon T, Michel G, Potin P, Kloareg B, Boyen C, Peters AF, Cock JM. 2008. Development and physiology of the brown alga *Ectocarpus siliculosus*: two centuries of research. New Phytol 177: 319-332.

Chaudhury MK, Finlay JA, Chung JY, Callow ME, Callow JA. 2005. The influence of elastic modulus and thickness on the release of the soft-fouling green alga *Ulva linza* (syn. *Enteromorpha linza*) from poly(dimethylsiloxane) (PDMS) model networks. Biofouling 21: 41-48.

Chen C, Wang J, Chen Z. 2004. Surface restructuring behavior of various types of poly(dimethylsiloxane) in water detected by SFG. Langmuir 20: 10186-10193.

Cho Y, Sundaram HS, Finlay JA, Dimitriou MD, Callow ME, Callow JA, Kramer EJ, Ober CK. 2012. Reconstruction of surfaces from mixed hydrocarbon and PEG components in water: Responsive surfaces aid fouling release. Biomacromolecules 13: 1864-1874.

Cho Y, Sundaram HS, Weinman CJ, Paik MY, Dimitriou MD, Finlay JA, Callow ME, Callow JA, Kramer EJ, Ober CK. 2011. Triblock copolymers with grafted fluorine-free, amphiphilic, non-ionic side chains for antifouling and fouling-release applications. Macromolecules 44: 4783-4792.

Christensen BE. 1989. The role of extracellular polysaccharides in biofilms. J Biotechnol 10: 181-202.

Clare AS, Aldred N. 2009. Surface colonisation by marine organisms and its impact on antifouling research. In: Eds Hellio C, Yebra DM. Advances in marine antifouling coatings and technologies. Woodhead Publishing Limited and CRC Press, Cambridge. pp. 46-79

Clare AS, Rittschof D, Gerhart DJ, Maki JS. 1992. Molecular approaches to nontoxic antifouling. J Invert Reprod Dev. 22: 67-76

Cooper SP, Finlay JA, Cone G, Callow ME, Callow JA, Brennan AB. 2011. Engineered antifouling microtopographies: Kinetic analysis of the attachment of zoospores of the green alga *Ulva* to silicone elastomers. Biofouling 27: 881-892.

Coppejans E, Kling R. 1995. Flore algologique des côtes du Nord de la France et de la Belgique. Jardin Botanique National de Belgique: Meise

D'Souza F, Bruin A, Biersteker R, Donnelly G, Klijnstra J, Rentrop C, Willemsen P. 2010. Bacterial assay for the rapid assessment of antifouling and fouling release properties of coatings and materials. J Ind Microbiol Biot 37: 363-370.

Dahlström M, Jonsson H, Jonsson PR, Elwing H. 2004. Surface wettability as a determinant in the settlement of the barnacle *Balanus Improvisus* (DARWIN). J Exp Mar Biol Ecol 305: 223-232.

Dafforn KA, Lewis JA, Johnston EL. 2011. Antifouling strategies: History and regulation, ecological impacts and mitigation. Mar Poll Bull 62(3): 453–465.

de Nys R, Guenther J. 2009. The impact and control of biofouling in marine finfish aquaculture. In: Eds Hellio C, Yebra DM. Advances in marine antifouling coatings and technologies. Woodhead Publishing Limited and CRC Press, Cambridge. pp. 177-219

Dexter SC. 1976. Influence of substrate wettability on the formation of bacterial slime films on solid surfaces immersed in natural sea water. In 'Proceedings of the 4th International Congress of Marine Corrosion and Biofouling'. Antibes, France pp. 137-144

Dexter SC. 1979. Influence of substratum critical surface tension on bacterial adhesion - in Situ studies. J Colloid Interface Sci 70: 346-354.

Dexter SC, Sullivan JD, Williams J, Watson SW. 1975. Influence of substrate wettability on the attachment of marine bacteria to various surfaces. Appl Microbiol 30: 298-308.

Dobretsov S. 2010. Marine biofilms. In: Eds Durr S, Thomason JC. Biofouling. Wiley-Blackwell. pp. 123-136

Dobretsov S, Thomason JC. 2011. The development of marine biofilms on two commercial non-biocidal coatings: a comparison between silicone and fluoropolymer technologies. Biofouling 27: 869-880.

Dobretsov S, Xiong H, Xu Y, Levin L, Qian P-Y. 2007. Novel antifoulants: Inhibition of larval attachment by proteases. Mar Biotechnol 9: 388-397.

Dobretsov SV, Qian P-Y. 2002. Effect of bacteria associated with the green alga *Ulva reticulata* on marine micro- and macrofouling. Biofouling 18: 217-228.

Du H, Chandaroy P, Hui SW. 1997. Grafted poly(ethylene glycol) on lipid surfaces inhibits protein adsorption and cell adhesion. BBA-Biomembranes 1326: 236-248.

Ederth T, Nygren P, Pettitt ME, Ostblom M, Du CX, Broo K, Callow ME, Callow J, Liedberg B. 2008. Anomalous settlement behavior of *Ulva linza* zoospores on cationic oligopeptide surfaces. Biofouling 24: 303-312.

Ederth T, Pettitt ME, Nygren P, Du CX, Ekblad T, Zhou Y, Falk M, Callow ME, Callow JA, Liedberg B. 2009. Interactions of zoospores of *Ulva linza* with arginine-rich oligopeptide monolayers. Langmuir 25: 9375-9383.

Edyvean RGJ. 2010. Consequences of fouling on shipping. In: Eds Durr S, Thomason JC. Biofouling. Wiley-Blackwell. pp. 217-225

Edyvean RGJ, Terry LA, Picken GB. 1985. Marine fouling and its effects on offshore structures in the North Sea: a review. Int Biodet 21: 277-284.

Ekblad T, Bergström G, Ederth T, Conlan SL, Mutton R, Clare AS, Wang S, Liu Y, Zhao Q, D'Souza F, Donnelly GT, Willemsen PR, Pettitt ME, Callow ME, Callow JA, Liedberg B. 2008. Poly(ethylene glycol)-containing hydrogel surfaces for antifouling applications in marine and freshwater environments. Biomacromolecules 9: 2775-2783.

Evariste E, Gachon CMM, Callow ME, Callow JA. 2012. Development and characteristics of an adhesion bioassay for ectocarpoid algae. Biofouling 28: 15-27.

Evariste E, Gatley CM, Detty MR, Callow ME, Callow JA. 2013. The performance of aminoalkyl/fluorocarbon/hydrocarbon-modified xerogel coatings against the marine alga *Ectocarpus crouaniorum*: Relative roles of surface energy and charge. Biofouling 29(2): 171-184.

Feinberg AW, Gibson AL, Wilkerson WR, Seegert CA, Wilson LH, Zhao LC, Baney RH, Callow JA, Callow ME, Brennan AB. 2003. Investigating the energetics of bioadhesion on microengineered siloxane elastomers: Characterizing the topography, mechanical properties, and surface energy and their effect on cell contact guidance. In. Clarson SJ, Fitzgerald JJ,

Owen MJ, Smith SD, van Dyke ME, editors. Synthesis and properties of silicones and silicone-modified materials. Am Chem Soc 838:196 – 211.

Field DE. 1976. Fluorinated polyepoxy and polyurethane coatings. J coating Technol 48: 43-47.

Finlay JA, Bennett SM, Brewer LH, Sokolova A, Clay G, Gunari N, Meyer AE, Walker GC, Wendt DE, Callow ME, Callow JA, Detty MR. 2010. Barnacle settlement and the adhesion of protein and diatom microfouling to xerogel films with varying surface energy and water wettability. Biofouling 26: 657 - 666.

Finlay JA, Callow ME, Ista LK, Lopez GP, Callow JA. 2002. The influence of surface wettability on the adhesion strength of settled spores of the green alga *Enteromorpha* and the diatom *Amphora*. Inter Comp Biol 42: 1116-1122.

Finlay JA, Fletcher BR, Callow ME, Callow JA. 2008. Effect of background colour on growth and adhesion strength of *Ulva* sporelings. Biofouling 24: 219-225.

Finnie AA, Williams DN. 2010. Paint and coatings technology for the control of marine fouling. In: Eds Durr S, Thomason J. Biofouling. Wiley-Blackwell. pp. 185-206

Fitridge I, Dempster T, Guenther J, de Nys R. 2012. The impact and control of biofouling in marine aquaculture: a review. Biofouling, 28(7): 649-669.

Flammang P, Lambert A, Bailly P, Hennebert E. 2009. Polyphosphoprotein-Containing Marine Adhesives. J Adhesion 85(8):447-464.

Fletcher RL. 1980. Catalogue of main marine fouling organisms. Vol. 6 Algae. Office d'études marines et atmosphériques: Brussels

Fletcher RL, Callow ME. 1992. The Settlement, attachment and establishment of marine algal spores. Br Phycol J 27: 303-329.

Floerl O. 2005. Factors that influence hull fouling on ocean-going vessels. In: Ed. Godwin LS. Hull fouling as a mechanism for marine invasive species introductions. Bishop Mus Tech Rep, Honolulu, Hawaii. pp. 6-13

Gachon CMM, Day JG, Campbell CN, Proschold T, Saxon RJ, Kupper FC. 2007. The culture collection of algae and protozoa (CCAP): A biological resource for protistan genomics. Gene 406: 51-57.

Gachon CMM, Strittmatter M, Muller DG, Kleinteich J, Kupper FC. 2009. Detection of differential host susceptibility to the marine oomycete pathogen *Eurychasma dicksonii* by real-time PCR: Not all algae are equal. Appl Environ Microbiol 75: 322-328.

Ganesan AM, Alfaro AC, Brooks JD, Higgins CM. 2010. The role of bacterial biofilms and exudates on the settlement of mussel (*Perna canaliculus*) larvae. Aquaculture 306: 388-392.

Geissler U. 1983. Die salzbelastete flussstrecke der werra-ein binnenlandstandort für *Ectocarpus confervoides* (Roth) Kjellman. Nova Hedwigia 37: 193-217.

Genzer J, Efimenko K. 2006. Recent developments in superhydrophobic surfaces and their relevance to marine fouling: A review. Biofouling 22(5):339-360.

Good RJ, Koo MN. 1979. The effect of drop size on contact angle. J Colloid Interface Sci 71: 283-292.

Gram L, Grossart H-P, Schlingloff A, Kiorboe T. 2002. Possible quorum sensing in marine snow bacteria: Production of acylated homoserine lactones by *Roseobacter* strains isolated from marine snow. Appl Environ Microbiol 68: 4111-4116.

Granhag LM, Finlay JA, Jonsson PR, Callow JA, Callow ME. 2004. Roughness-dependent removal of settled spores of the green alga *Ulva* (syn. *Enteromorpha*) exposed to hydrodynamic forces from a water jet. Biofouling 20: 117-122.

Greer SP, Amsler CD. 2002. Light boundaries and the coupled effects of surface hydrophobisity and light on spore settlement in the brown alga *Hincksia irregularis* (Phaeophyceae). J Phycol 38: 116-124.

Greer SP, Amsler CD. 2004. Clonal variation in phototaxis and settlement behaviors of *Hincksia irregularis* (Phaeophyceae) spores. J Phycol 40: 44-53.

Grozea CM, Walker GC. 2009. Approaches in designing non-toxic polymer surfaces to deter marine biofouling. Soft Matter 21(5): 4088-4100.

Gudipati CS, Finlay JA, Callow JA, Callow ME, Wooley KL. 2005. The antifouling and fouling-release perfomance of hyperbranched fluoropolymer (HBFP)-poly(ethylene glycol) (PEG) composite coatings evaluated by adsorption of biomacromolecules and the green fouling alga *Ulva*. Langmuir 21: 3044-3053.

Gunari N, Brewer LH, Bennett SM, Sokolova A, Kraut ND, Finlay JA, Meyer AE, Walker GC, Wendt DE, Callow ME, Callow JA, Bright FV, Detty MR. 2011. The control of marine biofouling on xerogel surfaces with nanometer-scale topography. Biofouling 27: 137-149.

Hall A. 1980. Heavy metal co-tolerance in a copper-tolerant population of the marine fouling alga, *Ectocarpus siliculosus* (Dillw.) Lyngbye. New Phytol 85: 73-78.

Hall A, Baker AJM. 1985. Settlement and growth of copper-tolerant *Ectocarpus siliculosus* (Dillwyn) Lyngbye on different copper-based antifouling surfaces under laboratory conditions.1. Corrosion trials in seawater and development of an algal culture system. J Mater Sci 20: 1111-1118.

Hall A, Baker AJM. 1986. Settlement and growth of copper-tolerant *Ectocarpus siliculosus* (Dillwyn) Lyngbye on different copper-based antifouling surfaces under laboratory conditions. 2. A comparison of the early stages of fouling using light and electron microscopy. J Mater Sci 21: 1240-1252.

Hall A, Fielding AH, Butler M. 1979. Mechanisms of copper tolerance in the marine fouling alga *Ectocarpus siliculosus* – evidence for an exclusion mechanism. . Mar Biol 54: 195-199.

Hamer JP, Walker G. 2001. Avoidance of dried biofilms on slate and algal surfaces by certain spirorbid and bryozoan larvae. J Mar Biol Ass UK 81: 167-168.

Harino H, Yamamoto Y, Eguchi S, Kawai Sc, Kurokawa Y, Arai T, Ohji M, Okamura H, Miyazaki N. 2007. Concentrations of antifouling biocides in sediment and mussel samples collected from Otsuchi Bay, Japan. Arch Environ Con Tox 52: 179-188.

Herth W, Schnepf E. 1980. The fluorochrome, calcofluor white, binds oriented to structural polysaccharide fibrils. Protoplasma 105: 129-133.

Hewitt C, Campbell M, Thresher R, Martin R, Boyd S, Cohen B, Currie D, Gomon M, Keough M, Lewis J, Lockett M, Mays N, McArthur M, O'Hara T, Poore GB, Ross DJ, Storey M, Watson J, Wilson R. 2004. Introduced and cryptogenic species in Port Phillip Bay, Victoria, Australia. Mar Biol 144: 183-202.

Hewitt CL. 2002. Distribution and biodiversity of australian tropical marine bioinvasions. Pac Sci 56: 213-222.

Holland R, Dugdale TM, Wetherbee R, Brennan AB, Finlay JA, Callow JA, Callow ME. 2004. Adhesion and motility of fouling diatoms on a silicone elastomer. Biofouling 20: 323-329.

Holm ER, Cannon G, Roberts D, Schmidt AR, Sutherland JP, Rittschof D. 1997. The influence of initial surface chemistry on development of the fouling community at Beaufort, North Carolina. J Exp Mar Biol Ecol 215: 189-203.

Howell D, Behrends B. 2006. A review of surface roughness in antifouling coatings illustrating the importance of cutoff length. Biofouling 22:401-410.

Hu DS-G, Tsai C-E. 1996. Correlation between interfacial free energy and albumin adsorption in poly(acrylonitrile–acrylamide–acrylic acid) hydrogels. In. pp. 1809-1817. (Wiley Subscription Services, Inc., A Wiley Company)

Hu ZK, Finlay JA, Chen L, Betts DE, Hillmyer MA, Callow ME, Callow JA, DeSimone JM. 2009. Photochemically cross-linked perfluoropolyether-based elastomers: Synthesis, physical characterization, and biofouling evaluation. Macromolecules 42: 6999-7007.

Huggett MJ, Nedved BT, Hadfield MG. 2009. Effects of initial surface wettability on biofilm formation and subsequent settlement of *Hydroides elegans*. Biofouling 25: 387-399.

Huijs FM, Klijnstra JW, Van ZJ. 2006. Antifouling coating comprising a polymer with functional groups bonded to an enzyme. European patent application EP1661955A1.

Iken KB, Amsler CD, Greer SP, McClintock JB. 2001. Qualitative and quantitative studies of the swimming behavior of *Hincksia irregularis* spores (Phaeophyceae):ecological implications and parameters for quantitative swimming assays. Phycologia 40: 359-366.

Jain A, Bhosle NB. 2009. Biochemical composition of the marine conditioning film: implications for bacterial adhesion. Biofouling 25: 13 - 19.

Jeffrey SW, Humphrey GF. 1975. New spectrophotometric equations for determining chlorophylls a, b, c1 and c2 in higher plants, algae and natural phytoplankton. Biochem Physiol Pfl 167: 191-194.

Jernakoff P. 1983. Factors affecting the recruitment of algae in a midshore region dominated by barnacles. J Exp Mar Biol Ecol 67: 17-31.

Jiang S, Cao Z. 2010. Ultralow-fouling, functionalizable, and hydrolyzable zwitterionic materials and their derivatives for biological applications. Adv Mater 22: 920-932.

Jordan JD, Dunbar RA, Hook DJ, Zhuang H, Gardella JA, Colon LA, Bright FV. 1998. Production, characterization, and utilization of aerosol-deposited sol-gel-derived films. Chem Mater 10: 1041-1051.

Kaffashi A, Jannesari A, Ranjbar Z. 2012. Silicone fouling-release coatings: Effects of the molecular weight of poly(dimethylsiloxane) and tetraethyl orthosilicate on the magnitude of pseudobarnacle adhesion strength. Biofouling 28: 729-741.

Kamino K. 2010. Molecular design of barnacle cement in comparison with those of mussel and tubeworm. J Adhesion 86 (1):96-110.

Kavanagh CJ, Schultz MP, Swain GW, Stein J, Truby K, Wood CD. 2001. Variation in adhesion strength of *Balanus eburneus, Crassostrea virginica* and *Hydroides dianthus* to fouling-release coatings. Biofouling 17: 155-167.

Kim J, Chisholm BJ, Bahr J. 2007. Adhesion study of silicone coatings: the interaction of thickness, modulus and shear rate on adhesion force. Biofouling 23(2): 113 – 120.

Kim J, Nyren-Erickson E, Stafslien S, Daniels J, Bahr J, Chisholm BJ. 2008. Release characteristics of reattached barnacles to non-toxic silicone coatings. Biofouling 24: 313-319.

Kirschner CM, Brennan AB. 2012. Bio-Inspired Antifouling Strategies. Annual Reviews of Materials Research. 42(1): 211-229.

Kloareg B, Quatrano R. 1988. Structure of the cell walls of marine algae and ecophysiological functions of the matrix polysaccharides. In. Oceanography and marine biology: An annual review. pp. 259-315

Krishnan S, Ayothi R, Hexemer A, Finlay JA, Sohn KE, Perry R, Ober CK, Kramer EJ, Callow ME, Callow JA, Fischer DA. 2006a. Anti-biofouling properties of comblike block copolymers with amphiphilic side chains. Langmuir 22: 5075-5086.

Krishnan S, Wang N, Ober CK, Finlay JA, Callow ME, Callow JA, Hexemer A, Sohn KE, Kramer EJ, Fischer DA. 2006b. Comparison of the fouling release properties of hydrophobic fluorinated and hydrophilic PEGylated block copolymer surfaces: Attachment strength of the diatom *Navicula* and the green alga *Ulva*. Biomacromolecules 7: 1449-1462.

Krishnan S, Weinman CJ, Ober CK. 2008. Advances in polymers for anti-biofouling surfaces. J Mater Chem 18: 3405-3413.

Lakshmi K, Muthukumar T, Doble M, Vedaprakash L, Kruparathnam, Dineshram R, Jayaraj K, Venkatesan R. 2012. Influence of surface characteristics on biofouling formed on polymers exposed to coastal sea waters of India. Colloids and Surfaces B: Biointerfaces 91: 205-211.

Lau SCK, Mak KKW, Chen F, Qian P-Y. 2002. Bioactivity of bacterial strains isolated from marine biofilms in Hong Kong waters for the induction of larval settlement in the marine polychaete *Hydroides elegans*. Mar Ecol Prog Ser 226: 301-310.

Le Bail A. 2009. Morphogénèse précose de l'algue brune *Ectocarpus siliculosus*. Universite Pierre et Marie Curie-Paris 6. PhD thesis.

Le Bail A, Billoud B, Maisonneuve C, Peters AF, Cock JM, Charrier B. 2008. Early development patern of the brown alga *Ectocqrpus siliculosus* (Ectocarpales, Phaeophyceae) sporophyte. J Phycol 44: 1269-1281.

Lee BP, Messersmith PB, Israelachvili JN, Waite JH. 2011. Mussel inspired wet adhesives and coatings. Annual Review of Materials Research 41: 99-132.

Lejars M, Margaillan A, Bressy C. 2012. Fouling release coatings: A nontoxic alternative to biocidal antifouling coatings. Chemical Reviews 112 (8): 4347-4390.

Lewis JA, Coutts ADM. 2010. Biofouling invasions. In: Eds Durr S, Thomason JC. Biofouling. Wiley-Blackwell. pp. 348-365

Linskens HF. 1966. Adhäsion von fortpflanzungszellen benthontischer algen. Planta 68: 99-110.

Magin CM, Cooper SP, Brennan AB. 2010. Non-Toxic antifouling strategies. Materials Today 13(4): 36-44.

Magin CM, Finlay JA, Clay G, Callow ME, Callow JA, Brennan AB. 2011. Antifouling performance of cross-linked hydrogels: Refinement of an attachment model. Biomacromolecules 12: 915-922.

Maldonado-Codina C, Morgan PB. 2007. In vitro water wettability of silicone hydrogel contact lenses determined using the sessile drop and captive bubble techniques. J Biomed Mater Res 83:496-502.

Maréchal J-P, Hellio C. 2009. Challenges for the development of new non-toxic antifouling solutions. Int J Mol Sci 10: 4623-4637.

Marshall K, Joint I, Callow ME, Callow JA. 2006. Effect of marine bacterial isolates on the growth and morphology of axenic plantlets of the green alga *Ulva linza*. Microbial Ecol 52: 302-310.

Martinelli E, Agostini S, Galli G, Chiellini E, Glisenti A, Pettitt ME, Callow ME, Callow JA, Graf K, Bartels FW. 2008. Nanostructured films of amphiphilic fluorinated block copolymers for fouling release application. Langmuir 24: 13138-13147.

Martinelli E, Galli G, Cwikel D, Marmur A. 2012a. Wettability and surface tension of amphiphilic polymer films: Time-dependent measurements of the most stable contact angle. Macromol Chem Physic 213: 1448-1456.

Martinelli E, Sarvothaman MK, Galli G, Pettitt ME, Callow ME, Callow JA, Conlan SL, Clare AS, Sugiharto AB, Davies C, Williams D. 2012b. Poly(dimethyl siloxane) (PDMS) network blends of amphiphilic acrylic copolymers with poly(ethylene glycol)-fluoroalkyl side chains for fouling-release coatings. II. Laboratory assays and field immersion trials. Biofouling 28: 571-582.

McMaster DM, Bennett SM, Tang Y, Finlay JA, Kowalke GL, Nedved B, Bright FV, Callow ME, Callow JA, Wendt DE, Hadfield MG, Detty MR. 2009. Antifouling character of 'active' hybrid xerogel coatings with sequestered catalysts for the activation of hydrogen peroxide. Biofouling 25: 21-33.

Michel G, Tonon T, Scornet D, Cock JM, Kloareg B. 2010. The cell wall polysaccharide metabolism of the brown alga *Ectocarpus siliculosus*. Insights into the evolution of extracellular matrix polysaccharides in Eukaryotes. New Phytol 188: 82-97.

Mieszkin S, Martin-Tanchereau P, Callow ME, callow JA. 2012. Effect of bacterial biofilms formed on fouling-release coatings from natural seawater and *Cobetia marina*, on the adhesion of two marine algae. Biofouling 28(9):953-968.
.
Mineur F, Johnson MP, Maggs CA, H S. 2007. Hull fouling on commercial ships as a vector of macroalgal introduction. Mar Biol 151: 1299-1307.

Mitik-Dineva N, Wang J, Truong VK, Stoddart PR, Malherbe F, Crawford RJ, Ivanova EP. 2009. Differences in colonisation of five marine bacteria on two types of glass surfaces. Biofouling 25: 621-631.

Molino PJ, Wetherbee R. 2008. The biology of biofouling diatoms and their role in the development of microbial slimes. Biofouling 24: 365-379.

Müller DG. 1967. Generationswelchsel, kernphasenweshsel und sexualitat der braunalge im kulturversuch. Planta 75: 39-54.

Müller DG. 1977. Sexual reproduction in british *Ectocarpus siliculosus* (Phaeophyta). Br Phycol J 12: 131-136.

Müller DG, Eichenberger W. 1994. Betaine lipid content and species delimitation in *Ectocarpus, Feldmannia* and *Hincksia* (Ectocarpales, Phaeophyceae). Eur J Phycol 29: 219-225.

Olsen SM, Pedersen LT, Laursen MH, Kiil S, Dam-Johansen K. 2007. Enzyme-based antifouling coatings: A review. Biofouling 23: 369-383.

Owens DK, Wendt RC. 1969. Estimation of the surface free energy of polymers. J Appl Polym Sci 13: 1741-1747.

Park D, Finlay JA, Ward RJ, Weinman CJ, Krishnan S, Paik M, Sohn KE, Callow ME, Callow JA, Handlin DL, Willis CL, Fischer DA, Angert ER, Kramer EJ, Ober CK. 2010. Antimicrobial behavior of semifluorinated-quaternized triblock copolymers against airborne and marine microorganisms. ACS Appl Mater Interfaces 2: 703-711.

Patel P, Callow ME, Joint I, Callow JA. 2003. Specificity in the settlement - modifying response of bacterial biofilms towards zoospores of the marine alga *Enteromorpha*. Environ Microbiol 5: 338-349.

Pereira M, Ankjaergaard C. 2009. Legislation affection antifouling products. In: Eds Hellio C, Yebra DM. Advances in marine antifouling coatings and technologies. Woodhead Publishing Limited and CRC Press, Cambridge. pp. 240-259

PerkinElmer (2008) Introduction to dynamic mechanical analyse. http://www.perkinelmer.com/CMSResources/Images/44-74546GDE_IntroductionToDMA.pdf.

Peters AF, Marie D, Scornet D, Kloareg B, Cock JM. 2004. Proposal of *Ectocarpus siliculosus* (Ectocarpales, Phaeophyceae) as a model organisms for brown algal genetics and genomics. J Phycol 40: 1079-1088.

Peters AF, Scornet D, Ratin M, Charrier B, Monnier A, Merrien Y, Corre E, Coelho SM, Cock JM. 2008. Life-cycle-generation-specific developmental processes are modified in the immediate upright mutant of the brown alga *Ectocarpus siliculosus*. Development 135: 1503-1512.

Peters AF, van Wijk SJ, cho GY, Scornet D, Hanyuda T, Kawai H, Schroeder DC, Cock JM, Boo SM. 2010. Reinstatement of *Ectocarpus crouaniorum* Thuret in Le Jolis as a third common species of *Ectocarpus* (Ectocarpales, Phaeophyceae) in Western Europe, and its phenology at Roscoff, Brittany. Phycol Res. 58: 157-170.

Petrone L, Di Fino A, Aldred N, Sukkaew P, Ederth T, Clare AS, Liedberg B. 2011a. Effects of surface charge and Gibbs surface energy on the settlement behaviour of barnacle cyprids (*Balanus amphitrite*). Biofouling 27: 1043-1055.

Petrone L, Easingwood R, Barker MF, McQuillan AJ. 2011b. In situ ATR-IR spectroscopic and electron microscopic analyses of settlement secretions of *Undaria pinnatifida* kelp spores. J R Soc Interface 8: 410-422.

Pettitt ME, Henry SL, Callow ME, Callow JA, Clare AS. 2004. Activity of commercial enzymes on settlement and adhesion of cypris larvae of the barnacle *Balanus amphitrite*, spores of the green alga *Ulva linza*, and the diatom *Navicula perminuta*. Biofouling 20: 299-311.

Phillips N, Burrowes R, Rousseau F, Reviers Bd, Saunders GW. 2008. Resolving evolutionary relationships among the brown algae using chloroplast and nuclear genes. J Phycol 44: 394-405.

Potin P, Leblanc C. 2006. Phenolic-based adhesives of marine brown algae. In: Eds Smith AM, Callow JA. Biological Adhesives. Springer, Heidelberg. pp. 105-124

Prendergast GS. 2007. Settlement and succession of benthic marine organisms: interactions between multiple physical and biological factors. Newcastle University. PhD thesis.

Pritchard A. 1988. The economics of fouling. In: Eds Melo L, Bott T, Bernado C. *Fouling Science and Technology*. Kluwer Academics, Dordrecht. pp. 31-45

Provasoli L, Pintner IJ. 1980. Bacteria induced polymorphism in an axenic laboratory strain of *Ulva lactuca* (Chlorophyceae). J Phycol 16: 196-201.

Pyefinch KA. 1950. Notes on the ecology of ship-fouling organisms. J Anim Ecol 19: 29-35.

Qian PY, Lau SCK, Dahms HU, Dobretsov S, Harder T. 2007. Marine biofilms as mediators of colonization by marine macroorganisms: Implications for antifouling and aquaculture. Mar Biotech 9(4):399-410.

Quinn GP, Keough MJ. 2002. Experimental design and data analysis for biologists. Cambridge University Press: Cambridge

Rasmussen K, Willemsen PR, Ostgaard K. 2002. Barnacle Settlement on Hydrogels. Biofouling 18: 177-191.

Ray B, Lahaye M. 1995. Cell-wall polysaccharides from the marine green alga *Ulva "rigida"* (ulvales, chlorophyta). Extraction and chemical composition. Carbohydr Res 274: 251-261.

Rittschof D, Costlow JD. 1989. Bryozoan and barnacle settlement in relation to initial surface wettability: a comparison of laboratory and field studies. In 'Topics in marine biology: proceedings of the 22nd European marine biological symposium'. Barcelona, Spain. (Ed. Ros JD) pp. 411-416. (Consejo Superior de Investigaciones Científicas, CSIC: Institut de Ciències del Mar)

Roberts D, Rittschof D, Holm E, Schmidt AR. 1991. Factors influencing initial larval settlement: temporal, spatial and surface molecular components. J Exp Mar Biol Ecol 150: 203-221.

Rosenhahn A, Finlay JA, Pettit ME, Ward A, Wirges W, Gerhard R, Callow ME, Grunze M, Callow JA. 2009. Zeta potential of motile spores of the green alga *Ulva linza* and the influence of electrostatic interactions on spore settlement and adhesion strength. Biointerphases 4: 7-11.

Rosenhahn A, Schilp S, Kreuzer HJ, Grunze M. 2010. The role of "inert" surface chemistry in marine biofouling prevention. Phys Chem Chem Phys 12: 4275-4286.

Roughgarden J, Gaines S, Possingham H. 1988. Recruitment dynamics in complex life cycles. Science 241: 1460-1466.

Russell G. 1973. The Phaeophyta: a synopsis of some recent developments. Oceanogr Mar Biol Ann Rev 11: 45-88.

Russell G, Morris OP. 1970. Copper tolerance in the marine fouling alga *Ectocarpus siliculosus*. Nature 228: 288-289.

Salta M, Wharton JA, Stoodley P, Dennington SP, Goodes LR, Werwinski S, Mart U, Wood RJK, Stokes KR. 2010. Designing biomimetic antifouling surfaces. Phil Trans R Soc A 368 **:** 4729-4754.

Sanchez A, Yebra DM. 2009. Ageing tests and long-term performance of marine antifouling coatings. In: Eds Hellio C, Yebra DM. Advances in marine antifouling coatings and technologies. Woodhead Publishing Limited and CRC Press, Cambridge. pp. 393-421

Scardino AJ, de Nys R. 2011. Mini review: Biomimetic models and bioinspired surfaces for fouling control. Biofouling 28: 73-86.

Schaffelke B, Smith J, Hewitt C. 2006. Introduced macroalgae a growing concern. J Appl Phycol 18: 529-541.

Schilp S, Kueller A, Rosenhahn A, Grunze M, Pettitt ME, Callow ME, Callow JA. 2007. Settlement and adhesion of algal cells to hexa (ethylene glycol)-containing self-assembled monolayers with systematically changed wetting properties. Biointerphases 2: 143-150.

Schmidt DL, Brady RF, Lam K, Schmidt DC, Chaudhury MK. 2004. Contact angle hysteresis, adhesion, and marine biofouling. Langmuir 20: 2830-2836.

Schultz MP. 2007. Effects of coating roughness and biofouling on ship resistance and powering. Biofouling 23: 331-341.

Schultz MP, Bendick JA, Holm ER, Hertel WM. 2011. Economic impact of biofouling on a naval surface ship. Biofouling 27: 87-98.

Schultz MP, Finlay JA, Callow ME, Callow JA. 2000. A turbulent channel flow apparatus for the determination of the adhesion strength of microfouling organisms. Biofouling 15: 243 - 251.

Schultz MP, Finlay JA, Callow ME, Callow JA. 2003. Three models to relate detachment of low form fouling at laboratory and ship scale. Biofouling 19: 17-26.

Schumacher JF, Carman ML, Estes TG, Feinberg AW, Wilson LH, Callow ME, Callow JA, Finlay JA, Brennan AB. 2007. Engineered antifouling microtopographies - effect of feature size, geometry, and roughness on settlement of zoospores of the green alga *Ulva*. Biofouling 23: 55-62.

Schwartz LW, Garoff S. 1985. Contact angle hysteresis on heterogeneous surfaces. Langmuir 1: 219-230.

Selvaggio P, Tusa S, Detty MR, Bright FV, Ciriminna R, Pagliaro M. 2009. Ecofriendly protection from biofouling of the monitoring system at Pantelleria's Cala Gadir underwater archaeological site, Sicily. Int J Naut Archaeol 38: 417-421.

Shea R, Chopin T. 2007. Effects of germanium dioxide, an inhibitor of diatom growth, on the microscopic laboratory cultivation stage of the kelp, *Laminaria saccharina*. J Appl Phycol 19: 27-32.

Shoaf WT, Lium BW. 1976. Improved extraction of chlorophyll a and b from algae using dimethyl sulfoxide. Limnol Oceanogr 21: 926-928.

Silberfeld T, Leigh JW, Verbruggen H, Cruaud C, de Reviers B, Rousseau F. 2010. A multi-locus time-calibrated phylogeny of the brown algae (Heterokonta, Ochrophyta, Phaeophyceae): Investigating the evolutionary nature of the "brown algal crown radiation". Mol Phylogenet Evol 56: 659-674.

Silverman H, Roberto F. 2007. Understanding marine mussel adhesion. Mar Biotechnol 9: 661-681.

Srinivasan M, Swain G. 2007. Managing the use of copper-based antifouling paints. Environ Manage 39: 423-441.

Starr R, Zeikus J. 1987. UTEX - The culture collection of algae at the University of Texas at Austin. J Phycol 23: 1-47.

Stein J, Truby K, Wood CD, Takemori M, Vallance M, Swain G, Kavanagh C, Kovach B, Schultz M, Wiebe D, Holm E, Montemarano J, Wendt D, Smith C, Meyer A. 2003. Structure-property relationships of silicone biofouling-release coatings: Effect of silicone network architecture on pseudobarnacle attachment strengths. Biofouling 19: 87-94.

Stewart RJ, Ransom TC, Hlady V. 2011. Natural Underwater Adhesives. J Polym Sci B Polym Phys (11):757-771.

Sundaram HS, Cho Y, Dimitriou MD, Weinman CJ, Finlay JA, Cone G, Callow ME, Callow JA, Kramerb EJ, Ober CK. 2011. Fluorine-free mixed amphiphilic polymers based on PDMS and PEG side chains for fouling release applications. Biofouling 27: 589-602.

Swain G, Anil AC, Baier RE, Chia FS, Conte E, Cook A, Hadfield M, Haslbeck E, Holm E, Kavanagh C, Kohrs D, Kovach B, Lee C, Mazzella L, Meyer AE, Qian PY, Sawant SS, Schultz M, Sigurdsson J, Smith C, Soo L, Terlizzi A, Wagh A, Zimmerman R, Zupo, Valerio. 2000. Biofouling and barnacle adhesion data for fouling-release coatings subjected to static immersion at seven marine sites. Biofouling 16: 331-344.

Swain GW. 1999. Redefining antifouling coatings. J Prot Coat Lining 16: 26-35.

Swain GW, Nelson WG, Preedeekanit S. 1998. The influence of biofouling adhesion and biotic disturbance on the development of fouling communities on non-toxic surfaces. Biofouling 12: 257 - 269.

Swain GW, Schultz MP. 1996. The testing and evaluation of non-toxic antifouling coatings. Biofouling 10: 187-197.

Tait K, Joint I, Daykin M, Milton DL, Williams P, Cámara M. 2005. Disruption of quorum sensing in seawater abolishes attraction of zoospores of the green alga *Ulva* to bacterial biofilms. Environ Microbiol 7: 229-240.

Tang Y, Finlay JA, Kowalke GL, Meyer AE, Bright FV, Callow ME, Callow JA, Wendt DE, Detty MR. 2005. Hybrid xerogel films as novel coatings for antifouling and fouling release. Biofouling 21: 59-71.

Terry LA, Picken GB. 1986. Algal fouling in North Sea. In: Eds Evans LV, Hoagland KD. Algal biofouling. Elsevier, Amsterdam. pp. 179-192

Thomason JC, Letissier MDAA, Thomason PO, Field SN. 2002. Optimising settlement tiles: The effects of surface texture and energy, orientation and deployment duration upon the fouling community. Biofouling 18: 293-304.

Thome I, Pettitt ME, Callow ME, Callow JA, Grunze M, Rosenhahn A. 2012. Conditioning of surfaces by macromolecules and its implication for the settlement of zoospores of the green alga *Ulva linza*. Biofouling 28: 501-510.

Thompson SEM, Callow ME, Callow JA. 2010. The effects of nitric oxide in settlement and adhesion of zoospores of the green alga *Ulva*. Biofouling 26: 167 - 178.

Thompson SEM, Taylor AR, Brownlee C, Callow ME, Callow JA. 2008. The role of nitric oxide in diatom adhesion in relation to substratum properties. J Phycol 44: 967-976.

Tribou M, Swain G. 2010. The use of proactive in-water grooming to improve the performance of ship hull antifouling coatings. Biofouling 26: 47-56.

Vadas RL, Johnson S, Norton TA. 1992. Recruitment and mortality of early post-settlement stages of benthic algae. Br Phycol J 27: 331-351.

Wahl M. 1989. Marine epibiosis. I. Fouling and antifouling: some basic aspects. Mar Ecol Prog Ser 58:175-189.

Walker G. 1973. The early development of the cement apparatus in the barnacle, *Balanus balanoides* (L.) (Crustacea: Cirripedia). J Exp Mar Biol Ecol 12: 305-314.

Wang Y, Betts DE, Finlay JA, Brewer L, Callow ME, Callow JA, Wendt DE, DeSimone JM. 2011. Photocurable amphiphilic perfluoropolyether/poly(ethylene glycol) networks for fouling-release coatings. Macromolecules 44: 878-885.

Weinman CJ, Finlay JA, Park D, Paik MY, Krishnan S, Sundaram HS, Dimitriou M, Sohn KE, Callow ME, Callow JA, Handlin DL, Willis CL, Kramer EJ, Ober CK. 2009. ABC triblock surface active block copolymer with grafted ethoxylated fluoroalkyl amphiphilic side chains for marine antifouling/fouling-release applications. Langmuir 25: 12266-12274.

West J, Kraft G. 1996. *Ectocarpus siliculosus* (Dillwyn) Lyngbye from Hopkins River Falls, Victoria - the first record of a freshwater brown alga in Australia. Muelleria 9: 29-33.

Wieczorek SK, Todd CD. 1998. Inhibition and facilitation of settlement of epifaunal marine invertebrate larvae by microbial biofilm cues. Biofouling 12: 81-118.

Wiegemann M. 2005. Adhesion in blue mussels (*Mytilus edulis*) and barnacles (genus *Balanus*): Mechanisms and technical applications. Aquat Sci 67: 166-176.

WHOI (Woods Hole Oceanographic Institution). 1952. Marine fouling and its prevention. US Naval Institute, Annapolis, Iselin, COD, 338p.

Yarbrough JC, Rolland JP, DeSimone JM, Callow ME, Finlay JA, Callow JA. 2006. Contact angle analysis, surface dynamics, and biofouling characteristics of cross-linkable, random perfluoropolyether-based graft terpolymers. Macromolecules 39: 2521-2528.

Yebra DM, Kiil S, Dam-Johansen K. 2004. Antifouling technology - Past, present and future steps towards efficient and environmentally friendly antifouling coatings. Prog Org Coat 50: 75-104.

Yu J, Wei W, Danner E, Ashley RK, Israelachvili JN, Waite JH. 2011. Mussel protein adhesion depends on interprotein thiol-mediated redox modulation. Nature Chem Biol 7: 588-590.

Zhang W, Wahlgren M, Sivik B. 1989. Membrane characterization by the contact angle technique: II. Characterization of UF-membranes and comparison between the captive bubble and sessile drop as methods to obtain water contact angles. Desalination 72: 263-273.

Zhang Z, Chen S, Jiang S. 2006. Dual-functional biomimetic materials: Nonfouling poly(carboxybetaine) with active functional groups for protein immobilization. Biomacromolecules 7: 3311-3315.

Zhang Z, Finlay JA, Wang LF, Gao Y, Callow JA, Callow ME, Jiang SY. 2009. Polysulfobetaine-grafted surfaces as environmentally benign ultralow fouling marine coatings. Langmuir 25: 13516-13521.

Zhao Q, Liu Y, Wang C, Wang S, Muller-Steinhagen H. 2005. Effect of surface free energy on the adhesion of biofouling and crystalline fouling. Chem Eng Sci 60: 4858-4865.

Zhao Q, Wang C, Liu Y, Wang S. 2007. Bacterial adhesion on the metal-polymer composite coatings. Int J Adhes Adhes 27: 85-91.